THE UNIVERSITY
OF MICHIGAN
SEP 12 1962
ENGINEERING
LIBRARY

АВТОМАТИКА
И
ТЕЛЕМЕХАНИКА

Vol. 22, No. 4, April, 1961

Translation Published October, 1961

SOVIET INSTRUMENTATION AND
CONTROL TRANSLATION SERIES

Automation and Remote Control

(The Soviet Journal *Avtomatika i Telemekhanika* in English Translation)

■ This translation of a Soviet journal on automatic control is published as a service to American science and industry. It is sponsored by the Instrument Society of America under a grant in aid from the National Science Foundation, continuing a program initiated by the Massachusetts Institute of Technology.

SOVIET INSTRUMENTATION AND CONTROL TRANSLATION SERIES

Instrument Society of America

Philip A. Sprague
President
Dr. Ralph H. Tripp
Past President
Nathan Cohn
President-elect-Secretary
Henry J. Noebels
Dept. Vice President
Dr. Benjamin W. Thomas
Dept. Vice President-elect
E. A. Adler
Dept. Vice President
Francis S. Hoag
Dept. Vice President
John J. McDonald
Dept. Vice President
John R. Mahoney
Dept. Vice President-elect
John C. Koch
Treasurer
Alonzo B. Parsons
Dist. I Vice President
H. Kirk Fallin
Dist. II Vice President
Harold J. Bowman
Dist. III Vice President
Fred R. Gilmer
Dist. IV Vice President
Charles H. Callier
Dist. V Vice President
Otto J. Lessa
Dist. VI Vice President
J. Howard Park, III
Dist. VII Vice President
C. Roy Horton
Dist. VIII Vice President
Max Curtis
Dist. IX Vice President
Kenneth S. Vriesen
Dist. X Vice President
Allan E. Lee
Dist. XI Vice President

International Headquarters

William H. Kushnick
Executive Director
Charles W. Covey
Editor, ISA Journal
Herbert S. Kindler
Director, Tech. & Educ. Services

ISA Publications Committee

Charles O. Badgett, *Chairman*

Jere E. Brophy	George A. Larsen	Joshua Stern
Dr. Enoch J. Durbin	Thomas G. MacAnespie	Frank S. Swaney
Prof. Richard W. Jones	John E. Read	Richard A. Terry

Translations Advisory Board of the Publications Committee

Jere E. Brophy, *Chairman*

T. J. Higgins	S. G. Eskin	G. Werbizky

■ This translation of the Soviet Journal *Avtomatika i Telemekhanika* is published and distributed at nominal subscription rates under a grant in aid to the Instrument Society of America from the National Science Foundation. This translated journal, and others in the Series (see back cover), will enable American scientists and engineers to be informed of work in the fields of instrumentation, measurement techniques, and automatic control reported in the Soviet Union.

The original Russian articles are translated by competent technical personnel. The translations are on a cover-to-cover basis and the Instrument Society of America and its translators propose to translate faithfully all of the scientific material in *Avtomatika i Telemekhanika*, permitting readers to appraise for themselves the scope, status, and importance of the Soviet work. All views expressed in the translated material are intended to be those of the original authors and not those of the translators nor the Instrument Society of America.

Publication of *Avtomatika i Telemekhanika* in English translation started under the present auspices in April, 1958, with Russian Vol. 18, No. 1 of January, 1957. The program has been continued with the translation and printing of the 1958-1961 issues.

Transliteration of the names of Russian authors follows the system known as the British Standard. This system has recently achieved wide adoption in the United Kingdom, and is currently being adopted by a large number of scientific journals in the United States.

Readers are invited to submit to the Instrument Society of America comments on the quality of the translations and the content of the articles. Pertinent correspondence will be published in the Society's monthly publication, the ISA JOURNAL. Space will also be made available in the ISA JOURNAL for such replies as may be received from Russian authors to comments or questions by the readers.

1961 Volume 22 Subscription Prices:

Per year (12 issues), starting with Vol. 22, No. 1

General:	*United States and Canada*	$35.00
	Elsewhere	38.00
Libraries of nonprofit academic institutions:		
	United States and Canada	$17.50
	Elsewhere	20.00
Single issues to everyone, each		$ 6.00

1957 Volume 18, 1958 Volume 19, 1959 Volume 20, and 1960 Volume 21 issues also available. Prices upon request.

See back cover for combined subscription to entire Series.

Subscriptions and requests for information on back issues should be addressed to the:

Instrument Society of America
530 William Penn Place, Pittsburgh 19, Penna.

Translated and printed by Consultants Bureau Enterprises, Inc.

Copyright © 1961 by the Instrument Society of America

Automation and Remote Control

A translation of Avtomatika i Telemekhanika, a publication of the Academy of Sciences of the USSR

EDITORIAL BOARD OF AVTOMATIKA I TELEMEKHANIKA

D. I. Ageikin
M. A. Aizerman
A. B. Chelyustkin *(Assoc. Editor)*
E. G. Dudnikov
N. Ya. Festa
V. A. Ilin
A. G. Iosuf'yan
V. V. Karibskii
A. V. Khramoi
B. Ya. Kogan
V. S. Kulebakin
S. A. Lebedev
A. Ya. Lerner
A. M. Letov *(Assoc. Editor)*
V. S. Malov
B. N. Petrov
Yu. P. Portnov-Sokolov
B. S. Sotskov
A. A. Tal' *(Corresp. Secretary)*
V. A. Trapeznikov *(Editor in Chief)*
Ya. Z. Tsypkin
G. M. Ulanov
A. A. Voronov
S. V. Yablonskii

Vol. 22, No. 4 Russian Original Dated April, 1961 October, 1961

CONTENTS

	PAGE	RUSS. PAGE
The Analytical Design of Control Systems. A. M. Letov	363	425
On New Stability Inequalities. I. S. Arzhanykh	373	436
On a Certain Method for Correcting the Dynamic Properties of Automatic Control Systems. V. S. Lerner	379	443
Analytical Solutions of Linear Equations Describing One Class of Dynamical Systems with Variable Parameters. Ts. G. Litovchenko	390	457
Problems of Nonlinear Filtration. I. The Case of One Parameter. I. A. Bol'shakov and V. G. Repin	397	466
The Errors Caused by a Measuring Apparatus, Checking the Variation of a Variable Quantity at Equal Time Intervals. V. A. Bolkonskii	408	479
Theory of a Single-Core Magnetic Amplifier with Rectification of the Load Current by Means of a Symmetrical Nonlinear Resistance. Dai Tse-Hsin	411	483
A Transistor Amplifier Operation in a Thyratron Mode. M. V. Ol'shvang	419	493
On the Theory of Selective Rectification of Even Voltage Harmonics by Means of Symmetrical Nonlinear Electrical Resistors. A. I. Kadochnikov, L. A. Fridman, and R. I. Yanus	426	501
A Simplified Method for Determining Stability Segments. V. E. Bogin	433	509
The Design of Automatic Control Systems (ACS). Yu. I. Borodin and V. N. Plotnikov	435	511
Determining the Optimal Transfer Function for "White Noise" in a Servosystem from the Figure of Merit and the Transient Response Duration for the System. A. S. Kul'chii	450	524
On the Properties of Single-Loop Control Systems. L. G. Sobolov	456	530
On Automatizing the Introduction of Certain Forms of Data into a Computer. V. S. Fain	461	536
A Wire Frequency Resonator for Telemetering. Yu. I. Pivovarov and Yu. M. Tsodikov	464	539
The Transfer Functions and Frequency Responses of a Carbon Pile Voltage Regulator. D. A. Popov	468	543
On Designing Functional Potentiometers. V. M. Frygin	477	552
REVIEWS		
"The Automation of Aviation Power Installations," by A. A. Shevyakov. Reviewed by B. N. Petrov, B. S. Voronkov, and N. P. Kolpakova	481	556

SOVIET INSTRUMENTATION AND CONTROL TRANSLATION SERIES

Automation and Remote Control

A Translation of Avtomatika i Telemekhanika, a Publication of the Academy of Sciences of the USSR

VOL. 22, NO. 4 PUBLISHED MONTHLY APRIL 1961 OCTOBER, 1961

CONTENTS

	PAGE	PAGE
	393	439
	399	456
	409	463
	419	473
	429	483
	439	493
	449	503
	459	513
	469	523
	477	532
	484	542

THE ANALYTICAL DESIGN OF CONTROL SYSTEMS

A. M. Letov
(Moscow)

Translated from Avtomatika i Telemekhanika, Vol. 22, No. 4,
pp. 425-435, April, 1961
Original article submitted November 4, 1960

A method of dynamic programming is obtained for the problem of the analytical design of control systems that are optimum relative to the integral square error.

1. The Method of Dynamic Programming

In [1-13], various methods are described for solving the problem of constructing an optimal system. Solutions obtained in these articles give the law of control as a known function of the time and of the initial and final states of the system. These solutions can be realized by using digital computers operating according to certain algorithms obtained. Discrete time intervals, during which the switching of the controlling unit occurs, are used for the output. In [1-7], the so-called "synthesis problem" is also formulated, i. e., the problem of presenting the control law as a known function of the coordinates of the system. In [14, 15], the authors discuss the simplest case of the solution of this problem, which is given the special name "analytical design."

The problem of the analytical design of control systems was formulated as a problem of classical calculus of variations, in which the law of automatic control is obtained relative to some previously stipulated optimizing functional. The law of control was obtained analytically and written in the form commonly used in actual applications with the corresponding sensing elements and servomotor.

The disadvantage of the methods applying the calculus of variations lies in the fact that they involve writing the equations of the variational problem, and these equations must be actually solved.

In the present article, we use the fact that the dynamic-programming method developed by R. Bellman in [8] permits us to obtain results already known by a new method that is sometimes more conveniently applicable in numerical work, and also to investigate some other possible methods. For clarity, we will describe the basis of the method of dynamic programming by using a simple example. (The original exposition of the method is given in [8]). We will assume that the differential equation

$$\dot{x} = G(x, y) \tag{1.1}$$

is given, with the initial condition $x(t_0) = u$, $t_0 = 0$.

We assume that $G(x, y)$ is a bounded, continuous function of x and y, differentiable with respect to y, defined in the open region $N(x, y)$. Here y is a control function that minimizes the functional

$$I(y) = \int_0^\infty F(x, y)\, dt \tag{1.2}$$

in the class C_1 of functions of x and y. Let y be a function minimizing (1.2). This minimum is some function $\psi(u)$ of the initial state u which we denote by

$$\psi(u) = \min_y I(y). \tag{1.3}$$

Let S be a positive number. We have

$$\psi(u) = \int_0^S F(x, y)\,dt + \int_S^\infty F(x, y)\,dt. \tag{1.4}$$

The essence of R. Bellman's optimization principle lies in the fact that if $y = y(t)$ minimizes the functional $\int_0^\infty F(x, y)\,dt$, then it also minimizes the functional $\int_S^\infty F(x, y)\,dt$ independently of the first integral. The principle expresses the natural condition of calculus of variations according to which any part of an extremal $y(t)$ is also extremal. Using this fact as a basis, R. Bellman developed the following original method. The equality 1.4 can be written in the form

$$\psi(u) = \min_{\underline{y}} \left[\int_0^S F(x, y)\,dt + \psi[x(S)]\right], \tag{1.5}$$

The notation $\min_{\underline{y}}$ denotes that the expression (1.5) is minimized by the function $\underline{y}$ of the class C_1. We will assume that the number S is sufficiently small and that $y(t_0) = v$. If ψ has a derivative for $x \in [x(0), x(S)]$, then according to the mean value theorem we have

$$\psi[u + GS] = \psi(u) + GS\left(\frac{\partial\psi}{\partial x}\right)_{x=\xi},$$

where $0 < \xi < S$. Then

$$\psi(u) = \min_{\underline{v}}\left[F(u, v)S + \psi(u) + GS\left(\frac{\partial\psi}{\partial x}\right)_{x=\xi} + O(S)\right].$$

Here $0(S)$ is the remainder, and it is assumed that $\lim 0(S)/S \to 0$ for $S \to 0$. Therefore when $S \to 0$ we obtain

$$\min_{\underline{v}}\left[F(u, v) + G(u, v)\frac{\partial\psi}{\partial u}\right] = 0. \tag{1.6}$$

In order that the expression in brackets actually yield a minimum relative to $\underline{y}$, its derivative with respect to $\underline{v}$ must be zero. Therefore

$$F(u, v) + G(u, v)\frac{\partial\psi}{\partial u} = 0, \qquad \frac{\partial F(u, v)}{\partial v} + \frac{\partial G(u, v)}{\partial v}\frac{\partial\psi}{\partial u} = 0. \tag{1.7}$$

After eliminating $\frac{\partial\psi}{\partial u}$, we arrive at the equation

$$F\frac{\partial G}{\partial v} = G\frac{\partial F}{\partial v}, \tag{1.8}$$

relating the values of $\underline{u}$ and $\underline{v}$ for any instant of time $t_0 = 0$. The principal aim of the dynamic-programming method is to obtain the functional equations (1.7). We will apply this method in solving the problem of analytical design. However, we first make two observations.

Observation 1. Since the equation (1.8) establishes the relation $v = v(u)$ for any instant t_0 of time, and since as a result of the optimal principle it does not depend on this time, the relation $v = v(u)$ is equivalent to $y = y(x)$ with the equation (1.1), we obtain the complete system. For simplicity, in what follows we will therefore write the functional equation immediately in terms of the original coordinates, since this will not cause any confusion.

Observation 2. In the case when the function G is defined in a closed region $\overline{N}(x, y)$ and the optimal solution can be obtained from the boundary condition, the requirement that the function y(t) be continuous and differentiable can in general be relaxed. The difficulty in solving a problem by the dynamic-programming method lies in the fact that the second of the expressions (1.7) can, in general, not be obtained, since it is uncertain what the expressions $\frac{\partial F}{\partial v}$ and $\frac{\partial G}{\partial v}$ signify along the boundary of $\overline{N}$. The originator of the dynamic-programming method proposes at this stage a very complex method for constructing the optimal solution. We have not applied this method. In the course of the solution of the analytical-design problem in the present work it will be shown that a simple optimal solution can be obtained, in the case of a closed region $\overline{N}$, of the problem for continuous functions y(t), and in a subsequent article for continuous x(t) and discontinuous functions y(t). The value of the method we will describe lies in the fact that it makes it possible to obtain a closed solution for the problem of analytical design in all these cases.

2. A First Order Object of Control

We will start by considering the simplest problem of optimizing the functional (1.2) in the class of functions C_1.

We have the equation of the object of control

$$\dot{\eta} = b\eta + m\xi, \qquad \eta(0) = \eta_0 \tag{2.1}$$

and the optimizing functional

$$I(\xi) = \int_0^\infty (a\eta^2 + c\xi^2)\, dt. \tag{2.2}$$

We write the dynamic programming equations (1.7) in the form

$$\begin{gathered} a\eta^2 + c\xi^2 + (b\eta + m\xi)\frac{\partial \psi}{\partial \eta} = 0, \\ 2c\xi + m\frac{\partial \psi}{\partial \eta} = 0. \end{gathered} \tag{2.3}$$

We thus obtain

$$mc\xi^2 + 2bc\eta\xi - am\eta^2 = 0 \tag{2.4}$$

with the solution

$$\xi = -\frac{k+b}{m}\eta, \quad k = \sqrt{b^2 + \frac{m^2 a}{c}}. \tag{2.5}$$

In the solution of (2.4) for ξ, we reject the solution

$$\xi = -\frac{b-k}{m}\eta,$$

which does not satisfy the requirements of control stability. The solution (2.5) was obtained in [14]. For what follows, it is important to obtain the form of the functional $\psi(u)$. After eliminating ξ from the equations (2.3), we obtain

$$a\eta^2 + b\eta\frac{\partial \psi}{\partial \eta} = \frac{m^2}{4c}\left(\frac{\partial \psi}{\partial \eta}\right)^2. \tag{2.6}$$

This nonlinear differential equation is satisfied by

$$\psi(\eta) = \frac{(b \pm k)c}{m^2}\eta^2 + B(\xi), \tag{2.7}$$

where $B(\xi)$ is an arbitrary function of ξ; we should probably set $B(\xi) = \text{const}$.

3. The Optimal Solution in a Closed Region

We turn again to the equations (2.1), (2.2), and we will investigate their solutions in the closed region $\bar{N}(\xi, \eta)$ characterized by the relation

$$|\xi| \leqslant \bar{\xi}, \tag{3.1}$$

where $\bar{\xi}$ is a given positive number. We will assume that the comparison functions are of the class C, since the optimal solution of the problem can be obtained from the boundary of the region (3.1). The case when $x(t)$ remains continuous while $y(t)$ is discontinuous at a finite number of points will be considered in a subsequent article.

We therefore consider the single-valued nonlinear transformation [15]

$$\xi = \varphi(\zeta). \tag{3.2}$$

The function $\varphi(\zeta)$ is continuous, piecewise differentiable, and defined as *

$$\varphi(\zeta) = \begin{cases} +\bar{\xi} \text{ for } \zeta \geqslant \zeta^*, \\ \varphi(\zeta) \text{ for } |\zeta| < \zeta^*, \\ -\bar{\xi} \text{ for } \zeta \leqslant -\zeta^*. \end{cases} \tag{3.3}$$

The number ζ^* is determined by the form of the function $\varphi(\zeta)$. The transformation (3.2) maps the closed region $\bar{N}(\xi, \eta)$ into an open region $N(\zeta, \eta)$ in which the role of the controlling function passes to ζ.

The functional equations (2.3) in the present case will be

$$\begin{gathered} a\eta^2 + c\varphi^2 + (b\eta + m\varphi)\frac{\partial \psi}{\partial \eta} = 0, \\ \left(2c\varphi + m\frac{\partial \psi}{\partial \eta}\right)\frac{\partial \varphi}{\partial \zeta} = 0. \end{gathered} \tag{3.4}$$

The last of the equations (3.4) breaks up into two equations:

$$2c\varphi + m\frac{\partial \psi}{\partial \eta} = 0, \tag{3.5}$$

$$\frac{\partial \varphi}{\partial \zeta} = 0. \tag{3.6}$$

It is evident that when $c \neq 0$, the equation (3.5) taken together with the first equation of (3.4) yields the known solution (2.5). In view of (3.2) and (3.3), this solution exists for

$$\left| -\frac{k+b}{m}\eta \right| < \zeta^*. \tag{3.7}$$

From Eq. (3.6) we also obtain

$$\varphi(\zeta) = \pm\bar{\xi}. \tag{3.8}$$

Then the first of the equations (3.4) becomes an ordinary differential equation for the functional ψ with the solution

$$\psi(\eta) = -\frac{a}{2b}\eta^2 + \frac{2am\bar{\xi}}{b^3}\eta - \frac{am^2 + cb^2}{b^3}\bar{\xi}^2 \ln|-(b\eta + m\bar{\xi})| + D. \tag{3.9}$$

* No specific form of the function $\varphi(\zeta)$ for $|\zeta| < \zeta^*$ is given, since it is not necessary in the present considerations.

For the purpose of analytical design, the expression for the functional (3.9) will be needed only to check on its continuity everywhere in $\overline{N}$. Before doing this, however, we write the control equation

$$\xi = \begin{cases} +\bar{\xi} & \text{for} \quad -\frac{k+b}{m}\eta \geqslant \bar{\xi}, \\ -\frac{k+b}{m}\eta & \text{for} \quad \left|-\frac{k+b}{m}\eta\right| < \bar{\xi}, \\ -\bar{\xi} & \text{for} \quad -\frac{k+b}{m}\eta \leqslant -\bar{\xi}. \end{cases} \tag{3.10}$$

We now assume that the initial deviation η_0 is sufficiently great in absolute value and that the system starts at the boundary of the region $\overline{N}$. We further assume that the system is stable [15]. The expression for the function in this case is obtained from the formula (3.9), where D is an arbitrary constant. Then the functional ψ is a bounded, continuous function of η, since the expression $b\eta = m\bar{\xi}$ is nowhere zero on the boundary. For $|\eta| = |m/(k+b)|\,\bar{\xi}$, the function $\psi(\eta)$ of (2.7) must take the same value as the function $\psi(\eta)$ of (3.9). This can always be arranged by the proper choice of the constants D and B.

The solution (3.10), although it is the same as the solution obtained in [15] by using the calculus of variations, is interesting because it was obtained by applying a nonlinear transformation of the form (3.3) which avoided the essential difficulties involved in investigating the functional equations, connected with the impossibility of differentiating the expression (1.6) with respect to $v = \xi$ for $\xi = \bar{\xi}$.

4. An nth Order Object of Control

Case of an open region. We consider the general case in which the disturbed motion of the object of control is given by the equations

$$\dot{\eta}_k = \sum_\alpha b_{k\alpha}\eta_\alpha + m_k\xi \qquad (k = 1, \ldots, n), \qquad \eta_k(0) = \eta_{k0} \tag{4.1}$$

and it is desired to find the function ξ minimizing the functional

$$I(\xi) = \int_0^\infty V dt, \tag{4.2}$$

where

$$V = \sum_k a_k\eta_k^2 + c\xi^2 \tag{4.3}$$

is a positive definite quadratic form.

The functional is to be minimized in the class of functions C_1.

The basic functional equation of Bellman has the form

$$\psi(\eta_{k0}) = \min_\xi \left\{ \int_0^S V dt + \psi[\eta_k(S)] \right\}. \tag{4.4}$$

When we take the limit when $S \to 0$, we obtain

$$0 = V + \sum_k \left(\sum_\alpha b_{k\alpha}\eta_\alpha + m_k\xi \right) \frac{\partial\psi}{\partial\eta_k}. \tag{4.5}$$

Since the function ξ must make the expression on the right-hand side of (4.5) a minimum,

$$2c\xi + \sum_k m_k \frac{\partial\psi}{\partial\eta_k} = 0. \tag{4.6}$$

The function ψ must therefore satisfy the partial differential equation (4.5), where the integral $\dot{\psi}$ must be chosen so that it satisfies the relation (4.6).

In order to find such an integral, we simplify Eq. (4.5) by using the equality (4.6). As a result we obtain

$$\sum_k a_k \eta_k^2 + \sum_k \sum_\alpha b_{k\alpha} \eta_\alpha \frac{\partial \psi}{\partial \eta_k} = \frac{1}{4c} \left(\sum_k m_k \frac{\partial \psi}{\partial \eta_k} \right)^2. \tag{4.7}$$

The solution of this nonlinear partial differential equation must be sought in the form of a quadratic form in the variables η_k:

$$\psi = \sum_k \sum_\alpha A_{k\alpha} \eta_k \eta_\alpha. \tag{4.8}$$

Here $A_{k\alpha}$ are completely definite numbers which can be found by comparing coefficients after the substitution of the expression (4.8) in the equation (4.7). The substitution of the expression (4.8) in (4.6) gives the equation of a perfect control with a fixed negative feedback [14].

$$\xi = \sum_\alpha p_\alpha \eta_\alpha. \tag{4.9}$$

We will show that (4.9) is the same equation for a perfect control (3.7) obtained in [14]. With this aim in view, we consider the equations (4.5) and (4.6). We will denote the right hand side of Eq. (4.5) by U. Taking (4.9) into account, we must assume that

$$U = U(\eta_1, \ldots, \eta_n) = 0. \tag{4.10}$$

Hence

$$dU = \sum_k \frac{\partial U}{\partial \eta_k} d\eta_k. \tag{4.11}$$

Since the equations (4.1) and (4.9) determine a system of independent solutions η_k, then (4.11) will be satisfied only when the equations

$$\frac{\partial U}{\partial \eta_k} = 0 \qquad (k = 1, \ldots, n). \tag{4.12}$$

are satisfied.

We now use the notation

$$\lambda_k = -\frac{\partial \psi}{\partial \eta_k} \qquad (k = 1, \ldots, n) \tag{4.13}$$

and write the equations (4.12) as

$$2a_k \eta_k - \sum_\alpha b_{\alpha k} \lambda_\alpha - \left(\sum_\alpha b_{k\alpha} \eta + m_k \xi \right) \frac{\partial \lambda_k}{\partial \eta_k} = 0.$$

But from (4.1),

$$\left(\sum_\alpha b_{k\alpha} \eta_\alpha + m_k \xi \right) \frac{\partial \lambda_k}{\partial \eta_k} = \dot{\lambda}_k,$$

and so along with (4.6) we obtain

$$\dot{\lambda}_k = -\sum_a b_{ak}\lambda_a + 2a_k\eta_k,$$
$$0 = 2c\xi - \sum_k m_k\lambda_k \qquad (k = 1, \ldots, n). \tag{4.14}$$

It follows from what has been said that the system of equations (4.14) is equivalent to the system (4.5), (4.6). But the equations (4.14) together with (4.1) are the equations of the variational problem of Lagrange, solved in sections 2 and 3 of the work [14]. The conclusions drawn concerning Eq. (4.9) follow from this. A second, no less important conclusion can now be drawn. Namely, as was shown in [14], the equations (4.1), (4.9) describe a stable control system having a control function that optimizes the functional (4.2) in all nonspecial cases as noted in [14].*

Case of a Closed Region. We again turn to the equations (4.1) and (4.2), and assume that the coordinate ξ is restricted by the inequality (3.1) and that the functional (4.2) is minimized in the class of functions C. If we repeat the reasoning in part 3, we obtain the basic functional equation in the form

$$V + \sum_k \left(\sum_a b_{ka}\eta_a + m_k\varphi\right)\frac{\partial\psi}{\partial\eta_k} = 0,$$
$$\left(2c\varphi + \sum_k m_k\frac{\partial\psi}{\partial\eta_k}\right)\frac{\partial\varphi}{\partial\zeta} = 0. \tag{4.15}$$

As before, we obtain two solutions; the first coincides with the solution (4.9) for the points $|\sum p_a\eta_a| < \bar{\xi}$, the second solution $\varphi = \pm\bar{\xi}$ exists for points $|\sum p_a\eta_a| \geq \bar{\xi}$. In order to check that in both cases the first equation of (4.15) defines a continuous functional, it is necessary, in addition to the solution (4.8), to find the solution of the partial differential equation

$$\sum_k a_k\eta_k^2 + c\bar{\xi}^2 + \sum_k\left(\sum_a b_{ka}\eta + m_k\bar{\xi}\right)\frac{\partial\psi}{\partial\eta_k} = 0. \tag{4.16}$$

We will, however, not consider this further.

It is obvious, from comparison, that the dynamic-programming method yields the same result as was obtained in [14, 15] by the methods of calculus of variations with the application of the functional (4.2). This makes it possible to obtain directly the law of control in the form in which it is usually realized with a known selection of sensing elements, transformations, amplifiers, and servomotors.

5. The Case of a Limited Servomotor Velocity

In this case (see [15]), addition to the equations (4.1), we must use the equation

$$\dot{\xi} = f(\sigma), \quad |f(\sigma)| < \bar{f}, \quad \xi(0) = \xi_0, \tag{5.1}$$

where $f(\sigma)$ is a function of the class A [16]. The function $f(\sigma)$ and its argument $\sigma(\eta_1, \ldots, \eta_n, \xi)$ must be chosen to minimize the functional

$$I = \int_0^\infty (V + \alpha\dot{\xi}^2)\,dt \tag{5.2}$$

in the class C of functions of η_1, η_n, and ξ.

*In this connection, see [5, 18].

Reasoning similar to that used above leads to the Bellman equations

$$V + \alpha f^2 + f\frac{\partial \psi}{\partial \xi} + \sum_k \Big(\sum_\alpha b_{k\alpha}\eta_\alpha + m_k\xi\Big)\frac{\partial \psi}{\partial \eta_k} = 0,$$
$$\Big(2\alpha f + \frac{\partial \psi}{\partial \xi}\Big)\frac{\partial f}{\partial \sigma} = 0. \tag{5.3}$$

The desired solution consists of two parts. The first part is determined by the limitations imposed on the velocity, and is obtained from the condition $\partial f/d\sigma = 0$. This means that

$$f(\sigma) = \pm \bar{f}, \quad |\sigma| \geqslant \sigma^*, \tag{5.4}$$

where σ^* is a positive number.

For obtaining the second part of the solution, we have

$$f(\sigma) = -\frac{1}{2\alpha}\frac{\partial \psi}{\partial \xi}, \quad |\sigma| < \sigma^*. \tag{5.5}$$

In combination with the first equation of (5.3), this yields the partial differential equation

$$V + \sum_k \Big(\sum_\alpha b_{k\alpha}\eta_\alpha + m_k\xi\Big)\frac{\partial \psi}{\partial \eta_k} = \frac{1}{4\alpha}\Big(\frac{\partial \psi}{\partial \xi}\Big)^2. \tag{5.6}$$

which can be satisfied by the function

$$\psi = \sum_k \sum_\alpha A_{k\alpha}\eta_k\eta_\alpha + \xi\sum_\alpha B_\alpha\eta_\alpha + R\xi^2. \tag{5.7}$$

The coefficients of the form (5.7) are obtained by the method already described. The equality (5.5) yields a linear function $f(\sigma)$ for $|\sigma| < \sigma^*$, i.e.,

$$f(\sigma) = h\sigma, \quad \sigma = -\frac{1}{2h\alpha}\Big(\sum_k B_k\eta_k + 2R\xi\Big). \tag{5.8}$$

The quantity σ^* is obtained from the condition $h\sigma^* = \bar{f}$.

As in the previous case, we can show that this solution of the problem coincides with the solution obtained in [15].

6. An Example

As an example, we will consider the problem of an aircraft flying at a specified height. With certain assumptions concerning the rate of damping of natural oscillations of the plane relative to its transverse axis, the equations for the disturbed motion can be written as

$$\begin{aligned} \dot{\eta}_1 &= b_{11}\eta_1 + b_{12}\eta_2 + m_1\xi, \\ \dot{\eta}_2 &= b_{21}\eta_1 + b_{22}\eta_2 + m_2\xi, \\ \dot{\eta}_3 &= \eta_1. \end{aligned} \tag{6.1}$$

The coefficients of the equations are given in terms of the initial parameters of the aircraft by the relations [17]

$$b_{11} = -c_{xc}, \quad b_{12} = 2k_2c_{yc}, \quad m_1 = -\rho c_{yc}^{\alpha}, \quad \tau = \frac{2m}{\rho SV},$$
$$b_{21} = -c_{yc}, \quad b_{22} = -2k_1c_{xc}, \quad m_2 = \rho c_{xc}^{\alpha}, \quad \rho = \frac{m_z^{\delta_b}}{m_z^{\alpha}}. \tag{6.2}$$

Here τ is a parameter of the aircraft. In the equations (6.1), η_1 is the inclination of the trajectory, η_2 a dimensionless velocity disturbance, and η_3 a dimensionless disturbance of the height.

The optimizing functional is given by the integral

$$I(\xi) = \int_0^\infty (\eta_3^2 + c\xi^2)\, dt. \tag{6.3}$$

The basic equation for the determination of the functional is

$$\eta_3^2 (b_{11}\eta_1 + b_{12}\eta_2)\frac{\partial \psi}{\partial \eta_1} + (b_{21}\eta_1 + b_{22}\eta_2)\frac{\partial \psi}{\partial \eta_2} + \eta_1 \frac{\partial \psi}{\partial \eta_3} = \frac{1}{4c}\left[m_1 \frac{\partial \psi}{\partial \eta_1} + m_2 \frac{\partial \psi}{\partial \eta_2}\right]^2. \tag{6.4}$$

and the solution of this equation will be sought in the form

$$\psi = \sum_k \sum_\alpha A_{k\alpha}\eta_k \eta_\alpha \qquad (k,\ \alpha = 1,\ 2,\ 3). \tag{6.5}$$

The equations for determining the coefficients are

$$\begin{gathered}
b_{11}A_{11} + b_{21}A_{12} + A_{13} = \frac{1}{2c}(m_1A_{11} + m_2A_{12})^2, \\
b_{12}A_{12} + b_{22}A_{23} = \frac{1}{2c}(m_1A_{13} + m_2A_{23})^2, \\
c = (m_1A_{13} + m_2A_{23})^2, \\
b_{12}A_{11} + (b_{22} + b_{11})A_{12} + b_{21}A_{22} + A_{23} = \frac{1}{c}[m_1^2A_{11}A_{12} + m_2^2A_{12}A_{22} + m_1m_2(A_{11}A_{22} + A_{12}^2)], \\
b_{11}A_{13} + b_{21}A_{23} + A_{33} = \frac{1}{c}[m_1^2A_{11}A_{13} + m_2^2A_{13}A_{23} + m_1m_2(A_{11}A_{23} + A_{13}A_{13})], \\
b_{12}A_{13} + b_{22}A_{23} = \frac{1}{c}[m_1^2A_{13}A_{13} + m_2^2A_{23}A_{23} + m_1m_2(A_{12}A_{23} + A_{13}A_{23})].
\end{gathered} \tag{6.6}$$

The equations (6.6) can be solved by the method of successive approximations, and as a result we obtain

$$\xi = -\frac{1}{c}[(m_1A_{11} + m_2A_{21})\eta_1 + (m_1A_{12} + m_2A_{23})\eta_2 + (m_1A_{13} + m_2A_{23})\eta_3]. \tag{6.7}$$

7. A Relation between Dynamic Programming and Lyapunov's Functions

In a discussion of the contents of the articles [14, 15], N. N. Krasovskii drew my attention to the fact that the functional (4.2), interpreted in these articles as an integral square error, can be considered as a Lyapunov function. N. N. Krasovskii pointed out this relation between Lyapunov functions and optimal systems in [7] and also in [18, 19]. R. E. Kalman noted it later in [13, 20].

We will show here that the relation of Lyapunov functions to the problem of optimizing the integral square error arises naturally from the formulas in section 4. Actually, using (4.9), we will calculate the total derivative of the function ψ defined in (4.8). This function must be positive everywhere that $\Sigma\eta_k^2 \neq 0$. It will have a meaning when the system (4.1) and (4.9) is stable.

Then the basic functional equation (4.5) becomes the partial differential equation we have used for constructing a Lyapunov function with a total derivative given by the formula

$$\frac{d\psi}{dt} = -V, \tag{7.1}$$

so that the functional ψ is the Lyapunov function for our problem. Conversely, we assume that by applying dynamic-programming methods we have found tha functional ψ (4.8). If there is some way of verifying that the function ψ is positive everywhere for $\Sigma\eta_k^2 \neq 0$, then it is a Lyapunov function for the problem. The condition that ψ be positive

is the stability criterion for the optimal system. This is of special interest, since the dynamic-programming method can be used to solve simultaneously both the problem of optimizing a system according to the criterion (4.2) and the problem of the stability of the optimal system. An optimal and stable system corresponds to a functional ψ that is positive for $\Sigma\eta_k^2 \neq 0$.

This latter fact is especially important in the case when the system to be optimized is nonlinear

$$\dot{\eta}_k = \Xi_k(\eta_1, \ldots, \eta_n, \xi). \tag{7.2}$$

In this case the basic functional equation will be

$$0 = V + \sum_k \Xi_k(\eta_1, \ldots, \eta_n, \xi)\frac{\partial\psi}{\partial\eta_k} \tag{7.3}$$

and the relation (7.1) remains valid.

The author wishes to thank E. A. Barbashin and N. N. Krasovskii sincerely for their very useful advice and comments.

LITERATURE CITED

1. V. G. Boltyanskii, R. V. Gamkrelidze, and L. S. Pontryagin, "The optimal processes," Dokl. Akad. Nauk SSSR, 110, 1 (1956).
2. R. V. Gamkrelidze, "The theory of optimal processes in linear systems. The theory of optimal processes," Izv. Akad. Nauk SSSR, ser. matem., 24, 1 (1960); Dokl. Akad. Nauk SSSR, 116, 1 (1957). "The theory of processes in linear systems, optimal with respect to rate of action," Izv. Akad. Nauk SSSR, ser. matem., 22 (1958).
3. V. G. Boltyanskii, "The maximum principle in the theory of optimal processes," Doklady Akad. Nauk SSSR, 119, 6 (1958).
4. R. V. Gamkrelidze, "Processes for bounded phase coordinates, optimal with respect to rate of action," Doklady Akad. Nauk SSSR, 125, 3 (1959).
5. N. N. Krasovskii, "The theory of optimal control," Avtomatika i telemekhanika, 18, 11 (1957).*
6. N. N. Krasovskii, "A problem in optimal control," Prikl. matem. i mekh., 21, 5 (1957).
7. N. N. Krasovskii, "A problem in optimal control," Prikl. matem. i mekh., 23, 1 (1959).
8. R. E. Bellman, J. Glicksberg, and O. A. Gross, Some Aspects of the Mathematical Theory of Control Processes. Report No. 313, 1959, RAND Corporation.
9. I. P. LaSall, Time Optimal Control Systems. Proc. National Ac. Sci., vol. 45, No. 4, 1958.
10. Ya. P. Roitenberg, "Some problems in dynamic programming," Prikl. matem. i mekh., 23, 4 (1959).
11. R. Kulikowski, Bulletin de L'Academie Polonaise des Sciences, vol. VII, No. 4, 1959; vol. VII, No. 6, 1959; vol. VII, No. 11, 1959; vol. VII, No. 12, 1959; vol. VIII, No. 4, 1960.
12. C. A. Desoer, The Bong–Bong Servo Problem, Treated by Variational Technique Information and Control, vol. 2, 1959.
13. R. E. Kalman and T. E. Bertram, Control System Analysis and Design Via the Second Method of Lyapunof. Journal of Basic Engineering, June, 1960.
14. A. M. Letov, "Analytical design of control systems," I, Avtomatika i telemekhanika, 21, 4 (1960).*
15. A. M. Letov, "Analytical design of control systems," II and III, Avtomatika i telemekhanika, 21, 5 and 6 (1960).*
16. A. M. Letov, The Stability of Nonlinear Control Systems [in Russian] State Technical Press (1955).
17. I. V. Ostoslavskii and G. O. Kalachev, The Longitudinal Stability of Aircraft [in Russian], Oborongiz (1951).
18. N. N. Krasovskii, "The calculation of optimal control by direct methods," Prikl. matem. i mekh., 2 (1960).
19. N. N. Krasovskii, "The choice of parameters for optimal stable systems," Doklady na Pervom kongresse IFAK (1960).
20. R. E. Kalman, "The general theory of control systems," Doklady na Pervom Kongresse IFAK (1960).

* Original Russian Pagination. See C. B. translation.

ON NEW STABILITY INEQUALITIES

I. S. Arzhanykh

(Tashkent)

Translated from Avtomatika i Telemekhanika, Vol. 22, No. 4,
pp. 436-442, April, 1961
Original article submitted October 25, 1960

New inequalities based on Shur's theorem are given; these are useful in the analysis of the stability of systems described by differential equations with constant or periodic coefficients.

Suppose the variational equations

$$\frac{d\xi_s}{dt} = \sum_{r=1}^{n} p_{sr}\xi_r \quad (s = 1, 2, \ldots, n) \tag{1}$$

ive constant or periodically varying coefficients. Then, as is known, the question of asymptotic stability may be solved by inequalities guaranteeing that the roots of the characteristic equation are distributed in the left half-plane or in the unit circle, respectively. With the help of a linear fractional transformation with real coefficients one may transform the left half-plane onto the unit circle and thus consider in both cases the question of whether the roots lie inside this circle. The criterion that the roots of the characteristic equation lie in the left half-plane is given by the Raus-Hurwitz inequalities. However this criterion is very inconvenient in application, since it is first necessary to write the equation in clear polynomial form, and then, from the coefficients of this polynomial, form the Hurwitz determinant. The question naturally arises: Is it possible to obtain an equivalent inequality without first reducing the equations to polynomial form?

A positive answer to this question is given in the present note. We shall seek inequalities guaranteeing that the roots be distributed inside the unit circle, and at the end we shall indicate the slight changes necessary in order to obtain inequalities guaranteeing that they lie in the left half-plane.

Thus suppose the characteristic equation has the form

$$f(x) \equiv c_0x^n + c_1x^{n-1} + \cdots + c_{n-1}x + c_n \equiv$$

$$\equiv [Ax + B] \equiv \begin{vmatrix} a_{11}x + b_{11}, \ldots, a_{1n}x + b_{1n} \\ \cdots\cdots\cdots\cdots\cdots \\ a_{n1}x + b_{n1}, \ldots, a_{nn}x + b_{nn} \end{vmatrix} = 0. \tag{2}$$

According to Shur's theorem [1] the necessary and sufficient conditions for the roots of equation (2) to lie inside the unit circle consist in the satisfaction of the inequality

$$|c_0| > |c_n| \tag{3}$$

and the condition that the polynomial

$$f_1(x) \equiv c_0^{(1)}x^{n-1} + \ldots + c_{n-1}^{(1)}, \tag{4}$$

defined by the equation

$$xf_1(x) \equiv c_0f(x) - c_nf^*(x), \tag{5}$$

where

$$f^*(x) = x^nf\left(\frac{1}{x}\right), \tag{6}$$

possess the same property.

Using these algorithmic rules, it is easy to construct stability inequalities without writing out f(x) explicitly. We have

$$f^*(x) = [A + Bx], \tag{7}$$

$$c_0 = [A + Bx]_{x=0} \equiv (a^n) \equiv \begin{vmatrix} a_{11}, \ldots, a_{1n} \\ \cdots\cdots\cdots \\ a_{n1}, \ldots, a_{nn} \end{vmatrix}, \tag{8}$$

$$c_n = [Ax + B] = (b^n). \tag{9}$$

We calculate $f_1(x)$ by the formula

$$xf_1(x) = c_0[Ax + B] - c_n[A + Bx]$$

and $f^*(x)$ by the formula

$$f_1^*(x) = x^{n-1} f_1\left(\frac{1}{x}\right) = x^{n-1}\left\{\left(\frac{1}{x}\right)^{-1}\left(c_0\left[A\frac{1}{x} + B\right] - c_n\left[A + B\frac{1}{x}\right]\right)\right\} =$$
$$= c_0[A + Bx] - c_n[Ax + B].$$

Suppose

$$f_1(x) = \frac{1}{x}(c_0[Ax + B] - c_n[A + Bx]) \equiv c_0^{(1)}x^{n-1} + \ldots + c_{n-1}^{(1)},$$
$$f_1^*(x) = c_0^{(1)} + \ldots + c_{n-1}^{(1)}x^{n-1}.$$

Then

$$c_0^{(1)} = \lim_{x\to 0} f_1^*(x) = c_0[A] - c_n[B] = c_0(a^n) - c_n(b^n) = c_0^2 - c_n^2, \tag{10}$$

$$c_{n-1}^{(1)} = \lim_{x\to 0} f_1(x) = \left\{\frac{d}{dx}(c_0[Ax + B] - c_n[A + Bx])\right\}_{x=0}.$$

Denoting

$$[Ax + B] = [ax + b,\ ax + b, \ldots,\ ax + b], \tag{11}$$

$$[A + Bx] = [a + bx,\ a + bx, \ldots,\ a + bx],$$

we find

$$c_{n-1}^{(1)} = c_0([a,\ b, \ldots,\ b] + [b,\ a, \ldots,\ b] + \ldots + [b,\ b, \ldots,\ a]) -$$
$$- c_n([b,\ a, \ldots,\ a] + [a,\ b, \ldots,\ a] + \ldots + [a,\ a, \ldots,\ b]) \equiv \tag{12}$$
$$\equiv c_0(ab^{n-1}) - c_n(ba^{n-1}).$$

After this we calculate

$$f_2(x) \equiv c_0^{(2)}x^{n-2} + \ldots + c_{n-2}^{(2)} = \frac{1}{x}\{c_0^{(1)}f_1(x) - c_{n-1}^{(1)}f_1^*(x)\} =$$
$$= \frac{1}{x}\left\{c_0^{(1)}\frac{1}{x}(c_0[Ax + B] - c_n[A + Bx]) - c_{n-1}^{(1)}(c_0[A + Bx] - c_n[Ax + B])\right\}$$

or

$$x^2 f_2(x) = [Ax + B]\,p_1(x) - [A + Bx]\,q_1(x). \tag{13}$$

where

$$p_1(x) = c_0^{(1)}p_0 + c_{n-1}^{(1)}xq_0^*, \tag{14}$$
$$q_1(x) = c_0^{(1)}q_0 + c_{n-1}^{(1)}xp^*,$$

$$p_0 = (a^n),\ q_0 = (b^n). \tag{15}$$

We show that the formula

$$x^k f_k(x) = [Ax + B]\, p_{k-1}(x) - [A + Bx]\, q_{k-1}(x), \tag{16}$$

holds, where

$$\begin{aligned} p_k(x) &= c_0^{(k)} p_{k-1}(x) + c_{n-k}^{(k)} x q_{k-1}^*(x), \\ q_k(x) &= c_0^{(k)} q_{k-1}(x) + c_{n-k}^{(k)} x p_{k-1}^*(x) \end{aligned} \tag{17}$$

for all values of $k = 1, 2, \ldots, n-1$. With this goal we compute

$$\begin{aligned} f_k^*(x) &= x^{n-k}\left\{\left(\frac{1}{x^k}\right)^{-1}\left(\left[A\frac{1}{x} + B\right] p_{k-1}\left(\frac{1}{x}\right) - \left[A + B\frac{1}{x}\right] q_{k-1}\left(\frac{1}{x}\right)\right)\right\} = \\ &= [A + Bx]\, p_{k-1}\left(\frac{1}{x}\right) - [Ax + B]\, q_{k-1}\left(\frac{1}{x}\right) \end{aligned}$$

and form the expression

$$\begin{aligned} x f_{k+1}(x) &\equiv c_0^{(k)} f_k(x) - c_{n-k}^{(k)} f_k^*(x) = \\ &= c_0^{(k)} \frac{1}{x^k}\{[Ax + B]\, p_{k-1}(x) - [A + Bx]\, q_{k-1}(x)\} - \\ &- c_{n-k}^{(k)}\left\{[A + Bx]\, p_{k-1}\left(\frac{1}{x}\right) - [Ax + B]\, q_{k-1}\left(\frac{1}{x}\right)\right\}. \end{aligned}$$

From this we find

$$\begin{aligned} x^{k+1} f_{k+1}(x) &= [Ax + B]\left(c_0^{(k)} p_{k-1}(x) + c_{n-k}^{(k)} x^{k-1} q_{k-}\left(\frac{1}{x}\right) x\right) - \\ &- [A + Bx]\left(c_0^{(k)} q_{k-1}(x) + c_{n-k}^{(k)} x^{k-1} p_{k-1}\left(\frac{1}{x}\right) x\right) \equiv \\ &\equiv [Ax + B]\, p_k(x) - [A + Bx]\, q_k(x), \end{aligned} \tag{18}$$

where the polynomials p_k and q_k are determined by formulas (17). For $k = 1$ the formulas (16) and (17) have the form (13), (14), and (15). We extend by induction formulas (16) and (17) to all values of $k = 1, 2, \ldots, n-1$. Suppose

$$f_k(x) \equiv c_0^{(k)} x^{n-k} + \cdots + c_{n-k}^{(k)}. \tag{19}$$

Then we have

$$c_{n-k}^{(k)} = \lim_{x \to 0} f_k(x) = \frac{1}{k!}\left\{\frac{d^k}{dx^k}([Ax + B]\, p_{k-1}(x) - [A + Bx]\, q_{k-1}(x))\right\}_{x=0}. \tag{20}$$

Moreover,

$$f_k^*(x) \equiv c_0^{(k)} + \cdots + c_{n-k}^{(k)} x^{n-k}, \tag{21}$$

$$x^{k-1} f_k^*(x) \equiv [A + Bx]\, p_{k-1}^*(x) - [Ax + B]\, q_{k-1}^*(x). \tag{22}$$

Consequently,

$$c_0^{(k)} = \lim_{x \to 0} f_k^*(x) = \frac{1}{(k-1)!}\left\{\frac{d^{k-1}}{dx^{k-1}}([A + Bx]\, p_{k-1}^*(x) - [Ax + B]\, q_{k-1}^*(x))\right\}_{x=0}. \tag{23}$$

Thus we obtain the following theorem.

Theorem. Necessary and sufficient conditions that the roots of equation (2) lie inside the unit circle are that the following inequalities be satisfied:

$$|c_0| > |c_n|, \tag{24}$$

$$|c_0^{(k)}| > |c_{n-k}^{(k)}| \quad (k = 1, 2, \ldots, n-1), \tag{25}$$

where the numbers $c_0^{(k)}$ and $c_{n-k}^{(k)}$ are defined by formulas (20) and (23), and the polynomials p_i and q_i are calculated recursively according to formulas (15) and (17).

We examine the application of the theorem to the cases n = 2 and n = 3. For n = 2 we have:

$$[Ax+B]=[ax+b,\ ax+b],\quad [A+Bx]=[a+bx,\ a+bx].$$
$$c_0=[a,\ a]=(a^2),\quad c_2=[b,\ b]=(b^2),\quad c_0^{(1)}=c_0^2-c_2^2,$$
$$c_1^{(1)}=\left\{\frac{d}{dx}(c_0[Ax+B]-c_2[A+Bx])\right\}_{x=0}=$$
$$=c_0([ab]+[ba])-c_2([ba]+[ab])=(c_0-c_2)(ab).$$

The stability condition is

$$|c_0|>|c_2|,\quad |c_0^{(1)}|>|c_1^{(1)}|.$$

By way of a numerical example we consider the equation

$$f(x)\equiv[Ax+B]=0,$$
$$a_{11}=1,\quad a_{12}=\alpha,\quad b_{11}=\beta,\quad b_{12}=-1,$$
$$a_{21}=-\alpha,\quad a_{22}=1,\quad b_{21}=1,\quad b_{22}=\beta.$$

For the roots to lie inside the unit circle it is necessary and sufficient that the inequalities

$$|c_0|>|c_2|,\quad |c_0^{(1)}|>|c_1^{(1)}|,$$
$$c_0=(a^2)=\begin{vmatrix}1, & \alpha\\ -\alpha, & 1\end{vmatrix}=1+\alpha^2,\quad c_2=(b^2)=\begin{vmatrix}\beta, & -1\\ 1, & \beta\end{vmatrix}=\beta^2+1,$$
$$c_0^{(1)}=c_0^2-c_2^2=(\alpha^2-\beta^2)(\alpha^2+\beta^2+2),$$
$$c_1^{(1)}=(c_0-c_2)(ab)=(\alpha^2-\beta^2)\left(\begin{vmatrix}1, & -1\\ -\alpha, & \beta\end{vmatrix}+\begin{vmatrix}\beta, & \alpha\\ 1, & 1\end{vmatrix}\right)=2(\alpha^2-\beta^2)(\beta-\alpha).$$

be satisfied.

Consequently, one should have

$$|\alpha|>|\beta|,\qquad \alpha^2+\beta^2+2>2|\beta-\alpha|.$$

For n = 3 we have

$$c_0=(a^3),\quad c_3=(b^3),\quad c_0^{(1)}=c_0^2-c_3^2,\quad c_2^{(1)}=c_0(ab)^2-c_3(a^2b),$$
$$c_0^{(2)}=(c_0^{(1)})^2-(c_2^{(1)})^2,\quad c_1^{(2)}=(c_0^{(1)}-c_2^{(1)})(c_0(a^2b)-c_3(ab^2)).$$

The stability inequalities have the form:

$$|c_0|>|c_3|,\quad |c_0^{(1)}|>|c_2^{(1)}|,\quad |c_0^{(2)}|>|c_1^{(2)}|.$$

If the variational equations (1) have constant coefficients, then it is necessary to transform the λ-plane into the x-plane so that the left half-plane is mapped onto the unit circle of the x-plane. This is accomplished by the substitution $x=(1+\lambda)/(1-\lambda)$, as a result of which the equation

$$\begin{vmatrix}p_{11}-\lambda, & p_{12}, & \dots, & p_{1n}\\ p_{21}, & p_{22}-\lambda, & \dots, & p_{2n}\\ \dots & \dots & \dots & \dots\\ p_{n1}, & p_{n2}, & \dots, & p_{nn}-\lambda\end{vmatrix}=0$$

goes into equation (2), where

$$A=(p_{rs}-\delta_{rs}),\quad B=(p_{rs}+\delta_{rs})$$

(δ_{rs} is the Kronecker symbol).

In those cases then the system of variational equations consists of equations of order higher than the first, by the introduction of new unknowns it may be brought into the form of a system in which each equation is of order one; then the inequalities indicated may be applied. But such a case may be investigated directly by computing the Shur polynomial in the above manner. We examine, for example, the variational equations of the form

$$a_{11}\ddot{\xi}_1 + a_{12}\ddot{\xi}_2 + b_{11}\dot{\xi}_1 + b_{12}\dot{\xi}_2 + c_{11}\xi_1 + c_{12}\xi_2 = 0,$$
$$a_{21}\ddot{\xi}_1 + a_{22}\ddot{\xi}_2 + b_{21}\dot{\xi}_1 + b_{22}\dot{\xi}_2 + c_{21}\xi_1 + c_{22}\xi_2 = 0$$

with constant coefficients. The characteristic equation will be

$$\begin{vmatrix} \lambda^2 a_{11} + \lambda b_{11} + c_{11}, & \lambda^2 a_{12} + \lambda b_{12} + c_{12} \\ \lambda^2 a_{21} + \lambda b_{21} + c_{21}, & \lambda^2 a_{22} + \lambda b_{22} + c_{22} \end{vmatrix} = 0.$$

We transform the left half-plane (Re $\lambda < 0$) onto the unit circle ($|x| < 1$) by the substitution

$$\lambda = \frac{x-1}{x+1}.$$

We examine the characteristic polynomial

$$\Delta(x) \equiv \begin{vmatrix} x^2\alpha_{11} + x\beta_{11} + \gamma_{11}, & x^2\alpha_{12} + x\beta_{12} + \gamma_{12} \\ x^2\alpha_{21} + x\beta_{21} + \gamma_{21}, & x^2\alpha_{22} + x\beta_{22} + \gamma_{22} \end{vmatrix} \equiv [x^2\alpha + x\beta + \gamma],$$

where

$$\alpha_{ik} = a_{ik} + b_{ik} + c_{ik}, \quad \beta_{ik} = 2(c_{ik} - a_{ik}), \quad \gamma_{ik} = a_{ik} - b_{ik} + c_{ik}.$$

The roots of the equation $\Delta(x) = 0$ should lie in the unit circle. To apply Shur's algorithmic rule it is necessary to compute the coefficients $c_0, c_4, c_0^{(1)}, c_3^{(1)}, c_0^{(2)}, c_2^{(2)}, c_0^{(3)}, c_1^{(3)}$. We have:

$$c_4 = (\gamma^2) \equiv \begin{vmatrix} \gamma_{11}\gamma_{12} \\ \gamma_{21}\gamma_{22} \end{vmatrix}, \qquad c_0 = (\alpha^2) \equiv \begin{vmatrix} \alpha_{11}\alpha_{12} \\ \alpha_{21}\alpha_{22} \end{vmatrix}.$$

Then we compute the third degree polynomial $\Delta_1(x)$ by the formula

$$x\Delta_1(x) = c_0\Delta(x) - c_4\Delta^*(x) \equiv c_0[x^2\alpha + x\beta + \gamma] - c_4[\alpha + \beta x + x^2\gamma]$$

and find

$$c_3^{(1)} = \lim_{x\to 0} \Delta_1(x), \qquad c_0^{(1)} = \lim_{x\to\infty} \frac{\Delta_1(x)}{x^3},$$

or

$$c_3^{(1)} = \left\{\frac{d}{dx}(c_0[x^2\alpha + x\beta + \gamma] - c_4[\alpha + \beta x + \gamma x^2])\right\}_{x=0} =$$
$$= c_0(\beta\gamma) - c_4(\beta\alpha) \equiv c_0([\beta\gamma] + [\gamma\beta]) - c_4([\beta\gamma] + [\alpha\beta]) \equiv$$
$$\equiv c_0\left\{\begin{vmatrix} \beta_{11}\gamma_{12} \\ \beta_{21}\gamma_{22} \end{vmatrix} + \begin{vmatrix} \gamma_{11}\beta_{12} \\ \gamma_{21}\beta_{22} \end{vmatrix}\right\} - c_4\left\{\begin{vmatrix} \beta_{11}\alpha_{12} \\ \beta_{21}\alpha_{22} \end{vmatrix} + \begin{vmatrix} \alpha_{11}\beta_{12} \\ \alpha_{21}\beta_{22} \end{vmatrix}\right\},$$

$$c_0^{(1)} = \lim_{\varepsilon\to 0}\{c_0[\alpha + \varepsilon\beta + \varepsilon^2\gamma] - c_4[\varepsilon^2\alpha + \varepsilon\beta + \gamma]\} = c_0(\alpha^2) - c_4(\gamma^2) = c_0^2 - c_4^2.$$

The second degree polynomial $\Delta_2(x)$ is calculated by the formula

$$x\Delta_2(x) = c_0^{(1)}\Delta_1(x) - c_3^{(1)}\Delta_1^*(x) =$$
$$= c_0^{(1)}\frac{1}{x}\{c_0[x^2\alpha + x\beta + \gamma] - c_4[\alpha + \beta x + x^2\gamma]) -$$
$$- c_3^{(1)}x^3\left(\left(\frac{1}{x}\right)^{-1}\left\{c_0\left[\frac{1}{x^2}\alpha + \frac{1}{x}\beta + \gamma\right] - c_4\left[\alpha + \beta\frac{1}{x} + \frac{1}{x^2}\gamma\right]\right\}\right) =$$
$$= \frac{1}{x}\{[x^2\alpha + x\beta + \gamma](c_0c_0^{(1)} + xc_4c_3^{(1)}) - [\alpha + \beta x + \gamma x^2](c_4c_0^{(1)} + xc_0c_3^{(1)})\}.$$

From this we find

$$c_2^{(2)} = \lim_{x\to 0} \Delta_2(x) = \frac{1}{2!}\left\{\frac{d^2}{dx^2}\left([x^2\alpha + x\beta + \gamma]\, p_1(x) - [\alpha + \beta x + \gamma x^2]\, q_1(x)\right)\right\}_{x=0} =$$
$$= \{(\alpha\gamma) + (\beta^2)\}\, c_0 c_0^{(1)} + (\beta\gamma)\, c_4 c_3^{(1)} - \{(\gamma\alpha) + (\beta^2)\}\, c_4 c_0^{(1)} - (\beta\alpha)\, c_0 c_3^{(1)},$$

$$c_0^{(2)} = \lim_{x\to\infty} \frac{\Delta_2(x)}{x^2} = \lim_{\varepsilon\to 0}\left\{[\alpha + \beta\varepsilon + \gamma\varepsilon^2]\left(c_0 c_0^{(1)} + \frac{1}{\varepsilon} c_4 c_3^{(1)}\right) -\right.$$
$$\left. - [\alpha\varepsilon^2 + \beta\varepsilon + \gamma]\left(c_4 c_0^{(1)} + \frac{1}{\varepsilon} c_0 c_3^{(1)}\right)\right\}_{\varepsilon=0} =$$
$$= (\alpha\beta)\, c_4 c^{(1)} + (\alpha^{(2)})\, c_0 c_0^{(1)} - (\gamma\beta)\, c_0 c_3^{(1)} - (\gamma^2)\, c_4 c_0^{(1)} = (c_0^{(1)})^2 - (c_3^{(1)})^2.$$

Finally, we compute the first degree polynomial $\Delta_3(x)$ by the formula

$$x\Delta_3(x) = c_0^{(3)}\Delta_2(x) - c_2^{(3)}\Delta_2^*(x) = c_0^{(3)}\frac{1}{x^2}\{[x^2\alpha + x\beta + \gamma]\,(c_0 c_0^{(1)} + x c_4 c_3^{(1)}) -$$
$$- [\alpha + \beta x + \gamma x^2]\,(c_4 c_0^{(1)} + x c_0 c_3^{(1)})\} -$$
$$- c_2^{(3)} x^{(2)}\left(\frac{1}{x^2}\right)^{-1}\left\{\left[\frac{1}{x^2}\alpha + \frac{1}{x}\beta + \gamma\right]\left(c_0 c_0^{(1)} + \frac{1}{x} c_4 c_3^{(1)}\right) -\right.$$
$$\left. - \left[\alpha + \beta\frac{1}{x} + \gamma\frac{1}{x^2}\right]\left(c_4 c_0^{(1)} + \frac{1}{x} c_0 c_3^{(1)}\right)\right\} =$$
$$= \frac{1}{x^2}\{[x^2\alpha + x\beta + \gamma]\, p_2(x) - [\alpha + \beta x + \gamma x^2]\, q_2(x)\}.$$

After this we find

$$c^{(3)} = \lim_{x\to 0} \Delta_3(x) = \frac{1}{3!}\left\{\frac{d^3}{dx^3}(x^3\Delta_3)\right\}_{x=0} =$$
$$= 2\,[c_0^{(1)} c_0^{(2)}\,(c_0\,(\alpha\beta) - c_4\,(\gamma\beta)) + c_0^{(2)} c_3^{(1)}\,(c_4 - c_0)\,((\alpha\gamma) + (\beta^2)) +$$
$$+ c_0 c_0^{(1)} c_2^{(2)}\,((\gamma^2) - (\alpha^2))],$$

$$c_0^{(3)} = \lim_{x\to\infty} \frac{\Delta_3(x)}{x} = \lim_{\varepsilon\to 0}\left\{[\alpha + \beta\varepsilon + \gamma\varepsilon^2]\, p_2\left(\frac{1}{\varepsilon}\right) - [\alpha\varepsilon^2 + \beta\varepsilon + \gamma]\, q_2\left(\frac{1}{\varepsilon}\right)\right\} =$$
$$= c_0^{(1)} c_0^{(2)}\,(c_0(\alpha^2) - c_4\,(\gamma^2)) + c_4 c_3^{(1)}\,(c_0^{(2)} + c_2^{(2)})\,(\beta\alpha) - c_3^{(1)}\,(c_0 c_0^{(2)} + c_4 c_2^{(2)})\,(\beta\gamma).$$

The stability inequalities have the form:

$$|c_0| > |c_4|, \quad |c_0^{(1)}| > |c_3^{(1)}|, \quad |c_0^{(2)}| > |c_2^{(2)}|, \quad |c_0^{(3)}| > |c_1^{(3)}|.$$

LITERATURE CITED

1. M. Krein and M. Neimark, Symmetric and Hermite Form Methods in the Theory of Distribution of Roots of Algebraic Equations [in Russian]. Gos. nauchno-tekhnicheckoe isd-vo Ukrainy. Kharkov, 1936.

ON A CERTAIN METHOD FOR CORRECTING THE DYNAMIC PROPERTIES OF AUTOMATIC CONTROL SYSTEMS

V. S. Lerner

(Ust' Kamenogorsk)

Translated from Avtomatika i Telemekhanika Vol. 22, No. 4,
pp. 443-456, April, 1961
Original article submitted February 22, 1960

The paper studies a method for correcting automatic control systems which is based on changing the structure of the system as a function of the signs for the deviation of the controlled parameter before and after those control system elements whose properties are to be corrected. The method is analyzed using the example of a relay automatic control system developed by the author for controlling the electric power supplied to an ore furnace. A comparative theoretical and experimental investigation of the system is performed for the cases of correction and no correction.

1. Statement of the Problem. A reduction of the effect of noise in automatic control systems (ACS) in those cases where the useful signal has a spectrum that consists of lower frequencies than the noise is achieved by introducing a series filter [1]. However, when this is done the narrowing of the frequency band causes a reduction in the stability margin of the system, and the duration of the transient response increases. Varying the gain in such a system can often lead to a worsening of the static or dynamic properties. In relay ACS the introduction of such a filter reduces the number of switching operations [2] and therefore increases the operational reliability, but (as in other systems) it worsens their static or dynamic properties. This contradiction could be eliminated if we were able to design an ACS with a narrow frequency passband relative to the perturbation and a wide passband relative to the useful signal.

In this paper we show that this problem can be solved by modifying the structure of a relay ACS . For this purpose it is necessary to cut in a filter, depending on the signs of the quantities at the input and output of the filter. This can be achieved by means of a special corrective network. Such a system will have good dynamic and static properties for a minimum number of switching operations for the relay elements.

2. The Essence of the Correction Method. The idea for the correction method treated in this paper consists of the following. Assume that after introduction of the filter the transient response at the input of the ACS is characterized by decaying oscillations 1 (Fig. 1). The variation of the quantity at the output of the filter which is connected in series with the detector element has the response given by curve 2 under these conditions. This same ACS with no filter does not cut off the high-frequency component of the perturbation. Its transient response is characterized by the curve 1'. The problem of making the transient response 1 approximate 1' while simultaneously filtering the perturbations can be solved as follows.

We shall introduce a network which compares the signs of the quantities at the input and output of the filter but worsens the dynamic properties of the ACS. Assume that at instants when the sign of the ordinate of curve 1 changes relative to the sign of the ordinate for curve 2, the structure of the original system will cahnge in such a way that during these periods the filter will be disconnected.

The nature of the transient response in such a system with a variable structure can be represented by the curves 3 and 4, respectively.

A sign-sensitive element is connected to point a at the instant the sign of curve 1 changes relative to curve 2; this element disconnects the filter. The curve ab is then characterized by a steeper slope than that of the corresponding curve bc. Then the sign sensitive element which changes the structure is again disconnected, and this restores the original structure for a smaller error magnitude.

It is evident from Fig. 1 that the transient response in the system with correction is completed during a shorter time and approaches the transient response in the system with no filter. Thus, any deviation which has appeared initially and has been caused by the perturbation passes through the network elements which assure the appropriate filtering of the high frequencies; the signal passing through the feedback loop is received in such a way that it bypasses the filtering unit.

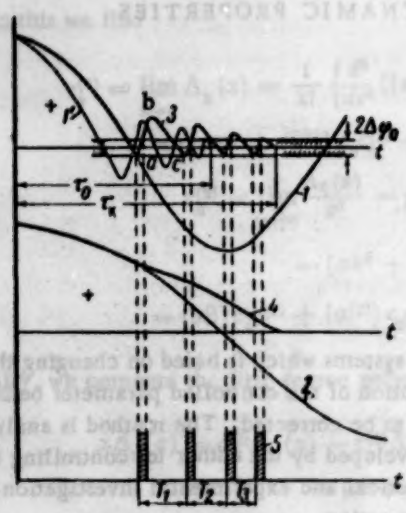

Fig. 1. 1) Transient response at the input to the filter in the ACS with no correction; 1') transient response in the ACS with no filter; 2) transient response at the output of the filter in the ACS with no correction; 3) transient response at the input to the filter in the ACS with correction; 4) transient response at the output of the filter in the ACS with correction; 5) connection of the sign-sensitive element $2\Delta\varphi_0$ is the dead band for the sign-sensitive element; τ_0 is the transient response time in the ACS with no filter; τ_c is the transient response time in the ACS with a filter when correction is present; T_1, T_2, and T_3 represent the periodicity for connection of the sign-sensitive element.

The general statment of the problem involved in changing the system structure as a function of its operating conditions was made by V. V. Solodovnikov [3], and for pulse and relay systems it was formulated by Ya. Z. Tsypkin [4, 5]. The literature indicates the expediency of using quantized devices for this purpose [5]. In [6] a study is made of the introduction of nonlinear feedback into a linear ACS for the purpose of achieving the optimal transient response. The paper describes the principle of stepwise variation of the speed feedback of a servosystem as a function of the product obtained by multiplying the sum of the error and its derivative by the error derivative. In [7] the possibility of controlling a neutral object with an astatic controller via the introduction of a quantized element is demonstrated.

In [8] the author proposes the introduction of a nonlinear element which varies the damping coefficient as a function of the error magnitude into a linear servosystem.

The block diagram for designing the ACS is shown in Fig. 2. Here 1 is the controlled object, 2 is the detecting element, 2a is the comparator element, 3 is the series corrective network (a filter that filters out the higher harmonics of the perturbations, 4 is the control network (for example, a relay system), 3' and 4', respectively, represent the corrective and control networks in the auxiliary control loop, 5 is the actuating organ, 5' is the corresponding actuating organ whose presence is not always mandatory when the element 5 can be connected to the circuit 6-3'-4-1, 6 is the network which responds to the sign of the controlled parameter deviation relative to its preceding value (x_5). In the relay system under study (Fig. 2) the total transient response time will be a minimum (other conditions being equal) if the pulse in the auxiliary circuit causes the actuating organ to be disconnected.

In a number of cases it is expedient to use quantities differing from the above-mentioned ones for correction purposes. In the general case we assume that the filter consists of a set of certain elements and sections in the ACS which has definite dynamic properties that are to be corrected.

In order to exclude the effect of noise on the corrective network it is important to match the static and dynamic characteristics of the sign-sensitive element 6 to the amplitude-frequency or spectral responses for the noise; these are not difficult to obtain on the basis of investigating the object and the operating conditions of the ACS*. The majority of industrial ACS are characterized by the effect of noise signals which have a relatively small amplitude compared to the amplitude of the basic perturbations, and a wider frequency spectrum. In order to suppress noise of this type we use a filter in the basic circuit. In that case the effect of noise on the corrective network can be practically eliminated if the sign-sensitive element 6 also responds to the absolute magnitude of the quantity x_3 and performs the switching when x_3 and x_5 are commensurate.

In the general case, eliminating the effects of noise on the corrective network is possible if the static and dynamic characteristics of the elements in this network are determined as functions of the amplitude-frequency responses for the noise. When this condition is not satisfied we will have a situation where sectors are cut out of the noise spectrum cutoff by the basic circuit; these sectors correspond to the passband for the corrective network frequencies at instants when the sign of the noise x_3 is opposite to the sign of x_5 after the transient response has arisen. This produces an appreciable lowering of the degree to which noise affects the ACS.

* Such characteristics are treated below on the basis of a specific example.

The method treated above for changing the structure of the system in order to obtain specific dynamic or static characteristics relative to the useful signal and the pertrubations (as a function of the signs of the signals at the inputs and outputs of the elements whose properties are to be corrected) can be used for improving the dynamic properties of a broad class of industrial ACS in which such a problem arises.

We shall study the application of this correction method to a specific relay system.

3. Description of the Network. We shall analyze the application of the method above to ACS which control the electric power delivered to an ore furance [10, 11]. The control network (Fig. 3)* is designed on the basis of measuring and controlling the phase admittance of the furnace by means of an electromechanical device for obtaining the quotient resulting from a division of the phase current by the corresponding voltage. In an electric ore furnace the variations in the phase admittances of the furnace are independent [12] when the proper distances between electrodes are chosen.

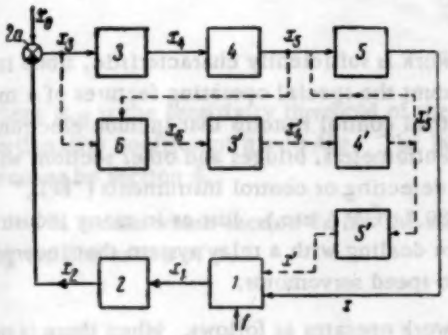

Fig. 2

If under these conditions the dynamic characteristics of the electromechanical computing device are matched with the corresponding characteristics of the network, then the autonomous operation of the controllers in individual phases is achieved in both the static and dynamic modes. In order to ensure the reliability of the network and correspondence between the conditions governing the operation of the ore furnace it is important to obtain cutoff of the high-frequency noise components and a minimum displacement of the electrodes. This is achieved by choosing the frequency responses of the electromechanical device that measures the ratio and by assuring autonomous operation of the controllers in neighboring phases.

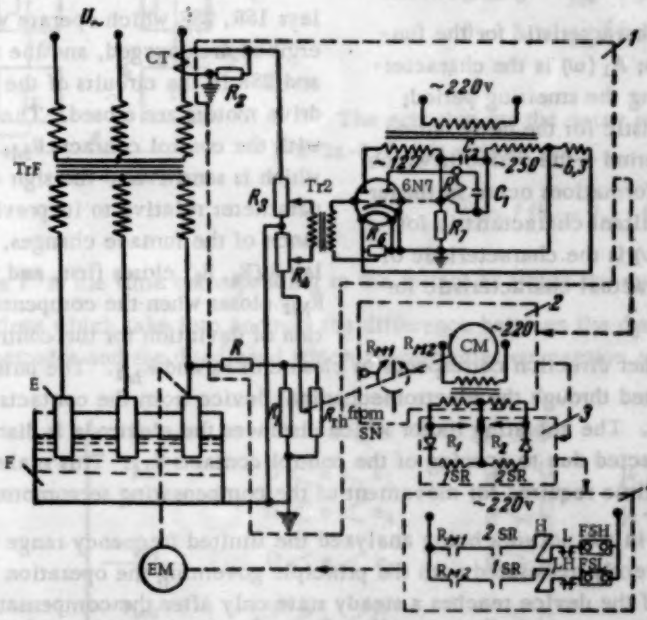

Fig. 3. TrF is the furnace transformer; E are the electrodes; F is the furnace. 1) Detecting block; 2) compensation servomotor (CM) with control contacts (R_M); 3) auxiliary relay units; 4) control network. EM is the motor for the electrode drive; H, L are the starting coils for the electrode-drive motor; S. N. is the setting network; FSH and FSL are the final cutouts for the electrode drive.

* The network is shown for one phase of the furnace; the networks for the remaining two phases are analogous.

Figure 4 shows the amplitude-frequency responses for the noise and fundamental perturbations, obtained on the basis of investigating the ore furnace as an object for automatic control of electric power. The curves are plotted in percent of nominal value of furnace phase power for a lead-smelting electric furnace; the data for the furnace is given in the Appendix. From Fig. 4 it is evident that the noise has a spectrum with higher frequencies and an amplitude-frequency response that lies appreciably below that of the fundamental perturbations; this verifies the reasoning cited above and demonstrates the expediency of introducing a filter for the purpose of excluding the effect of noise on the system and eliminating excess oscillations of the controlled parameter at a frequency close to the noise frequency. From these curves it is also evident that the superposition of noise on the fundamental curve has practically no effect on the average value of the controlled parameter.

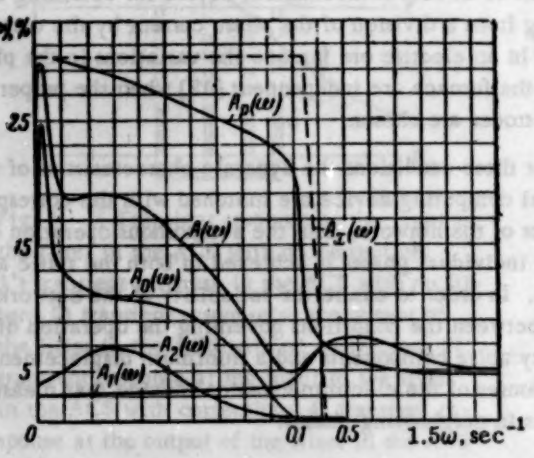

Fig. 4. $A_0(\omega)$ is the characteristic for the fundamental perturbations; $A_1(\omega)$ is the characteristic for the noise during the smelting period; $A_2(\omega)$ is the characteristic for the noise during the second smelting period —the period in which physicochemical transformations occur in the furnace; $A(\omega)$ is the resultant characteristic for the perturbations; $A_X(\omega)$ is the characteristic of the ACS; $A_p(\omega)$ is the actual characteristic for the basic ACS circuit.

Our network is sufficiently characteristic, since it takes into account the special operating features of a majority of industrial control systems that include electronic automatic potentiometers, bridges and other sections with compensation detecting or control instruments ("ÉPD," "ÉMD," "IR-130," "ÉPP," etc.). Just as in many industrial systems, we are dealing with a relay system that incorporates a constant-speed servomotor.

The network operates as follows. When there is no deviation of the controlled quantity the contacts R_{M1} and R_{M2} (Fig. 3) of the electromechanical device are open, the armature of the null-relay R which controls the connection of the compensation motor CM is in the intermediate position, and both contacts R_1, R_2 are open. The relays 1SR, 2SR, which operate when the contacts of R are energized, are engaged, and the normally open contacts 1SR and 2SR in the circuits of the starting coils for the electrode drive motors are closed. The relays 1SR and 2SR together with the control contacts R_{M1} and R_{M2} form an element which is sensitive to the sign of the variation in the control parameter relative to its previous value. When the admittance of the furnace changes, one of the contacts of the relay R (R_1, R_2) closes first, and then the contact R_{M1} and R_{M2} closes when the compensation motor turns. One direction of deviation for the control parameter corresponds to closure of R_1 and R_{M1}; the other direction corresponds to closure of R_2 and R_{M2}. The pulse for connection of the eletrode drive motor is transmitted through the electromechanical device from the contacts R_M; the cutout pulse is sent from the contact 2SR and 1SR. The actuating motor which displaces the electrode is disconnected before the instant at which it would be disconnected due to opening of the control contacts R_M. This makes it possible to eliminate the effect of the inertia and the time required for movement of the compensating servomotor in the detecting instrument.

It should be noted that in the network being analyzed the limited frequency range of the instrument used for frequency measurement is directly associated with the principle governing the operation of the electromechanical device; the output quantity of the device reaches a steady state only after the compensation process has been completed.

Analysis of the control System. Based on the analysis of the automatic control network, its block diagram (which takes into account the dynamic properties of the individual elements) can be represented as in Fig. 5; in this figure 1 is the controlled object (the electrical ore furnace); φ is the deviation of the controlled quantity in relative units $\varphi = G/G_b$, where G is the running value of the phase admittance for the furnace, G_b is the admittance of the furnace when it is used as the base quantity. The input quantity for the object is the displacement of the electrodes $\mu = h_e/h_{eb}$, where h_e and h_{eb}, respectively, denote the running and base values for the electrode displacement. Studying small deviations μ and φ, we obtain the linearized equation for the object in the form

$$\varphi = k\mu \qquad (1)$$

The transfer coefficient $\underline{k}$ for the object determines the slope of the static characteristic and depends substantially on the engineering conditions governing the operation of the furnace (temperature, the state of the melt); this coefficient varies as the smelting process proceeds. The detecting organ includes the relay amplifier 2 and the integrating section 2a (Fig. 5) in accordance with the network shown in Fig. 3. For the condition that the frequency responses of the instrument and the network are matched, the output quantity of the instrument reflects the input quantity with practically no inertia: the presence of the integrating element in this case is equivalent to introducing a constant lag corresponding to the maximum transient response time for the instrument. Then the equation for the detecting instrument is written as:

$$\begin{aligned} &\sigma = 0 \quad \text{for} \quad |\varphi| < |\varphi_{\sigma 0}|, \\ &\sigma = \eta\varphi \quad \text{for} \quad |\varphi_{\sigma m}| > |\varphi| > \varphi_{\sigma 0}, \end{aligned} \tag{2}$$

where $\varphi_{\sigma 0}$ is the sensitivity threshold of the instrument; $\varphi_{\sigma m}$ is the upper limit for the measurement, and η is a proportionality coefficient $\eta = d\sigma/d\varphi$. The lag introduced by the instrument in the other network elements is taken into account by section 4.

In a case where section 2a has the characteristic of an integrator*, φ' (Fig. 5) corresponds to a pulse representing the derivative of σ.

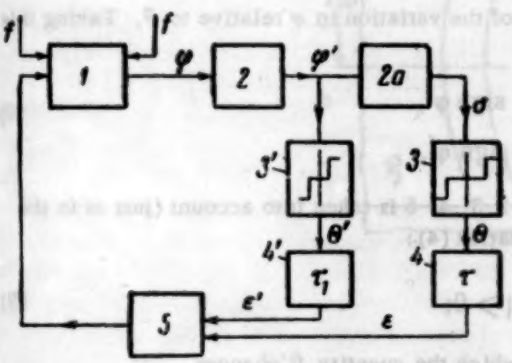

Fig. 5.

The function for the transducing element 3 (Fig. 5) is fulfilled by the main contact of the power controller. The equation for element 3 corresponds to the equation for a relay with a dead band ($2\Delta\sigma$) which is determined by the controller adjustment

$$\begin{aligned} &\theta = 0 \quad \text{for} \quad |\sigma| < |\Delta\sigma|, \\ &\theta = \theta_0 \quad \text{for} \quad |\sigma| > |\Delta\sigma|. \end{aligned} \tag{3}$$

The equation for the delay section 4 in the basic circuit 1-2-2a-3-4-5 is written as

$$\varepsilon = f(\theta - \theta_\tau) \quad \text{for} \quad |\theta| > 0, \tag{4}$$

where $\theta_\tau = \theta(t^* - \tau)$, where t^* is the time corresponding to the instant at which the quantity θ changes ($d\theta/d\sigma \neq 0$).

The servomotor equations which take into account the difference between the dynamic torques of the drive for raising and lowering the electrodes and the dead band which accompanies connection and cutout are written as follows:

$$\dot{\mu} = \begin{cases} 0 & \varepsilon \leqslant 0 \quad \ddot{\mu} > 0 \\ & 0 < \varepsilon < \varepsilon_1 \quad \ddot{\mu} < 0 \quad \dot{\mu} > 0 \\ & 0 < \varepsilon < \varepsilon_2 \quad \ddot{\mu} < 0 \quad \dot{\mu} < 0 \\ \dfrac{m_{v01}\varepsilon}{T} & 0 < \varepsilon < \varepsilon_{01} \quad \ddot{\mu} > 0 \\ \dfrac{m_{v02}\varepsilon}{T} & \varepsilon_{02} < \varepsilon < 0 \quad \ddot{\mu} > 0 \\ \dfrac{m_{v1}\varepsilon}{T} & \varepsilon_1 < \varepsilon < \varepsilon_{01} \quad \ddot{\mu} < 0 \\ \dfrac{m_{v2}\varepsilon}{T} & \varepsilon_{01} < \varepsilon < \varepsilon_2 \quad \ddot{\mu} < 0 \\ \dot{\mu}_{m1} & \varepsilon > \varepsilon_{01} \\ \dot{\mu}_{m2} & \varepsilon < \varepsilon_{02} \end{cases} \tag{5}$$

* In the particular case involving the correction under study.

Here ϵ_{01} and ϵ_{02}, respectively, determine the dead band for connecting the servomotor (for movement up and down); ϵ_1 and ϵ_2 analogously determine the dead band for disconnection of the servomotor when it moves up and down; m_{y01} and m_{y02} are the dynamic torques of the servodrive when it is connected for upward and downward displacement; m_{y1} and m_{y2} are the analogous dynamic torques for cutout:

$$m_{y01} = \frac{M_{s.av.} - M_s}{M_n}, \qquad m_{y1} = \frac{M_{b.av.} + M_s}{M_n},$$

$$m_{y02} = \frac{M_{s.av.} + M_s}{M_n}, \qquad m_{y2} = \frac{M_{b.av.} - M_s}{M_n},$$

where $M_{s.av.}$ and $M_{b.av.}$ are the average starting and braking torques for the motor which are determined on the basis of its mechanical characteristics; M_n is the nominal torque; T is the electromechanical time constant

$$T = \frac{GD^2 n_0}{\dot{\mu}_m 375 M_n}, \qquad \dot{\mu}_m = \frac{\dot{\varphi}_m}{k},$$

and $\dot{\varphi}_m$ is the maximum rate of change for the controlled parameter (φ) of the object.

The auxiliary relay unit 3' (Fig. 5) takes into account the sign of the variation in φ' relative to θ. Taking this into account, we write the equation for the element 3' in the form

$$\begin{aligned} \theta' &= 0 \quad \text{for} \quad \operatorname{sign}\theta = \operatorname{sign}\varphi', \\ \theta' &= \theta'_0 \quad \text{for} \quad \operatorname{sign}\theta \neq \operatorname{sign}\varphi'. \end{aligned} \tag{6}$$

The lag introduced by the elements of the corrective circuit 1-2-3'-4'-5 is taken into account (just as in the basic circuit) by the delay section 4' whose equation is written as equation (4):

$$\varepsilon' = f'(\theta' - \theta'_{\tau_1}) \quad \text{for} \quad |\theta'| > 0; \tag{7}$$

$\theta'_{\tau_1} = \theta'(t'^* - \tau_1)$, t'^* is the time corresponding to the instant at which the quantity θ' changes.

The equations (5) for the servomotor when it operates in the corrective circuit will include ϵ' instead of ϵ while keeping the same form.

The block diagram under study differs substantially on the networks used in industrial systems with quantized stopping of the actuating mechanism. In these systems the cutout signal is not associated with a variation in the properties of the ACS elements and their static and dynamic characteristics due to the effect of ac perturbations; rather, it is determined by a constant standard input introduced from the outside. In that case, for example, the variation of the system gain can lead either to the appearance of oscillations or to the prolongation of the transient response (i.e., in the final analysis it leads to a deviation of the static or dynamic characteristics of the ACS from the desired ones). In the block diagram under study both the basic and the correcting pulses pass through the object; this permits us to associate the introduction of the correcting pulse with the variation in the properties of the stabilized object (or has its output quantities varied according to some definite law) by the ACS.

In order to analyze the method of correction under study and to determine its effectiveness we shall perform a comparative investigation of two networks: a) with no corrective circuit (the control system 1-2-2a-4-5-1 (Fig. 5)), and b) with a corrective circuit (the control system which depends on the sign of $\varphi' - \theta$: 1-2-2a-3-4-5-1 or 1-2-3'-4'-5-1). We analyze each of these systems on the basis of investigating the corresponding phase trajectories.

It follows from eqs. (1)–(7) and the block diagram in Fig. 5 that the investigated system can be treated from the point of view of dynamics as the combination of a relay servomechanism which is derived by a second order equation (in the general case with variable coefficients) and a delay section. Under these conditions the characteristic of the servomotor has a dead band and is asymmetrically arranged relative to the axis of abscissas; the time delay may be different, depending on the direction in which the servomotor is made to rotate. An analysis of such systems in the general case requires an examination of the possible movements on a many-sheet phase surface [9].

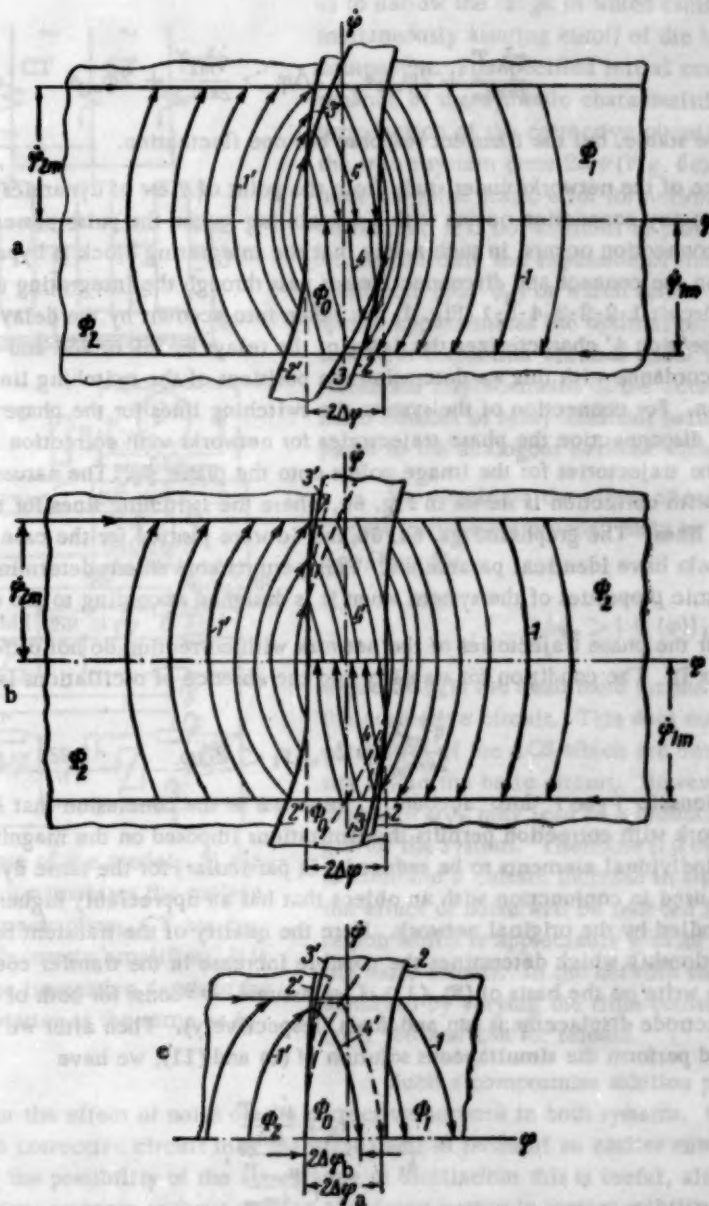

Fig. 6. Phase trajectories for the ACS: a) with no correction; b, c) for introduction of the corrective circuit. The broken lines show the trajectories for an analogous network without correction.

Based on a simultaneous analysis of equations (1)–(7), it is not difficult to eliminate the intermediate variables and to obtain the equations of motion for the ACS on the phase plane*. For a system with no corrective circuit the phase representation is shown in Fig. 6a. It follows from an examination of the phase trajectory that the limiting cycles will be absent if we have

$$\varphi < 2\Delta\varphi \quad \text{for} \quad \dot{\varphi} = 0, \tag{8}$$

for all curves of the form 4' (Fig. 6a); here $2\Delta\varphi$ is the dead band for the controller ($\Delta\varphi = \Delta\sigma/\eta$). From this the necessary and sufficient condition for an absence of periodic modes and for a transient response without oscillations is written in the form

$$\frac{\dot{\varphi}_{2m}^2 T}{2km_{v2}} + 2\dot{\varphi}_{m2}\tau < 2\Delta\varphi. \tag{9}$$

* The derivations of the equations of motion for the ACS are given in the Appendix.

For

$$\frac{\dot{\varphi}_{m2}^2 T}{2km_{y2}} + 2\dot{\varphi}_{m2}\tau \geqslant 2\Delta\varphi > \frac{\dot{\varphi}_{m1}^2 T}{2km_{y1}} + 2\dot{\varphi}_{m1}\tau. \tag{10}$$

the system may also be stable, but the transient response has one fluctuation.

The main feature of the networks under study from the point of view of dynamics resides in the fact that in a network with correction any connection occurs with a certain lag when the pulse passes through the integrating block of the instrument; disconnection occurs in such a way that the integrating block is bypassed. However, in the network without correction the connect and disconnect pulses pass through the integrating unit in both cases. The filtering properties of the circuit 1-2-2-3-4-5-1 (Fig. 1) are taken into account by the delay section 4. The time delay τ_1 determined by the section 4' characterizes the delay of the relays R, 1SR or 2SR and the servomotor; it is much smaller than τ. In accordance with this we determine the positions of the switching lines on the phase plane for the network with correction. For connection of the system the switching lines for the phase trajectories of both networks are analogous, and for disconnection the phase trajectories for networks with correction are shifted in the direction of an earlier transfer of the trajectories for the image points onto the plane Φ_0. The nature of the phase trajectories for the analyzed network with correction is shown in Fig. 6b, where the switching lines for the network without correction are denoted by broken lines. The graphs in Figs. 6a, 6b, and 6c were plotted for the case where all analogous sections of the compared networks have identical parameters. This permits convenient determination of the effect achieved in improving the dynamic properties of the system when it is designed according to the described method.

The equations for the phase trajectories of the network with correction do not differ in form from the original equations (cf. Appendix I). The condition for stability and the absence of oscillations is written analogously with (9):

$$\frac{\dot{\varphi}_{m2}^2 T}{2km_{y2}} + 2\dot{\varphi}_{m2}\tau_1 < 2\Delta\varphi. \tag{11}$$

Taking the relationship $\tau_1 \ll \tau$ into account, we come to the conclusion that for equal object and controller parameters the network with correction permits the limitations imposed on the magnitude of the dead band and the characteristics for individual elements to be reduced. In particular, for the same dynamic properties a network with correction can be used in conjunction with an object that has an appreciably higher transfer coefficient than the value which can be handled by the original network. Here the quality of the transient response in both networks may be identical. The relationship which determines the possible increase in the transfer coefficient for comparable networks is not difficult to write on the basis of (9), (11) if we assume φ = const for both of the compared networks and an identical rate of electrode displacement (up and down, respectively). Then after we substitute $\varphi_{m2} = k\dot{\mu}_{m2}$ in (9), $\varphi_{m2} = k_1\dot{\mu}_{m2}$ in (11) and perform the simultaneous solution of (9) and (11), we have

$$\frac{k}{k_1} = \frac{\tau_1 + \frac{\dot{\mu}_{m2} T}{4m_{y2}}}{\tau + \frac{\dot{\mu}_{m2} T}{4m_{y2}}}, \tag{12}$$

where k_1 and k are the maximum allowable transfer coefficients in the network with and without correction. For the condition $\tau_1 > \frac{\dot{\mu}_{m2} T}{4m_{y2}}$ we have approximately

$$\frac{k}{k_1} \approx \frac{\tau_1}{\tau}. \tag{13}$$

Based on the resulting relationships we determine the boundary value of the transfer coefficient and the possible limits for the improvement of the dynamic properties of the network under study. The use of the network with correction for the specified object permits us to reduce the dead band of the controller* or to narrow the range over which oscillations exist for possible deviations of the system gain (the variation of the transfer coefficients of the object and other ACS elements during the process of operation).

The phase trajectories cited in Fig. 6 illustrate the use of the described correction method in a specific nonlinear system. Here the phase trajectories are plotted for the case where introduction of the corrected circuit permits

* For an equal degree of stability.

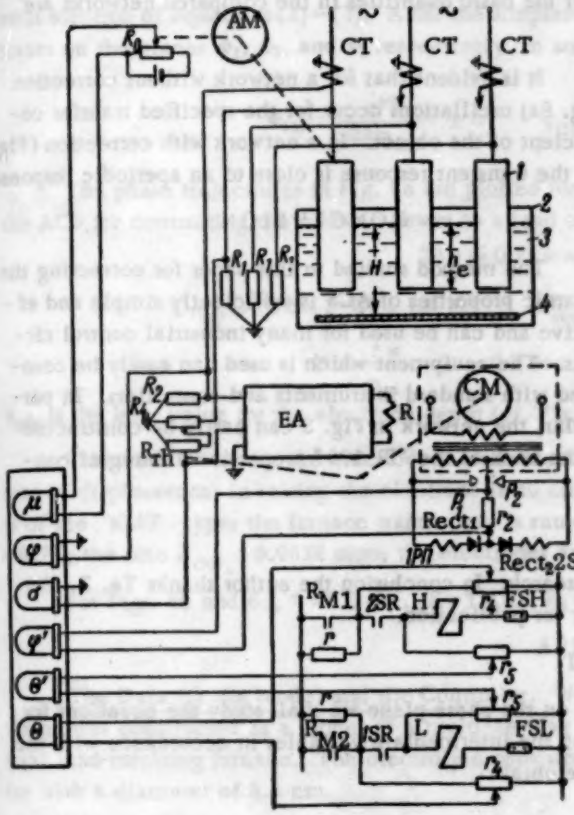

Fig. 7. 1) Electrodes; 2) frame of the model; 3) electrolyte; 4) metal trough which stimulates the molten metal. AM is the actuating mechanism; CT are current transformers; EA is an electronic amplifier; H is the electrolyte level; h_e is the immersion depth of the electrode. The remaining notation is the same as in Fig. 3.

us to narrow the range in which oscillations exist while simultaneously assuring cutoff of the high-frequency noise component. For specified initial conditions and for maintenance of the dynamic characteristics of the system, the introduction of the corrective circuit permits reduction of the static system error $2\Delta\varphi$ (Fig. 6c). Assuming that we have the same static error for networks with and without correction, it is not difficult to plot the phase trajectories which illustrate the expansion of the region for the initial conditions (φ_n, $\dot{\varphi}_n$) or which assure that the transient response approximates the optimal response. Here the system with correction which is under study can assure the minimum displacements of the actuating organ for a minimum number of relay-element switching operations as compared to the analogous network without correction.

We eliminate the effect of noise on the corrective circuit in the system under study by satisfying the condition (Fig. 4):

$$2\Delta\varphi_0 > [A_1(\omega)]_{\max}. \qquad (14)$$

where $2\Delta\varphi_0$ is the dead band for the auxiliary relay unit in the corrective circuit. This does not affect the static characteristics of the ACS which are determined by the quantity $\Delta\varphi$ in the basic circuit. However, an appreciable increase in $\Delta\varphi_0$ may lead to a reduction in the stability margin for the system. Therefore it is evidently most expedient to combine a certain increase in $\Delta\varphi_0$ with a guarantee that the effect of noise will be reduced in the high-frequency region which is appreciably greater than the pass band for the basic circuit. In the network shown in Fig. 3 this is achieved by varying the time constant in the circuit of the coils 1SR and 2SR for release.

Such a compromise solution permits us to assure the desired degree of reduction for the effect of noise on the corrective network in both systems. On the other hand, the possible effect of noise on the corrective circuit may manifest itself in terms of an earlier cutout of the system; from the point of view of reducing the possibility of the appearance of oscillations this is useful, although it may lead to a certain extension of the transient response without causing any deterioration in system stability.

For the analyzed system the effect of noise on the corrected circuit is not substantial*. The introduction of a corrective network, even when the analyzed effect of noise on the corrective network proper is taken into account, solves the problem on an over-all increase in the stability region for the ACS.

The analysis above illustrates a particular case where the correction method is applied. In general form the investigation and the choice of parameters for ACS with correction will be studied separately.

5. The Experimental Characteristics of the Network. An experimental investigation of the compared networks was performed in an electrolytic bath (an electrical model of the electrical ore furnace**) by connecting both controllers to it. The scheme illustrating the tests and the method of obtaining oscillograms is shown in Fig. 7. For instantaneous variation of the setting input to the regulator we fixed the following variable quantities: the phase current in the model (φ), the voltage across the rheochord R_{Th} (σ), the operation of the null-relay contacts R (φ'), the operation of the controller contacts (θ) and the contacts of the intermediate relays 1SR and 2SR(θ'), and the displacement

* Taking into account the imposition of a limitation in the sense of the sign, amplitude, and instant of appearance of the noise (cf. Section 2).

** The experimental characteristics for the basic perturbations and the noise are shown in Fig. 4 for an actual electrical ore furnace for smelting lead.

μ of the electrode motor. The oscillograms for the variations of the basic quantities in the compared networks are shown in Fig. 8 for identical conditions.

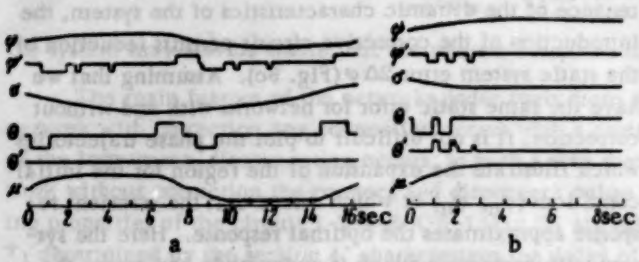

Fig. 8. Oscillograms for the transient response: a) in the network without correction; b) in the network with correction

It is evident that for a network without correction (Fig. 8a) oscillations occur for the specified transfer coefficient of the object. In a network with correction (Fig. 8b) the transient response is close to an aperiodic response.

CONCLUSION

The method studied in this paper for correcting the dynamic properties of ACS is sufficiently simple and effective and can be used for many industrial control circuits. The equipment which is used can easily be combined with standard instruments and controllers. In particular, the network in Fig. 3 can easily be constructed on the basis of the "IR-130" proportional-integral controller.

The adjustment of the network is also simple.

Engineer A. N. Ryndin participated in the experimental research. In conclusion the author thanks Ya. Z. Tsypkin for his valuable remarks and his help in preparing the paper for publication.

APPENDIX I

In order to determine the equations of motion for the ACS on the phase plane we shall study the equations for the individual elements (1)–(7) simultaneously while eliminating the intermediate variables in accordance with the method described in [1]. For an input deviation $|\varphi| > |\Delta\varphi|$ we obtain

$$\varphi_{out} = -\int \frac{km_{y0}(t-\tau)}{T}\,dt.$$

at the output of the system.

In order to fix the deviation φ_ϵ we have

$$\varphi_{\epsilon\,out} = -\frac{km_{y0}t_\epsilon^2}{2T} + \frac{km_{y0}\tau t_\epsilon}{T}. \tag{15}$$

after integration.

If the ACS under study were not to have lag, then the cut-in time would be t_ϵ. In an ACS with a delay τ the variation of φ_ϵ during the cut-in time t_ϵ is smaller by an amount $km_y\tau t_\epsilon/T$; however, for switching it is necessary that the cut-in time for the system be the same in both cases in order to liquidate the perturbation. Therefore, the increase in speed in both cases must be determined by the equation

$$\varphi = \frac{km_{y0}t_\epsilon}{2T}, \tag{16}$$

which is derived on the basis of (5), (1). From this it is not difficult to derive the equation which determines the switching line for the ACS on the phase plane when lag and a dead band are present. For an input deviation $\varphi_\epsilon - \Delta\varphi$ we have the equation for the switching line 2 (Fig. 6a) after substituting (16) into (15):

$$\varphi_{\epsilon\,(2)} = -\frac{\dot\varphi^2 T}{2m_{y02}k} + \dot\varphi\tau + \Delta\varphi. \tag{17}$$

Analogously, we determine the equations for the switching lines 2', 3, 3' (Fig. 6a):

$$\varphi_{\epsilon\,(2')} = \frac{\dot\varphi^2 T}{2m_{y02}k} + \dot\varphi\tau + \Delta\varphi, \quad \varphi_{\epsilon\,(3)} = \varphi_{\epsilon\,(2)} - \Delta\varphi - \dot\varphi\tau, \quad \varphi_{\epsilon\,(3')} = \varphi_{\epsilon\,(2')} - \Delta\varphi - \dot\varphi\tau.$$

The equations for the phase trajectories on the planes Φ_1, Φ_2, Φ_3, that characterize the acceleration and brak-

ing modes when the servodrive is connected in different directions are also determined on the basis of the simultaneous solution of equations (1)—(7). After the simplest substitutions [1] we obtain the equations for the phase trajectories on the planes Φ_1, Φ_2, and Φ_3 respectively, in analogous fashion:

$$\varphi_{(1)} = \frac{\dot{\varphi}^2 T}{2km_{y01}} + C, \quad \varphi_{(2)} = \frac{\dot{\varphi}^2 T}{2km_{y02}} + C, \quad \varphi_0 = \frac{\dot{\varphi}^2 T}{2km_{y1,2}} + C.$$

The phase trajectories in Fig. 6a are plotted for the following values of the basic parameters corresponding to the ACS for controlling the electric power to a lead smelting electric furnace:

$$2\Delta\varphi = 0.2;\ k = 0.8;\ m_{y01} = 1;\ k = k_0 \frac{h_{eb}}{G_b};$$

$$h_{eb} = 20\text{ cm};\ T = 7.6\text{ sec};\ m_{y02} = 1.2;\ G_b = 400\text{ cm}^{-1};\ \dot{\mu}_{m1} = 0.75;\ m_{y1} = 1.5;$$

$$T = \frac{T_M}{\dot{\mu}_m};\ \tau = 0.3\text{ sec};\ \dot{\mu}_{m2} = 0.96;\ m_{y2} = 0.75;\ k_0 = 16\frac{\text{ohm}^{-1}}{\text{cm}};$$

h_{eb} is the base value for the electrode depth (cf. Fig. 7).

The drive motor for the electrode is an induction motor with a short-circuited rotor (type MA-142 2/6); the rate of displacement in raising the electrode is 80 cm/min, and it is 90 cm/min for lowering the electrode; the brake is of the KMT type; the furnace transformer is rated at $P_L = 3600$ kva, $I_L = 14{,}000$ amp, short-circuit voltage $l_{s.c.} = 9.7\%$; the line $Z_{cor.} = 0.0012$ ohm; the electrodes are graphite with a diameter of 700 mm.

For Figs. 6b and 6c, $\tau_1 = 0.1$ sec., $K = 1.4K_1$, $K_1 = 1.12$. The remaining quantities correspond to Fig. 6a.

APPENDIX II

The Data for the Model and the Controller. We used an electrolytic bath (of the three-phase type; cf. Fig. 7) which was constructed as a model of a multiple-slag electrical ore furnace on scale 1:10 with respect to an industrial lead-smelting furnace. The electrolyte consisted of an aqueous solution of table salt. The electrodes were graphite with a diameter of 5.5 cm.

A transformer of the type TOS rated at 1.5 kw with three legs and $l_{s.c.} = 4.8\%$ was used; the nominal voltages for the primary and secondary windings were $U_1/U_2 = 220/21$ v, and the nominal secondary current was $I_{21} = 23$ amp.

The electrode drive motors are actuating mechanisms of the type IM 2/120 with a pulley; $D = 40$ cm, $G_b = 1.5\text{ ohm}^{-1}$, $h_{eb} = 4$ cm, $k_0 = 0.2\text{ ohm}^{-1}/\text{cm}$, $k = 0.55$. The controller dead band corresponded to $\Delta G = 0.03\text{ ohm}^{-1}$, $T_M = 0.0245$ sec, $T = 0.08$ sec, $\tau = 0.2$ sec, $\tau_1 = 0.04$ sec, $\dot{\mu}_{m1} = 0.36$; $\dot{\mu}_{m2} = 0.43$.

The limiting value of $\underline{k}$ for which there are no oscillations in the network with correction was equal to $k_1' = 1.2$ on the basis of the experimental data. Computations according to formula (12) yield $k_1 \approx 2k$, i.e., $k_1 = 1.1$, which is close to k_1'.

In our experiments the maximum perturbations at the controller input were equal to $\Delta G_{max} = 0.5\text{ ohm}^{-1}$ (or $\sim 33\% G_b$), $\Delta h_{e.\,max} = 2.5$ cm.

LITERATURE CITED

1. Foundations of Automatic Control Theory. Edited by V. V. Solodovnikov [in Russian] (Machinery Press, 1954).
2. Yu. E. Efroimovich and V. I. Feigin, Automatic Control of Metallurgical Arc Furnaces [in Russian] Metallurgy Press (1951).
3. V. V. Volodovnikov, Certain Design Principles and Theoretical Problems Associated with Self-Adaptive Automatic Control Systems. Reports to the Session of the Academy of Sciences USSR on Scientific Problems of Production Automation [in Russian] (Academy of Sciences USSR Press, 1957).
4. Ya. Z. Tsypkin, Theory of Relay Automatic Control Systems [in Russian] (State Technical Press, 1955).
5. Ya. Z. Tsypkin, "Correction of pulsed regulation and control systems," Avtomatika i Telemekhanika, 18, 2 (1957).*
6. G. M. Ostrovskii, "The use of nonlinear corrective networks in second-order automatic control systems," Avtomatika i Telemekhanika 17, 11 (1956).*
7. V. A. Maslennikov, "Quality control of a neutral object using an astatic controller," Avtomatika i Telemekhanika 17, 2 (1956).
8. Lewis, "The use of nonlinear feedback for improving the transient response in automatic control systems," Voprosy Raketnoi Tekhniki 4 [Russian translation] (1954).

* Original Russian Pagination. See C. B. translation.

9. V. V. Petrov, V. Yu. Rutkovskii, "The theory of the simplest servomechanism with log, "Izvestiya Akad. Nauk, Otdelenie Tekhnicheskikh Nauk 4 (1956).
10. V. S. Lerner, A Device for the Automatic Control of the Power Supply to an Electrical Ore Furnace, Author's Certificate No. 12772, (Feb. 20, 1959).
11. V. S. Lerner, An Instrument for Measuring the Ratio between Two Quantities which are Electrically Specified, Author's Certificate No. 112773 (Nov. 10, 1956).
12. V. S. Lerner, An Electric Ore Furnace as An Object for the Automatic Control of Electric Power, Symposium of the Transactions of the All-Union Scientific-Research Institute of Nonferrous Metals, No. 6 [in Russian] (Metallurgy Press, 1950).

ANALYTICAL SOLUTIONS OF LINEAR EQUATIONS DESCRIBING ONE CLASS OF DYNAMICAL SYSTEMS WITH VARIABLE PARAMETERS

Ts. G. Litovchenko

(Moscow)

Translated from Avtomatika i Telemekhanika, Vol. 22, No. 4, pp. 457-465, April, 1961

Operational calculus is applied to obtain the solution of linear equations with linearly varying coefficients in general form. Conditions under which this solution may be represented in closed form, i.e., expressed in terms of elementary functions and tabulated special functions, are established.

The mathematical investigation of the behavior of nonlinear automatic control systems in the neighborhood of stable motions, with first order accuracy, reduces to the analysis of linear equations with variable coefficients, the equations of first approximation for certain unstable motions of the system. A general solution to these equations, as is known, may not be obtained; and therefore it will be valuable to single out certain classes of equations which, on the one hand, have a practical value, and on the other hand, may be solved in closed form. This will permit a simple analysis of the automatic control systems corresponding to them.

In this paper we examine one class of equations of the form

$$\sum_{\nu=0}^{\nu=N} (a_\nu + b_\nu t)\, \mathrm{F}_{\nu,t}\, x(t) = u(t), \tag{1}$$

where $\mathrm{F}_{\nu,t}$ is a certain linear stationary operator defined by

$$\mathrm{F}_{\nu,t} x(t) = \int_0^t f_\nu(t-\tau)\, x(\tau)\, d\tau. \tag{2}$$

The structure of the system corresponding to equation (1) is represented in Fig. 1. In the particular case when $f_\nu(t-\tau) = \delta^{(\nu+1)}(t-\tau)$, equation (1) takes on the form of a differential equation:

$$\sum_{\nu=0}^{\nu=N} (a_\nu + b_\nu t)\, x^{(\nu)}(t) = u(t). \tag{3}$$

One deals with equations of type (1) or (3) in planning various linear automatic control systems whose variable parameters may be considered to the linearly varying.

Examples of such automatic control systems are gyroscopes in those stages of motion when the kinetic moment changes approximately linearly in time, tracking systems with linearly varying driving moment of inertia, radiolocation systems in conjunction with automatic escort with variable band pass, and also the control systems of the type examined, for example, in [1, 2].

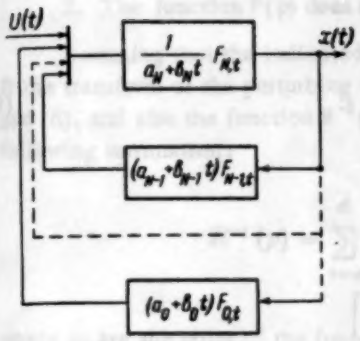

Fig. 1.

Equations (1) or (3) are equations with singular points, and their solutions may be represented by infinite power series [3], which, however, are not convenient for the analysis of the properties of automatic control systems. Therefore it is of interest to distinguish those cases when these solutions may be put into closed form, i.e. when they may be expressed in terms of elementary functions and tabulated special functions. The fact that many particular types of equation (3) for N = 2 have such solutions (Bessel's, Laguerre's, the degenerate hypergeometric equation, etc. [3]) lends itself to this idea.

The problem posed in conveniently solved by application of the Laplace transform. Applying it to the equation (1) or (2), we obtain, by virtue of the linearity of the variable coefficients, an equation of first order, the solution of which is easily obtained by quadratures. Then we determine, firstly, the conditions under which the transform obtained has an inverse, and secondly, we obtain the inverse itself. As a result we find all particular cases in which it is possible to solve in finite (analytic) form, and also find the solutions themselves of equations of type (1) independently of the form of the operators $\mathbf{F}_{\nu,t}$, and of equations of type (3) independently of the order N.

We apply the Laplace transform to equation (1). Considering that inverses of the form (2) correspond to the product of transforms, and also the fact that the product of a certain function of time by t corresponds to differentiating its transform with opposite sign [4], we obtain the equation

$$\sum_{\nu=0}^{N}\left(a_\nu - b_\nu \frac{d}{dp}\right)F_\nu(p)\,X(p) = U(p), \tag{4}$$

in which $\mathbf{F}_\nu(p)$ is the transform of an impulse transient function $f_\nu(t)$. In the case when equation (1) takes the form of differential equation (3), $F_\nu(p) = p^\nu$.

After transformation,

$$\sum_{\nu=0}^{N}\left(a_\nu - b_\nu \frac{d}{dp}\right)F_\nu(p)\,X(p) = X(p)\left[\sum_{\nu=0}^{N} a_\nu F_\nu(p) - b_\nu F'(p)\right] - X'(p)\sum_{\nu=0}^{N} b_\nu F_\nu(p)$$

equation (4) may be written in the form

$$X'(p) + P(p)\,X(p) = Q(p), \tag{5}$$

where

$$P(p) = \frac{\sum_{\nu=0}^{N} b_\nu F'_\nu(p)}{\sum_{\nu=0}^{N} b_\nu F_\nu(p)} - \frac{\sum_{\nu=0}^{N} a_\nu F_\nu(p)}{\sum_{\nu=0}^{N} b_\nu F_\nu(p)}, \qquad Q(p) = -\frac{U(p)}{\sum_{\nu=0}^{N} b_\nu F_\nu(p)}. \tag{6}$$

The functions $\mathbf{F}_\nu(p)$, forcing functions of linear stead systems possessing together with variable parameters $(a_\nu + b_\nu t)$ the same structure as the system examined may be represented in the form of rational functions of the argument p. Therefore the functions $P(p)$ as well is a rational function, with the order of the numerator for all $a_\nu \neq 0$ and $b_\nu \neq 0$ equal to the order of the denominator. The latter fact follows from the obvious fact that the second term of the function P(p) for $p \to \infty$ approaches a constant limit equal to

$$c_0 = \lim_{p\to\infty}\left[-\sum_{\nu=0}^{N} a_\nu F_\nu(p) \Big/ \sum_{\nu=0}^{N} b_\nu F_\nu(p)\right],$$

and the first term approaches zero.

On this basis, the function P(p) may be represented in the form of a whole part and the sum of proper fractions:

$$P(p) = c_0 + \sum_{n=1}^{N}\sum_{m=1}^{M_n}\frac{c_{n,m}}{(p-p_n)^m}, \tag{7}$$

where p_n are the poles of the function, N is the number of poles, and M_n the order of the nth pole, and $c_{n,m}$ expansion coefficients defined by the formula

$$c_{n,m} = \lim_{p\to p_n}\frac{d^{M_n-m}}{dp^{M_n-m}}\left[(p-p_n)^{M_n}P(p)\right]\frac{1}{(M_n-m)!}. \tag{8}$$

In the case when the functional equation (1) takes the form of a differential equation (3), the function P(p) is equal to

$$P(p) = \frac{\sum_{\nu=0}^{N} \nu b_\nu p^{\nu-1} - a_\nu p^\nu}{\sum_{\nu=0}^{N} b_\nu p^\nu}. \tag{9}$$

In this, the whole part is equal to $c_0 = \lim_{p\to\infty} P(p) = -\frac{a_N}{b_N}$.

The general solution of equation (5)

$$X(p) = e^{-\int P(p)dp}\left[C + \int e^{\int P(p)\,dp} Q(p)\,dp\right]$$

after substitution of the expression for P(p) from formula (7) takes the form

$$X(p) = e^{-c_0 p} R^{-1}(p)\left[C + \int e^{c_0 p} V(p)\,dp\right], \tag{10}$$

in which the functions R(p) and V(p) are equal to:

$$R(p) = \exp\left[\int \sum_{n=1}^{N}\sum_{m=1}^{M_n} \frac{c_{n,m}}{(p-p_n)^m}\,dp\right], \tag{11}$$

$$V(p) = R(p)\,Q(p). \tag{12}$$

Simple transformations lead to the following formula for the function R(p):

$$R(p) = \exp\left\{\int \sum_{n=1}^{N}\sum_{m=1}^{M_n} \frac{c_{n,m}}{(p-p_n)^m}\,dp\right\} = \exp\left\{\sum_{n=1}^{N}\sum_{m=1}^{M_n} \frac{c_{n,m}}{(p-p_n)^m(m-1)} + \right. \tag{13}$$

$$\left. + \sum_{n=1}^{N} c_{n,1}\ln(p-p_n)\right\} = \prod_{n=1}^{N}(p-p_n)^{c_{n,1}} \prod_{n=1}^{N}\prod_{m=2}^{M_n} e^{-\frac{c_{n,m}}{(m-1)(p-p_n)^m}}$$

We further determine the inverse x(t) of the function X(p). Using the convolution rule [4] and operational relations (27) established in Appendix I, from formula (10) we obtain

$$x(t) = -\int_0^t r^*(t-\tau)\,\frac{v(\tau)}{\tau - c_0}\,d\tau, \tag{14}$$

where the functions $r^*(t)$ and v(t) are the inverses of the functions $R^{-1}(p)$ and V(p).

Thus formula (14) gives the general solution of the original equation (1) independently of the form of the operators $\mathbf{F}_{\nu,t}$. In this the formula (13) shows in which cases the integral (14) may be taken in closed form, i.e., expressed in terms of elementary and tabulated special functions. This is possible when the coefficients $c_{n,m}$ of series (7) for $m \geq 2$ are equal to zero, and for $m = 1$ they are actually whole numbers. In this case the function

$$R(p) = \prod_{n=1}^{N}(p-p_n)^{c_{n,1}} \tag{15}$$

is a rational function; the functions $R^{-1}(p)$ and V(p), also rational functions, have inverses expressable by sums of terms of the form $t^k e^{at}$. Then integral (14) in taken in the general form (see Appendix III) and the solution x(t) is expressed in the form of some combination of functions $t^k e^{at}\bar{E}_i(t)$. If, however, the numbers $c_{n,m}$ for $m \geq 2$ are not equal to zero and at least one number $c_{n,1}$ is not whole, then the inverse r(t) of the function R(p) may not be obtained in closed form, and the solution x(t) of the original equation (1) or (3) may not be obtained in such a form either. This follows from the fact that for $c_{n,m} \neq 0$ and $m \geq 2$ the function R(p) contains a factor of the form $e^{a/p-p_1}$, for which in inverse, on the basis of Appendix II and the displacement theorem [4], is expressed by Bessel functions of the form $-\left(\frac{a}{t}\right)^{1/2} I_1(2\sqrt{at})\,e^{p_n t}$. However, the convolution integrals of these functions, defining r(t), are not expressible in terms of known tabulated functions [5, 6].

As a result one may formulate the following conditions under which it is possible to solve equations (1) or (3) in closed form.

1. The function P(p), defined by formula (6) or (9), does not contain multiple poles; this guarantees that the numbers $c_{n,m}$ for $m \geq 2$ are zero.

2. The function P(p) does not contain complex poles and their residues $c_{n,1}$ are whole numbers.

Assuming that the indicated conditions are fulfilled, we find the solution of equation (1) or (3) in finite form. If the transform of the perturbing function U(p) is a rational function, then the function V(p) defined by formulas (12) and (6), and also the function $R^{-1}(p)$, are rational. This allows one to represent $R^{-1}(p)$ and V(p) in the form of the following summation:

$$R^{-1}(p) = \sum_{s=0}^{S} B_s p^s + \sum_{k=1}^{K} \sum_{l=1}^{L_k} \frac{g_{k,l}}{(p-p_k)^l}, \qquad V(p) = \sum_{j=0}^{J} A_j p^j + \sum_{i=1}^{I} \sum_{\vartheta=1}^{\Theta_i} \frac{q_{i,\vartheta}}{(p-p_i)^\vartheta}, \tag{16}$$

where p_k are the poles of the function $R^{-1}(p)$, K is the number of its poles, L_k the order of the kth pole, $g_{k,l}$ the coefficients of expansion defined by the formula

$$g_{k,l} = \lim_{p \to p_k} \frac{d^{L_k - l}}{dp^{L_k - l}} [(p-p_k)^{L_k} R^{-1}(p)] \frac{1}{(L_k - l)!}, \tag{17}$$

S is the excess of the order of the numerator of the function $R^{-1}(p)$ over that of the denominator, B_s are the expansion coefficients defined by the formula

$$B_s = \lim_{p \to \infty} \frac{1}{p^s} \left[R^{-1}(p) - \sum_{x=s+1}^{S} B_x p^x \right], \tag{18}$$

p_i are the poles of the function V(p), I the number of its poles, Θ_i the order of ith pole, $q_{i\vartheta}$ the expansion coefficients defined by the formula

$$q_{i\vartheta} = \lim_{p \to p_i} \frac{d^{\Theta_i - \vartheta}}{dp^{\Theta_i - \vartheta}} [(p-p_i)^{\Theta_i} V(p)] \frac{1}{(\Theta_i - \vartheta)!}; \tag{19}$$

J the excess of the order of the numerator of the function V(p) over that of its denominator, and A_j the expansion coefficients defined by the formula

$$A_j = \lim_{p \to \infty} \frac{1}{p^j} \left[V(p) - \sum_{x=j+1}^{J} A_x p^x \right]. \tag{20}$$

The inverses $r^*(t)$ and $v(t)$ of the functions $R^{-1}(p)$ and V(p) are obtained, after applying to formula (16) the inverse transform formula, in the form:

$$r^*(t) = \sum_{s=0}^{S} B_s \delta^{(s+1)}(t) + \sum_{k=1}^{K} \sum_{l=1}^{L_k} \frac{g_{k,l}}{(l-1)!} e^{p_k t} t^{l-1},$$

$$v(t) = \sum_{j=0}^{J} A_j \delta^{(j+1)}(t) + \sum_{i=1}^{I} \sum_{\vartheta=1}^{\Theta_i} \frac{q_{i,\vartheta}}{(\vartheta-1)!} e^{p_i t} t^{\vartheta-1}.$$

Finally, the last step is to take the integral (14), in which we substitute $r^*(t)$ and $v(t)$ defined by (21):

$$x(t) = -\sum_{j=0}^{J} A_j \int_0^t \frac{r^*(t-\tau)\,\delta^{(j+1)}(\tau)}{\tau - c_0} d\tau - \sum_{i=1}^{I} \sum_{\vartheta=1}^{\Theta_i} \frac{q_{i,\vartheta}}{(\vartheta-1)!} \int_0^t \frac{r^*(t-\tau)\, e^{p_i \tau} \tau^{\vartheta-1}}{\tau - c_0} dt =$$

$$= \frac{1}{c_0} \sum_{j=0}^{J} A_j \left[\sum_{s=0}^{S} B_s \delta^{(s+j+1)}(t) + \sum_{k=1}^{K} \sum_{l=1}^{L_k} \frac{g_{k,l}}{(l-1)!} \int_0^t \frac{e^{p_k(t-\tau)}(t-\tau)^{l-1}}{\tau - c_0} \delta^{(j+1)}(\tau)\, d\tau \right] -$$

$$- \sum_{i=1}^{I} \sum_{\vartheta=1}^{\Theta_i} \frac{q_{i,\vartheta}}{(\vartheta-1)!} \left[\sum_{s=0}^{S} B_s \frac{d^s}{dt^s} \left(\frac{e^{p_i t} t^{\vartheta-1}}{t - c_0} \right) + \sum_{k=1}^{K} \sum_{l=1}^{L_k} \frac{g_{k,l}}{(l-1)!} \int_0^t \frac{e^{p_k(t-\tau)}(t-\tau)^{l-1} e^{p_i \tau} \tau^{\vartheta-1}}{\tau - c_0} d\tau \right].$$

Introducing the function

$$J_{i,k}(t, m, n) = \int_0^t \frac{e^{(p_i - p_k)\tau}(t-\tau)^m \tau^n}{\tau - c_0} d\tau,$$

determined in Appendix III for $p_i - p_k = a$, we obtain the final expression for $x(t)$:

$$x(t) = \frac{1}{c_0}\sum_{j=0}^{J} A_j \left[\sum_{s=0}^{S} B_s \delta^{(s+j+1)}(t) + \sum_{k=1}^{K}\sum_{l=1}^{L_k} \frac{g_{k,l}}{(l-1)!}\frac{d^j}{dt^j}\left(e^{p_k t} t^{l-1}\right)\right] - \tag{22}$$

$$-\sum_{i=1}^{I}\sum_{\vartheta=1}^{\Theta_i}\frac{q_{i,\vartheta}}{(\vartheta-1)!}\left[\sum_{s=0}^{S} B_s \frac{d^s}{dt^s}\left(\frac{e^{p_i t} t^{\vartheta-1}}{t-c_0}\right) + \sum_{k=1}^{K}\sum_{l=1}^{L_k}\frac{g_{k,l}}{(l-1)!} e^{p_k t} J_{ik}(t, l-1, \vartheta-1)\right].$$

Thus to obtain the general solution of equations (1) or (3) in closed form it is necessary:

1) to compose the functions P(p) and Q(p) in formula (6) or (9),

2) expand the function P(p) according to formula (7), (8) in a series and establish the possibility of obtaining the solution in finite form according to the conditions introduced above;

3) compose the functions $R^{-1}(p)$ and V(p) according to formulas (15) and (12) and calculate the coefficients of their expansion in the series of the form (16) according to formulas (17), (18), (19), (20):

4) obtain the final solution of the original equation (1) or (3) by formula (22).

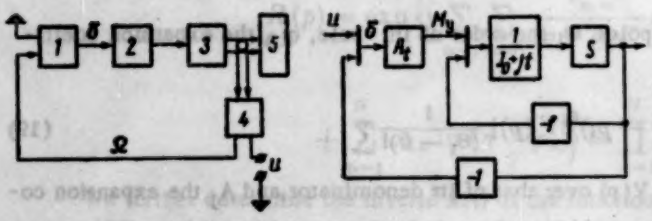

Fig. 2.

The method presented for solving equation (1) or (3) with linearly varying coefficients differs in that it depends neither on the order of the differential equation (3), nor on the complexity of the operators $F_{\nu,t}$ entering into equation (1). Since for a large number of terms of the series (for large values c_n) calculations by formula (22) are somewhat complicated, in these cases an approximate method of obtaining the solution may be recommended. This approximate method is based on graphically calculating the integral convolution (14), determining the functions $r(t)$ and $v(t)$ beforehand by the corresponding transformations (for example, by the known method of trapezoidal frequency characteristics [7]).

Example. We shall examine a control system for the velocity of rotation of a body of variable mass. The system (Fig. 2) contains an amplifier of the mismatch signal 1, a rotary amplifier 2, a motor 3, and tachogenerator 4. The moment of inertia of the load 5 changes according to the linear law $J = J_0 + jt$. The equations of motion of the system have the form

$$\delta(t) = u(t) - \Omega(t), \quad M_y(t) = A_t\delta(t), \quad J\Omega(t) + f\Omega(t) = M_y(t), \quad J = J_0 + jt, \tag{23}$$

where the operator A_t corresponds to the transformation of the signal $\delta(t)$ at the controlled moment $M_y(t)$ according to the transfer function $\frac{M_y(p)}{\delta(p)} = A(p) = \frac{K}{(1+T_1 p)(1+T_2 p)}$, describing the circuit amplifier and the transformation of the signal in the amplifier and motor. Initial data: $K = 0.12$ kgm/$\frac{1}{\text{sec}}$; $f = 0.01$ kgm/$\frac{1}{\text{sec}}$; $j = 0.06$ kgm sec^2/sec; $J_0 = 0.06$ kgm sec^2; $T_1 = 1$ sec; $T_2 = 0.5$ sec.

The system of equations (25) we write in the form

$$(J_0 + jt)\dot{\Omega}(t) + (f + A_t)\Omega(t) = A_t u(t). \tag{24}$$

Comparing equation (26) with equation (1), we obtain

$$a_0 = 1, \quad b_0 = 0, \quad F_0(p) = f + A(p),$$
$$a_1 = J_0, \quad b_1 = j, \quad F_1(p) = p.$$

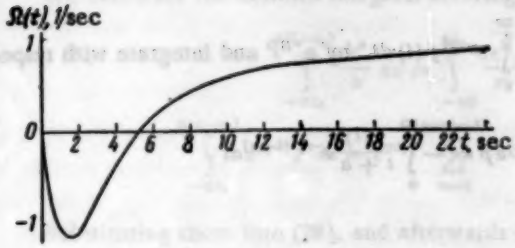

Fig. 3.

We determine the reaction of the system to the signal of the form $u(t) = 1(t)$.

1. According to formula (6) we compare the functions P(p) and Q(p):

$$P(p) = \frac{1}{p} - \frac{f + A(p)}{fp} - \frac{J_0}{f};$$

$$Q(p) = -\frac{A(p)}{fp^2} = -\frac{K}{f(1 + T_1 p)(1 + T_2 p)p^2}.$$

2. We determine the expansion coefficients by formula (8)

$$c_{1,1} = 1 - \frac{K + f}{f} \approx 1 \quad \text{for} \quad p_1 = 0,$$

$$c_{2,1} = \frac{K}{f} \frac{1}{\left(1 - \frac{T_2}{T_1}\right)} = 4 \quad \text{for} \quad p_2 = -\frac{1}{T_1} = -1,$$

$$c_{3,1} = \frac{K}{f\left(1 - \frac{T_2}{T_1}\right)} = -2 \quad \text{for} \quad p_3 = -\frac{1}{T_2} = -2.$$

For $m \geq 2$ $c_{n,m} = 0$.

3. We compare the functions $R^{-1}(p)$ and V(p) according to formulas (15) and (12):

$$R^{-1}(p) = \frac{p(p+2)^3}{(p+1)^4}, \qquad V(p) = -\frac{(p+1)^3}{p^3(p+2)^3}.$$

We calculate the coefficient g_{kl} according to (17). In this, $K = 1$, $p_{k=1} = -1$, $L_{k=1} = 4$.

$$g_{1,4} = \lim_{p \to -1} p(p+2)^3 = -1, \qquad g_{1,3} = \lim_{p \to -1} [(p+2)^3 + 2p(p+2)] = -1,$$

$$g_{1,2} = \frac{1}{2} \lim_{p \to -1} [2(p+2) + 2(p+2) + 2p] = 1, \quad g_{1,1} = \frac{1}{6} \lim_{p \to -1} [4 + 2] = 1.$$

The coefficients $B_s = 0$.

We calculate the coefficients g_{ij} according to formula (19). Here $I = 2$, $p_{i=1} = 0$, $\Theta_{i=1} = 3$; $p_{i=2} = -2$, $\Theta_{i=2} = 3$.

$$q_{1,3} = \lim_{p \to 0} \left[-\left(\frac{p+1}{p+2}\right)^3 = -\frac{1}{8} \right], \qquad q_{2,2} = \lim_{p \to -2} \left[-\frac{(p+1)^3}{p^3} = -\frac{1}{8} \right],$$

$$q_{1,2} = \lim_{p \to 0} \left[-\frac{d}{dp}\left(\frac{p+1}{p+2}\right)^3 = -\frac{3}{16} \right], \qquad q_{2,2} = \lim_{p \to -2} \left[-\frac{d}{dp}\frac{(p+1)^3}{p^3} = \frac{3}{16} \right],$$

$$q_{1,1} = \frac{1}{2} \lim_{p \to 0} \left[-\frac{d^2}{dp^2}\left(\frac{p+1}{p+2}\right)^3 = 0 \right] \qquad q_{2,1} = \frac{1}{2} \lim_{p \to -2} \left[-\frac{d^2}{dp^2}\frac{(p+1)^3}{p^3} = 0 \right].$$

The coefficients $A_j = 0$.

4. We obtain the final solution according to formula (22)

$$\Omega(t) = \left(-\frac{1}{6} - \frac{1}{16}t + \frac{1}{8}t^2 + \frac{1}{48}t^3\right) e^{-t-1}[\overline{Ei}(t+1) - \overline{Ei}(1)] +$$

$$+ \left(1 + \frac{3}{8}t - \frac{1}{4}t^2 - \frac{1}{24}t^3\right) e^{-t+1}[\overline{Ei}(-t-1) - \overline{Ei}(-1)] + \left(\frac{15}{16} - \frac{1}{8}t - \frac{1}{48}t^3\right) +$$

$$+ \left(-\frac{1}{24}t^3 + \frac{1}{16}t^2 - \frac{15}{16}t - \frac{5}{4}\right) e^{-t} + \left(\frac{1}{32}t^3 - \frac{1}{16}t^2 - \frac{10}{24}t + \frac{5}{16}\right) e^{-2t}.$$

The corresponding graph is given in Fig. 3.

Appendix I

We multiply the left and right sides of the relation $F(p)=\int_0^\infty e^{-pt} f(t)\,dt$ by e^{-ap} and integrate with respect to p. We obtain

$$\int F(p)\,e^{-ap}dp + C = \int_0^\infty f(t)\,dt \int e^{-p(t+a)}dp = -\int_0^\infty \frac{f(t)}{t+a}\,e^{-p(t+a)}dt\,.$$

From this follows the operational relation

$$-\frac{f(t)}{t+a} \doteq e^{ap}\left[C+\int e^{-ap}F(p)\,dp\right]. \tag{25}$$

The quantity C may be chosen arbitrarily, since it corresponds to adjoining to the function f(t)/(t+a), having a discontinuity at t = -a, the term cδ(t+a), defined only at the point of discontinuity. In the particular case when the function f(t)/(t=a) does not contain a discontinuity (for f(-a) + 0 and f'(-a) ≠ ∞), one must take C = 0.

Appendix II

We apply the inverse Laplace transform to the function $e^{\frac{a}{p}}=\sum_{i=0}^{\infty}\frac{a^i}{p^i i!}$ We obtain the operational relation

$$e^{\frac{a}{p}} \doteq \sum_{i=0}^{\infty}\frac{a^i t^i}{i!\,(i-1)!}\,,$$

for which the transformations

$$\sum_{i=0}^{\infty}\frac{a^i t^{i-1}}{i!\,(i-1)!} = \frac{|a|}{\sqrt{|a|\,t}}\sum_{i=0}^{\infty}\frac{(-1)^i}{i!\,(i-1)!}\left(2\sqrt{|a|\,t}\right)^{2i-1} = -\left(\frac{|a|}{t}\right)^{1/2} J_1\left(2\sqrt{|a|\,t}\right) \quad \text{for} \quad a<0,$$

$$\sum_{i=0}^{\infty}\frac{a^i t^{i-1}}{i!\,(i-1)!} = \frac{a}{\sqrt{at}}\sum_{i=0}^{\infty}\frac{1}{i!\,(i-1)!}\left(2\sqrt{at}\right)^{2i-1} = -\left(\frac{a}{t}\right)^{1/2} I_1\left(2\sqrt{at}\right) \quad \text{for} \quad a>0$$

lead to the operational relation

$$e^{\frac{a}{p}} \doteq \begin{cases} -\left(\frac{|a|}{t}\right)^{1/2} J_1\left(2\sqrt{|a|\,t}\right) & \text{for} \quad a<0, \\ -\left(\frac{a}{t}\right)^{1/2} I_1\left(2\sqrt{at}\right) & \text{for} \quad a>0. \end{cases} \tag{26}$$

Appendix III

We calculated the function $J(t, m, n)=\int_0^t \frac{e^{a\tau}(t-\tau)^m\tau^n}{\tau-c_0}\,d\tau$. Representing $(t-\tau)^m$ in the form of an expansion, we obtain

$$J(t,\ m,\ n) = \sum_{\mu=0}^{m}\binom{m}{\mu}(-1)^\mu t^{m-\mu}\int_0^t \frac{\tau^{\mu+n}}{\tau-c_0}\,e^{a\tau}d\tau\,. \tag{27}$$

The integral entering into (29) may be brought, after a series of transformations, into the form

$$\int_0^t \frac{\tau^{\mu+n}}{\tau-c_1}\,e^{a\tau}d\tau = e^{ac_0}\int_{-ac_0}^{a(t-c_0)}\frac{\left(\frac{x}{a}+c_0\right)^{\mu+n}}{x}\,e^x dx = \tag{28}$$

$$= e^{ac_0}c_0^{\mu+n}\left[\int_{-ac_0}^{a(t-c_0)}\frac{e^x}{x}\,dx + \sum_{\rho=1}^{\rho=\mu+n}\binom{\mu+n}{\rho}(ac_0)^{-\rho}\int_{-ac_0}^{a(t-c_0)} x^{\rho-1}e^x dx\right].$$

We calculate the definite integrals entering into (28):

$$\int_{-ac_0}^{a(t-c_0)} \frac{e^x}{x}\,dx = \int_{-\infty}^{ac_0} \frac{e^x}{x}\,dx - \int_{-\infty}^{a(t-c_0)} \frac{e^x}{x}\,dx = \overline{Ei}\,(at-ac_0) - \overline{Ei}\,(-ac_0),$$

$$\int_{-ac_0}^{a(t-c_0)} x^{\rho-1}e^x dx = e^{ac_0} \sum_{\nu=0}^{\nu=\rho-1} (-1)^\nu \frac{(\rho-1)!}{(\rho-1-\nu)!}\left[e^{at}(at-ac_0)^{\rho-1-\nu} - (-ac_0)^{\rho-1-\nu}\right].$$

Substituting them into (28), and afterwards into (27), we obtain finally

$$J(t, m, n) = \sum_{\mu=0}^{m} \binom{m}{\mu} (-1)^\mu t^{m-\mu} c_0^{\mu+n} \left\{ e^{ac_0}\left[\overline{Ei}\,(at-ac_0) - \overline{Ei}\,(-ac_0)\right] + \right.$$

$$\left. + \sum_{\rho=1}^{\rho=\mu+n} \binom{\mu+n}{\rho} c_0^{-\rho} \sum_{\nu=0}^{\nu=\rho-1} (-1)\, a^{-\nu-1} \frac{(\rho-1)!}{(\rho-1-\nu)!}\left[e^{at}(t-c_0)^{\rho-1-\nu} - (-c_0)^{\rho-1-\nu}\right]\right\}.$$

Tables for integral exponents of this function are given, for example in [5].

LITERATURE CITED

1. Ch'ien Hsüeh-sên, Technical Cybernetics [in Russian] Izd-vo inostr. liter., 1956.
2. A. S. Kel'zon, Dynamical Problems of Cybernetics [in Russian] Sudpromgiz, 1959.
3. E. Kamke, Handbook on Ordinary Differential Equations [Russian translation] Izd-vo inostr. liter., 1951.
4. B. Van der Pol and Bremmer, H. Operational Calculus of the Two-Sided Laplace Transformation [Russian translation] Izd-vo inostr. liter., 1952.
5. E. Jahnke and F. Emde, Tables of Functions with Formulas and Curves. Gostekhizdat, 1949.
6. I. M. Ryzhik, Tables of Integrals, Sums, Series, and Products. [in Russian] Gostekhizdat, 1948.
7. Fundamentals of Automatic Control Theory [in Russian] V. V. Solodovnikov, Editor.

PROBLEMS OF NONLINEAR FILTRATION

I. THE CASE OF ONE PARAMETER

I. A. Bol'shakov and V. G. Repin

(Moscow)

Translated from Avtomatika i Telemekhanika, Vol. 22, No. 4,
pp. 466-478, April, 1961
Original article submitted October 11, 1960

The problem is solved of the filtration of a random process (parameter) from a nonadditive mixture with another random process (the carrier signal for the parameter) under certain assumptions concerning both random processes. Operators are found that carry out the filtration; the applicability of the principle of feedback is shown in this realization. An example from radio technology is described.

There has been a great deal of work done on the linear filtration of a random process from an additive mixture with another random process, starting with the fundamental articles by Kolmogorov and Wiener. In practice, however, cases often occur when the function to be determined is in a nonadditive mixture with other signals. Thus the radiotechnological methods of measuring various quantities (frequency, signal delay, etc.) are essentially to separate a random variable from a misture with a signal of which it is the modulation parameter and with various types of interference. In a more common case, the elements of control systems are interconnected by channels in which the desired information is coded in the parameters of certain carrier signals. In the transmission process, the latter signals

fluctuate and are mixed with noise. Since these random disturbances are nonadditively mixed with the desired information, methods of reproducing the information can hardly be considered to be in the realm of linear theory. Methods for constructing filters in the general case will be discovered in the theory of statistical solutions, where it is not necessary to make any previous assumptions concerning the structure of these filters. Complete statistical information on the carrier signal and possibly on the parameter is needed, however.

In what follows, we will consider filtration to be the continuous measurement (estimation) of some random quantity which is a parameter of the received signal; in the general case the received signal is also random. In the present series of articles, we will solve the Bayes filtration problem when the a priori statistics of the parameter are known. Here we will consider the case when the signal depends on a single parameter with a Gaussian distribution. In subsequent articles we will consider the cases of many parameters, and cases of sampling depending on the estimate. Since we are mainly interested in practical applications, we will not aim to give the rigorour mathematical basis of all the results obtained.

1. The Design of a Nonlinear Filter

Let the function y(t) and one of its parameters $\lambda(t)$ at times $t_1, t_2, \ldots, t_n$ from the interval (t_0, t) take, respectively, the values $\{y_1, y_2, \ldots, y_n\} = \mathbf{y}$ and $\{\lambda_1, \lambda_2, \ldots, \lambda_n\} = \boldsymbol{\lambda}$. Let their joint probability density distribution be

$$P(y_1, y_2, \ldots, y_n \mid \lambda_1, \lambda_2, \ldots, \lambda_n) P_0(\lambda_1, \lambda_2, \ldots, \lambda_n) = P(\mathbf{y} \mid \boldsymbol{\lambda}) P_0(\boldsymbol{\lambda}),$$

where $P(\mathbf{y} \mid \boldsymbol{\lambda})$ is the conditional density distribution of $\mathbf{y}$ for given $\boldsymbol{\lambda}$ or the probability function [1,2] and $P_0(\boldsymbol{\lambda})$ is the a priori density distribution of the parameter. The filtration problem is to obtain a function $\lambda(t)$ from the selected values of y(t), where this function is the approximation to $\lambda(t)$, and is in some sense the best possible approximation to the real values of the parameter. In the theory of the solution, the closeness of this approximation is characterized by the "function loss," which is a minimum for agreement between the estimate and the real value of the parameter. The most common is the square function loss, which leads to the requirement of a minimum mean square error. We can see that in this case, $\boldsymbol{\lambda}^*$ satisfies the vector equation

$$\int (\boldsymbol{\lambda}^* - \boldsymbol{\lambda}) P(\mathbf{y} \mid \boldsymbol{\lambda}) P_0(\boldsymbol{\lambda}) d\boldsymbol{\lambda} = 0 \qquad \left(d\boldsymbol{\lambda} = \prod_{i=1}^{n} d\lambda_i\right), \tag{1}$$

the known formal solution of which is the conventional mathematical expectation $\boldsymbol{\lambda}$ for a given $\mathbf{y}$

$$\boldsymbol{\lambda}^* = \frac{\int \boldsymbol{\lambda} P(\mathbf{y} \mid \boldsymbol{\lambda}) P_0(\boldsymbol{\lambda}) d\boldsymbol{\lambda}}{\int P(\mathbf{y} \mid \boldsymbol{\lambda}) P_0(\boldsymbol{\lambda}) d\boldsymbol{\lambda}}. \tag{2}$$

However, except in the additive case ($y = \lambda + n$, where $n = n(t)$ is the interference), the integration in (2) cannot be carried out, and so the structure of the optimal operator remains unknown.

We note that in practice, only the case of a sufficiently accurate parameter measurement is of interest. It is natural, that for a relatively low interference level, the error made in measuring the parameter when an optimal operator is used will actually be small compared to the width of the a priori distribution. If we also take into account the fact that the rate of variation of the parameter $\lambda(t)$ is usually small in comparison with the rate of variation of the signal y(t) in which this parameter is coded, then $P(\mathbf{y} \mid \boldsymbol{\lambda})$ can be represented approximately in the form

$$P(\mathbf{y} \mid \boldsymbol{\lambda}) \approx \exp\left\{-L(\boldsymbol{\lambda}^*) + \mathbf{z}'(\boldsymbol{\lambda} - \boldsymbol{\lambda}^*) - \frac{1}{2}(\boldsymbol{\lambda} - \boldsymbol{\lambda}^*)' \mathbf{A} (\boldsymbol{\lambda} - \boldsymbol{\lambda}^*)\right\}, \tag{3}$$

where

$$L(\boldsymbol{\lambda}) = -\ln P(\mathbf{y} \mid \boldsymbol{\lambda}), \quad \boldsymbol{\lambda}, \ \boldsymbol{\lambda}^*; \qquad \mathbf{z} = (z_1, \ldots, z_n) = \left\{-\frac{\partial L(\boldsymbol{\lambda}^*)}{\partial \lambda_1}, \ldots, -\frac{\partial L(\boldsymbol{\lambda}^*)}{\partial \lambda_n}\right\}$$

is a columa vector, $\mathbf{A} = \|a_{ik}\| = \left\|\frac{\partial^2 L(\boldsymbol{\lambda}^*)}{\partial \lambda_i \partial \lambda_k}\right\|$ is a square matrix, and a' denotes the transpose. Thus the probability function, as a function of $\boldsymbol{\lambda}$, is approximated by a many-dimension Gaussian distribution near the point $\boldsymbol{\lambda}^*$ with coefficients depending on the realization y(t). The basis for such a substitution is the convergence of the logarithm of the probability function as a function of the parameter $\lambda(t)$ to a parabola, near the real value of $\lambda_0(t)$ for time intervals considerably longer than the correlation interval of y(t), but shorter than the time of variation of $\lambda(t)$. By assumption, such time intervals actually exist. It is clear that the expansion of the logarithm in a series can be carried out to a point close to $\lambda_0(t)$ that gives the same parabola.

The approximation (3) makes it possible to construct optimal filters for a whole series of important cases of parameter statistics. Of prime interest is the Gaussian distribution for λ:

$$P_0(\lambda) = (2\pi)^{-n/2} \det^{-1/2} \mathbf{R} \exp\left[-\frac{1}{2}(\lambda - \overline{\lambda})' \mathbf{V} (\lambda - \overline{\lambda})\right], \tag{4}$$

where $\mathbf{R} = \|R(t_i, t_k)\|$ is the correlation matrix of $\lambda(t)$, $\mathbf{V} = \mathbf{R}^{-1}$ the inverse matrix, and $\overline{\lambda} = \{\overline{\lambda}_1, \overline{\lambda}_2, \ldots, \overline{\lambda}_n\}$ the column vector of mean values.

If we substitute (3) and (4) in (1), we obtain the result:

$$\lambda_n^* = \sum_{k=1}^{n} c_{nk}\left[z_k + \sum_{i=1}^{n} a_{ki}(\lambda_i^* - \overline{\lambda}_i)\right] + \overline{\lambda}_n, \tag{5}$$

where c_{nk} is an element of the matrix $\mathbf{C}$, which is the inverse of the matrix $\mathbf{V} + \mathbf{A}$ in the interval (t_0, t_n). The equality (5) related the estimate at the last instant of time $t = t_n$ with its values at all the preceding instants. In (3), (5), etc., the estimate of λ_k^* for the times $t_k (k = 1, \ldots, n)$ is formed according to the realization of $y(t)$ in the interval (t_0, t_k), which corresponds to the requirement of physical realizability of the operators sought. If the choice of $y(t)$ is discrete then (5) is already the solution to the problem, while is the realization of $y(t)$ is continuous, we introduce new functions by the relations

$$C(t_n, t_k) = c_{nk}, \quad \int_{t_k - \Delta t/2}^{t_k + \Delta t/2} Z(t)\,dt = z_k, \quad \int_{t_k - \Delta t/2}^{t_k + \Delta t/2} d\tau \int_{t_i - \Delta t/2}^{t_i + \Delta t/2} ds\, A(\tau, s) = a_{ki} \tag{6}$$

and transform (5) from a summation to an integral by carrying out the limiting processes $t_{i+1} - t_i = \Delta t \to 0$, $n \to \infty$ $(i = 1, 2, \ldots, n;\ n\Delta t = t - t_0)$, which yields

$$\lambda^*(t) = \int_{t_0}^{t} C(t, \tau)\left\{Z(\tau) + \int_{t_0}^{t} A(\tau, s)[\lambda^*(s) - \overline{\lambda}(s)]\,ds\right\} d\tau + \overline{\lambda}(t). \tag{7}$$

The physical interpretation of the relation (7) is shown in the block diagram in Fig. 1. The given realization is led to the element 1, which forms the quantity $Z(t)$ equal to the mismatch between $\lambda(t)$ and $\lambda^*(t)$. The element 1 can thus be appropriately named the discriminator. Simultaneously, $y(t)$ is lead to the elements 2 and 3 for the formation of the impulse reactions $C(t, \tau)$ and $A(t, \tau)$ of the linear variable of the filters. The output of the element 2 is added to the quantity $\overline{\lambda}(t)$, and the result led to the elements 1, 2, and 3 for the adjustment of their parameters. The output of 2 also passes through the filter 3, is combined with the output of the discriminator 1, and the result is again led to the filter 2. This system is essentially a self-regulating system, the characteristics of the elements of which depend on the form of the realization $y(t)$. It can be seen that the variations of the characteristics of the filters 2 and 3 tend to decrease the influence of the filtration component at the output of the discriminator, the strength of which increases with increasing mismatch $\epsilon = \lambda - \lambda^*$. Such a component occurs both in basic radiotechnical measurements of a parameter and in the system we are considering. When the noise is strong enough, however, this component does not play an important part. We can therefore reject the formation of the filters 2 and 3 by using the given realization, and using instead of $A(t, \tau)$ its mean value obtained from the over-all properties of $y(t)$, known to us a priori. In this case, the dotted line in Fig. 1 can be omitted, and we obtain a considerable simplification of the scheme of solution. If we use the assumption concerning the smallness of the mismatch and the rate of variation of the signal, we can set

$$\frac{\partial^2 L(\lambda^*)}{\partial\lambda_i\,\partial\lambda_k} \approx \frac{\partial^2 L(\lambda)}{\partial\lambda_i\,\partial\lambda_k} \approx \overline{\frac{\partial^2 L(\lambda)}{\partial\lambda_i\,\partial\lambda_k}} \approx K\Delta t\,\delta_{ik}; \quad A(t, \tau) = K\delta(t - \tau), \tag{8}$$

where the bar denotes the mean over the set of values of $y(t)$, and K is a coefficient which is determined from the coding of the parameter in the signal and the statistics of $y(t)$, and which, under rather general conditions, is independent of the time and the measured parameter (see section 2).

When we solve (7) for $\lambda^*(t)$, we obtain

$$\lambda^*(t) = \int_{t_0}^{t} G(t, \tau) Z(\tau)\,d\tau + \overline{\lambda}(t), \tag{9}$$

where the impulse reaction G(t, τ) from (7) and (8) satisfies

$$C(t, \tau) + K\int_{\tau}^{t} C(t, s)\, G(s, \tau)\, ds = G(t, \tau). \tag{10}$$

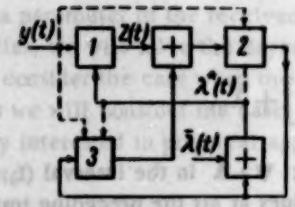

Fig. 1. Block diagram of a nonlinear filter: 1) discriminator; 2) filter with impulse reaction C(t, τ); 3) filter with impulse reaction A(t, τ)

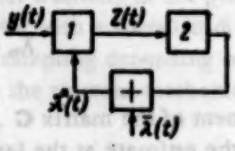

Fig. 2. Simplified single-loop system: 1) discriminator; 2) smoothing circuit.

Since $\mathbf{C} = [\mathbf{V} + \mathbf{A}]^{-1} = [\mathbf{V} + K\Delta t\mathbf{I}]^{-1}$, where $\mathbf{I}$ is the unit matrix, then C(t, τ), in its turn satisfies the equation

$$C(t, \tau) + K\int_{t_0}^{t} C(t, s)\, R(s, \tau)\, ds = R(t, \tau). \tag{11}$$

A similar relation also holds for the discrete case.

The expression (9) shows that under the assumptions made, an optimum nonlinear filter is a single-loop servo system (Fig. 2) with a nonlinear discriminator which isolates the derivative from the logarithm of the probability function for λ(t) at the point $\lambda^*(t)$. The system is closed by linear smoothing units with impulse reaction G(t, τ) depending on the correlation function R(t, τ) of the parameter, and through the coefficient K on the statistics of y(t). It will be shown, in what follows, that the smoothing units are linear only for Gaussian parameter distributions.

In general, Z(t) depends nonlinearly on $\epsilon = \lambda - \lambda^*$, but if the probability is high that the quantity ε(t) is small, then for the analysis of the accuracy of measurement we can set

$$Z(t_i) = \lim_{\Delta t \to 0} \frac{1}{\Delta t} \frac{\partial L(\lambda^*)}{\partial \lambda_i} \approx \lim_{\Delta t \to 0} \frac{1}{\Delta t} \left[\frac{\partial L(\lambda)}{\partial \lambda_i} + \sum_k \frac{\overline{\partial^2 L(\lambda)}}{\partial \lambda_i \partial \lambda_k} (\lambda_k^* - \lambda_k) \right] = \tag{12}$$

$$= \xi(t_i) + K\varepsilon(t_i),$$

where ξ(t) is the fluctuation component, which is not dependent on $K\delta(t_1 - t_2)$. Here the spectral density of the fluctuations ξ(t)/K, converted to a value of the parameter, is evidently equal to 1/K, so that K characterizes the signal/interference ratio in the discriminator. We also note that the quantity 1/KT is the dispersion of the estimate of the probability maximum of the parameter λ, which can be obtained from the realization y(t) after a time T, if the parameter is constant during this time.

From (9) and (12) it is easy to see that KC(t, τ) is the impulse reaction of some linear system which is equivalent to the system in Fig. 2 for small mismatch. To the input of the equivalent system is lead the total "signal" $\lambda(t) - \bar{\lambda}(t)$ and the "interference" ξ(t)/K converted to a value of the parameter. Thus with the neglect of a fluctuation component proportional to the mismatch, for small ε(t) the parameter and the interference are additive and independent to an equivalent degree. If we take into account the fact that the parameter has a Gaussian distribution, then in the light of what has been said, it becomes clear why the equation (11) coincides with the equation for a Wiener filter, for the isolation of a parameter with correlation function R(t, τ) from a mixture with white noise with a spectral density 1/K for a finite time of observation (t_0, t). The main difference from the Wiener filter is the presence in the scheme in Fig. 2 of a doubly nonlinear discriminator element (for the input signal y(t)) and the necessity in principle of the feedback, which shifts that part of the discriminator characteristic that is linear with respect to the parameter, immediately following a variation in the parameter.

When we use (9)-(12), we obtain the following expressions for the mean value and the correlation function of $\lambda^*(t)$:

$$\overline{\lambda^*(t)} = \overline{\lambda(t)},\ \overline{[\lambda^*(t_1) - \overline{\lambda(t_1)}][\lambda^*(t_2) - \overline{\lambda(t_2)}]} = R(t_1, t_2) - C(t_1, t_2).$$

Finally, the error of measurement of the parameter has the variance

$$\sigma^2_{\text{out}}(t) = \overline{\varepsilon^2(t)} = C(t, t). \tag{13}$$

2. Discriminator Characteristics

The results obtained above determine the operations carried out by the discriminator in the formation of the function Z(t), this function being a measure of the current mismatch and also of its basic characteristic, i.e., the quantity K; but in practice these operations depend on the statistics of y(t) and the method by which they are coded in the parameter $\lambda(t)$. Certain general considerations can, however, be introduced, that make it possible to use a model for a quick determination of the operation of the discriminator and of its characteristics in the most interesting practical cases.

If we ignore difficulties concerning the limiting transitions, the logarithm of the probability functional can always be written in the form

$$L_{(t_0, t)}(y, \lambda) = \int_{t_0}^{t} l(y, \lambda; \tau)\, d\tau, \tag{14}$$

where $l(y, \lambda, \tau)$ depends in principle on the realizations y(t) and $\lambda(t)$ in the interval (t_0, τ), but in actuality only on the values of y(t) and $\lambda(t)$ in an internal of the order of the correlation time τ_y of the signal y(t) preceding the time τ. According to the assumption concerning the relation between the rate of change of the signal and the parameter, during this interval $\lambda(t)$ maintains an almost constant value which determines the function $l(y, \lambda; t)$ in the interval $(t - \tau_y, t)$, but has no influence on its value for other time intervals. On the basis of these considerations, it can be seen that Z(t) is statistically equivalent to the derivative of $-l(y, \lambda; t)$ with respect to λ for a constant value of λ equal to the value of the estimate $\lambda^*(t)$ for the given time; i.e., the operation of the discriminator for optimal measurement reduces to the formation of the quantity

$$Z(t) = -\frac{\partial l(y, \lambda^*(t); t)}{\partial \lambda}. \tag{15}$$

from the values of the signal realization y(t) that have been taken, and from the current estimate $\lambda^*(t)$.

The quantity K characterizing the optimal discriminator is here given by the formula

$$K = \lim_{T \to \infty} \frac{1}{T} \int_0^T \overline{\frac{\partial^2 l(y, \lambda; t)}{\partial \lambda^2}}\, dt. \tag{16}$$

The operation (15) can be realized physically in several ways. First of all, in certain cases, the derviative of $l(y, \lambda; t)$ can be formed exactly. Secondly, in practice we can replace the derivative by the difference

$$Z(t) \approx \frac{1}{\Delta\lambda}\left[l\left(y, \lambda^* + \frac{\Delta\lambda}{2}; t\right) - l\left(y, \lambda^* - \frac{\Delta\lambda}{2}; t\right)\right];$$

i.e., in the measuring device we use two channels which form $l(y, \lambda; t)$ at distances of $\pm\Delta\lambda/2$ from the value of the parameter being considered. We note that each of these channels is an ordinary optimal receiver for the signal $y(t, \lambda)$ without final integration [2]. It is also possible to use only one channel which is successively shifted in both directions from $\lambda^*(t)$. All approximate methods must be evaluated relative to the characteristics they give compared with the characteristics of an optimal discriminator that forms Z(t) accurately.

Since we have not yet chosen any definite parameter form or any system by which it may be coded, we will now give some examples of the representation of the logarithm of the probability functional in the form (14). The realization of the operation for the formation of Z(t) by using (15) or one of the approximate methods will be almost obvious.

A. A regular signal $v(t, \lambda)$ in white noise with a spectral density N_0. Here

$$l(y, \lambda; t) = \frac{1}{2N_0}[y(t) - v(t, \lambda)]^2; \quad K = \lim_{T\to\infty}\frac{1}{TN_0}\int_0^T\left[\frac{\partial v(t, \lambda)}{\partial\lambda}\right]^2 dt.$$

There is no difficulty in generalizing this to the case of correlated noise.

B. A noncoherent signal in white noise. The case of a periodically modulated signal with independent, random phases of a high-frequency filler in each modulation period T_r is sufficiently well known [2]. For sufficiently large values of the signal/noise ratio, the quantity $l(y; \lambda; t)$ coincides with the voltage envelope at the output of the adjusted filter [2], and for a symmetric signal spectrum the quantity K is given by

$$K = \frac{1}{N_0T_r}\int_0^{T_r}\left\{\left[\frac{\partial u(t, \lambda)}{\partial\lambda}\right]^2 + u^2(t, \lambda)\left[\frac{\partial\psi(t, \lambda)}{\partial\lambda}\right]^2\right\}dt,$$

where $u(t, \lambda)$ is the amplitude and $\psi(t, \lambda)$ the phase-modulation of the signal.

C. A fluctuating signal in normal noise. In practice, the most interesting case is that of a normal, fluctuating, high-frequency signal, with arbitrary amplitude modulation $u(t, \lambda)$ and phase modulation $\psi(t, \lambda)$, and with a correlation function equal to $R_c(t_1, t_2) = u(t_1, \lambda)\,u(t_2, \lambda)\cos[\omega_0(t_1 - t_2) + \psi(t_1, \lambda) - \psi(t_2, \lambda)]\,\rho(t_1 - t_2)$,

where $\rho(t_1 - t_2) = \frac{1}{2\pi}\int_{-\infty}^{+\infty} S_c(\omega)\cos\omega(t_1 - t_2)\,d\omega$ is the correlation-signal envelope in the absence of modulation and $S_c(\omega)$ is the corresponding spectral density. If the function $\rho(t)$ varies slowly in comparison with $u(t, \lambda)$ and $\psi(t, \lambda)$, then neglecting terms that are independent of λ, we can write

$$l(y, \lambda; t) =$$

$$= \left[\int_{-\infty}^{t} h(t-\tau)\cos\omega_{arb}(t-\tau)\,y(\tau)\,u(\tau, \lambda)\cos[(\omega_0+\omega_{arb})\tau + \psi(\tau, \lambda)]\,d\tau\right]^2. \tag{17}$$

Here the function h(t), representing the impulse reaction of a filter, has the square of the absolute value of its frequency characteristic given by the expression

$$|H(i\omega)|^2 = \frac{8}{N_0}\frac{S_c(\omega)/2N_0}{1 + S_c(\omega)/2N_0}, \tag{18}$$

and an arbitrary phase characteristic, $u(t, \lambda)$ is normalized so that $\lim_{T\to\infty}\frac{1}{T}\int_0^T u^2(t, \lambda)\,dt = 1$, and ω_{arb} is an arbitrary intermediate frequency. The quantity K for this case is given by

$$K = \left\{\lim_{T\to\infty}\frac{1}{T}\int_0^T\left[\left(\frac{\partial u(t, \lambda)}{\partial\lambda}\right)^2 + u^2(t, \lambda)\left(\frac{\partial\psi(t, \lambda)}{\partial\lambda}\right)^2\right]dt - \right. \tag{19}$$

$$\left. -\left[\lim_{T\to\infty}\frac{1}{T}\int_0^T u^2(t, \lambda)\frac{\partial\psi(t, \lambda)}{\partial\lambda}\,dt\right]^2\right\}\frac{1}{\pi}\int_{-\infty}^{+\infty}\frac{(S_c(\omega)/2N_0)^2}{1 + S_c(\omega)/2N_0}\,d\omega.$$

3. The Characteristics of Smoothing Circuits

Although the methods of designing Wiener filter are known for several cases (see, for example [3]), the representation of the filters in the form of servo systems can be used to obtain the known results by new methods, and also to obtain some new results.

A. The parameter a linear combination of known functions with random coefficients [3]. Let $\lambda(t) = \mu f(t) + \overline{\lambda}(t)$, where $f(t)$, $\overline{\lambda}(t)$ are known functions and μ is a normally distributed function for which $\overline{\mu} = 0$, $\overline{\mu^2} = \sigma^2$ so that

$$R(t_1, t_2) = \sigma^2 f(t_1) f(t_2).$$

The relation (11) is now an integral equation with a degenerate kernel, having the solution

$$C(t, \tau) = \frac{\sigma^2 f(t) f(\tau)}{1 + K\sigma^2 \int_{t_0}^{t} f^2(s)\, ds}.$$

Thus the error in measuring the parameter $\sigma_{out}(t)$ always tends to zero for increasing t:

$$\sigma^2_{out}(t) = \frac{\sigma^2 f^2(t)}{1 + K\sigma^2 \int_{t_0}^{t} f^2(s)\, ds}.$$

The impulse reaction G(t, τ) of the smoothing unit, according to (11) is given by

$$G(t, \tau) = \frac{\sigma^2 f(t) f(\tau)}{1 + K\sigma^2 \int_{t_0}^{\tau} f^2(s)\, ds}.$$

The smoothing consists of multiplying the output of the discriminator $Z(\tau)$ by the function $f(\tau)/\left[1 + K\sigma^2 \int_{t_0}^{\tau} f^2(s)\, ds\right]$ (Fig. 3) and then integrating. As a result, we obtain the value of the coefficient μ, which can be used as a multiplier for the law of variation of the parameter f(t) generated by the system. After adding $\bar{\lambda}(t)$, we obtain an estimate of $\lambda(t)$.

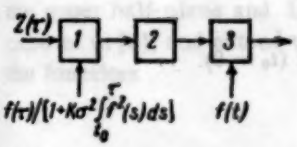

Fig. 3. The smoothing unit for a parameter in the form $\lambda(t) = \mu f(t) + \bar{\lambda}(t)$: 1) multiplier; 2) integrator; 3) multiplier.

The gradual "switching off" of the discriminator is typical of this setup, and the larger the value of K, the more rapidly this takes place. The law of variation $\lambda(t)$ is known except for a multiplying factor, and so a finite realization interval is sufficient to predict the behavior of the parameter at all succeeding times. During this interval the main error has already been eliminated, and only very large overshoots will correct the estimate.

We now consider the general case where $\lambda(t) = \sum_{k=1}^{m} \mu_k f_k(t) + \bar{\lambda}(t)$, with $f_1(t), \ldots f_m(t)$ known linearly independent functions and μ_k random coefficients for which $\bar{\mu}_i = 0$, $\overline{\mu_i \mu_j} = S_{ij}$ (i, j = 1, . . . , m), and we find that

$$R(t, \tau) = \sum_{i, j=1}^{m} S_{ij} f_i(t) f_j(\tau) = \mathbf{f}'(t)\, \mathbf{S}\mathbf{f}(\tau),$$

where $\mathbf{f}(t) = \{f_1(t), \ldots, f_m(t)\}$ is a column vector and $\mathbf{S} = |S_{ij}|$ is a square matrix. The solution (11) has the form

$$C(t, \tau) = \mathbf{f}'(t)\, [\mathbf{I} + \mathbf{S}\mathbf{U}(t)]^{-1}\, \mathbf{S}\mathbf{f}(\tau), \tag{20}$$

where $\mathbf{U}(t) = \left| K \int_{t_0}^{t} f_j(s) f_i(s)\, ds \right|$. Then from the equation (10) we obtain

$$G(t, \tau) = \mathbf{f}'(t)\, [\mathbf{I} + \mathbf{S}\mathbf{U}(\tau)]^{-1}\, \mathbf{S}\mathbf{f}(\tau). \tag{21}$$

It follows from (21) that the smoothing unit consists of m parallel channels. In the kth channel the function Z(t) is multiplied by a function depending on all the functions $f_i(\tau)$ (i = 1, . . . , m) and on K, the resulting function is integrated, and the result of this integration is multiplied by $f_k(t)$. All m outputs are then added, together with $\bar{\lambda}(t)$.

B. The parameter a stationary process. This case has been more thoroughly investigated than any other, because of its great theoretical and practical interest. For a finite time of observation, C(t, τ) is obtained by methods described in [3]. If the time of observation exceeds the correlation interval of the parameter, then if we let t_0 tend to $-\infty$ and try to find $C(t, \tau) = C(t - \tau)$, the relation (11) yield the well known Wiener-Hopf equation

$$C(t) + K \int_{0}^{\infty} C(\tau)\, R(t - \tau)\, d\tau = R(t) \quad (t > 0). \tag{22}$$

The physical realization of the solution (22) has the form [3]

$$C(i\omega) = \frac{1}{\Psi(i\omega)}\left[\frac{S(\omega)}{\Psi(-i\omega)}\right]_+ = \frac{1}{2\pi\Psi(i\omega)}\int_0^\infty e^{-i\omega t}\,dt\int_{-\infty}^{+\infty}\frac{S(u)}{\Psi(-iu)}e^{iut}\,du, \tag{23}$$

where

$$C(i\omega) = \int_0^\infty C(t)\,e^{-i\omega t}\,dt,\ S(\omega) = \int_{-\infty}^{+\infty} R(t)\,e^{-i\omega t}\,dt,\ \Psi(i\omega)\,\Psi(-i\omega) = 1 + KS(\omega) \tag{24}$$

is a special representation (factorization) as a product of factors with zeros and poles in the upper and lower complex half-plane, respectively. Such a representation is possible everywhere, for example if $S(\omega)$ is a rational function of ω^2. The operation $[\ ]_+$ is the separation of that part of the expression in brackets that has a pole in the upper ω half-plane; analytically, this is expressed by using the two integrals in (23).

C. The parameter is a Wiener process, i.e. the integral of white noise. Its correlation function is

$$R(t, \tau) = B\min(t, \tau) \qquad (B = \text{const}).$$

In this case, when we differentiate (11) with respect to τ we obtain

$$\frac{\partial^2}{\partial\tau^2}C(t, \tau) - KBC(t, \tau) = 0,$$

the solution of which is

$$C(t, \tau) = \sqrt{\frac{B}{K}}\frac{\sinh\sqrt{BK}\tau}{\cosh\sqrt{BK}t}; \qquad \sigma^2_{out}(t) = \sqrt{\frac{B}{K}}\tanh\sqrt{BK}\,t \quad (t_0 = 0).$$

in the region $\tau < t$.

After a period of $(t < (BK)^{-1/2})$, of the regime with $\sigma^2_{out}(t)$ increasing like the variance for the parameter Bt, a regime is established in which

$$\sigma^2_{out}(t) \approx \lim_{t\to\infty}\sigma^2_{out}(t) = \sqrt{B/K}. \tag{25}$$

From (10), the impulse reaction of the smoothing units is

$$G(t, \tau) = \sqrt{B/K}\tanh\sqrt{BK}\tau. \tag{26}$$

Because of the previous knowledge of the continuity of $\lambda(t)$ and the zero initial error of measurement, the output of the discriminator for $\tau < (BK)^{-1/2}$ is suppressed. For $\tau \gg (BK)^{-1/2}$ the smoothing becomes a constant amplification and integration, and $C(t, \tau)$ tends to

$$\sqrt{B/K}\exp\{-\sqrt{BK}(t-\tau)\}. \tag{27}$$

Thus the use of one integrator in the smoothing circuit of a servo system, often occurring in practice, is optimal for a parameter in the form of a Wiener process.

D. The parameter a process with stationary growth. In C (para. 4), for a nonstationary process with a long observation time, the filter appeared to be particularly simple in the case of the class of circuits with constant parameters.

Since a Wiener process is a particular case of processes with stationary parameters [4], it is natural in the case of stationary parameters to seek general algorithms for obtaining limiting operators.

For a process with stationary parameters of the kth order, the statistical characteristics of the kth difference

$$\Delta^k_\tau x(t) = \sum_{m=0}^{k}\binom{k}{m}(-1)^m x(t - m\tau)$$

are independent of the time. The spectral density $S(\omega)$ of such a process is defined by the relation

$$\overline{[\Delta^k_{\tau_1} x(t_1) - \overline{\Delta^k_{\tau_1} x(t_1)}]\,[\Delta^k_{\tau_2} x(t_2) - \overline{\Delta^k_{\tau_2} x(t_2)}]} = d(t_1 - t_2;\ \tau_1, \tau_2) = \tag{28}$$

$$= \frac{1}{2\pi}\int_{-\infty}^{+\infty} e^{i\omega(t_1-t_2)}\left(1 - e^{-i\omega\tau_1}\right)^k \left(1 - e^{i\omega\tau_2}\right)^k S(\omega)\, d\omega.$$

The transition in (27) to the limit for $\tau_1, \tau_2 \to 0$ gives the relation between $S(\omega)$ and the correlation function $\rho(t_1 - t_2)$ of the kth derivative of $x(t)$

$$\lim_{\tau_1,\ \tau_2 \to 0} \frac{d(t_1 - t_2;\ \tau_1, \tau_2)}{\tau_1^k \tau_2^k} = \overline{\frac{d^k}{dt_1^k} x(t_1) \frac{d^k}{dt_2^k} x(t_2)} = \rho(t_1 - t_2) = \tag{29}$$

$$= \frac{1}{2\pi}\int_{-\infty}^{\infty} e^{i\omega\,(t_1 - t_2)} \omega^{2k} S(\omega)\, d\omega.$$

In (11), we replace the function $R(t, \tau)$ by its expression in terms of $\rho(t_1 - t_2)$:

$$R(t, \tau) = \int_{t_0}^{t} dt_1 \int_{t_0}^{\tau} dt_2\, (t - t_1)^{k-1} (\tau - t_2)^{k-1} \rho(t_1 - t_2).$$

We further set $t_0 = -\infty$, and seek $C(t, \tau)$ in the form $C(t - \tau)$. When we take the Fourier transform and use (29), we find that $C(i\omega)$ is expressed by the same formula (23). Here the factorization (24) involves the representation of the factor ω^{2k} in the denominator of $S(\omega)$ in the form $(i\omega)^k(-i\omega)^k$, where $1/(i\ \omega)$ is formally assumed to be a pole in the upper half-plane and $1/(-i\omega)$ a pole of the lower ω half-plane. For the justification of this method we can proceed as in [3], and extend the class of functions differing from zero on the half-axis $(0 \leq t < +\infty)$, by the addition of the functions

$$f_m(t) = \begin{cases} t^m & t \geqslant 0 \\ 0 & 0 < 0 \end{cases} \qquad (m = 1, 2, \ldots)$$

and introduce similar function on the half-axis $(-\infty < t \leq 0)$. For example, in the case of the Wiener process,

$$1 + KS(\omega) = 1 + \frac{BK}{\omega^2} = \frac{\sqrt{BK} + i\omega}{i\omega} \frac{\sqrt{BK} - i\omega}{-i\omega},$$

and so from (23) we have

$$C(i\omega) = \frac{-i\omega}{\sqrt{BK} + i\omega}\left[\frac{B}{i\omega\left(\sqrt{BK} - i\omega\right)}\right]_+ = \sqrt{\frac{B}{K}} \frac{1}{\sqrt{BK} + i\omega},$$

and this agrees with the Fourier transform (27).

For another example, we can consider the process obtained by taking the double integral of white noise with a spectral density $D(S(\omega) = D/\omega^4)$. It can be seen that

$$C(i\omega) = \left(\frac{4D}{K^3}\right)^{1/4} \frac{i\omega + (KD/4)^{1/4}}{(i\omega)^2 + (4KD)^{1/4} i\omega + (KD)^{1/2}}, \tag{30}$$

and so σ^2_{out} is equal to $(4D/K^3)^{1/4}$. In this case, the smoothing units have the transfer function

$$\sqrt{\frac{D}{K}} \frac{1 + (4/KD)^{1/4} p}{p^2},$$

i.e. they consist of a double integrator and a correlating RC-circuit with constant time $(4/KD)^{1/4}$. Such smoothing filters are very often applied in practice, but the conditions for their optimization are still unknown.

E. The mixed case. It is sometimes important to represent the parameter as a combination of two terms—a linear combination of known functions with random coefficients and a certain nondegenerate process (for example, with stationary growth) with correlation function $r(t, \tau)$. Then

$$R(t, \tau) = \sum_{i,\ j=1}^{m} \sum S_{ij} f_i(t) f_j(\tau) + r(t, \tau),$$

where we will assume that $r(t, t) \ll \sum_{i,j} S_{ij} f_i(t) f_j(t)$. To a first approximation, the equation (11) takes the same form as in A (para. 4), with the solution $C_1(t,\tau)$ given by (20). For a second approximation $C_2(t,\tau)$ we have

$$C_2(t, \tau) + K\int_{t_0}^{t} C_2(t, s)\, r(s, \tau)\, ds = r(t, \tau) - \int_{t_0}^{t} C_1(t, s)\, r(s, \tau)\, ds. \tag{31}$$

When $t - t_0 \to \infty$, the term containing $C_1(t,\tau)$ vanishes in (31) as well as in all subsequent approximations to $C(t,\tau)$. The smoothing circuits in this case can be approximately realized by two parallel channels: a channel for estimating the linear combination, which is gradually disconnected from the discriminator, and a channel for maintaining the nondegenerate process. The outputs of these channels are combined. For processes with stationary growth in a steady regime, the second channel contains circuits with constant parameters.

4. A Practical Example

We consider a radio transmission of random information coded in the delay of a harmonic frequency modulation. When there are fluctuations, the correlation function of the signal (see B of para. 3) is

$$R_c(t_1, t_2) = \rho(t_1 - t_2)\cos\left[\omega_0(t_1 - t_2) + \frac{\omega_m}{\Omega}(\sin\Omega(t_1 - \lambda) - \sin\Omega(t_2 - \lambda))\right],$$

where ω_m and Ω are the amplitude and frequency of the modulation, and λ is the measured delay. According to (15) and (17), the operation of the discriminator is described by the formula

$$Z(t) = \left\{\int_{-\infty}^{t} h(t-\tau)\cos\omega_{int}(t-\tau)\, y(\tau)\cos\left[(\omega_0 + \omega_{int})\tau + \frac{\omega_m}{\Omega}\sin\Omega(\tau - \lambda^*)\right] d\tau\right\} \times$$

$$\times\left\{\int_{-\infty}^{t} h(t-\tau)\cos\omega_{int}(t-\tau)\, y(\tau)\,\omega_m\cos\Omega(\tau-\lambda^*)\sin\left[(\omega_0+\omega_{int})\tau + \frac{\omega_m}{\Omega}\sin\Omega(\tau-\lambda^*)\right] d\tau\right\}$$

and an exact realization can be obtained in the form of that part of the block diagram in Fig. 4 within the dotted lines. The signal is combined in two mixers 1 and 2 with the heterodyne signals from the heterodyne generator 16 with a phase shift of $\pi/2$, obtained by the phase-changer 15, and with identical frequency modulation with delay time corresponding to the measured value of λ^* and imposed by the control delay line 17. In one of the channels there is also a mixer 3 with frequency ChM, which transmits to the intermediate frequency ω_{interm} the ChM side bands that arise at the output of the mixer 2 for the mismatch between λ and λ^* with a strength proportional to $\lambda - \lambda^*$. There are also filters 4 and 5 with frequency characteristics (18) tuned to the intermediate frequency. In the phase detector 6, the error Z(t) is obtained from the filter outputs. The quantity K which characterizes the operation of the discriminator, in the case of a signal with a rectangular fluctuation spectrum of width Δf_c is, according to (19),

$$K = \frac{h^2}{1+h}\,\omega_m^2\,\Delta f_c, \tag{32}$$

where $h = P_c/2N_0\Delta f_c$ is the signal/noise ratio in the signal band and $P_c = \rho(0) = \frac{1}{2\pi}\int_{-\infty}^{+\infty} S_c(\omega)\, d\omega$.

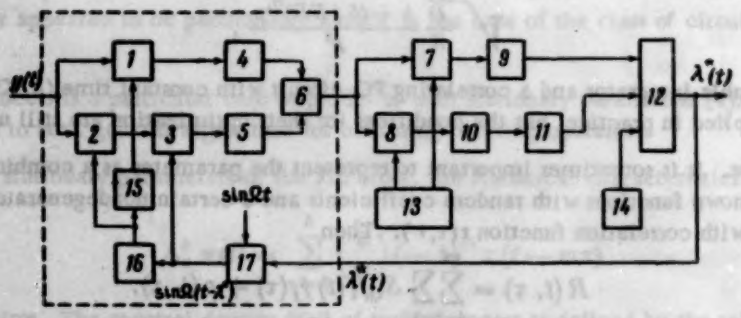

Fig. 4. Block diagram of the delay-measuring unit.

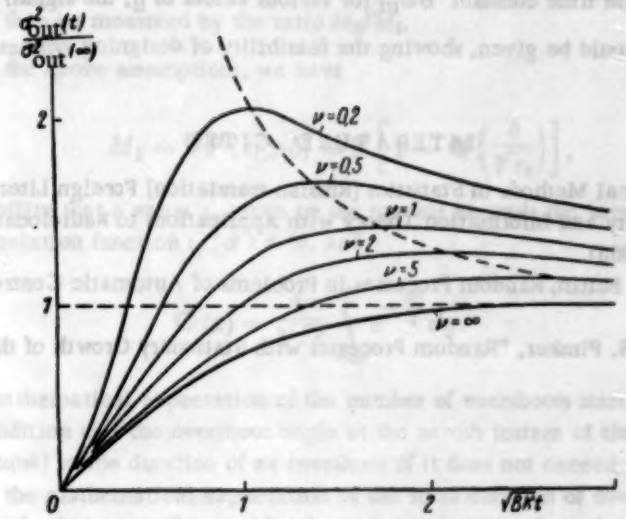

Fig. 5. Dependence of the delay-measurement error on the time

Let the measured quantity vary according to the law $\lambda(t) = \overline{\lambda(t)} + \mu t + \xi(t)$, where $\overline{\lambda(t)}$ is the known mean value, μ a random, normally distributed variable ($\bar{\mu} = 0$, $\overline{\mu^2} = \sigma^2$), and $\xi(t)$ a Wiener process with variance Bt. Then the impulse reaction of the smoothing units, according to (10) and (11) is

$$G(t,\tau) = \sqrt{\frac{B}{K}} \frac{\sinh\sqrt{BK}\tau \exp\left\{\int\limits_{\sqrt{BK}\tau}^{\sqrt{BK}t} \frac{\sinh s\, ds}{\cosh s - \sinh s \left(s + \frac{\sqrt{B^3K^1}}{\sigma^3}\right)^{-1}}\right\}}{\cosh\sqrt{BK}t - \sinh\sqrt{BK}t \left(\sqrt{BK}t + \frac{\sqrt{B^3K}}{\sigma^3}\right)^{-1}} \qquad (33)$$

and it is realized approximately by the remaining part of the block diagram in Fig. 4. The discriminater output is led to the tracking channel and the channel for evaluating the velocity. The channels have controllable amplifiers 7 and 8, and integrators 9, 10, and 11.

The tracking channel is gradually triggered, while the estimation channel is gradually disconnected from the discriminator. The element 13 controls the amplifier, and the programming mechanism 14 introduces the mean value which is summed in 12 with the outputs of the two channels. The output of 12 is the estimate of $\lambda(t)$, and is led to the discriminator, thus closing the system.

By using (11) and (13), we obtain the variance of the measurement error

$$\sigma^2_{out}(t) = \sqrt{B/K}\left\{\coth\sqrt{BK}t - 1/\left[\sqrt{BK}t + (B^3t)^{1/3}/\sigma^2\right]\right\}^{-1}, \qquad (34)$$

where $\sqrt{B/K} = \sigma^2_{out}(\infty)$ is the steady variance, and $v = (B^3K)^{\frac{1}{2}}/\sigma^2$ is the ratio of $\sigma^2_{out}(\infty)$ to the variance of the linear term μt through the interval $(BK)^{-1/2}$, equal to the time for the establishment of a steady state in the system and calculated only for the Wiener process. In the steady smoothing regime, the system becomes a simple integrator with the introduction of a mean value, and for $\sigma_{out}(\infty)$, from (32) and (34) we obtain the formula

$$\sigma_{out}(\infty) = \left[\frac{B}{\Delta f_c \omega_m^2}\,\frac{1+h}{h^2}\right]^{1/4}. \qquad (35)$$

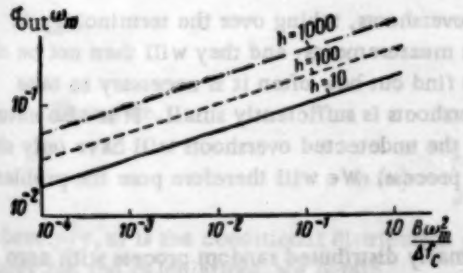

Fig. 6. The dependence of delay-measurement error on the parameter variance and the signal/noise ratio.

Figure 5 shows the time dependence of $\sigma^2_{out}(H/\sigma^2_{out}(\infty))$ for some values of $\nu=(B^3K)^{\frac{1}{2}}/\sigma^2$, obtained from (34). The dotted curves show the geometrical location of the maximal values and the asymptotic value. Figure 6 shows the relation of $\sigma_{out}\omega_m$ and the ratio of the growth $B/\Delta f_c$ of the a priori variance in the correlation interval of the

signal to the square of the ChM time constant $1/\omega_m^2$ for various values of h, the signal/noise ratio.

Many other examples could be given, showing the feasibility of designing synthesizing, nonlinear measuring and filtering apparatus.

LITERATURE CITED

1. G. Kramer, Mathematical Methods in Statistics [Russian translation] Foreign Literature Press (1948)
2. F. Woodward, Probability and Information Theory with Applications to Radiolocation [Russian translation], Izv-vo "Sov. radio" (1955).
3. G. H. Lening and R. G. Bettin, Random Processes in Problems of Automatic Control [Russian translation] Foreign Literature Press (1958)
4. A. M. Yaglom and M. S. Pinsker, "Random Processes with Stationary Growth of the kth Order," Doklady Akad. Nauk SSSR, 90 (1953).

THE ERRORS CAUSED BY A MEASURING APPARATUS, CHECKING THE VARIATION OF A VARIABLE QUANTITY AT EQUAL TIME INTERVALS

V. A. Bolkonskii

Translated from Avtomatika i Telemekhanika, Vol. 22, No. 4, pp. 479-482, April, 1961
Original article submitted June 23, 1960

We consider an apparatus for measuring the values of a variable quantity at discrete instants of time and signalling when this quantity has exceeded a certain allowable level. An estimate is obtained for the mean sum of the durations of those time intervals during which the controlled quantity is beyond the permitted level, that are not observed by the discrete control.

During the course of a technological process, it is often necessary to ensure that certain variables characterizing this process (for example, the supply of heating gas for a blast furnace, or its temperature and pressure) do not pass beyond certain limits. This result is obtained by determining the value of the variable at certain fixed intervals of time (we will call these intervals measurement cycles), and if it is observed that the measured value passes outside the allowable range, a signal is transmitted indicating the necessity for regulation.

These excursions beyond the allowable limits (we will call them overshoots, taking over the terminology in radio-technical literature) can occur, however, in the intervals between measurements and they will then not be observed by the controlling apparatus. It would therefore be interesting to find out how often it is necessary to take measurements, to ensure that the time of duration of the undetected overshoots is sufficiently small. It is also natural to take into account the fact that for a high frequency of measurement, the undetected overshoots will have only short durations and can not strongly influence the course of the technological process. We will therefore pose the problem in the following way.

We will assume that the variation of interest to us is that of a normally distributed random process with zero mathematical expectation and known correlation function r_t.

We will find the mean sum of the durations of the undetected overshoots beyond a level δ for a long time of observation T, with a given time Δ between successive measurements.* We denote the mathematical expectation of

*In a similar way, we can take into account the fact that undetected overshoots can only exceed the level δ by small amounts, and it is possible, for example, to derive the dependence of the mean number of undetected overshoots, exceeding not only the level δ, but also the level $\delta(1+\epsilon)$ on $\epsilon(\epsilon > 0)$. In this form, the problem can be applied in answering a question that is important in metrology: At how many points of a scale must a measuring apparatus be checked, in order to ensure the correctness of readings taken by it?

the total duration of all overshoots (detected or not detected) by M_1. The effectiveness of the control for a given frequency of measurement can then be measured by the ratio M_2/M_1.

It is obvious that with the above assumptions, we have

$$M_1 = TP(x_t > \delta) = T\left[1 - \Phi\left(\frac{\delta}{\sqrt{r_0}}\right)\right], \tag{1}$$

where $P(x_t > \delta)$ is the probability that a value x_t taken by the process exceeds the level δ, r_0 is the variance of the process (the value of the correlation function r_t for $t = 0$), and

$$\Phi(x) = \frac{1}{\sqrt{2\pi}} \int_{-\infty}^{x} e^{-\frac{y^2}{2}} dy.$$

We denote by μ the mathematical expectation of the number of overshoots starting in a unit time, and by $m(x)$ the conditional (with the condition that the overshoot begin at the zeroth instant of time) mathematical expectation of the quantity τ_x which is equal to the duration of an overshoot if it does not exceed x, and equal to zero if it does exceed x. It is evident that the mathematical expectation of the total duration of overshoots beginning during the time interval $[t, t+dt]$, $0 < t < \Delta$, that are undetected by the measurement made at the instant Δ, is $\mu\, dt\, m(\Delta - t)$. Therefore,

$$M_2 = \frac{T}{\Delta} \int_0^{\Delta} m(\Delta - t)\, \mu dt = T \frac{\mu}{\Delta} \int_0^{\Delta} m(x)\, dx \tag{2}$$

(we take T/Δ as integer). As is known (see, for example, [1])

$$\mu = \frac{1}{2\pi} \sqrt{\frac{-r_0''}{r_0}}\, e^{-\frac{\delta^2}{2r_0}}, \tag{3}$$

where r_0'' is the value of the second derivative r_t'' for $t = 0$ ($-r_0''$ is the variance of the process x_t'). In the calculation of the function $m(x)$ we will assume that the second derivative x_t'' of the process x_t remains constant during the whole overshoot, equal to its value at the beginning of the overshoot.

This is a natural assumption, as can be seen from the following considerations. It is obvious that the measurement cycle Δ must be chosen so that it can be expected that the majority of overshoots will be detected. This is possible only in the case when the main part of the spectrum of the process consists of frequencies that are considerably lower than the frequency of measurement. Since only overshoots with durations not greater than Δ are considered, then the probability is small of a sharp change in the quantity x_t or even in x_t'' during the overshoot. In any case, this assumption becomes all the more valid when $\Delta \to 0$.

With this assumption, the duration of an overshoot beginning at the zeroth instant is given by the expression

$$\tau = -2\frac{x_0'}{x_0''}. \tag{4}$$

Therefore,

$$m(x) = \iint \frac{2y}{-z} p(y, z)\, dy dz \quad \left(z < 0, \frac{2y}{-z} < x\right), \tag{5}$$

where $p(y, z)$ is the conditional distribution density of the vector (x_δ', x_δ'') under the condition that $x_0 = \delta$. When we carry out the calculations, we obtain

$$m(x) = \frac{1}{\pi} \sqrt{\frac{-r_0''}{B}} \int_{-\infty}^{0} \exp\left[-\frac{\left(z - \frac{r_0''}{r_0}\delta\right)^2}{2B}\right]\left(1 - e^{\frac{z^2 x^2}{r_0''}}\right) \frac{dz}{-z},$$

where

$$B = r_0^{IV} - \frac{r_0''^2}{r_0}$$

and

$$M_2 = T\frac{-r_0''\Delta^2\delta}{6(2\pi r_0)^{3/2}}e^{-\frac{\delta^2}{2r_0}}\left[1+\frac{6r_0}{\Delta\delta}\sqrt{\frac{2}{-r_0''}}\int_{-\infty}^{\infty}f(bu)\,p(u)\,du\right], \tag{6}$$

where

$$p(u)=\frac{1}{\sqrt{2\pi}}e^{-\frac{1}{2}\left(u-\frac{r_0''\delta}{r_0\sqrt{B}}\right)^2},$$

$$f(G)=\begin{cases}\frac{1}{G}\left[1-\frac{G^2}{6}-\sqrt{2\pi}\,\frac{\Phi(G)-\Phi(0)}{G}\right] & \text{for } G>0,\\ -\frac{G}{6} & \text{for } G<0,\end{cases} \tag{7}$$

$$b=\Delta\sqrt{\frac{1}{2}\left(\frac{r_0^{IV}}{-r_0''}+\frac{r_0''}{r_0}\right)}.$$

To simplify this expression, we note that the quantity M_1 can be assumed to be small in comparison with T. We may therefore assume that $\delta \geq 2$.

It can be verified that if the spectrum of the process is concentrated in a frequency band from 10% to 20% of the integration frequency, then the expression in the square brackets in (6) is close to unity (for example, if the frequencies in the spectrum do not exceed $2\pi/5\Delta$ and the spectral density does not increase with increasing frequency, then this expression is between 0.8 and 1.2). If we note that the assumption that the process is stationary and has a normal distribution is usually valid only to a first approximation, and also that the statistical character of the process is not known accurately, it is obviously not usually sensible to use the complicated formula (6). It can, in fact, be replaced by the approximate expression

$$M_2 \approx T\ 0.026\left(1-\frac{r_\Delta}{r_0}\right)\frac{\delta}{\sqrt{2\pi r_0}}e^{-\frac{\delta^2}{2r_0}}. \tag{8}$$

If we also use the approximate relation

$$\frac{1}{\sqrt{2\pi}}e^{-\frac{x^2}{2}}:(1-\Phi(x))\approx x,$$

which is accurate to within 15% for $x \geq 2$; then for $\frac{\delta}{\sqrt{r_0}} \geq 2$ we obtain

$$\frac{M_2}{M_1}\approx 0.026\left(1-\frac{r_\Delta}{r_0}\right)\frac{\delta^2}{r_0}. \tag{9}$$

Example A. A process with spectral density

$$f(\lambda)=\begin{cases}\frac{5\Delta}{\pi}, & |\lambda|<\frac{2\pi}{5\Delta},\\ 0, & |\lambda|>\frac{2\pi}{5\Delta},\end{cases}$$

and correlation function

$$r_t=\frac{\sin\frac{2\pi}{5\Delta}t}{\frac{2\pi}{5\Delta}t}.$$

B. $f(\lambda)=\frac{5\Delta}{\pi\sqrt{2\pi}}\exp\left[-\frac{\lambda^2 25^2\Delta}{2\pi^2}\right]$, $r_t=\exp\left[-\frac{\pi^2t^2}{50\Delta^2}\right]$.

$\delta/\sqrt{r_0}$	M_1/T	M_2/T		M_2/M_1	
		A	B	A	B
2	0.023	$6.7 \cdot 10^{-4}$	$5.1 \cdot 10^{-4}$	0.029	0.022
3	0.00135	$8.2 \cdot 10^{-6}$	$6.2 \cdot 10^{-6}$	0.06	0.047

The results of this example show that if the spectrum of the process is in a band with frequency about 1/5 of the measurement frequency, then the total duration of the undetected overshoots is on the average 2-6% of the total duration of all overshoots beyond the prescribed level.

SUMMARY

1. A method is obtained for calculating the fraction undetected of the total duration of overshoots of a controlled variable quantity beyond a permissible level when the time interval between successive measurements is Δ.

The mean sum of the durations of all overshoots and the mean sum of the duration of undetected overshoots occurring during a time interval of length T can be calculated for a measurement cycle Δ from the formulas (1) and (8).

2. If, with sufficient accuracy, the process can be assumed to be stationary and to have a normal distribution, and if the variance of the process and its derivatives (r_0, r_0'', r^{IV}_0) are known with sufficient accuracy, then the calculation of M_2 can be carried out with considerable accuracy by applying numerical-graphical methods of integration and the formulas (6) and (7).

LITERATURE CITED

1. S. Rice, The Theory of Fluctuational Noise [Russian translation] Collection of Translations "The Theory of the Transmission of Electrical Signals in the Presence of Noise," Foreign Literature Press (1953).

THEORY OF A SINGLE-CORE MAGNETIC AMPLIFIER WITH RECTIFICATION OF THE LOAD CURRENT BY MEANS OF A SYMMETRICAL NONLINEAR RESISTANCE

Dai Tse-Hsin

(Moscow)

Translated from Avtomatika i Telemakhanika, Vol. 22, No. 4, pp. 483-492, April, 1961
Original article submitted June 21, 1960

It is demonstrated that when a nonlinear resistance is connected in series with a single-core saturable reactor, the current in the ac circuit contains a dc component which is proportional to the dc magnetizing signal.

An expression is derived for the dc component of current in the ac circuit; this expression establishes a relationship between the dc component in the load circuit and in the input signal.

We know that there are magnetic amplifiers which rectify the even voltage harmonics by means of symmetrical nonlinear resistances. Push-pull magnetic amplifiers based on this principle have a lower sensitivity threshold of the order of 10^{-14}-10^{-12} [1].

However, the theory for magnetic amplifiers of this type has not been developed sufficiently. Therefore, we have posed the problem of clarifying the physics involved in the operation of amplifiers designed according to the principle of combining ideal saturable reactors and symmetrical nonlinear resistances (Fig. 1).

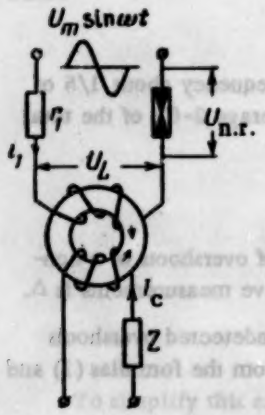

Fig. 1.

In this paper we make the following assumptions.

a) The characteristic for the symmetrical nonlinear resistance is approximated by three straight-line segments shown in Fig. 2:

$$r = \frac{du}{di} = \infty \quad \text{for} \quad |u| \leqslant |u_0|, \qquad (1)$$
$$r = \frac{du}{di} = 0 \quad \text{for} \quad |u| \geqslant |u_0|.$$

Such a volt-ampere characteristic can be obtained by connecting semiconductor diodes in a bridge circuit as shown in Fig. 3; here ordinary diodes are connected in the arms, and a reference silicon diode (stabilitron) of the type "D808-813" is connected in the diagonal. If we use silicon diodes as the rectifying diodes, then the volt-ampere characteristic for such a bridge is very close to the characteristic shown in Fig. 2. Even at a high temperature (of the order of 90° C) a high reverse resistance is maintained in diodes of this type. The forward resistance of the diodes, as well as the reverse dynamic resistance of the reference diode, can be treated as a resistance connected in series with the bridge. The reference diode does not affect the symmetry of the volt-ampere characteristic for the bridge, since the voltage across the reference diode connected in the diagonal always bucks the voltage applied to the bridge. Carborundum resistances are good as far as stability is concerned, but they have high losses.

b) the magnetization curve is represented by three straight-line segments (Fig. 4):

$$\mu = \frac{dB}{dH} = \text{const} \quad \text{for} \quad |B| \leqslant |B_s|, \qquad (2)$$
$$\mu = \frac{dB}{dH} = 0 \quad \text{for} \quad |B| \geqslant |B_s|.$$

c) The network is supplied with a sinusoidal voltage.

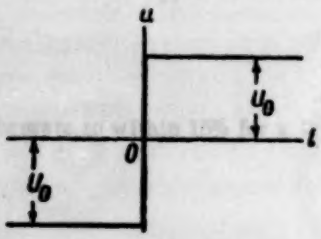

Fig. 2.

Fig. 3.

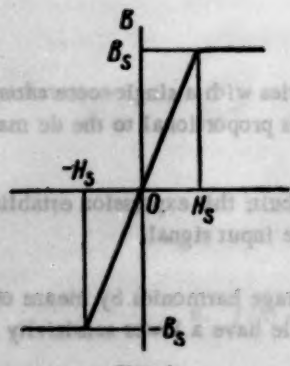

Fig. 4.

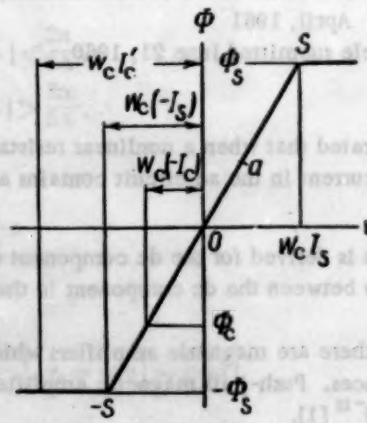

Fig. 5.

d) The current in the control circuit does not vary for variations in the ac circuit. This is achieved by connecting a large ac impedance in the circuit (in particular, a large inductance).

e) In this paper we shall study only the steady-state mode.

f) A resistor is connected in series with the symmetrical nonlinear resistance and the saturable reactor in the load circuit.

The network which is studied in this paper contains only one core. However, the results obtained here can be used for combining single-core networks to form multiple-core networks.

The Operation of a Saturable Reactor with a Symmetrical Nonlinear Resistance

For the network in Fig. 1, it is expedient to examine three modes of operation.

Mode 1. This mode occurs when the magnetizing force produced by the maximum control current is less than or equal to the magnetizing force corresponding to the knee of the curve in Fig. 4 (i.e., $|w_c I_c| \leq |w_c I_s|$, Fig. 5).

This mode is of greatest interest. It shall be demonstrated that there exists an approximately linear relationship between the dc component I_0 of the current i_1 in the load circuit and the control current I_c.

We shall study how the voltage U_L across the saturable reactor, the flux Φ in the saturable reactor, the voltage across the nonlinear resistance U_{nr}, and the current i_1 in the load current vary (in Fig. 6 $I_y = 0$).

When there is no signal during the interval $0 \leq t \leq t_1$ the supply voltage $U_m \sin \omega t$ is less than the reference voltage U_0 across the stabilitron, and all of the supply voltage appears across the nonlinear symmetrical resistance.

At the instant $t = t_1$ at which $U_m \sin \omega t_1 = U_0$, the current i_1 begins to increase according to the equation

$$U_m \sin \omega t - U_0 = L_1 \frac{di_1}{dt} + i_1 r_1 = U_L + i_1 r_1 = W 10^{-8} \frac{d\Phi}{dt} + i_1 r_1, \tag{3}$$

where L_1 is the inductance of the winding W_1 of the unsaturated core, r_1 is the resistance in the load circuit.

Keeping in mind the fact that $\omega L_1 \gg r_1$, it is possible to neglect the voltage drop $i_1 r_1$. Then from Eq. (3) we have

$$W_1 10^{-8} \frac{d\Phi}{dt} \approx U_m \sin \omega t - U_0.$$

The flux varies according to the expression

$$\Delta\Phi \approx \frac{1}{W_1 10^{-8}} \int_{t_1}^{t} (U_m \sin \omega t - U_0)\, dt. \tag{4}$$

Henceforth we shall assume that the values of U_m and U_0 are such that the quantity $\Delta\Phi$ defined by formula (4) is equal to Φ_s. Then, if the flux varies from zero, we obtain $\Phi = \Phi_s$ for $t = t_2$.

The current i_1 varies according to the expression

$$i_1 = \frac{W_1 10^{-8}}{L_1} \Phi. \tag{5}$$

For $t_1 \leq t \leq t_2$ the voltage across the nonlinear resistance does not vary and remains equal to U_0.

At the instant $t + t_2$ the supply voltage again becomes equal to U_0, the voltage across the saturable reactor decrease to zero, the flux reaches and value Φ_s, and the current i_1 reaches the value I_s (Figs. 5 and 6).

For $t > t_2$ the voltage difference $U_m \sin \omega t - U_0$ becomes negative, and the reference diode starts to block the load circuit. But a reduction of the flux from the value $+\Phi_s$ produces an emf which maintains the reference diode

in a conducting state; therefore a positive current i_1 flows through the load circuit. This continues until the flux decreases to the original value $\Phi = 0$.

We see that when a symmetrical nonlinear resistance is present there is a negative voltage across the saturable reactor, whereas the supply voltage is positive.

For $t > t_3$ the process is repeated, but in the opposite direction. The average value of the current i_1 over the entire cycle is equal to zero.

When a signal $(-I_c)$ is present, where $|w_c I_c| \leq |w_c I_s|$ in the time interval $t_1 \leq t \leq t_3$ (Fig. 7), the process occurs in the same manner as when there is no signal, except for the fact that the flux Φ_c is displaced downward by the amount

$$\Phi_c = L_c(-I_c)\frac{1}{W_c 10^{-8}}, \tag{6}$$

where L_c is the inductance of the saturable reactor from the control circuit side.

At the instant $t = t_1$, when $U_m \sin \omega t = U_0$, the flux Φ begins to increase when the original value Φ_c. At the instant $t = t_3$ the flux returns to the same original value.

Thus when there is a negative signal $-I_c$, it is possible to have a change in flux during the positive half-cycle of flux density which is equal to

$$\Delta\Phi_{+m} = \left|\Phi_s - \left[L_c(-I_c)\frac{1}{W_c 10^{-8}}\right]\right| = \left|\Phi_s + \frac{L_c I_c}{W_c 10^{-8}}\right| > |\Phi_s|; \tag{7}$$

but the actual flux change $\Delta\Phi$ when the signal is present remains the same as when there is no signal. The variations in the fluxes with and without a signal are, respectively, equal to (Fig. 5)

$$\Delta\Phi = \Phi_s - \Phi_0 = \Phi_s - 0 = \Phi_s, \qquad \Delta\Phi = \Phi_a - \Phi_c = \Phi_s. \tag{8}$$

The shape of the variation in the curve i_1 for $t_1 \leq t \leq t_3$ (Figs. 6 and 7) is identical with and without a signal.

For $t_4 \leq t \leq t_5$ the current i_1 and the flux vary according to equation (3). The initial conditions are

$$t = t_4, \quad i_1 = 0, \quad \Phi = \Phi_c = \frac{L_c(-I_c)}{W_y 10^{-8}}.$$

It should be noted that now the maximum possible flux change in the negative direction is equal to

$$\Delta\Phi_{-m} = \left|-\Phi_s - \left(-\frac{L_c I_c}{W_c 10^{-8}}\right)\right| = \left|-\Phi_s + \frac{L_c I_c}{W_c 10^{-8}}\right| < |-\Phi_s|. \tag{9}$$

At the instant $t = t_5$ the core is saturated. Determining t_4 in the equation $U_m \sin \omega t_4 - U_0 \approx 0$, we find the instant t_5 from the equation

$$\int_{t_4}^{t_5} (U_m \sin \omega t - U_0 - i_1 r_1)\, dt \approx \int_{t_4}^{t_5} (U_m \sin \omega t - U_0)\, dt \approx W_1 10^{-8}(-\Phi_s) + L_c I_c. \tag{10}$$

The negative current i_1 for $t_5 \leq t \leq t_6$ is determined by the expression

$$i_1 = \frac{U_m \sin \omega t - U_0}{r_1}.$$

For $t_5 \leq t \leq t_6$ there is no voltage across the saturable reactor, the flux Φ does not change, and $\Phi = -\Phi_s$.

At the instant $t = t_6$ the current i_1 reaches the value $(-I_s + I_c)$, and the saturable reactor emerges from its saturation state. The instant t_6 is determined from the equation

$$U_m \sin \omega t_4 - U_0 = r_1(-I_s + I_c) \approx 0. \tag{11}$$

Usually it is possible to assume $(-I_s + I_c)r_1 \approx 0$.

From Fig. 7a it is immediately evident that $U_m \sin \omega t_4 \approx 0 - U_0 \approx 0$ and $U_m \sin \omega t_6 - U_0 \approx 0$, but $\omega t_6 = \pi - \omega t_4$.

The instant t_7 is determined by the condition that the flux at that instant becomes equal to

$$\int_{t_4}^{t_6} (U_m \sin \omega t - U_0 - i_1 r_1)\, dt + \int_{t_6}^{t_7} (U_m \sin \omega t - U_0 - i_1 r_1)\, dt = 0.$$

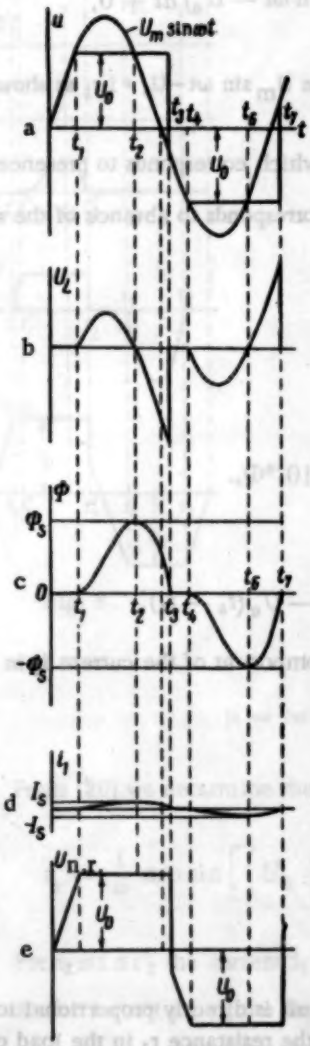

Fig. 6.

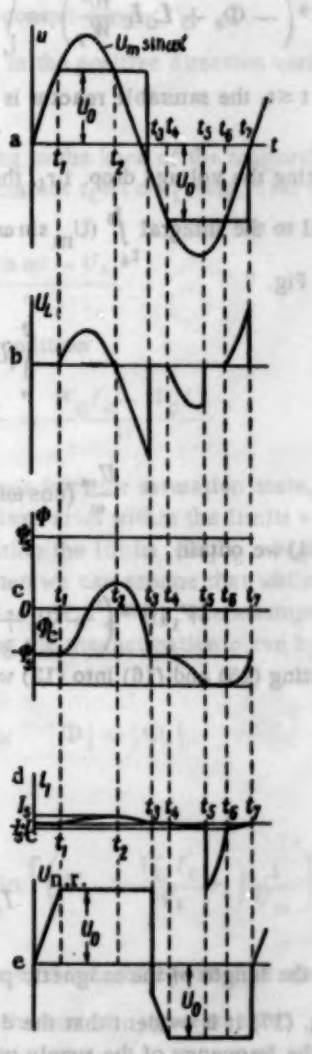

Fig. 7.

If we neglect the voltage drop $i_1 r_1$, then the latter expression becomes

$$\int_{t_4}^{t_6} (U_m \sin \omega t - U_0)\, dt + \int_{t_6}^{t_7} (U_m \sin \omega t - U_0)\, dt \approx 0. \tag{12}$$

We shall derive the expression for the dc component I_0 of the current i_1 in the load circuit.

When the saturable reactor is unsaturated, the magnetizing current i_1 in the load circuit is small and can be neglected.

Then

$$I_0 = \frac{1}{T}\frac{1}{r_1}\int_{t_4}^{t_5}(U_m \sin \omega t - U_0)\,dt = \frac{1}{T}\frac{1}{r_1}\left[\frac{U_m}{\omega}(\cos \omega t_5 - \cos \omega t_4) - U_0(t_5 - t_4)\right]. \quad (13)$$

We shall express the current I_0 in terms of the network parameters.

The integral of the voltage across the saturable reactor with respect to time for $t_4 \leq t \leq t_5$ is equal to the change $\Delta\Phi_{-m}$ (Fig. 7):

$$W_1 10^{-8}\left(-\Phi_s + L_c I_c \frac{10^8}{W_7}\right) = \int_{t_4}^{t_5} U_L dt = \int_{t_4}^{t_5} U_L dt + \int_{t_5}^{t_5} U_L dt = \int_{t_4}^{t_5}(U_m \sin \omega t - U_0)\,dt + 0, \quad (14)$$

since for $t_5 \leq t \leq t_6$ the saturable reactor is saturated, $\int_{t_5}^{t_6} U_L dt = 0$, and the voltage $U_m \sin \omega t - U_0 = i_1 r_1$ as shown in Fig. 7.

Neglecting the voltage drop $i_1 r_1$, the integral $\int_{t_4}^{t_6}(U_m \sin \omega t - U_0)dt$ (Fig. 7) which corresponds to presence of the signal is equal to the integral $\int_{t_4}^{t_6}(U_m \sin \omega t - U_0)dt = -W_1 10^{-8}\Phi_s$ (Fig. 6) which corresponds to absence of the signal. Therefore, for Fig. 7

$$\int_{t_4}^{t_5}(U_m \sin \omega t - U_0)\,dt = -W_1 10^{-8}\Phi_s,$$

or

$$\frac{U_m}{\omega}(\cos \omega t_4 - \cos \omega t_5) - U_0(t_5 - t_4) = -W_1 10^{-8}\Phi_s. \quad (15)$$

From (14) we obtain

$$W_1 10^{-8}\left(-\Phi_s + L_c I_c \frac{10^8}{W_c}\right) = \frac{U_m}{\omega}(\cos \omega t_4 - \cos \omega t_5) - U_0(t_5 - t_4). \quad (16)$$

Substituting (15) and (16) into (13) we find the final expression for the dc component of the current i_1 in the load circuit:

$$I_0 = \frac{f}{r_1}\left(-\frac{W_1}{W_c} L_c I_c\right) \quad (17)$$

or

$$I_0 = \frac{f}{r_1}\left(-W_1 \frac{0.4\pi W_c \mu 10^{-8}}{l_{st}} I_c\right), \quad (17a)$$

where l_{st} is the length of the magnetic path in the core.

From Eq. (17) it is evident that the dc component of current in the load circuit is directly proportional to the signal I_c and the frequency of the supply voltage, and is inversely proportional to the resistance r_1 in the load circuit. For an increase (in absolute value) of the signal in the negative direction from zero to I_s, the magnetizing current i_1 in the positive direction remains constant; the average value of the current i_1 in the negative direction increases. The average value of the current i_1 in the negative direction reaches the maximum negative value $I_{1\,\text{neg. max}}$ for a control current equal to $-I_s$. Substituting $-I_c = -I_s$ into Eq. (17), we obtain the maximum dc component

$$I_{0\max} = I_{1\text{neg.max}} = \frac{f}{r_1}\left(-\frac{W_1}{W_c} L_c I_s\right). \quad (18)$$

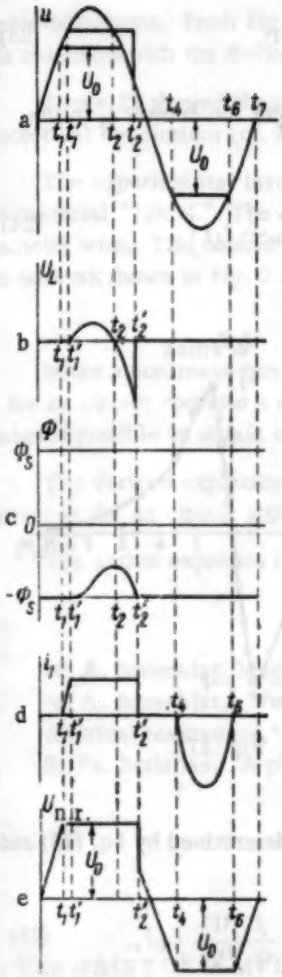

Fig. 8.

Mode 2. This mode occurs when the magnetizing force produced by the dc control current is greater than the magnetizing force corresponding to the knee on the magnetization curve (Fig. 5) and less than the maximum possible magnetizing force produced by the current i_1 in the load circuit (that is, $|W_c I_s| < |W_c I_c| < \left|W_1 \frac{U_m - U_0}{r_1}\right|$, cf. Fig. 8).

For a further increase in the modulus of the negative signal above $|-I_s|$, the current i_1 in the negative direction will remain constant. Its average value, in accordance with Eq. (18), is equal to $I_{1\,neg.\,max}$. However, as we shall demonstrate below, for $|I_c| > |I_s|$ the current i_1 in the positive direction becomes greater than for $0 < |I_c| < |-I_s|$.

For mode 2 we shall denote the control current I'_c.

We shall wee how the current i_1 in the positive direction varies for $|I'_c| > |-I_s|$.

Until the instant t'_1, corresponding to the knee of the magnetization curve, the saturable reactor is saturated and the current $t_1 \le t \le t'_1$ (Fig. 8) is determined from the expression

$$i_1 = \frac{U_m \sin \omega t - U_0}{r_1}. \qquad (19)$$

When at the instant $t = t'_1$ the condition

$$\frac{U_m \sin \omega t'_1 - U_0}{r_1} = \frac{W_c I'_c - W_c I_s}{W_1} \qquad (20)$$

is satisfied, the saturable reactor emerges from the saturation state, and the flux rises from the value $-\Phi_s$. When the flux varies within the limits $+\Phi_s$ to $-\Phi_s$, the current i_1 in the load circuit varies within the limits $(W_c I'_c + W_c I_s)/W_1$ to $(W_c I'_c - W_c I_s)/W_1$. If $|I_s| \ll |I'_c|$, then we can assume that while the flux varies the current maintains the constant value $W_c I'_c / W_1$. The assumption that $|I_s| \ll |I'_c|$ is equivalent to approximating the magnetization curve by three straight-line segments (Fig. 9):

$$\mu = \infty \quad \text{for} \quad |\Phi| < |\Phi_s|, \quad \mu = 0 \quad \text{for} \quad |\Phi| = |\Phi_s|. \qquad (21)$$

From (20) we determine the instant t'_1:

$$t'_1 = \frac{1}{\omega} \arcsin \left[\left(U_0 + \frac{W_c I'_c - W_c I_s}{W_1} r_1\right) \frac{1}{U_m}\right] \approx \frac{1}{\omega} \arcsin \left[\left(U_0 + \frac{W_c I'_c}{W_1} r_1\right) \frac{1}{U_m}\right]. \qquad (22)$$

For $t_2 \le t \le t'_2$ the current i_1 has its sign maintained constant by the emf induced by the flux change.

At the instant $t = t'_2$ the flux returns to its original value $-\Phi_s$, and the current i_1 goes to zero.

The instant t'_2 is determined by equality of the time integrals of the voltage across the saturable reactor:

$$\int_{t'_1}^{t_2} (U_m \sin \omega t - U_0 - i_1 r_1)\, dt + \int_{t_2}^{t'_2} (U_m \sin \omega t - U_0 - i_1 r_1)\, dt = 0,$$

or

$$\int_{t'_1}^{t_2} \left(U_m \sin \omega t - U_0 - \frac{W_c I'_c}{W_1} r_1\right) dt \approx 0,$$

$$-\left(U_0 + r_1 \frac{W_c I_c'}{W_1}\right)(t_2' - t_1') + \frac{U_m}{\omega}(\cos \omega t_1' - \cos \omega t_2') \approx 0. \quad (23)$$

Computing t'_1 and t'_2 from (22) and (23), it is possible to obtain the average value for the current i_1 in the positive direction:

$$I_{1\,\text{пол}} \approx \frac{1}{T}\left[\frac{W_y I_y'}{W_1}(t_2' - t_1') + \frac{U_m}{\omega r_1}(\cos \omega t_1 - \cos \omega t_1') - \frac{U_0}{r_1}(t_1' - t_1)\right]. \quad (24)$$

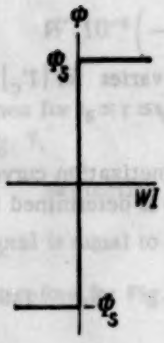

Fig. 9.

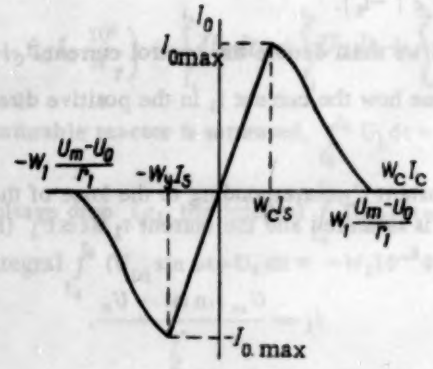

Fig. 10.

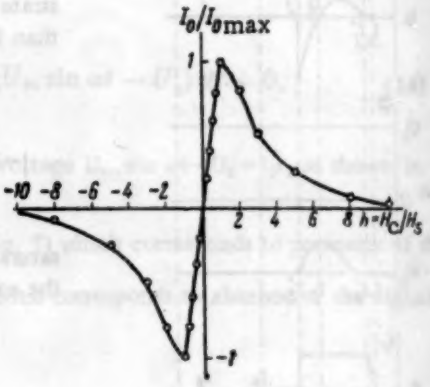

Fig. 11.

In this mode the dc component I_0 of the current is equal to the sum of the currents determined by Eq. (18) and (24):

$$I_0 = \frac{1}{T}\left[\frac{W_c I_c'}{W_1}(t_2' - t_1') + \frac{U_m}{\omega r_1}(\cos \omega t_1 - \cos \omega t_1') - \frac{U_0}{r_1}(t_1' - t_1)\right] - \frac{f}{r_1}\frac{W_1}{W_c} L_c I_s. \quad (25)$$

From Fig. 8d, Eq. (18), (24), (25), and from the discussion above it is evident that for $|I_s| < |I_c| < \left|\frac{1}{W_c} W_1 \frac{U_m - U_0}{r_1}\right|$ the current $I_{1\,\text{pos.}}$ (for $t_1 \leq t \leq t'_2$) increases in magnitude in the positive direction as I_c increases, while the current $I_{0\,\max}$ from Eq. (18) remains constant. Therefore the dc component I_0 from Eq. (25) decreases as the control current increases.

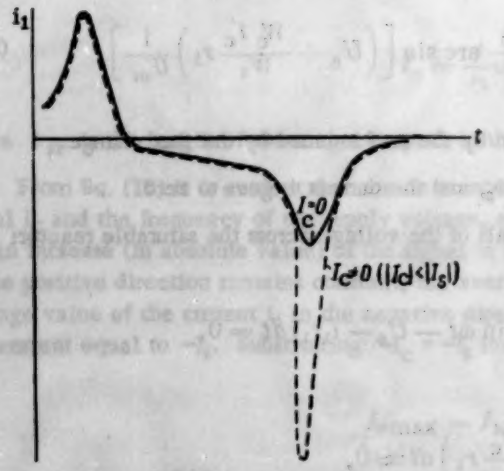

Fig. 12.

Mode 3. This mode occurs for a further increase in the signal I_c to the value $|I_c| \geq \left|\frac{1}{W_c} W_1 \frac{U_m - U_0}{r_1}\right|$; under these conditions the magnetizing force produced by the dc control current I_c in the load circuit. Thus the saturable reactor cannot become desaturated. The current i_1 in the load circuit does not contain a dc component. When the signal increases, the current i_1 for $t_1 \leq t \leq t'_2$ tends toward the shape shown in Fig. 8d for $t_4 \leq t \leq t_6$.

Thus modes 2 and 3 are not working modes. For mode 1 the dc component I_0 is proportional to the signal I_c (for $0 < |W_c I_c| < |W_c I_s|$).

The control characteristic computed from Eqs. (17) and (25) is shown in Fig. 10. The characteristic which is taken experimentally for $H_s = 0.05$ oerst, $I_s = 0.5$ ma, is shown in Fig. 11. It is evident that its shape is close to the

theoretical shape. From Fig. 11 it is evident that the characteristic is practically a straight line for $|I_c| < |I_s|$, and this coincides with the theoretical conclusion (cf. Fig. 10).

Figure 12 showed the oscillogram for the current i_1 in the load circuit. The nature of the curve verifies the theoretical conclusions (cf. Fig. 7d).

The experimental investigation was performed on a core with the dimensions 20 × 28 × 7 that was made of the material "79MN." The core was made of a ribbon 0.04 mm thick. The ac winding had 400 turns of 0.2 mm diameter wire. The control winding had 1000 turns of the same wire. As a symmetrical nonlinear resistance we used the network shown in Fig. 3 and a carborundum resistor (ϕ 20 × 5). The supply voltage had a frequency of 500 cps.

SUMMARY

When a nonlinear symmetrical resistance is connected in series with a single-core saturable reactor the current in the ac circuit contains a dc component which is proportional to the magnetizing current for $|I_c| < |I_s|$. This makes it possible to obtain controlled rectification.

The derived expression (17) provides a preliminary quantitative relationship between the dc component of the current in the ac circuit and the network parameters.

The author expresses his appreciation to M. A. Rozenblat for his valuable remarks and advice.

LITERATURE CITED

1. M. A. Rozenblat, Magnetic Amplifiers [in Russian] (Soviet Radio Press, 1960).
2. M. A. Rozenblat, "Fundamentals of the theory and design of selective rectifiers based on nonlinear symmetrical resistances," Avtomatika i Telemekhanika 15, 4 (1954).
3. R. Ya. Berkman, "A phase detector for multiple frequencies," Avtomatika i Telemekhanika 19, 4 (1958).*

A TRANSISTOR AMPLIFIER OPERATIONING IN A THYRATRON MODE†

M. V. Ol'shvang

(Moscow)

Translated from Avtomatika i Telemekhanika, Vol. 22, No. 4,
pp. 493-500, April 1961
Original article submitted July 22, 1960

The paper studies the operation of a transistor amplifier in a switching mode in which the transistors are maintained fully conducting up until the instant that the collector current passes through zero [1].

The characteristics of the amplifier are clarified when a magnetic amplifier is used to control the circuit. Experimental results are cited.

A switching mode of operation provides the following basic advantages in a transistor amplifier in comparison to the proportional mode:

1) A high coefficient of utilization for the transistor—up to 100 and greater;

* Original Russian Pagination. See C. B. translation.

† From a report made to a seminar in the Institute of Automation and Remote Control of the Academy of Sciences USSR on contactless magnetic elements, May 25, 1960.

2) a high efficiency—up to 95-98%;

3) a high temperature stability.

As a consequence of this the use of the switching mode is especially favorable for use in power output stages. In control systems such an amplifier often operates into a reversive RL dc or ac load (collector and induction motors, electromagnetic clutches, etc.).

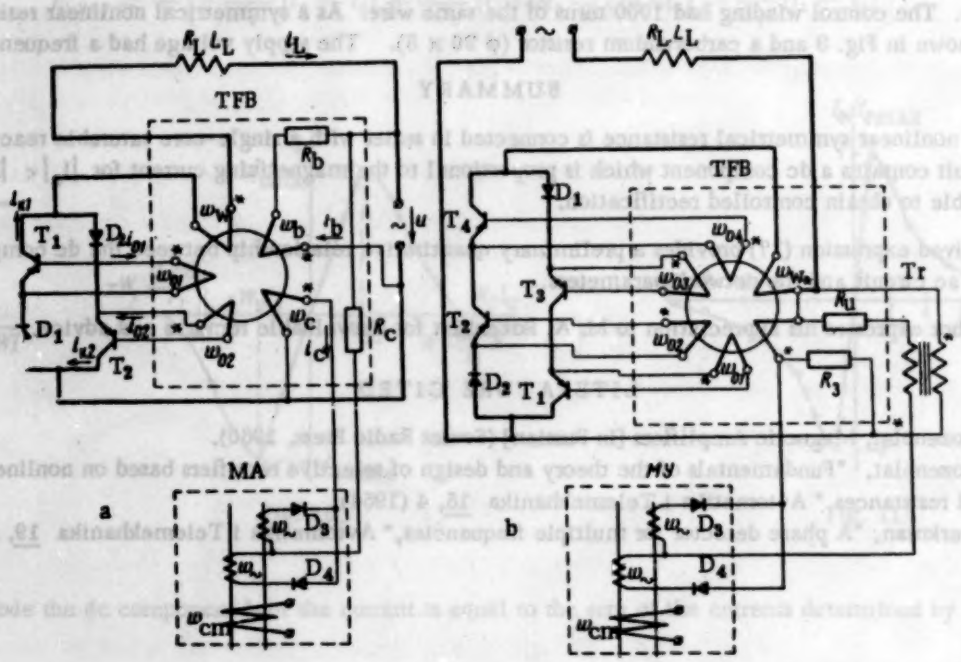

Fig. 1.

However, a switching mode involves a substantial shortcoming where RL loads are concerned: when the "switch" opens (the transistor is cut off), the breaking of the current through the inductance causes overvoltages to develop across the transistor, and the energy stored in the inductance is dissipated in the transistor.

For the case of a nonreversive dc RL load, this shortcoming is eliminated by shunting the load with a reversed rectifier. The use of uncontrolled reversed rectifiers for reversive amplifiers and for amplifiers with an ac output is impossible.

The breaking of the current by the transistor can also be avoided when the load current periodically drops to zero due to supply from the ac line. Then the transistor operates in the following mode: before the arrival of the control signal it is cut off; at the instant the control signal arrives it is fully conducting and remains in this state as long as the load current flows through it, irrespective of the magnitude of the control signal; after the current passes through zero the transistor is again cut off. Thus the transistor made in this network is analogous to the operating mode of a thyratron [1].

The Principle of Operation for the Circuit

The amplifier circuit is shown in Fig. 1a. The transistors T_1 and T_2 are connected in common-emitter fashion with a positive feedback signal through the current transformer TFB. The diodes D_1 and D_2 block the transistor from any voltage with the nonworking polarity.

The TFB has the following windings: the working winding w_w through which the load current i_L flows, the feedback windings $w_{01} = w_{02} = w_0$ through which the transistor base currents i_{01} and i_{02} flow, the windings w_b and w_c which are subjected to the blocking i_b and control i_c signals, respectively, through the ballast resistors R_b and R_c.

The wave shapes of the currents and voltages are shown in Fig. 2. We shall study the operation of the network by assuming that the feedback transformer is ideal. During the positive half-cycle the voltage is applied to the transistor T_1 and the diode D_2. Assume that at the instant voltage is applied to T_1 the relationship

$$i_b w_b \geqslant i_c w_c \tag{1}$$

is satisfied.

Here the direction of the magnetizing force (mmf) $i_b w_b$ is such that the transistor T_1 is cut off, and the current

$$i_{02} = \frac{i_b w_b - i_c w_c}{w_{02}} \tag{2}$$

flows through the winding w_{02}; i. e., if (1) is taken into account we have

$$i_{02} \approx \frac{i_b w_b}{w_{02}}. \tag{2a}$$

Under these conditions the magnitude of the voltage which blocks T_1 is determined from the formula

$$-e_{01} = e_{02} = i_{02} r_{02} = w_0 S \frac{dB}{dt}. \tag{3}$$

Here B is the flux density in the core of the TFB; S is the cross section of the core; $r_{02} = R_{w2} + r_{in.2}$, where R_{w2} is the resistance of the winding w_{02}, and $r_{in.2}$ is the input resistance of T_2.

Assume that at the instant $\Theta = \Theta_0$ a control signal appears whose mmf is directed opposite to the mmf of the blocking signal; assume further that its magnitude satisfies the inequality

$$i_c > \frac{i_b w_b}{w_c}. \tag{4}$$

Here the resultant mmf will change sign, and the flux in the core will begin to decrease ($dB/dt < 0$). As a result the conditions $e_{01} > 0$, $e_{02} < 0$ will be satisfied; i. e., T_1 will shift into the active region. The process of a further shift of T_1 toward full conduction proceeds to completion in avalanche fashion (until T_1 is in the region of collector current saturation).

After T_1 has become conducting, the inequality

$$i_L w_p \geqslant i_c w_c > i_b w_b \tag{5}$$

is satisfied.

From the instant Θ_0 we have

$$i_L w_w - i_{01} w_{01} + i_c w_c - i_b w_b = 0. \tag{6}$$

From (5) and (6) we obtain the expression for the base current

$$i_{b1} = i_{01} = \frac{i_L w_w}{w_{01}}. \tag{6a}$$

The transistor is fully conducting if

$$i_b \geqslant \frac{i_{col.}}{\beta_0}, \tag{7}$$

where β_0 is the current gain in a common-emitter circuit when $U_{col.} = 0$, and the specified value of collector current is i_{col}.

From (6a) and (7) we obtain the condition governing full conduction for the transistor:

$$n = \frac{w_0}{w_w} < \beta_0. \tag{8}$$

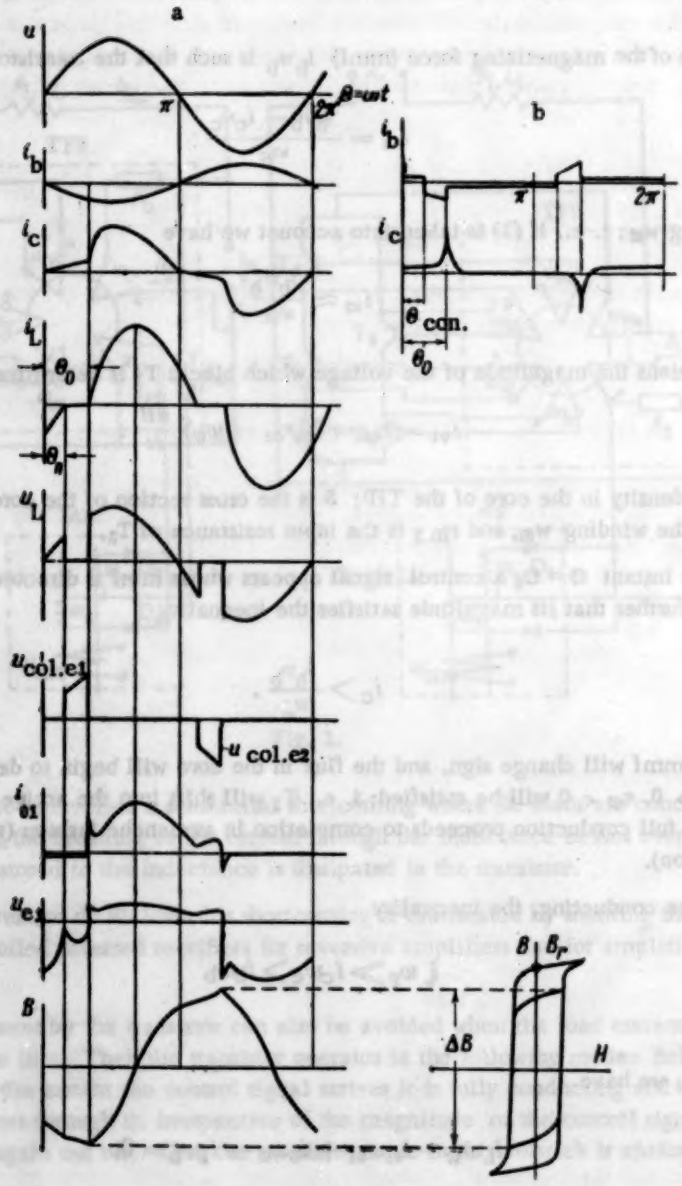

Fig. 2.

After the transistor shifts into the active region it is encompassed by positive feedback with a coefficient

$$k_{fb} = \frac{\beta w_w}{w_0}, \tag{9}$$

where β is current gain of the transistor in a common-emitter circuit for the specified collector current and a collector voltage $U_{col.} < 0$.

After the transistor has been shifted into the active region by the control signal, the inequality $\beta > \beta_0$ is valid in the entire region where the current i_L increases. If (8) is satisfied then $k_{fb} > 1$, and thus at the instant Θ_0 the avalanche process of transistor conduction occurs and the transistor shifts into the region of collector current saturation.

Condition (8) is sufficient for assuring avalanche conduction of the triode after the control signal satisfying (4) has been applied, provided that the process of reaching full conduction in the transistor occurs sufficiently rapidly in comparison to a cycle of the supply frequency. The necessary and sufficient condition for assuring that the process of reaching transistor conduction is an avalanche process when the transistor is connected in a common-emitter circuit with feedback through a current transformer is cited in [2] for the case where the dynamic characteristics of the transistor and the core are taken into account.

The time required to reach full conduction in the circuit whose parameters are cited below amounted to 30-40 μsec for a resistive load, and 5-10 μsec for an RL load. The latter value is explained by the fact that the diode becomes fully conducting at the very beginning of the next rise of the load current from zero to the maximum, since the time constant for the RL load appreciably exceeds the time constant for the process of reaching full conduction. Therefore, when the transistor operates into an RL load the power dissipated during commutation can be neglected, and the power dissipated in the transistor is in practice determined solely by the power dissipated in the region of collector current saturation.

At the instant $\theta = \theta_{con.}$ ($\theta = \pi + \Theta_{con.}$) the current $i_{col.1}$ ($i_{col.2}$) becomes equal to zero. The quantity $\theta_{con.}$ is determined by the instant at which the transistor becomes fully conducting and by the quantity $\varphi_L = \text{arc tan } (\omega L_L/R_L)$.

The presence of the switching mode and the control of the transistors through the transformer permits easy realization of parallel and series connection of transistors; for this purpose the corresponding number of feedback windings are added to the TFB.

The Control of the Amplifier

Changing the power to the load is achieved by changing the conduction angle θ_0 of the transistor. Therefore, in order to control the amplifier it is possible to use various phase-shift networks. The most expedient network for this purpose is a magnetic amplifier (MA).

Figure 1a shows a variant of a control circuit using an MA whose supplied directly from the line voltage. The amplifier in Fig. 1 shall henceforth be called a magnetic-transistor amplifier (MTA); the MA is its input stage, and the transistor section plus the TFB is the output stage.

While the MA is unsaturated (the excitation interval) inequality (1) is satisfied; after saturation inequality (4) is satisfied (i.e., at the instant the MA is saturated the transistor becomes fully conducting).

On the basis of studying the graphs in Fig. 2a it is possible to come to a conclusion concerning the input-output response for the MTA. For operation into a resistive load it is the same as the response of the input stage (the MA), since the excitation interval of the MA coincides with the intervals during which the transistor is blocked. For operation into an RL load, the interval during which the transistor is in the blocked state proves to be less than the excitation interval of the MA due to the lag of the load current relative to the supply voltage (cf. Fig. 2a); therefore the input-output response is steeper. Even for an MA saturation angle equal to the load angle φ_L, the load current reaches a maximum value and then remains constant.

Evidently the most expedient form of control signal is a pulse. Under these conditions the next pulse must arrive only after the load current has dropped to zero. On the other hand, the blocking signal can be applied only during the interval for which the transistor is in the blocked state.

These conditions can be realized if the control and blocking circuits are connected in parallel with the output stage. Then the voltage across these circuits will be applied synchronously with the voltage applied to the transistors. Such a network is shown in Fig. 1b. The transistors T_1, T_3 and T_2, T_4 are connected in series. The voltage across the magnetic amplifier MA is applied through a step-down and isolating transformer Tr. This lowers the weight and dimensions of the MA and permits the control and blocking signals to be applied to the same winding of the TFB.

The waveshape diagrams for i_c and i_b are shown in Fig. 2b for this case. The excitation interval for the MA and the interval during which the transistor is in the blocked state coincide for this network irrespective of the nature of the load. Therefore, the input-output response of the amplifier shown in Fig. 1b also repeats the MA response irrespective of the type of load. Since the response of the MA depends only slightly on the load angle, it follows that the resultant response of the MTA will also have this property.

Figure 3 shows the input-output responses for an MTA with the transistors connected in series according to the network shown in Fig. 1b. The supply voltage is U = 80 v (U_m = 115 v), f = 400 cps; the load impedance is Z_L = 30 ohm.

We shall cite the basic parameters for the network. The TFB core is made of 80NKh material with 20 rings; w_w = 12, w_0 = 70 (n = 11.7), and w_c = 500. The MA core is identical with that of the TFB; w_∞ = 2400, w_{cm} = 3000 (R_{cm} = 300 ohm). The transistors T_1–T_4 are germanium transistors of the type P4B (without additional cooling fins). D_1–D_2 are germanium diodes of the type D302 ; D_3–D_4 are germanium diodes of the type D2V . The MA is connected through a step-down transformer with a ratio 6/1.

The characteristic 1 (Fig. 3) was taken for the network shown in Fig. 1b and is practically indepndent of the load angle. It is easy to see that it repeats the conventional response for a self-saturating magnetic amplifier. The input-output response for the network shown in Fig. 1a (with the transistors connected in series as for Fig. 1b) coincides with the characteristic 1 for $\varphi_L = 0$. The characteristic 2 was obtained for $\varphi_L = 40°$. It has a pronounced limiting of the output current and a large linear segment; this verifies the reasoning cited above.

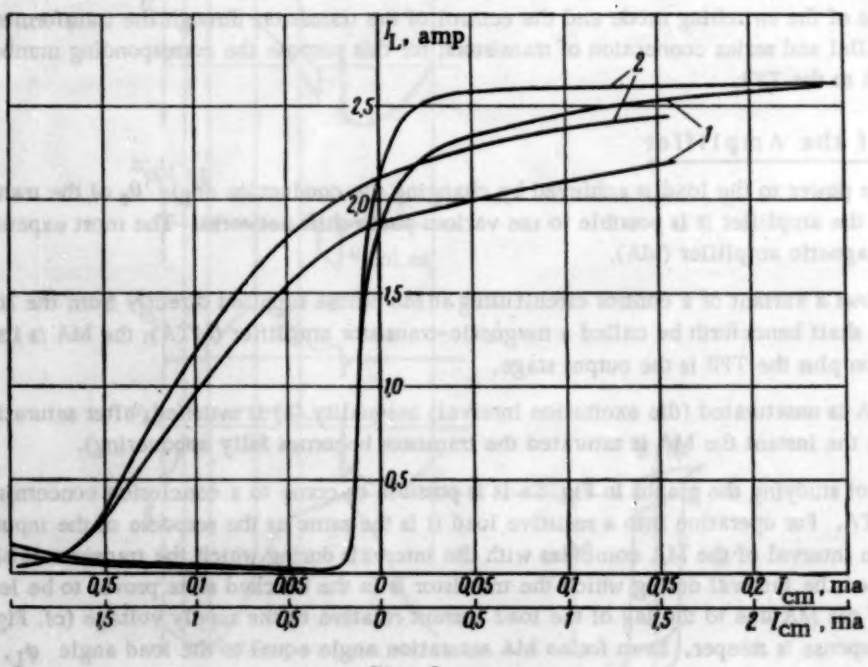

Fig. 3.

The average value of the current at the output of the MA in the network shown in the Fig. 1b did not exceed 2.5 ma. Thus the power gain for the output stage in Fig. 1b is $5 \cdot 10^3$; in Fig. 1a it is $1 \cdot 10^3$. Such a high gain for the output stage is achieved due to the fact that the control signal must merely bring the transistor into the active region.

The over-all power gain of the MTA over the linear segment of the characteristic is approximately $2 \cdot 10^7$. The efficiency of the amplifier is 95-98%.

The network was tested under conditions where the ambient temperature was varied through the range from -50 to +60°C. Under these conditions the instability of the MTA characteristic was determined solely by the temperature drift of the MA characteristic.

We shall compare MTA networks with synchronous and independent connections. The advantage of the network in Fig. 1a is the fact that for operation into an RL load the MTA corrects the characteristic of the MA in the region of maximum output (where the gain of the MA drops sharply), since the region of maximum output from the MA is not used for controlling the output stage. However, in view of the necessity of synchronizing the voltage across the control circuits with the voltage across the output stage the use of Fig. 1a is difficult for polyphase circuits. The network in Fig. 1b is more flexible and can be used in all those cases where an MA is usually used. The other advantage of the network in Fig. 1b is its higher power gain for the output stage.

Special Operational Feature of the TFB

The magnetic state of the TFB core varies along a hysteresis loop as shown in Fig. 2. Here the core must not saturate; i.e., the condition

$$\Delta B < 2B_s, \tag{10}$$

must be satisfied, where B_s is the saturation flux density.

From (3), (6a), and (8) we obtain

$$\Delta B = \frac{R_0 I_L}{2fnSw_0}, \tag{10a}$$

$$R_0 = R_w + R_{in},$$

as a result of integration; here I_L is the average value of the load current; f is the frequency of the supply source; R_w is the resistance of the winding w_0, and R_{in} is the average value of the resistance r_{in} over a half cycle.

For the case of TFB saturation before the instant Θ_n, premature blocking of the transistor occurs due to disruption of the feedback.

An appreciable difference in the magnitudes of the resistances R_{01} and R_{02} in the feedback circuits leads to saturation of the TFB during that half cycle when the transistor operates with a larger distance R_0 [this follows from Eq. (12a)]. An insignificant deviation in the values of R_{01} and R_{02} will have no effect due to the fact that inequality (8) is satisfied with some margin.

The output stage of the MTA is practically inertialess.

For a nonuniform and asymmetrical arrangement of the windings on the core of the TFB, the normal mode of operation of the MTA is violated; this is a consequence of the harmful effect of the leakage inductances. The leakage inductance of the feedback winding causes a certain lag in the current i_0 with respect to the current i_L in the primary winding during the interval for which the output stage is fully conducting, and with respect to i_b during the interval for which the transistor is in the blocked state. At the instant the primary current passes through zero, the current $i_0 \neq 0$; this current then becomes the magnetizing current, the flux begins to change in the opposite direction, and a positive voltage is applied to the emitter junction of the second transistor at that moment when it must be blocked.

In view of this, the leakage inductance of the feedback winding relative to the windings w_b leads to a growth of the no-load current, and the leakage inductance of the feedback winding relative to the working winding may cause the appearance of step variations on the input-output response of the MTA.

These phenomena are absent when the distribution of the windings on the toroid of TFB is uniform. In the network shown in Fig. 1a the no-load current did not exceed 10 ma for the parameters indicated above.

Another method for eliminating these phenomena is to shunt one of the TFB windings with a capacitor whose magnitude (normalized to the winding w_0) is 0.2-2 μf. However, a capacitor of several microfarads leads to an appreciable retardation of the process involved in reaching full conduction and thus causes an increase in the losses.

The effect of the leakage inductance is the smaller, the greater the magnetic permeability of the core material. As tests have shown, it is possible to use either permalloy cores or cores made of steel E31C for the TFB.

The feedback transformer can be treated as ideal if we choose the value of blocking current in such a way that during the greater part of the cycle the inequality $i_b \gg i_\mu$ is satisfied, where i_μ is the magnetizing current nor-

malized to the winding w_b. In practice it is sufficient for the current I_b to exceed the magnitude of the magnetizing current by a factor of 5 to 10.

SUMMARY

In the proposed magnetic-transistor amplifier the transistor operates in a mode which is analogous to a thyratron mode: when the control signal is applied it becomes conducting via an avalanche process and remains fully conducting while current flows through it. This is achieved by introducing positive feedback through a current transformer.

As a result the amplifier acquires the following advantages: 1) the possibility of operating into an RL load; 2) a small time required to reach full conduction (this time is practically independent of the wave front of the control signal, and thus a high use coefficient for the transistors and high stability are achieved); 3) a large gain for the output stage and a low inertia.

Based on the network analyzed above, we designed and successfully tested amplifiers with an output working into a reversive induction motor (two-phase and three-phase). A somewhat modified version of the network can be used for feeding the armature of the dc reversive motor.

The author expresses his deep appreciation to R. A. Lipman who made a number of valuable suggestions when this paper was edited.

LITERATURE CITED

1. M. V. Ol'shvang, A Power Amplifier Based on Switching Transistors, Patent Application Number 1311785, February 27, 1960.
2. R. A. Lipman and M. V. Ol'shvang, "A magnetic-transistor amplifier," Avtomatika i Telemekhanika 21, No. 7 (1960).*

ON THE THEORY OF SELECTIVE RECTIFICATION OF EVEN VOLTAGE HARMONCIS BY MEANS OF SYMMETRICAL NONLINEAR ELECTRICAL RESISTORS

A. I. Kadochnikov, L. A. Fridman, and R. I. Yanus

(Sverdlovsk)

Translated from Avtomatika i Telemekhanika, Vol. 22, No. 4, pp. 501-508, April, 1961
Original article submitted June 24, 1960

The paper studies one of the networks which is used for selective rectification of even voltage harmonics using symmetrical nonlinear electrical resistors. The application of this network in the output circuit of a "ferroprobe" (or a magnetic amplifier of the even harmonic type) is studied. A simple formula is derived which makes it possible to evaluate the sensitivity of such a "ferroprobe." Experimental data are cited which verify the theoretical conclusions.

In a number of papers [1-9] a study is made of selective rectifiers based on symmetrical nonlinear electrical resistors (SNER). In [7, 8] a study is made of the operation of SNER that are used for selective rectification of the even harmonics in a voltage obtained from the output (indicating) winding of a "ferroprobe." It is demonstrated that the presence of a sharp knee near a certain point on the volt-ampere characteristic of the SNER is of great significance in increasing the sensitivity of the network. In this regard the SNER network treated by R. Ya. Berkman [9] is very favorable. It consists of a Gretz bridge consisting of four rectifier elements connected to a common blocking voltage.

* Original Russian Pagination. See C. B. translation

The volt-ampere characteristics for such SNER is shown schematically in Fig. 1. Near the points U_b and $-U_b$ whose position is regulated by the magnitude of the blocking voltage, there is the required sharp knee.

R. Ya. Berkman uses an expansion of the measured voltage into a Fourier series; as a result the final formula contains the sum of the series and essentially makes it possible to draw merely the qualitative conclusion that the network under study achieves selective rectification of the even harmonics in the measured voltage. As far as quantitative computations are concerned, this formula can be used for simple computation only in certain particular cases (for example, the case where one of the even harmonics is isolated). We have derived a sufficiently exact and at the same time simple solution for the SNER network cited above which has been justified by experimental results.

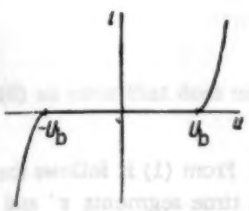

Fig. 1.

Theory

The network under study is shown in Fig. 2. We assume that: a) the capacitances are sufficiently great so that the ac component of the potential difference across their plates can be neglected in the steady-state mode;

b) the characteristics of the rectifier elements are identical, and in order to achieve additional simplification of the computations we assume that the reverse resistances of the rectifier elements are infinitely large;

c) the supply voltage $u_\sim$ does not contain even harmonics;

d) the amplitude e_m of the measured voltage e is considerably less than the amplitude u_{cm} of the commutating voltage u_c:

$$e \ll u_c = \frac{n_2}{n_1} u_\sim \qquad (1)$$

(n_1 and n_2, respectively, denote the number of turns on windings I and II).

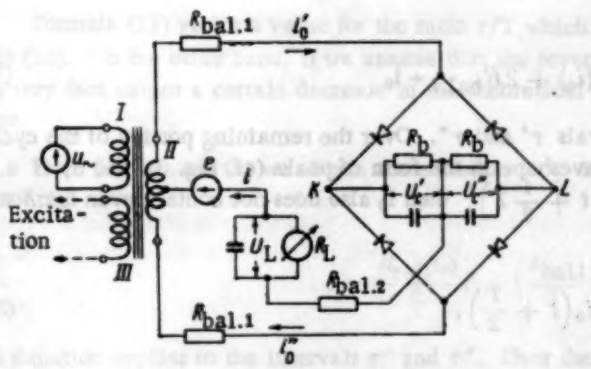

Fig. 2.

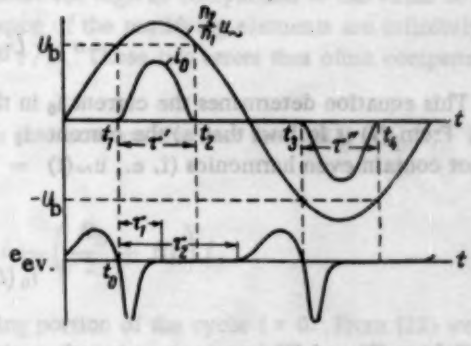

Fig. 3.

Between points K and L in the steady-state mode, a practically constant potential difference $U_b = U'_b + U''_b$ is formed. For $|U_c| \leq U_b$ the bridge is blocked and $i'_0 = i''_0 = i = 0$. For $|U_c| > U_b$ (i.e., in the "transmission intervals" τ' and τ''; cf. Fig. 3) the bridge is unblocked and

$$\tau' = \tau'' = \tau. \qquad (2)$$

If the measured voltage is e = 0, then in view of the symmetry of the network we have:

$$i = 0, \quad i'_0 = i''_0 = i_0,$$

$$U'_b = U''_b = \frac{U_b}{2}.$$

For $e \neq 0$ we have

$$i_0' = i_0 + \frac{i}{2}, \qquad i_0'' = i_0 - \frac{i}{2},$$

$$U_b' = \frac{U_b}{2} + \Delta U_b, \quad U_b'' = \frac{U_b}{2} - \Delta U_c.$$

in view of the same symmetry.

It is evident that

$$\Delta U_b = R_b \frac{I}{2}, \tag{3}$$

where $\underline{I}$ denotes the dc component of the current $\underline{i}$ flowing through the load resistance R_L. From (1) it follows that $i \ll i_0$. Choosing the conditional directions of the currents i'_0, i''_0, and $\underline{i}$ (cf. Fig. 2) for the time segments τ' and τ'' when the bridge is unblocked, we shall obtain the following Kirchhoff equations for the symmetrical loops:

$$\frac{u_c}{2} + e \mp \frac{U_b}{2} - \Delta U_b - U_L = u_{r.}\left(i_0 + \frac{i}{2}\right) + \left(i_0 + \frac{i}{2}\right) R_{bal.1} + i R_{bal.2} \tag{4}$$

$$\frac{u_c}{2} - e \mp \frac{U_b}{2} + \Delta U_b + U_L = u_{r.}\left(i_0 - \frac{i}{2}\right) + \left(i_0 - \frac{i}{2}\right) R_{bal.1} - i R_{bal.2} \tag{5}$$

Here $U_L = R_L I$ is the potential difference across the load resistance, U_r $(i_0 \pm i/2)$ is the potential difference across the rectifying element, $R_{bal.}$, $R_{bal.}$ are ballast resistors, where $R_{bal.}$ includes one-half the resistance of the winding II; the upper sign in front of $U_b/2$ corresponds to the interval τ', and the lower sign corresponds to the interval τ''. Since $i \ll i_0$, it is possible to write approximately

$$u_{r.}\left(i_0 \pm \frac{i}{2}\right) = u_{r.}(i_0) \pm \frac{du_{r.}(i_0)}{di_0}\frac{i}{2} = u_{r.}(i_0) \pm \frac{i}{2} R_{r.d}(i_0), \tag{6}$$

where $R_{r.d.}(i_0)$ is the differential resistance of the rectifying element. Adding (4) and (5) and taking (6) into account, we obtain

$$u_c \mp U_b = 2u_{r.}(i_0) + 2R_{bal.1} + i_0 \tag{7}$$

This equation determines the current i_0 in the intervals τ' and τ''. Over the remaining portion of the cycle, $i_0 = 0$. From (7) it follows that a) the current i_0 has a waveshape in the form of peaks (cf. Fig. 3), and b) if $u_\sim$ does not contain even harmonics (i. e., $u_\sim(t) = -u_\sim\left(t + \frac{1}{2}T\right)$, then i_0 also does not contain even harmonics; i.e.,

$$i_0(t) = -i_0\left(t + \frac{T}{2}\right). \tag{8}$$

Taking (8) and (2) into account together with the rectifying effect of the bridge, we have

$$U_b = 2R_b \frac{2}{T}\int_{t_1}^{t_2} i_0\, dt. \tag{9}$$

We shall integrate (7) over the limits of the interval τ' while assuming $u_c = u_{cm} \sin \omega t$. Taking into account the fact that $U_b = u_{cm} \cos \omega\tau/2$ and that according to the generalized theorem of the mean we have

$$\int_{t_1}^{t_2} u_{r.}(i_0)\, dt = \int_{t_1}^{t_2} R_{r.}(i_0)\, i_0\, dt = \bar{R}_{r.} \int_{t_1}^{t_2} i_0\, dt$$

where $\bar{R}_r$ is a certain "average" value for the resistance of the rectifying element, and taking (9) into account, we obtain

$$2\tan\frac{\omega\tau}{2}-\omega\tau=\pi\frac{\overline{R}_{r.}+R_{bal.1}}{R_b}. \qquad (10)$$

This equation can easily be solved graphically. However, for practical computations it can be further simplified. For $\omega\tau < 100°$ we have

$$2\tan\frac{\omega\tau}{2}-\omega\tau\approx\frac{2}{3}\left(\frac{\omega\tau}{2}\right)^3.$$

with an error that does not exceed 30%.

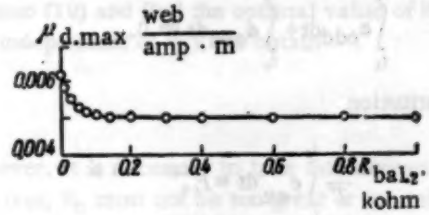

Fig. 4.

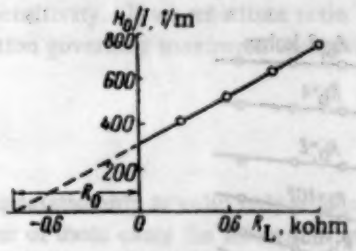

Fig. 5.

Substituting this into (7) we obtain

$$\left(\frac{\tau}{T}\right)^3\approx 0.15\frac{\overline{R}_{r.}+R_{bal.1}}{R_b} \qquad (11)$$

Formula (11) yields a value for the ratio τ/T which is somewhat too high in comparison to the value obtained from (10). On the other hand, if we assume that the reverse resistance of the rectifying elements are infinitely large, this very fact causes a certain decrease in the theoretical value of τ/T. These two errors thus often compensate each other.

From (4), (5), and (6) we obtain the equation for i if we take into account the fact that $\Delta U_b = (R_b/2)\cdot I$ and $U_L = R_L I$:

$$e=\frac{R_{r.d}(i_0)}{2}i+\left(\frac{R_{bal1}}{2}+R_{bal2}\right)i+\left(\frac{R_b}{2}+R_L\right)I, \qquad (12)$$

this equation applies to the intervals τ' and τ''. Over the remaining portion of the cycle $i = 0$. From (12) we obtain

$$\frac{1}{T}\left(\int_{t_1}^{t_2}e\,dt+\int_{t_3}^{t_4}e\,dt\right)=\frac{1}{2T}\left(\int_{t_1}^{t_2}R_{r.d}(i_0)\,i\,dt+\int_{t_3}^{t_4}R_{r.d}(i_0)\,i\,dt\right)+\left(\frac{R_{bal1}}{2}+R_{bal2}\right)I+\left(\frac{R_b}{2}+R_L\right)\frac{2\tau}{T}I. \qquad (13)$$

From the generalized theorem of the mean we have

$$\frac{1}{2T}\left(\int_{t_1}^{t_2}R_{r.d}(i_0)\,i\,dt+\int_{t_3}^{t_4}R_{r.d}(i_0)\,i\,dt\right)=\frac{\overline{R}_{r.d.1}}{2}\frac{1}{T}\left(\int_{t_1}^{t_2}i\,dt+\int_{t_3}^{t_4}i\,dt\right)=\frac{\overline{R}_{r.d.}}{2}I, \qquad (14)$$

where $\overline{R}_{r.d.}$ is a certain "average" differential resistance of the rectifying element. We shall study the left-hand side

of Eq.(13). The voltage $\underline{e}$, generally speaking, consists of two components e_{ev} and e_{odd}, where e_{ev} denotes the sum of the even harmonics of the voltage $\underline{e}$ and has the property

$$e_{ev.}(t) = e_{ev.}\left(t + \frac{T}{2}\right), \tag{15}$$

the quantity e_{odd} represents the sum of the odd harmonics of the voltage $\underline{e}$ and has the property

$$e_{odd}(t) = -e_{odd}\left(t + \frac{T}{2}\right). \tag{16}$$

From (16) and (2) it follows that

$$\int_{t_1}^{t_2} e_{odd}\,dt + \int_{t_2}^{t_4} e_{odd}\,dt = 0. \tag{17}$$

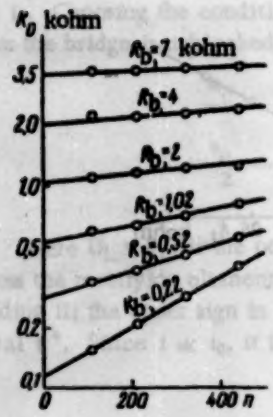

Fig. 6.

Using the substitution

$$\frac{2}{T}\int_{t_1}^{t_2} e_{ev.}\,dt = E_\tau \tag{18}$$

and taking (2), (14), (15), and (17) into account, we obtain

$$I = \frac{E_\tau}{\frac{\bar{R}_{r.d.}}{2} + \frac{R_{bal1}}{2} + R_{bal2} + \left(\frac{R_b}{2} + R_L\right)\frac{2\tau}{T}}. \tag{19}$$

from (13).

Thus the dc component of the current flowing through the load resistance R_L proved to be proportional to the average value of the sum of the even harmonics in the measured voltage over the transmission interval τ.

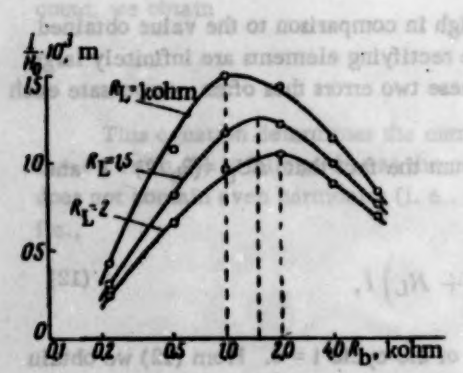

Fig. 7.

The SNER network under study can be used, in particular, for rectifying the sum of the even harmonics in an emf excited in the output winding of a "ferroprobe" (or an even-harmonic magnetic amplifier). In that case we have the following well-known relationship [8] for an operating mode close to no-load:

$$e_{ev} = 2nS\frac{d\mu_d}{dt}H_0 \tag{20}$$

(In the MKSA system). Here H_0 is the "controlling" field, μ_d is the differential permeability of the core, $\underline{n}$ is the number of turns on the indicator winding, S is the cross section area of the core. Substituting (20 into (18), we obtain

$$E_\tau = \frac{4nS}{T}(\mu_{d2} - \mu_{d1})H_0. \tag{21}$$

Here $\mu_{d.1}$ and $\mu_{d.2}$ are the values of the differential permeability at the instants t_1 and t_2, respectively. In order to obtain the maximum proportionality coefficient between I and H_0 (i.e., the maximum sentivity of the network) it is necessary for the "phase shift" between $e_{ev.}$ and the commutating voltage $u_c = n_2 u_\sim / n_1$ to be in accordance with that shown in Fig. 3 (i.e., the instants t_1 and t_0 coincide). Under these conditions the magnitude of the interval τ must be confined to the limits delineated by τ_1 and τ_2. In that case $\mu_{d.2} \approx 0$, $\mu_{d.1} = \mu_{d.\,max.}$, and, therefore,

$$E_\tau = -\frac{4nS}{T}\mu_{d.max}H_0. \qquad (22)$$

The indicated optimal phase shift between e_{ev} and u_c can be achieved practically by using a phase shifter or simply by choosing the appropriate resistance for the excitation circuit.

From (19) it follows, in particular, that the sensitivity of the network depends substantially on the ratio τ/T which can be computed approximately from (11). The quantity $\bar{R}_{\tau.}$ which appears in this formula can be evaluated from the characteristic of the rectifier element only in a very approximate fashion [it can often be assumed that $\bar{R}_{\tau.} = R_{\tau.}(i_0/2)$]. Notwithstanding this, computations according to formula (11) will prove to be sufficiently exact since the ballast resistors $R_{bal.}$ are introduced into the network to compensate the effect of instability in the rectifier element characteristics on the operation of the network; they must thus be appreciably greater than $\bar{R}_{\tau.}$. However, $R_{bal.}$ must not be too great in order to avoid lowering the network sensitivity. If we substitute ratio τ/T found from (11) into (19) and find the optimal value of R_b from the condition governing maximum sensitivity (assuming that E_τ is independent of R_b), we obtain

$$R_{b.opt} = R_L. \qquad (23)$$

However, it is necessary to take into account the fact that this relationship is valid only within restricted limits. In fact, R_b must not be too great or too small, since in either of those cases the interval τ may, in accordance with (11), prove to be greater than τ_2 or less than τ_1. From (11) and (19) it also follows that an increase in $R_{bal.1}$, $R_{bal.2}$, and R_L leads only to a lowering of the sensitivity.

If the forward resistance of the rectifying element on the working segment of the characteristic and the value of the ballast resistance $R_{bal.}$ are small compared to the load resistance, then the terms $(1/2)R_{\tau.d.}$ and $(1/2)R_{bal.1}$ in the denominator of formula (19) can be neglected. Substituting (22) into (19) we have

$$I = -\frac{\frac{4nS}{T}\mu_{d.max}H_0}{R_{bal.2} + \left(\frac{R_b}{2} + R_L\right)\frac{2\tau}{T}}. \qquad (24)$$

for this case.

For approximate computations that give a rough value for the sensitivity of "ferroprobes" in which the network under study is used for rectifying the sum of the even harmonics of the emfs excited in the output winding, we obtain the following results from (24) if we assume that $R_{bal.} = 0$ and take (23) and (11) into account:

$$\frac{I}{H_0} \approx -\frac{nS\mu_{d.max}}{\sqrt[3]{R_L^2(\bar{R}_\tau + R_{bal.1})}}. \qquad (25)$$

Here f is the excitation frequency.

For a magnetic amplifier with the same output circuit, the current gain can be computed approximately from the formula

$$\frac{I}{I_0} \simeq -\frac{\frac{S}{l}nn_0\mu_{d.max}f}{\sqrt[3]{R_L^2(\bar{R}_\tau + R_{bal.1})}}, \qquad (26)$$

where I is the control current, n_0 is the number of turns on the control winding, and l is the length of the magnetic path in the core.

In concluding this section we shall note that, as subsequent detailed analysis shows, the proportionality between

R_b kohm	0.22	0.52	1.02	2.00	4.00	7.00
$\left(\frac{\tau}{T}\right)_{comp.}$	0.31	0.24	0.20	0.16	0.13	0.11
$\left(\frac{\tau}{T}\right)_{meas.}$	0.31	0.26	0.22	0.19	0.16	0.14
$\mu_{d.max}$, $\frac{web}{amp \cdot m}$	0.020	0.040	0.053	0.053	0.053	0.049

I and H_0 is still maintained for the case where the reverse resistances of the rectifying elements are finite (for the condition that their volt-ampere characteristics are identical).

Experimental Data

An experimental verification of the derived theoretical results was obtained using magnetic amplifiers of the even harmonic type with an excitation frequency of 500 cps. We used germanium diodes of the type DGTs-24 as the rectifying element. The capacitors had a value of 20 μf.

A. The table cites a comparison of the ratio τ/T for various R_b computed according to formula (11) and measured directly by means of an oscilloscope.

The agreement is satisfactory.

B. It is best to perform the direct verification of formula (24) using magnetic amplifiers with ferrite cores for which the quantity $\mu_{d.max.}$ does not depend on the excitation mode and can therefore be measured easily. It is necessary to take into account the fact that formula (24) was derived on the basis of assuming no-load operation. Therefore in performing the measurements the ballast resistor $R_{bal.2}$ is introduced into the network. Figure 4 shows the dependence of $\mu_{d.max.}$ computed according to formula (24) from the experimental data on $R_{bal.2}$. It is evident that the curve $\mu_{d.max.} = \mu_{d.max.}(R_{bal.2})$ asymptotically approaches the value corresponding to no-load operation. For various R_b the no-load values of $\mu_{d.max.}$ obtained in this manner fluctuate within the limits of from $4.8 \cdot 10^{-3}$ to $5.1 \cdot 10^{-3}$ (web/amp · m). Direct measurement by the simplest method yields $\mu_{d.max.} = (4.7 \pm 0.3)10^{-3}$ web/amp · m.

C. Further experiments were performed using toroidal cores made of 79NM permalloy. The mean diameter of the toroids was 3.0 cm, and the cross section area was 0.25 cm^2. The number of turns on the excitation winding was 63. Formula (24) can be used for this case in order to perform an approximate computation of $\mu_{d.max.}$ from the measured ratios I/H_0 and τ/T. The results of such a computation for various R_b are cited in the table. The "valleys" in the function $\mu_{d.max.} = \mu_{d.max.}(R_b)$ at the edges are explained by the fact that for $R_b < 1$ kohm the transmission interval proves to be greater than τ_2, whereas for $R_b > 4$ kohm it is less than τ_1.

D. In accordance with (21) the function $H_0/I = f(R_L)$ must be a straight line. This is verified by experimental results (cf. Fig. 5 which shows a typical curve for H_0/I as a function of R_L from among the series of curves which we obtained). According to (24) the segment R_0 shown in Fig. 5 must equal $R_b/2$ for $R_{bal.2} = 0$. Figure 6 shows the experimentally obtained functions $R_0 = R_0(n)$ for various R_b. For $n \to 0$ (this corresponds approximately to no-load operation) we have $R_0 = (1/2)R_b$.

E. From Fig. 7, which shows the experimentally obtained curves for the sensitivity I/H_0 as a function of R_b for various load resistances R_L, it is evident that the maximum sensitivity corresponds to a value of R_b that equals R_L; i.e., relationship (23) is also verified experimentally.

SUMMARY

1. For the indicated network the dc component of the current flowing through the load resistance is proportional to the average value of the sum of the even harmonics in the measured voltage over the transmission interval. It also depends substantially both on the load resistance R_L and on the resistance R_b across which the blocking voltage is produced.

2. An approximate computation of the sensitivity for a "ferroprobe" in which the network under study is used for selective rectification of the sum of the even harmonics in the emf excited in the output winding can be performed according to formula (25). The approximate computation of the current gains for a magnetic amplifier with the same output circuit can be performed according to formula (26).

LITERATURE CITED

1. M. A. Rozenblat, "rectification in nonlinear symmetrical electric and magnetic circuits," Doklady Akad. Nauk. 68, 3 (1949).
2. M. A. Rozenblat, "selective rectification by means of nonlinear resistances," Doklady Akad. Nauk. 74, 4 (1950).
3. I. G. Miles, Types of Magnetic Amplifiers Survey, Trans. AIEE Vol. 71, 1952.
4. E. H. Frost-Smith, The Study of a Magnetic Inverter for Amplification of Low-Input-Power D. C. Signals. Proc. IEE Vol. 100, No. 76, Part II, 1953.
5. M. A. Rozenblat, "fundamentals of the theory and design of selective rectifiers based on nonlinear symmetrical resistances," Avtomatika i Telemekhanika 15, 4 (1954).
6. M. A. Rozenblat, "fundamentals of designing magnetic amplifiers with a low sensitivity threshold," Avtomatika i Telemekhanika 17, 1 (1956).*
7. R. I. Yanus, L. A. Fridman, and V. I. Drozhzhina, "A method for rapid monitoring of the coercive force of electrical-engineering sheet iron," Zavodskaya Laboratoriya 21, 10 (1955).
8. L. A. Fridman, On Using Semiconductor Rectifiers in the Phase-Sensitive Indicator Circuits of "Ferroprobe" Magnetomers [in Russian] Transactions of the Institute of Metal Physics of the Acad. Sci. USSR, No. 21 (1959).
9. R. Ya. Berkman, "A phase detector for multiple frequencies," Avtomatika i Telemekhanika 19, 4 (1958).*

A SIMPLIFIED METHOD FOR DETERMINING STABILITY SEGMENTS

V. E. Bogin

(Moscow)

Translated from Avtomatika i Telemekhanika, Vol. 22, No. 4, pp. 509-510, April, 1961
Original article submitted August 6, 1960

As we know, in investigating the stability of linear automatic control systems the method of D-subdivision is used for determining the set of parameter values for which the system remains stable.

In investigating systems by this method it is necessary to plot a D-subdivision curve which is associated with rather cumbersome computations. In practice, it is often necessary to determine a stability segment (i.e., a segment of the positive abscissa semiaxis which located within the stability region.

Stability segments can be determined using a simplified method that is a corollary of the D-subdivision method involving one parameter.

As usual, it is assumed that the coefficients of the characteristic equation for the closed-loop system depends linearly on the investigated parameter w; i.e., $G(p) = Q(p) + wR(p)$, where G(p) is the left-hand side of the characteristic equation for the closed-loop system.

As we know, the equation for the D-subdivision curve is given by

$$w = -\frac{Q(j\omega)}{R(j\omega)}.$$

* Original Russian Pagination. See C. B. translation.

After separating the real and imaginary parts we obtain

$$w(\omega) = A_1(\omega) + jA_2(\omega).$$

An example of the D-subdivision curve is shown in the figure.

From the figure we derive the following:

1) the boundaries of the stability segments are determined by the values of $A_1(\omega_k)$, where ω_k are the real positive roots of the equation $A_2(\omega) = 0$;

2) by computing $A_1(\omega_k + \Delta\omega)$ and $A_2(\omega_k + \Delta\omega)$ it is possible to determine the direction of the hatching (i.e., it is possible to isolate the segments which are "candidates" for the stability segments).

Thus the problem of determining stability segments reduces to the following operations:

1) determining the real positive roots of the equation $A_2(\omega) = 0$;

2) computing the values $A_1(\omega_k)$;

3) computing the values $A_1(\omega_k + \Delta\omega)$, $A_2(\omega_k + \Delta\omega)$;

4) verifying the system for stability for a value of the parameter $\underline{w}$ taken from the segment which is a candidate for the stability segment.

The reduction of the computations in the method cited above is obvious, since here there is no need to determine the large number of values $w = w(\omega)$ which must be found for accurate plotting of a D-subdivision curve.

The number of computations required for an approximate determination of the roots w_k is small, since such an approximation can be rather rough.

There exist effective methods for determining the roots of the equations. For an approximate determination of the real roots it is convenient to use the method based on the Viet formula and the Bernoulli method. The results obtained by these methods can be refined using linear interpolation, the iteration method, the Newton method etc. [1].

For equations which are not of high degree (up to the sixth) it is possible to use the Kryzhanovskii iteration method [2] if the upper boundary for the real roots is first determined according to the Maclaurin method [1] and the variable ω is substituted for according to the formula

$$\omega = \theta + b,$$

here $\underline{b}$ is the upper boundary for the positive roots and θ is a new variable.

The computation of the values for the polynomials and their derivatives is conveniently performed according to the Horner scheme.

In conclusion it should be noted that the method cited above is not expedient if the curve for D-subdivision with respect to one parameter is used for judging the system performance etc. (cf., for example, [3]).

LITERATURE CITED

1. V. L. Zaguskin, Handbook on Numerical Methods for Solving Algebraic and Transcendental Equations [in Russian] (Physics and Mathematics Press, 1960).

2. O. M. Kryzhanovskii, "On an Iteration Method for Determining the Approximate Roots of Equations," Avtomatika i Telemekhanika 11, 5 (1950).
3. M. V. Meerov, Synthesis of Block Diagrams for High-Precision Automatic Control Systems [in Russian] (Physics and Mathematics Press, 1959).

THE DESIGN OF AUTOMATIC CONTROL SYSTEMS (ACS)

Yu. I. Borodin and V. N. Plotnikov

(Moscow)

Translated from Avtomatika i Telemekhanika, Vol. 22, No. 4,
pp. 511-523, April,1961
Original article submitted October 31, 1960

The paper develops a method for designing automatic control systems without lag for the case of first and second order objects when four types of controllers are used. The method is generalized to include systems with lag. Nomograms are given for choosing the parameters of the desired transfer function and for determining the type of controller.

A number of papers [2-6, 9-13] have been devoted to the adjustment of controllers and the synthesis of corrective networks in ACS.

In this paper we present a method for choosing the controller parameters on the basis of the primary performance indices in the case of first and second order objects (for the case of no pure lag and for the case where lag is present), and for four types of controllers: a) with respect to deviation (D); b) with respect to the integral (I); c) with respect to both deviation and integral (DI); d) with respect to deviation, derivative and integral (DDI). The method under study is a concretization of the method for synthesizing corrective networks in ACS which was based on choosing the desired logarithmic amplitude response (LAR) [4].

We shall study the block diagram of the ACS (Fig. 1a). It consists of a controlled object with the transfer function K_0W_0 and a controller with a transfer function $K_cW_c(s)$ whose type and parameters are unknown.

The transfer function for many objects can be represented by one of the expressions cited in Table 1; the transfer functions of the controller types indicated above are cited in Table 2.

As the primary dynamic indices characterizing the automatic stabilization system (Fig. 1b) we shall analyze:

1. The magnitude of the maximum deviation x_{max} caused by a unit stop perturbation.

2. The transient response time T caused by the same perturbation. (The minium time after which the deviation of the controlled quantity differs from its steady-state value by an amount less than or equal to Δ. For static systems T is determined by the formula $x_{st} - \Delta \leq |x(T)| \leq x_{st} + \Delta$, and for astatic systems by the formula $|x(T)| \leq \Delta$. The quantity Δ is determined by the engineering conditions. Here Δ is equal to 5% of the unit step perturbation).

3. The time t_c during which the deviation reaches its maximum value.

4. The relative dynamic deviation of the controlled quantity, which characterizes the shape of the transient response; it is given by $\eta_s = x_{21}/x_{11}$ (for a static system—the curve 1) or $\eta_c = x_{22}/x_{max}$ (for an astatic system—curve 2).

5. The static system error x_{st} which is characterized by the deviation of the controlled quantity from the nominal value after the transient response caused by a unit step perturbation has been completed.

First we shall study the method of choosing the type of controller and its parameters for objects that have a transfer function of the type (1) and (2); then we shall generalize the method to include systems whose object has pure lag.

TABLE 1

$K_0W_0(s)$	$\frac{K_0}{T_0s+1}$ (1)	$\frac{K_0}{T_0^2s^2+2\zeta_0T_0s+1}$ (2)	$\frac{K_0e^{-\tau s}}{T_0s+1}$ (3)	$\frac{K_0e^{-\tau s}}{T_0^2s^2+2\zeta_0T_0s+1}$ (4)

TABLE 2

Type of controller	D	I	DI	DPI
transfer function $K_CW_C(s)$	K_C (5)	$\frac{K_p}{s}$ (6)	$\frac{K_C(\tau_Cs+1)}{s}$ (7)	$\frac{K_C(\tau_C^2s^2+2\zeta_C\tau_Cs+1)}{s}$ (8)

TABLE 3

Type of object	1st order		2nd order	
type of controller	D	I, DI, DDI	D	I, DI, DDI
transfer function for Y(s)	$\frac{K}{T_1s+1}$ (9)	$\frac{Ks}{T_1^2s^2+2\zeta_1T_1s+1}$ (10)	$\frac{K}{T_1^2s^2+2\zeta_1T_1s+1}$ (11)	$\frac{Ks}{(T_2s+1)(T_1^2s^2+2\zeta_1T_1s+1)}$ (12)

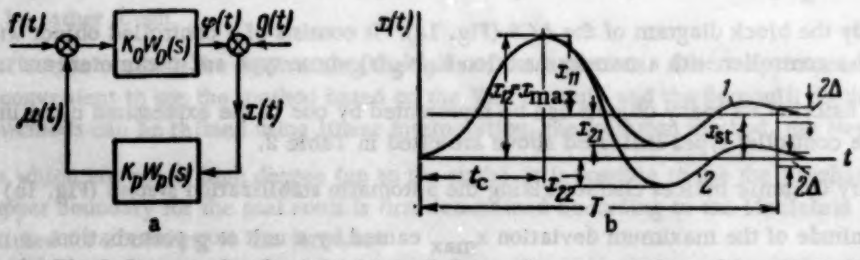

Fig. 1. Block diagram for the ACS (a), and the performance indices (b). g(t) is the standard input signal [g(t) = const], f (t) is the perturbation, φ (t) is the controlled quantity, x (t) is the deviation of the controlled quantity, μ (t) is the control signal.

Nomograms for choosing the desired transfer function of the closed-loop system. These nomograms establish the relationship between the parameters of the transient response and the transfer function for the closed-loop ACS. The transfer functions Y (s) for the ACS corresponding to the objects and controllers under study are shown in Table 3.

The nomograms were plotted using formulas which determine the relationship between the primary performance indices T, x_{max}, t_c and η, and the parameters of the transfer function for the closed-loop system K, T_1, and ζ_1 (Table 4). The formulas were derived using the inverse Laplace transform.

The nomograms are plotted for the transfer function (10) of the closed-loop ACS in the coordinates 20 log K vs. ζ_1; t_c/T_1; η vs. ζ_1 (Fig. 2) for the transfer functions (11) and (12) they are plotted in the coordinates 20 log K/T_1 vs. ζ_1; t_c/T_2, η vs. ζ_1 (Figs. 3 and 4). The curves in Fig. 4 are plotted only for the case $T_2 = T_1$; however, they

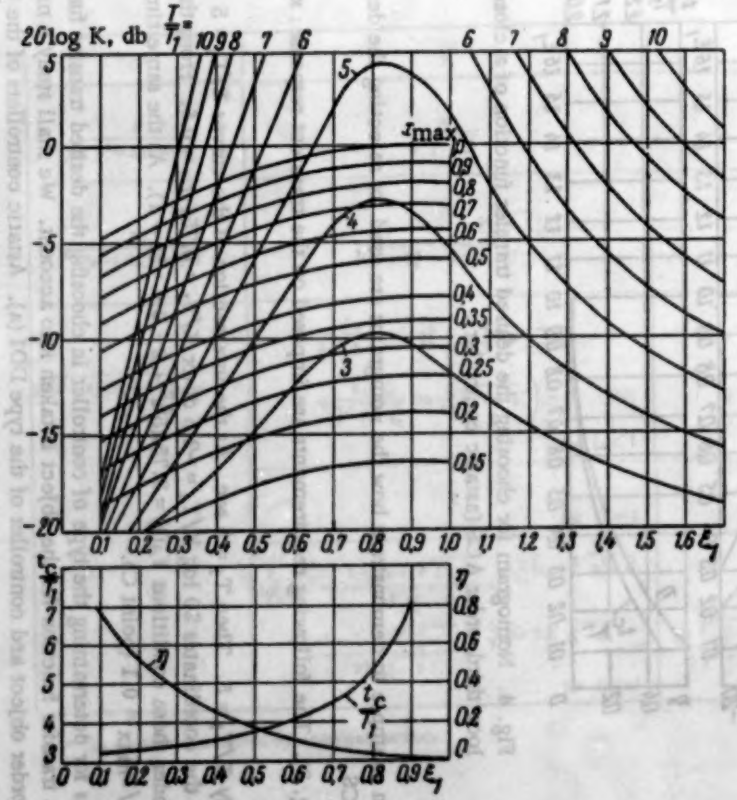

Fig. 2. Nomogram for choosing the desired transfer function of a closed-loop second order ACS (static controller).

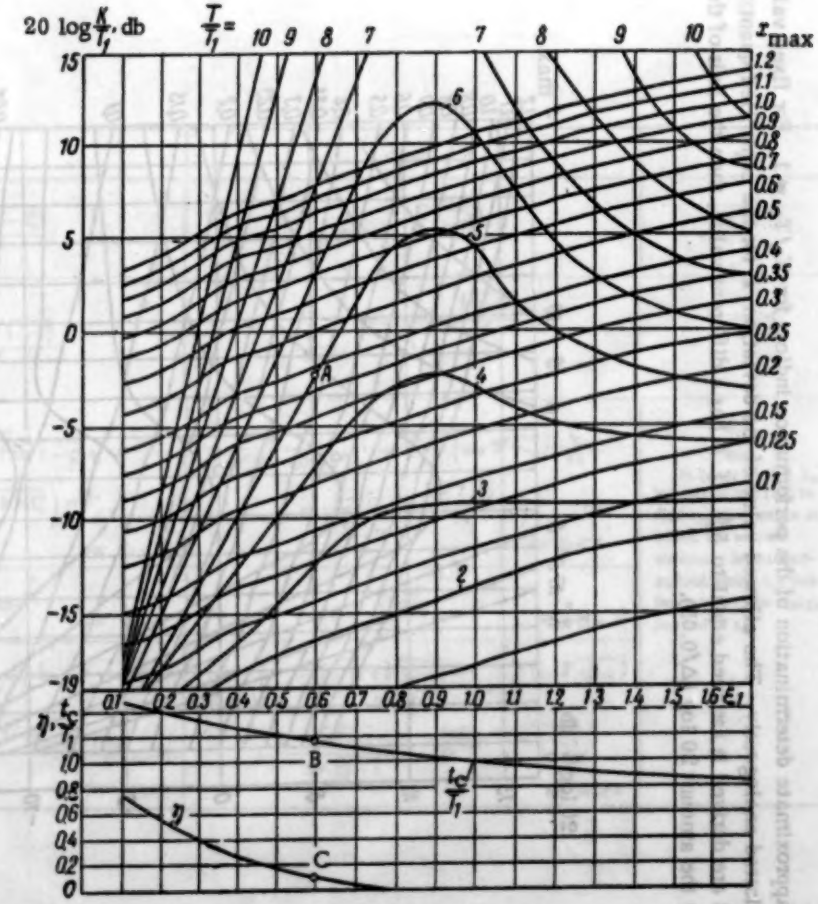

Fig. 3. Nomogram for choosing the desired transfer function of a closed-loop second order ACS (astatic controller).

can be used for an approximate determination of the performance indices for $T_2/T_1 \neq 1$. For fixed values $T_2/T_1 \neq 1$ the curves can be plotted analogously. The allowed value of the deviation Δ for the controlled quantity when the formulas in Table 4 are derived is assumed equal to 5%. If Δ has a different value, then the axis of the abscissas should be shifted by the amount 20 log (Δ/0.05).

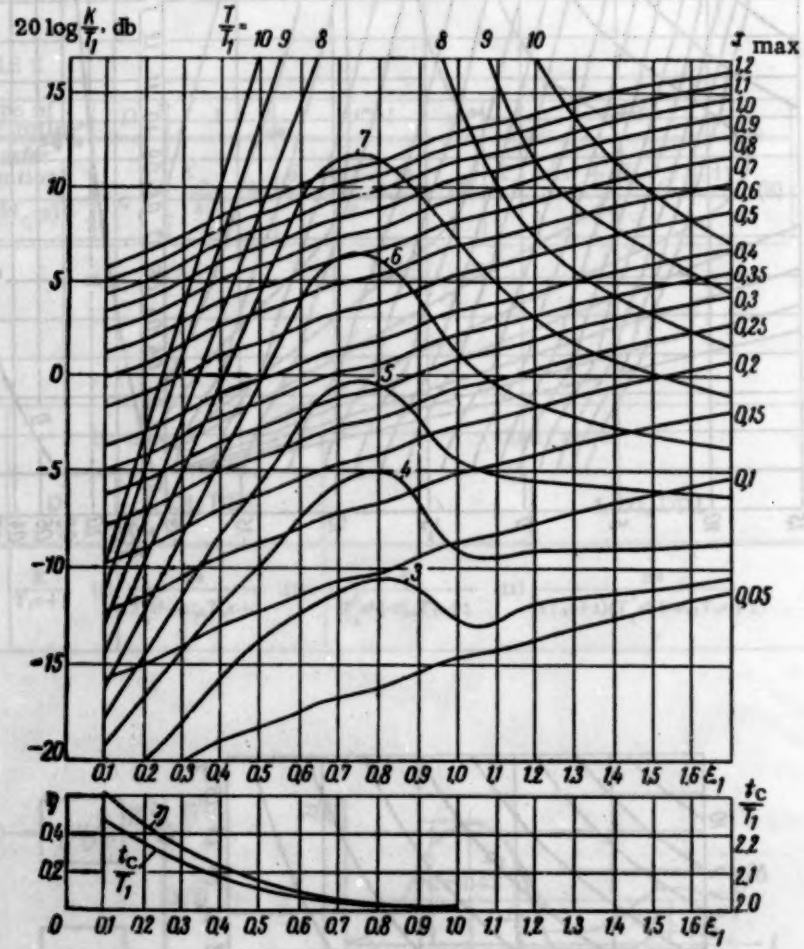

Fig. 4. Nomogram for choosing the desired transfer function of a closed-loop third-order ACS (astatic controller).

We shall use an example to demonstrate how the nomgrams are used for selecting the desired transfer functions of the closed-loop ACS.

Example 1 (Fig. 3). The following requirements are imposed on the transient response: $x_{st} = 0$; $x_{max} \leq 0.4$; $T \leq 25$ sec.

We shall specify $T/T_1 = 5$. Then $T_1 = 5$ sec. At the intersection of the curves $T/T_1 = 5$ and $x_{max} = 0.4$ we find the point A with the coordinates 20 log $K/T_1 = -2.5$ db or $K/T_1 = 0.75$; $\zeta_1 = 0.6$. From this we have $K = 5 \cdot 0.75 = 3.75$. Under these conditions $Y_d(s) = 3.75s(5^2s^2 + 2 \cdot 0.6 \cdot 5s + 1)$. At the same time, $t_c = T_1 \cdot 1.2 = 6$ (point B) and $\eta = x_{22}/x_{max} = 0.1$ (point C).

The nomograms for determining the type of controller in choosing the desired transfer function for the closed-loop system when the transfer function for the object is taken into account. We shall study a method of plotting nomgrams for a first order object and controller of the type DDI (a). Astatic controllers of the type DI (7) and I (6) shall be treated throughout as particular cases of (8) when the coefficients of the derivative and the deviation (or just

$Y_d(s)$	$\frac{t_c}{T_1}$	$\frac{T}{T_1}$	x_{max}	η
$\frac{K}{T_1^2s^2+2\zeta_1T_1s+1}$	$\frac{\pi}{\sqrt{1-\zeta_1^2}}$	$-\frac{1}{\zeta_1}\ln\frac{\Delta\sqrt{1-\zeta_1^2}}{K}$	$K\left(1-e^{-\frac{\pi\zeta_1}{\sqrt{1-\zeta_1^2}}}\right)$	$e^{-\frac{\pi\zeta_1}{\sqrt{1-\zeta_1^2}}}$
$\frac{Ks}{T_1^2s^2+2\zeta_1T_1s+1}$	$\frac{1}{\sqrt{1-\zeta_1^2}}\arctan\frac{\sqrt{1-\zeta_1^2}}{\zeta_1}$	$-\frac{1}{\zeta_1}\ln\frac{\Delta T_1\sqrt{1-\zeta_1^2}}{K}$	$\frac{K}{T_1}e^{-\frac{\zeta_1}{\sqrt{1-\zeta_1^2}}\arctan\frac{\sqrt{1-\zeta_1^2}}{\zeta_1}}$	$e^{-\frac{\pi\zeta_1}{\sqrt{1-\zeta_1^2}}}$
$\frac{Ks}{(T_1s+1)(T_1^2s^2+2\zeta_1T_1s+1)}$	$e^{-\frac{t_c}{T_1}}-e^{-\zeta_1\frac{t_c}{T_1}}\left(\cos\frac{t_c}{T_1}\sqrt{1-\zeta_1^2}+\right.$ $\left.+\frac{1-\zeta_1}{\sqrt{1-\zeta_1^2}}\sin\frac{t_c}{T_1}\sqrt{1-\zeta_1^2}\right)=0^*$ (13) for $\zeta_1<1$	$e^{-\frac{T}{T_1}}-e^{-\zeta_1\frac{T}{T_1}}\left(\cos\frac{T}{T_1}\sqrt{1-\zeta_1^2}+\right.$ $\left.+\frac{1-\zeta_1}{\sqrt{1-\zeta_1^2}}\sin\frac{T}{T_1}\sqrt{1-\zeta_1^2}\right)=0^*$ for $\zeta_1<1$	$\frac{K}{T_1^2(1-\zeta_1)}\left[e^{-\frac{t_c}{T_1}}-e^{-\zeta_1\frac{T_c}{T_1}}\left(\cos\sqrt{1-\zeta_1^2}\,\frac{t_c}{T_1}-\right.\right.$ $\left.\left.-\frac{1-\zeta_1}{\sqrt{1-\zeta_1^2}}\sin\frac{\sqrt{1-\zeta_1^2}}{T_1}t_c\right)\right]$ (14) for $\zeta_1<1$	$\frac{x_{m2}}{x_{max}}$ In order to find X_{m2} we should use (13) to find t_{c2}-the instant at which the second extremum is reached- and substitute t_{c2} into formula (14) for X_{max} instead of t_c.
	2 for $\zeta_1=1$	$\frac{K}{T_1}\left(\frac{T}{T_1}\right)^2=2\Delta e^{\frac{T}{T_1}}$ for $\zeta_1=1$	$\frac{2K}{e^2T_1}$ for $\zeta_1=1$	
	$\frac{t_c}{T_1}e^{-\frac{t_c}{T_1}}-\frac{1-\zeta_1+\sqrt{\zeta_1^2-1}}{2\sqrt{\zeta_1^2-1}}e^{-\frac{t_c}{T_1}\left(\zeta_1-\sqrt{\zeta_1^2-1}\right)}+$ $+\frac{1-\zeta_1-\sqrt{\zeta_1^2-1}}{2\sqrt{\zeta_1^2-1}}e^{-\frac{t_c}{T_1}\left(\zeta_1+\sqrt{\zeta_1^2-1}\right)}=0^*$ for $\zeta_1>1$	$e^{-\frac{T}{T_1}}\frac{\zeta_1+\sqrt{\zeta_1^2-1}-1}{2\sqrt{\zeta_1^2-1}}e^{-\frac{T}{T_1}\left(\zeta_1-\sqrt{\zeta_1^2-1}\right)}-$ $-\frac{\sqrt{\zeta_1^2-1}-1}{2\sqrt{\zeta_1^2-1}}e^{-\frac{T}{T_1}\left(\zeta_1+\sqrt{\zeta_1^2-1}\right)}=\frac{0{,}1T}{K}(\zeta_1-1)$ for $\zeta_1>1$	$\frac{K}{T_1^2(\zeta_1-1)}\left[-e^{-\frac{t_c}{T_1}}+\frac{\zeta_1+\sqrt{\zeta_1^2-1}-1}{2\sqrt{\zeta_1^2-1}}e^{-\frac{t_c}{T_1}\left(\zeta_1-\sqrt{\zeta_1^2-1}\right)}-\right.$ $\left.-\frac{\zeta_1-\sqrt{\zeta_1^2-1}-1}{2\sqrt{\zeta_1^2-1}}e^{-\frac{t_c}{T_1}\left(\zeta_1+\sqrt{\zeta_1^2-1}\right)}\right]$ for $\zeta_1>1$	

* The equations are solved by empirical methods.

TABLE 5

ζ_1	f_{11}	f_{12}
$\zeta_1 < 1$	$e^{-\frac{\zeta_1}{T_1}\tau}\left[\cos\frac{\sqrt{1-\zeta_1^2}}{T_1}\tau - \frac{\zeta_1-\frac{T_1}{T_0}}{\sqrt{1-\zeta_1^2}}\sin\frac{\sqrt{1-\zeta_1^2}}{T_1}\tau\right]$	$e^{-\frac{\zeta_1}{T_1}\tau}\left[\cos\frac{\sqrt{1-\zeta_1^2}}{T_1}\tau - \frac{\frac{T_0}{T_1}-\zeta_1}{\sqrt{1-\zeta_1^2}}\sin\frac{\sqrt{1-\zeta_1^2}}{T_1}\tau\right]$
$\zeta_1 = 1$	$e^{-\frac{\tau}{T_1}}\left[1-\frac{\tau}{T_1}\left(1-\frac{T_1}{T_0}\right)\right]$	$e^{-\frac{\tau}{T_1}}\left[1+\frac{\tau}{T_1}\left(\frac{T_0}{T_1}-1\right)\right]$
$\zeta_1 > 1$	$\frac{1}{2\sqrt{\zeta_1^2-1}}e^{-\frac{\zeta_1}{T_1}\tau}\times$ $\times\left[\left(\zeta_1+\sqrt{\zeta_1^2-1}-\frac{T_1}{T_0}\right)e^{\frac{\sqrt{\zeta_1^2-1}}{T_1}\tau} - \left(\zeta_1-\sqrt{\zeta_1^2-1}-\frac{T_1}{T_0}\right)e^{\frac{\sqrt{\zeta_1^2-1}}{T_1}\tau}\right]$	$\frac{1}{2\sqrt{\zeta_1^2-1}}e^{-\frac{\zeta_1}{T_1}\tau}\times$ $\times\left[\left(\zeta_1+\sqrt{\zeta_1^2-1}-\frac{T_0}{T_1}\right)e^{\frac{\sqrt{\zeta_1^2-1}}{T_1}\tau} - \left(\zeta_1-\sqrt{\zeta_1^2-1}-\frac{T_0}{T_1}\right)e^{\frac{\sqrt{\zeta_1^2-1}}{T_1}\tau}\right]$

of the derivative) are equal to zero. Setting the transfer function for the closed-loop system equal to the desired transfer function (11), we have:

$$Y(s)=\frac{\frac{1}{K_C}s}{\left(\frac{T_0}{K_0K_C}+\tau_C^2\right)s^2+\left(2\zeta_C\tau_C+\frac{1}{K_CK_0}\right)s+1}=\frac{}{T_1^2s^2+2\zeta_1T_1s+1}=Y_d(s). \tag{15}$$

In order to satisfy the latter equation it is necessary that the condition

$$K_C=\frac{1}{K},\quad \frac{T_0}{K_0K_C}+\tau_C^2=T_1^2,\quad 2\zeta_C\tau_C+\frac{1}{K_0K_C}=2\zeta_1T_1. \tag{16}$$

be satisfied.

Solving these equations simultaneously, we obtain:

$$\tau_C^2=T_1^2-\frac{K}{K_0}T_0;\quad 2\zeta_C\tau_C=2\zeta_1T_1-\frac{K}{K_0}. \tag{17}$$

If $\tau^2 = 0$, the coefficient of the derivative is equal to zero; then we obtain the condition for a proportional-integral controller of the type DI:

$$\tau_C^2=T_1^2-\frac{K}{K_0}T_0=0. \tag{18}$$

For the case of a type I controller the coefficient of the deviation must also be equal to zero:

$$2\zeta_c\tau_c = 2\zeta_1 T_1 - \frac{K}{K_0} = 0. \tag{19}$$

Writing Eqs. (18) and (19) in the form

$$20\log\frac{K}{T_1K_0} = 20\log\frac{T_1}{T_0} \tag{20}$$

and

$$20\log\frac{K}{T_1K_0} = 20\log 2\zeta_1. \tag{21}$$

we plot the curves in the coordinates $20\log\frac{K}{T_1K_0}$ vs. ζ_1 (Fig. 5) on the same scale as that used for the nomogram in Fig. 3 for various values of T_1/T_0 (the thin solid line) and $K_0 = 1$. The think solid line corresponds to Eq. (21). If $K_0 \neq 1$, then it is necessary to shift the axis of abscissas by $20\log K_0$. In choosing the desired transfer function for the closed-loop system it is necessary to make use of the nomogram in Fig. 5 in conjunction with the nomogram in Fig. 3. For this purpose it is necessary to superimpose one nomogram on the other in such a way that the distance between the axes of abscissas equals $20\log K_0$. For convenience in using the nomograms it is desirable to plot one of them (for example, the nomogram used to choose the type of controller) on transparent paper.

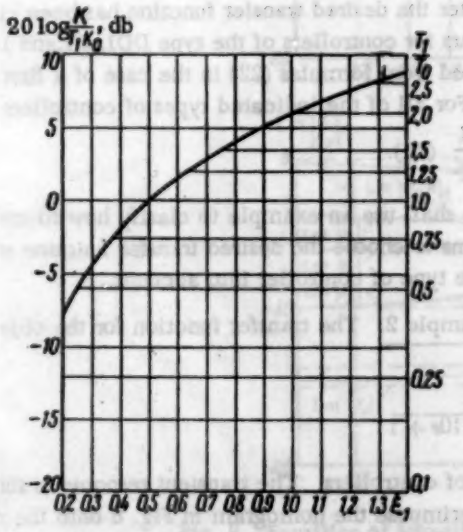

Fig. 5. Nomogram for determining the type of controller for a first order object without lag.

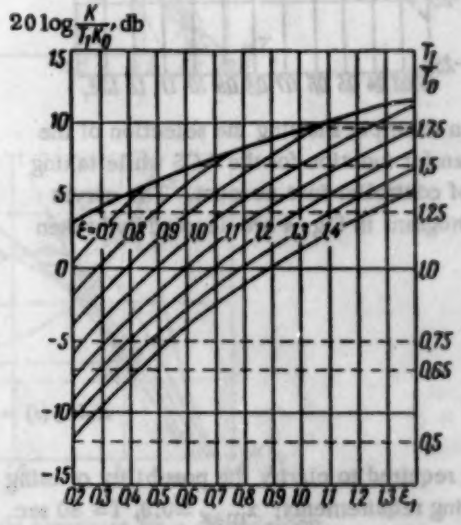

Fig. 6. Nomogram for determining the type of controller for a second order object without lag.

The parameters of the desired transfer function in the case of a type DI controller should be determined from the thin solid curve; in the case of an I controller they are determined from the intersection of the thick solid line with thin solid line.

For a second order object and a type DDI controller (8) we set $Y(s)$ and $Y_{d.}(s)$ equal to one another and find:

$$T_0^2\frac{K}{K_0} = T_1^2,\quad 2\zeta_0 T_0\frac{K}{K_0} + \tau_c^2 = T_1^2(1+2\zeta_1),\quad \frac{K}{K_0} + 2\zeta_c\tau_c = T_1(1+2\zeta_1). \tag{22}$$

The first condition (22) is necessary for the case where all three types of controllers are used (this condition corresponds to coincidence of the high-frequency asymptotes of the desired logarithmic amplitude response (LAR)

and the LAR of the object; the second condition ($\tau^2 = 0$) is necessary for a controller of the type DI, and the third condition ($2\zeta_c\tau_c = 0$) is for a controller of the type I. Solving Eq. (22) relative to K/T_1 and taking the logarithm, we obtain formulas from which curves in the coordinates $20 \log (K/T_1K_0)$ vs. ζ_1 (Fig. 6) for various values of T_1/T_0 (the broken-line curves) and ζ_0 (the thin solid curve); the thick solid line corresponds to the latter equation. The nomograms were plotted for $K_0 = 1$.

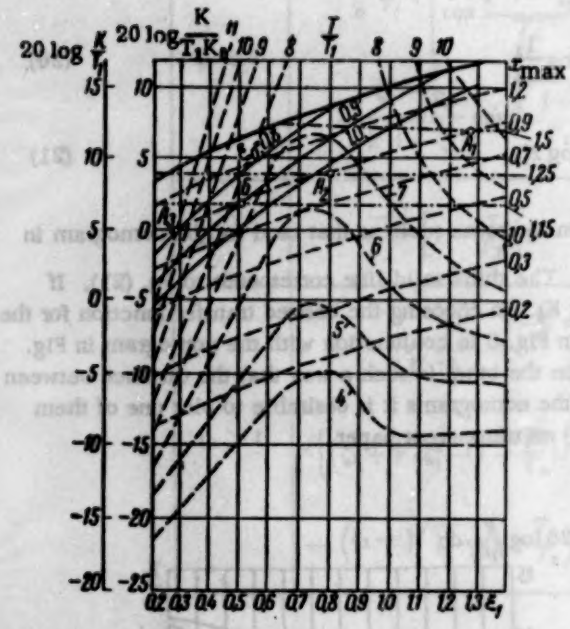

Fig. 7. An example showing the selection of the desired transfer function for the ACS while taking the type of controller into account. The curves of the nomogram in Fig. 4 are denoted by broken lines.

If $K_0 \neq 1$, then it is necessary to shift the axis of abscissas by $20 \log K_0$. In choosing the desired transfer function for the closed-loop system the nomogram in Fig. 6 should be used in the same way as the nomogram in Fig. 5 (i.e., in conjunction with the nomogram in Fig. 4). The parameters of the desired transfer function for the case of a DDI controller are determined from the broken-line curves (T_1/T_0); the parameters for the desired transfer function in the case of a DI controller are determined at the intersection of the broken-line curves (T_1/T_0 = const) and the thin solid curves (ζ_0 = const); the parameters of the desired transfer function for the case of an I controller are determined at the intersection of three curves; i.e., under these conditions the latter equation in the system (22) is taken into account (the thick solid curve).

After the desired transfer function has been chosen, the parameters for controllers of the type DDI, DI, and I can be determined from formulas (22) in the case of a first order object. For all of the indicated types of controllers the gain is $K_c = \frac{1}{K}$ (23).

We shall use an example to clarify how to use the nomograms to choose the desired transfer function while taking the type of controller into account.

Example 2. The transfer function for the object is

$$K_0W_0(s) = \frac{1.78}{10^2s^2 + 2 \cdot 0.9 \cdot 10s + 1}.$$

It is required to clarify the possibility of using various types of controllers. The transient response is subject to the following requirements: $x_{max} \leq 0.9$, $T \leq 80$ sec. We shall superimpose the nomogram in Fig. 6 onto the nomogram in Fig. 4 (Fig. 7) by raising the axis of abscissas by an amount equal to $20 \log K_0 = 5$ db.

The parameters of the desired transfer function in the case of a DDI are determined at the intersection of curve $x_{max} = 0.9$ with the straight line T_1/T_0 = const. If $T_1/T_0 = 1.5$ (point A_1), then $T/T_1 = 9.5$ and $T = 143$ sec. If $T_1/T_0 = 1.25$ (point A_2), then $T = 81$ sec. If $T_1/T_0 = 1.0$ (point A_3), then $T/T_1 = 11$ and $T = 110$ sec. Thus for a specified value of x_{max} the transient response with the minimal duration will be that corresponding to the desired transfer function

$$Y_d(s) = \frac{35s}{(12.5s + 1)(156s^2 + 20s + 1)}.$$

The transient response time for the case where a controller of the type DDI is used can be reduced if x_{max} is less. Thus, for example, if $x_{max} = 0.4$, then $T = 45$ sec.

In choosing a controller of the type DI the parameters of the desired transfer function are determined on the intersection of the curves $x_{max} = 0.9$ and $\zeta_0 = 0.9$ (point B) and the straight line $T_1/T_0 = 1.15$ passing through this point.

Thus we find $T_1 = 11.5$ sec, $T/T_1 = 7.5$ and $T = 86$ sec. The desired transfer function is written as

$$Y_d(s) = \frac{25.8s}{(11.5s+1)(132s^2+11.5s+1)},$$

whereas $K/T_1 = 2.24$; $\zeta_1 = 0.5$.

The transient response time here is greater than the required value, and it is not possible to reduce it for the type of controller specified. From Fig. 7 it follows that a controller of the type I cannot be used in this case, since this would lead to a large deviation of the controlled quantity (the curve $2\zeta_c\tau_c = 0$ is above the curve $x_{max} = 1.2$).

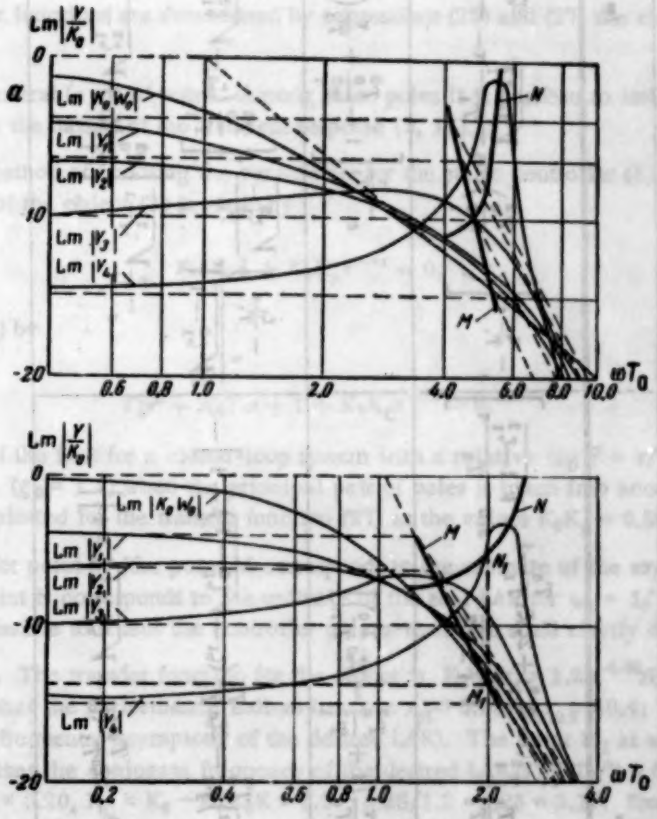

Fig. 8. Families of logarithmic amplitude responses for a closed-loop ACS with lag. a) First order object; b) second order object, $\zeta_0 = 1.0$.

We shall generalize the method for determining the controller parameters to include systems whose objects have pure lag (3) and (4). The transfer function for an object with lag is written as

$$K_0W_{0\tau}(s) = K_0W_0(s)e^{-\tau s}, \tag{24}$$

where $K_0W_0(s)$ is the transfer function for the object without lag; $e^{-\tau s}$ is the transfer function for the lag section.

The transfer function for the closed-loop ACS in that case is

$$Y_\tau(s) = \frac{K_0W_{0\tau}(s)}{1 + K_0W_{0\tau}(s)K_cW_c(s)} = \frac{K_0W_0(s)e^{-\tau s}}{1 + K_0W_0(s)K_cW_c(s)e^{-\tau s}} \tag{25}$$

TABLE 6

ζ_1	f_{12}	f_{22}
$\zeta_1 < 1$	$e^{-\frac{\zeta_1}{T_1}\tau}\left[2\left(\zeta_0-\frac{T^0}{T_1}\zeta_1\right)\cos\frac{\sqrt{1-\zeta_1^2}}{T_1}\tau-\frac{T_1}{T_0}\frac{\frac{T_0^2}{T_1^2}(1-2\zeta_1^2)+2\zeta_0\zeta_1\frac{T_0}{T_1}-1}{\sqrt{1-\zeta_1^2}}\sin\frac{\sqrt{1-\zeta_1^2}}{T_1}\tau\right]$	$e^{-\frac{\zeta_1}{T_1}\tau}\left[\left(1-\frac{T_0^2}{T_1^2}\right)\cos\frac{\sqrt{1-\zeta_1^2}}{T_1}\tau-\frac{2\zeta_0\frac{T_0}{T_1}-\zeta_1\left(1+\frac{T_0^2}{T_1^2}\right)}{\sqrt{1-\zeta_1^2}}\sin\frac{\sqrt{1-\zeta_1^2}}{T_1}\tau\right]$
$\zeta_1 = 1$	$e^{-\frac{\tau}{T_1}}\left[2\left(\zeta_0-\frac{T_0}{T_1}\right)+\frac{\tau}{T_0}\left(1+\frac{T_0^2}{T_1^2}-2\zeta_0\frac{T_0}{T_1}\right)\right]$	$e^{-\frac{\tau}{T_1}}\left[1-\frac{T_0^2}{T_1^2}+\frac{\tau}{T_1}\left(1+\frac{T_0^2}{T_1^2}-2\zeta_0\frac{T_0}{T_1}\right)\right]$
$\zeta_1 > 1$	$\frac{e^{-\frac{\zeta_1}{T_1}\tau}}{2\sqrt{\zeta_1^2-1}}\frac{T_1}{T_0}\left\{e^{\frac{\sqrt{\zeta_1^2-1}}{T_1}\tau}\left[\left(\zeta_1-\sqrt{\zeta_1^2-1}\right)\frac{T_0^2}{T_1^2}-2\zeta_0\frac{T_0}{T_1}\left(\zeta_1-\sqrt{\zeta_1^2-1}\right)+1\right]-\right.$ $\left.-e^{-\frac{\sqrt{\zeta_1^2-1}}{T_1}\tau}\left[\frac{T_0^2}{T_1^2}\left(\zeta_1+\sqrt{\zeta_0^2-1}\right)^2-2\zeta_0\frac{T_0}{T_1}\left(\zeta_1+\sqrt{\zeta_1^2-1}\right)+1\right]\right\}$	$\frac{e^{-\frac{\zeta_1}{T_1}\tau}}{2\sqrt{\zeta_1^2-1}}\left\{e^{\frac{\sqrt{\zeta_1^2-1}}{T_1}\tau}\left[\frac{T_0^2}{T_1^2}\left(\zeta_1-\sqrt{\zeta_1^2-1}\right)-2\zeta_0\frac{T_0}{T_1}+\zeta_1+\sqrt{\zeta_1^2-1}\right]-\right.$ $\left.-e^{-\frac{\tau}{T_1}\sqrt{\zeta_1^2-1}}\left[\frac{T_0^2}{T_1^2}\left(\zeta_1+\sqrt{\zeta_1^2-1}\right)-2\zeta_0\frac{T_0}{T_1}+\zeta_1-\sqrt{\zeta_1^2-1}\right]\right\}$

and includes as multiplier the same lag-section transfer function as does the object. Therefore the desired transfer function can be written conditionally as

$$Y_{d\tau}(s) = Y'_{d}(s)\, e^{-\tau s}, \tag{26}$$

where

$$Y'_{d}(s) = \frac{K_0 W_0(s)}{1 + K_0 W_0(s)\, K_C W_C(s)\, e^{-\tau s}}. \tag{27}$$

The transient response in a system that has the transfer function $Y'_d(s)$ differs from the transient response in a system that has a transfer function of the form (25) by a time displacement in the amount τ.

For systems whose transfer functions are determined by expressions (25) and (27) the characteristic equations are identical.

The equation has an innumerable set of poles. Among these poles it is possible to isolate the principal pair of complex poles which determine the nature of the transient response [9, 11].

First we shall study the method of choosing the parameters for the static controller (5). The characteristic equation for the system in the case of the object (3) is given by

$$T_0 s + 1 + K_0 K_p e^{-\tau s} = 0, \tag{28}$$

and in the case of the object (4) by

$$T_0^2 s^2 + 2\zeta_0 T_0 s + 1 + K_0 K_C e^{-\tau s} = 0. \tag{29}$$

Figure 8 shows families of the LAR for a closed-loop system with a relative lag $\bar{\tau} = \tau/T_0 = 0.3$ and first order (a) and second order (b) objects ($\zeta_0 = 1.0$) when the principal pair of poles is taken into account. The LAR $L_m|Y_1|$, $L_m|Y_2|$, $L_m|Y_3|$, $L_m|Y_4|$ are plotted for the transfer function (27) as the values $K_0K_C = 0.58; 1.0; 2.16; 4.6$.

Figure 8 shows the lines for point M (the point M corresponds to the ordinate of the asymptotic LAR for $\omega_1 = 1/T_1$) and the point N (the point N corresponds to the ordinate of the real LAR for $\omega_1 = 1/T_1$). The families of LAR which are cited make it possible to select the controller parameters. We shall clarify this using an example.

Example 3 (cf. Fig. 8b). The transfer function for the object is $K_0W_0(s) = 1.2e^{-0.6s}/(12^2s^2 + 2 \cdot 12s + 1)$. It is required to determine K_C such that the performance indices become $x_{st} \leq 0.25$; $x_{max} \leq 0.4$; $T \leq 60$ sec. Then $20 \log (K/K_0) \leq -13.6$ (the low-frequency asymptote of the desired LAR). The point M_1 at which this straight line interesects the curve M determines the conjugate frequency of the desired LAR. $T_1 = T_0/2 = 6$. The segment $M_1N_1 = 20 \log 2\zeta_1 = -8$ db, whence $\zeta_1 = 0.20$, $K_C = K_0 - K/K_0K = 1.2 - 0.25/1.2 \cdot 0.25 = 3.17$. From the nomogram in Fig. 2a we find that the chosen desired transfer function corresponds to a transient response with the following performance indices: $x_{max} = 0.4$; $T/T_1 = 8$; $T = 48 + 3.6 = 51.6$ sec.

Families of LAR similar to those shown in Fig. 8 can be plotted for systems with controllers of the type I, DI, and DDI; they can then be used to choose parameters that insure the required performance indices. However, it is simpler to generalize the method treated above for ACS with no lag and astatic controllers to include systems with lag.

For the case of a first order object with lag (3) and a controller of the type DDI (8) the transfer function for the closed-loop ACS is determined by the expression

$$Y'_{\tau}(s) = Y'_{\tau}(s)\, e^{-\tau s}. \tag{30}$$

Here

$$Y'_{\tau}(s) = \frac{\frac{1}{K_C} s}{\frac{1}{K_0 K_C} T_0 s^2 + \frac{1}{K_0 K_C} s + (\tau_C^2 s^2 + 2\zeta_C \tau_C s + 1)\, e^{-\tau s}}, \tag{31}$$

where $1/K_C = K$.

The desired transfer function $Y'_{\tau}(s)$ [cf. (26), (27)] will be written as

$$Y'_d(s) = \frac{Ks}{T_1^2 s^2 + 2\zeta_1 T_1 s + 1}. \tag{32}$$

Requiring that the roots of the characteristic equation (31) must be equal to the desired roots, we determined the roots of the characteristic equation (32) by substituting them successively into (31); solving the resulting equations relative to τ_c^2 and $2\zeta_c\tau_c$, we find

$$\tau_c^2 = T_1^2 - \frac{K}{K_0} T_0 f_{11} \;\&\; 2\zeta_c\tau_c = 2\zeta_1 T_1 - \frac{K}{K_0} f_{21}, \tag{33}$$

where f_{11} and f_{21} are determined by the formulas in Table 5 as a function of ζ_1. Formulas (33) differ from the analogous formulas (17) for a system without lag in that they have the multipliers f_{11} and f_{21} (corrections to the lag). For convenience in determining the corrections, the formulas in Table 5 can be used to plot the curves $f_{11} = f(\zeta_1)$ and $f_{21} = f(\zeta_1)$ for various τ/T_0 and T_1/T_0.

For the case of a second order object with lag (4) and a controller of the type DDI (8) we have $Y_{\tau}(s) = Y'_{\tau}(s)e^{-\tau s}$. Here

$$Y'_{\tau}(s) = \frac{\frac{1}{K_c} s}{\frac{K}{K_0} T_0^2 s^3 + 2\zeta_0 \frac{T_0}{K_0} K s^2 + \frac{K}{K_0} s + (\tau_c^2 s^2 + 2\zeta_c\tau_c s + 1) e^{-\tau s}}, \tag{34}$$

where $K = 1/K_c$.

The desired transfer function is

$$Y'_d(s) = \frac{Ks}{(T_2 s + 1)(T_1^2 s^2 + 2\zeta_1 T_1 s + 1)}. \tag{35}$$

Originating from the requirements that the roots of the characteristic equation for the ACS (34) must be equal to the roots of the desired characteristic equation, we determine the roots of the characteristic equation (35), substitute them into (34), and obtain the following solutions by solving the resulting equations for τ_c and ζ_c:

$$\tau_c^2 = T_1^2 - \frac{K}{K_0} T_0 f_{12}, \quad 2\zeta_c\tau_c = 2\zeta_1 T_1 - \frac{K}{K_0} f_{22}. \tag{36}$$

An additional condition is imposed on the transfer function; this condition is based on the presence of a third pole

$$\frac{K}{K_0 T_1} = \frac{T_1^2}{T_0^2} f_{32}, \tag{37}$$

where

$$f_{32} = \frac{2(\zeta_1 - 1)\, e^{-\frac{\tau}{T_1}}}{-1 + 2\zeta_0 \frac{T_1}{T_0} - \frac{T_1^2}{T_0^2} + e^{\frac{\tau}{T_1}} \left(f_{22} \frac{T_1^2}{T_0^2} - f_{12} \frac{T_1}{T_0} \right)}.$$

The formulas are written in the same form as that used for an object with no lag. The corrections f_{12} and f_{22} for the lag are determined from the expressions in Table 6.

For convenience in determining the corrections from the formulas in Table 6 we plot the curves $f_{21} = f(\zeta_1)$, $f_{22} = f(\zeta_1)$, and $f_{32} = f(\zeta_1)$ for various values of τ/T_0, ζ_0, T_1/T_0, and T_1/T_2.

Setting the right-hand sides of Eqs. (33) and (36) to zero and converting (33) to the form

$$20\log\frac{K}{K_0T_1}=20\log\left(\frac{T_1}{T_0}\frac{1}{f_{11}}\right),\qquad 20\log\frac{K}{K_0T_1}=20\log\frac{2\zeta_1}{f_{21}}, \tag{38}$$

and (36) and (37) to the form

$$\begin{aligned}
20\log\frac{K}{K_0T_1}&=20\log\left(\frac{T_1}{T_0}\right)^2 f_{22},\\
20\log\frac{K}{K_0T_1}&=20\log\left(\frac{T_1}{T_0}\frac{1}{f_{12}}\right),\\
20\log\frac{K}{K_0T_1}&=20\log\frac{2\zeta_1}{f_{22}},
\end{aligned} \tag{39}$$

we plot the nomograms in Figs. 9 and 10 in the coordinates 20 log K/K_0T_1 vs. ζ_1 in order to determine the type of controller in an ACS with lag for fixed values of T_1/T_0, ζ_0 (for a second order object), and $\tau/T_0 = 0.3$. They are analagous to the nomograms in Figs. 5 and 6 for determining the type of controller in an ACS with no lag.

Formulas (33) and (36) make it possible to choose the control parameters in such a way that the roots of the closed-loop ACS which determine the nature of the transient response correspond to the desired ones. However, in this case for the performance indices of the ACS with lag to be close to the desired indices of the ACS without lag (the transient response time differs by the amount τ), it is necessary that the remaining poles of the transfer function for the ACS with lag lie considerably further away from the imaginary axes than the desired poles. Therefore there are limitations placed on the choice of the desired transfer function for the system with lag; these are determined by the relationship between the object parameters and the desired transfer function for the ACS. The critical relationship between these parameters is determined by the minimal distance between the desired and the remaining poles for which it is still possible to estimate the transient response using only the principal poles. We adopt the phase stability margin for the open-loop system as a criterion which makes it possible to estimate the location of the poles of the transfer function of the system with pure lag.

Under these conditions the formulas derived above are valid for those parameter values which cause the phase stability margin of the system with lag to be no less than the phase stability margin of the system with no lag.

In order to determine the critical values of the parameters we computed the phase stability margins for the system with and without lag for various parameter values; we then compared the transfer functions of these systems for equal stability margins and found the relationships corresponding to the critical values of the parameters; i. e., $K/K_0T_1 = f(\zeta_1; T_1/T_0; \zeta_0)$. The curves for the critical values were plotted in the coordinates 20 log K/K_0T_1 and ζ_1 for fixed values of τ/T_0 and T_1/T_0; they were plotted on a nomogram for determining the type of controller in the system with lag (the dash-dot curves in Figs. 9 and 10). It should be noted that in Fig. 10 the curves for the additional conditions and the critical values coincide for the values $T_1/T_0 = 0.5$ and 1.0. Making use of the nomograms in Figs. 9 and 10, it is possible to choose the desired transfer function for the system while taking the type of controller into account. Here we take into account the limitations governing the choice of controller parameters (these limitations were discussed above). After choosing the desired transfer function the controller parameters can be found from formulas (23), (33) and (36).

We shall analyze an example which clarifies the method presented above.

Example 4 (Fig. 11). The transfer function for the object is

$$K_0W_0(s)=\frac{1.6e^{-3s}}{10^2s^2+2\cdot0.75\cdot10s+1}.$$

The following requirements are imposed on the transient response: $x_{max} \le 0.5$; $T \le 30$ sec. We must determine the type of controller and the numerical values of its parameters. We superimpose the nomogram in Fig. 10 onto the nomogram in Fig. 4 and shift the axis of abscissas of the former by the amount 20 log $K_0 = 4$ db.

The desired transfer function is determined by the coordinates of the point A which is chosen on the intersection of the curve corresponding to the additional condition for $T_1/T_0 = 0.5$ and the curve $x_{max} = 0.5$.

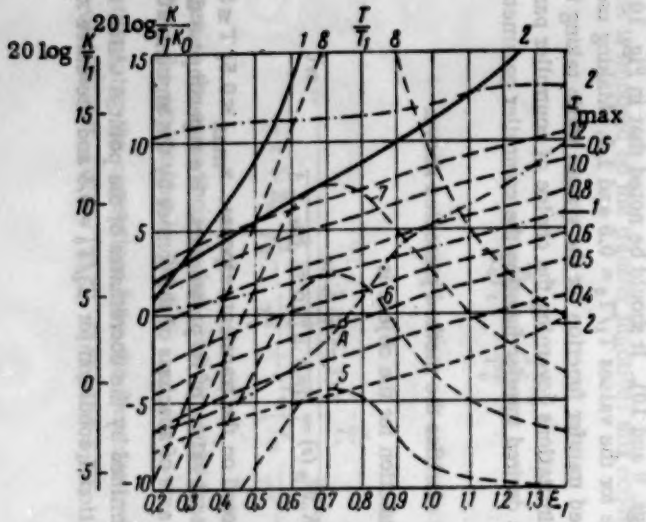

Fig. 9. Nomogram for determining the type of controller for a first order object with lag.

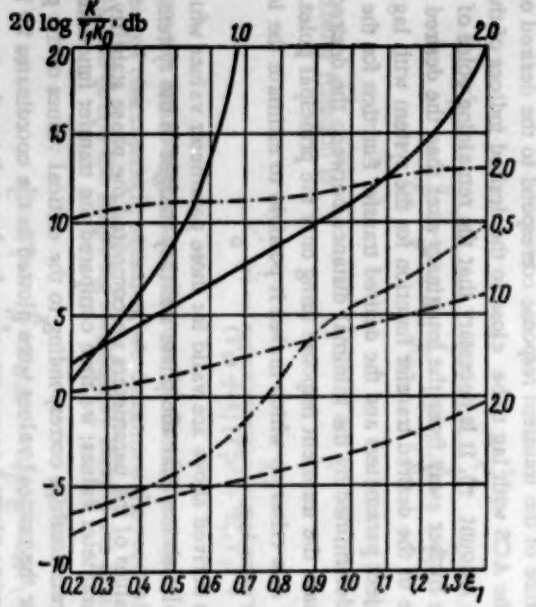

Fig. 10. Nomogram for determining the type of controller for a second order object with lag.

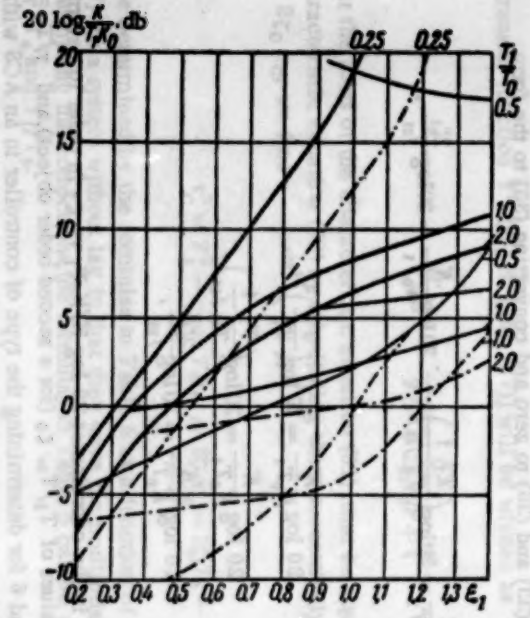

Fig. 11. Example illustrating the choice of the desired transfer function for the ACS with lag when the type of controller is taken into account. The curves from the nomogram in Fig. 4 are denoted by dash-dot lines.

The desired transfer function is written as

$$Y'_d(s) = \frac{7.5s}{(5s+1)(25s^2+7.4s+1)},$$

since $T_1 = 0.5T_0 = 5$ sec; $20 \log (K/T_1) = 3.5$ db; $K = 7.5$; $\zeta_1 = 0.74$; $T_2 = T_1$. The parameters of the transient response are $x_{max} = 0.5$; $T = 5 \cdot 5.5 = 27.5$ sec. The corrections f_{12}, f_{22} are found from the formulas in Table 6 (or from the graph): $f_{12} = -1.02$; $f_{22} = -1.5$. The parameters of the controller are determined from formulas (23) and (36):

$$K_p = 1/K = 0.132; \quad \tau_c^2 = 72; \quad 2\zeta_c\tau_c = 14.4.$$

The transfer function for the controller is

$$K_c W_c(s) = 0.132(72s^2 + 14.4s + 1)/s.$$

SUMMARY

The proposed method permits the choice of the simplest type of controller and the determination of its parameters either analytically or from the logarithmic frequency responses on the basis of specified performance indices.

LITERATURE CITED

1. Fundamentals of Automatic Control. Theory. Edited by V. V. Solodovnikov [in Russian] (Machinery Press, 1954).
2. E. G. Dudnikov, Fundamentals of the Automatic Control of Thermal Process [in Russian] (State Power Engineering Press, 1956).
3. A. Ya. Lerner, Introduction to the Theory of Automatic Control [in Russian] (Machinery Press, 1958).
4. P. S. Matveev and V. N. Plotnikov, "Nomograms for analyzing and synthesizing automatic stabilization systems," Avtomatika i Telemekhanika 20, 7 (1959).*
5. G. K. Krug and E. K. Krug, Electrical Corrective Elements in Automatic Control and Regulation Systems [in Russian] (State Power Engineering Press, 1959).
6. N. T. Kuzovkov, "Synthesis of automatic control systems from logarithmic root loci and generalized frequency responses," Izvestiya Akad. Nauk, Otdelenie Tekhnicheskikh Nauk, Énergetika i Avtomatika 5 (1959).
7. V. V. Solodovnikov, "Synthesis of corrective networks in servosystems for typical inputs," Avtomatika i Telemekhanika 12, 5 (1951).
8. V. V. Solodovnikov, "Synthesis of corrective networks in servosystems by means of optimal and typical logarithmic frequency responses," Avtomatika i Telemekhanika 14, 5 (1953).
9. V. V. Solodovnikov, Synthesis of Corrective Networks in Automatic Control Systems," Transactions of the Second All-Union Conference on the Theory of Automatic Control, Vol. II [in Russian](Academy of Sciences USSR Press, 1955).
10. K. L. Chien, J. A. Hrones, and J. B. Reswick, On the automatic control of generalized passive systems. Trans. ASME vol. 74, 1952, pp. 175-185.
11. J. H. Mulligan, The effect of pole and zero locations on the transient response of linear dynamic systems. Proc. Inst. of Rad. Eng. vol. 37, May, 1949.
12. W. Oppelt, Kleines Handbuch technischer Regelvorgänge. Verlag Chemie, 1960.
13. J. Traxel, Synthesis of Automatic Control Systems [Russian translation] (Machinery Press, 1959).

* Original Russian Pagination. See C. B. translation.

DETERMINING THE OPTIMAL TRANSFER FUNCTION FOR "WHITE NOISE" IN A SERVOSYSTEM FROM THE FIGURE OF MERIT AND THE TRANSIENT RESPONSE DURATION FOR THE SYSTEM

A. S. Kul'chii

(Leningrad)

Translated from Avtomatika i Telemekhanika, Vol. 22, No. 4,
pp. 524-529, April,1961
Original article submitted July 24, 1960

The paper establishes a relationship between the coefficients of the systematic error and the time required for the transient response when the minimum mean square error is ensured. Formulas are derived for determining the optimal transfer function for "white noise" in cases where the first two or three error coefficients are taken into account.

A number of papers have been devoted to developing engineering methods for obtaining optimal block diagrams and dynamic-accuracy estimates for automatic control systems. In [1], for example, a study is made of the problem of finding the optimal values of certain parameters for a servosystem with a specified structure on the basis of assuring the minimum mean square error (MSE) under conditions where it is equal to the square of the systematic error. In [2] the method of determining the optimal pulse transient response is generalized to include the case where the dynamic accuracy with which the regular useful signal is reproduced is determined by a priori specified coefficients of a certain polynomial time function which characterizes this accuracy (the error coefficients C_i). The sampling time T in [2] is chosen to be the transient response time for a unit step input. The amplitude-frequency and phase-frequence responses are approximated semianalytically by means of the corresponding desired responses.

In [3] K. I. Kurakin solves the problem of obtaining the responses for systems that are physically reliable and deviate the least amount from the optimal system; this was achieved using an analytical method for approximating the transfer function $\Phi(p, e^{-pT})$ by means of a fractionally rational Padeh function. The deviations from the optimal conditions are in this case also reduced to a situation where the error coefficients do not equal zero; i.e., the steady-state error with which the regular useful signal is reproduced is chosen equal to some allowable value.

The satisfaction of the optimal conditions therefore assures a minimum MSE for a specified value of the systematic error. Thus, in order to determine the optimal transfer function and its corresponding MSE it is necessary to know the coefficients C_i of the systematic error and the transient response duration T.

In a number of cases the useful signal is a slowly varying time function; then the analysis can be limited to just the first two or three error coefficients. The coefficient C_1, which is a quantity that is the inverse of the figure of merit for the system with respect to speed, is usually specified; the error coefficients C_2 and C_3 in the cases indicated above have a comparatively small effect on the magnitude of the systematic error, and therefore it is expedient to determine them from the conditions which govern the assurance of the minimum MSE.

Based on the results of [3], we study the problem of determining the optimal transfer function for "white noise" in this paper; we achieve this by finding those values of the coefficients C_2 and C_3 for which the MSE is minimal. We consider C_1 and T to be the specified quantities.

In order words, the purpose of the paper is to determine the relationship between the accuracy of the system for random and regular inputs, and the time required for the transient response to be completed.

1. Original Equations

We shall cite the expressions for the optimal transfer function and MSE of the servosystem in the case when: a) a stationary random noise of the "white noise" type with the spectral density $G_{nn}(\omega) = \epsilon^2 = \text{const}$ acts at the input of the system, and b) the first two error coefficients satisfying the dynamic accuracy requirements are given together with the transient response duration T [3].

The expression for the MSE in [3] becomes

$$\overline{\delta_n^2} = \frac{4.5\,\varepsilon^2}{T}\left(1 - \frac{8\,C_1}{T} - \frac{20\,C_2}{3T^2} + \frac{64\,C_1^2}{3T^2} + \frac{40\,C_1C_2}{T^3} + \frac{20\,C_2^2}{T^4}\right). \tag{1}$$

Here T is the duration of the transient response; C_1 and C_2 are the coefficients of the systematic error δ_c,

$$\delta_c(t) = C_1\frac{d\beta(t)}{dt} + \frac{C_2}{2!}\frac{d^2\beta(t)}{dt^2},$$

where $\beta(t)$ is the useful signal at the system input.

From here on we shall operate with the relative value of the MSE which can be written in the form of the equation

$$\overline{\eta^2} = \frac{\overline{\delta_n^2}}{\varepsilon^2} = \frac{4.5}{T} - \frac{36C_1}{T^2} - \frac{30C_2}{T^3} + \frac{96C_1^2}{T^3} + \frac{180C_1C_2}{T^4} + \frac{90C_2^2}{T^5}. \tag{2}$$

The equations for the optimal transfer function of the servosystem in the closed-loop $\Phi_{opt.}(p)$ and open-loop $W_{opt.}(p)$ states are given in [3] by means of the following expressions:

$$\Phi_{opt}(p) = \frac{\frac{T^2}{10}\left[1 - \frac{5}{T}\left(C_1 + \frac{C_2}{T}\right)\right]p^2 + \frac{T}{2}\left(1 - \frac{2}{T}C_1\right)p + 1}{\frac{T^3}{120}p^3 + \frac{T^2}{10}p^2 + \frac{T}{2}p + 1}, \tag{3}$$

$$W_{opt}(p) = \frac{1}{C_1}\frac{\frac{T^2}{10}\left[1 - \frac{5}{T}\left(C_1 + \frac{C_2}{T}\right)\right]p^2 + \frac{T}{2}\left(1 - \frac{2}{T}C_1\right)p + 1}{p\left[\frac{T^3}{120C_1}p^2 + \frac{T}{2}\left(1 + \frac{C_2}{TC_1}\right)p + 1\right]}. \tag{4}$$

For the system to be a stable and minimal-phase system in both the closed-loop and open-loop states the error coefficients C_1 and C_2 must satisfy the following inequalities:

$$C_1 > 0, \tag{5}$$

$$C_1 < \frac{T}{2}, \tag{6}$$

$$C_2 < \frac{T^2}{5} - TC_1, \tag{7}$$

$$C_2 > -TC_1. \tag{8}$$

For the case where it is necessary to take into account the first three error coefficients C_1, C_2, C_3, the expression for the optimal transfer function will be given by the equation [3]

$$\Phi_{opt}(p) = \frac{\frac{T^2}{84}\left[1 - \frac{9}{T}\left(C_1 + \frac{7C_2}{3T} + \frac{14C_3}{9T^2}\right)\right]p^3 + \frac{3T^2}{28}\left[1 - \frac{14}{3T}\left(C_1 + \frac{C_2}{T}\right)\right]p^2 + \frac{T}{2}\left(1 - \frac{2C_1}{T}\right)p + 1}{\frac{T^4}{1680}p^4 + \frac{T^3}{84}p^3 + \frac{3T^2}{28}p^2 + \frac{T}{2}p + 1}. \tag{9}$$

Under these conditions the relationships between the error coefficients must be determined by the set of inequalities (6) and the inequalities

$$C_2 < \frac{3T^2}{14} - TC_1, \tag{10}$$

$$C_3 < \frac{T^3}{14} - \frac{9T^2}{14}C_1 - \frac{3T}{2}C_2. \tag{11}$$

We shall now give the expression for the relative value of the mean square error for the optimal system when "white noise" appears at its input; this expression was derived on the basis of (9) using the formulas cited in [4]:

$$\overline{\eta^2} = \frac{784}{89T}\left(1 - \frac{15C_1}{T} - \frac{30C_2}{T^2} - \frac{35C_3}{2T^3} + \frac{675C_1C_2}{2T^5} + \frac{210C_1C_3}{T^4} + \frac{525C_2C_3}{T^6} + \frac{75C_1^2}{T^2} + \frac{405C_2^2}{T^4} + \frac{175C_3^2}{T^6}\right). \quad (12)$$

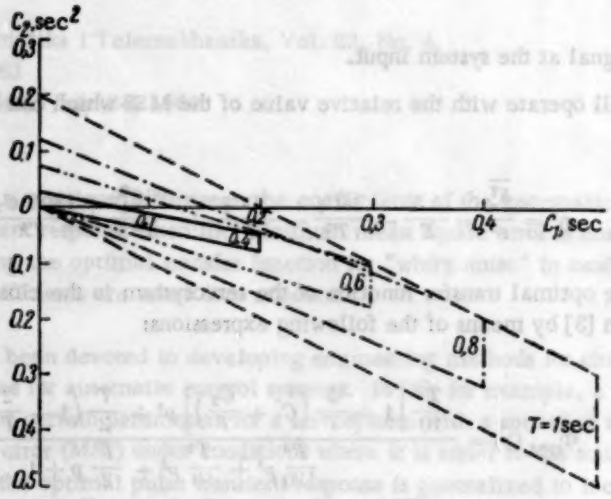

Fig. 1.

2. The Regions of Allowable Values for C_2

From the inequalities (5)-(8) it is possible to plot the regions of allowable values for the error coefficient of the second derivative of the useful signal C_2 as a function of C_1 for specified T; these regions permit us to perform a direct estimate of the applicability of one or another value of C_2 from the point of view of the requirements imposed on the optimal transfer function of the system. The indicated region for certain values of T are shown in Fig. 1. Each of the regions is bounded from the left by the axis of ordinates ($C_1 = 0$), and above and below by straight lines whose equations are $C_2 = 0.2T^2 - TC_1$ and $C_2 = -TC_1$, respectively. On the right the region is bounded by the straight line $C_1 = 0.5\ T$.

Knowing C_1 and T, it is thus possible immediately to determine the allowable limits for the values of C_2. However, this does not provide an answer to the question of whether or not we have chosen the optimal values of C_2 from the point of view of the magnitude of the MSE.

The solution of this problem shall be sought, as indicated above, on the basis of the proposition that the error coefficients of the second and third derivatives have only a small effect on the magnitude of the systematic error; therefore they must be determined in such a way as to assure the minimum MSE.

3. Determining the Optimal Transfer Function with Respect to the Figure of Merit and the Transient Response Duration

Assuming that the magnitude of the figure of merit with respect to speed ($1/C_1$) and the duration T of the transient response are specified, we find the expressions for the error coefficients which cause the relative value of the MSE to be a minimum. For this purpose we use known rules to determine the minimum for the function (2) by assuming that the value of C_2 in it is variable; then we determine the minimum of the function (12), assuming that the coefficients C_2 and C_3 are the variables. Having performed these operations, we obtain the following results. The function (2) has a minimum for

$$C_2 = \frac{T^2}{6} - TC_1. \quad (13)$$

It is evident that (13) satisfies both inequality (7) and inequality (8). Substituting (13) into (2), (3), and (4), we obtain the formulas for the relative value of the MSE and for the transfer function of the optimal system in the closed-loop and open-loop states in cases where it is possible to treat only the first two error coefficients. The enumerated formulas are written as:

$$\overline{\eta_*^2} = \frac{2}{T}\left(\frac{3C_1^2}{T^2} - \frac{3C_1}{T} + 1\right), \tag{14}$$

$$\Phi^*_{opt}(p) = \frac{\frac{T^3}{60}p^3 + \frac{1}{2}(T - 2C_1)p + 1}{\frac{T^3}{120}p^3 + \frac{T^2}{10}p^2 + \frac{T}{2}p + 1}, \tag{15}$$

$$W^*_{opt}(p) = \frac{1}{C_1 p}\,\frac{\frac{T^3}{60}p^3 + \frac{1}{2}(T - 2C_1)p + 1}{\frac{T^3}{120C_1}p^3 + \frac{T^2}{12C_1}p + 1}. \tag{16}$$

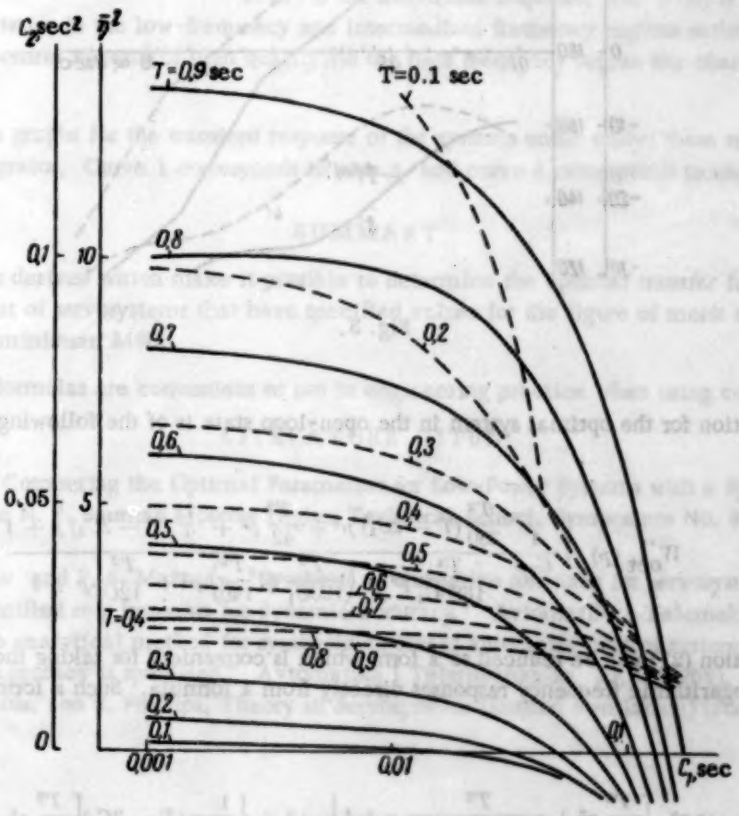

Fig. 2.

An analysis of the function (12) shows that it has a minimum for the values of the error coefficients C_2 and C_3 which are defined by the equations

$$C_2 = \frac{T^2}{6} - TC_1, \tag{17}$$

$$C_3 = -\frac{T^3}{5} + \frac{9}{10}T^2C_1. \tag{18}$$

If we substitute (17) and (18) into (12) and (9), then we obtain formulas for determining the MSE and the transfer function for the system in the open-loop state in the case where it is necessary to take into account the first three coefficients of the systematic error C_1, C_2, and C_3 in finding the optimal parameters:

$$\overline{\eta_{**}^2} = \frac{196}{89T}\left(\frac{3C_1^2}{T^2} - \frac{3C_1}{T} + 1\right), \tag{19}$$

$$\Phi_{opt}^{**}(p) = \frac{\frac{T^2}{280}(T-2C_1)p^3 + \frac{T^2}{42}p^2 + \frac{1}{2}(T-2C_1)p + 1}{\frac{T^4}{1680}p^4 + \frac{T^3}{84}p^3 + \frac{3T^2}{28}p^2 + \frac{T}{2}p + 1}. \tag{20}$$

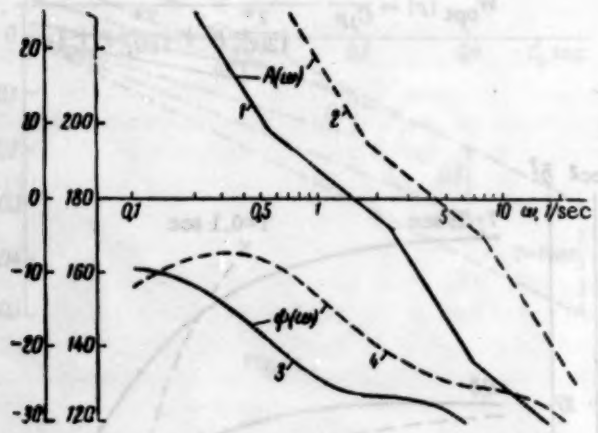

Fig. 3.

The transfer function for the optimal system in the open-loop state is of the following form for the case under study:

$$W_{opt}^{**}(p) = \frac{1}{C_1 p}\,\frac{\frac{T^2}{280}(T-2C_1)p^3 + \frac{T^2}{42}p^2 + \frac{1}{2}(T-2C_1)p + 1}{\frac{T^4}{1680C_1}p^3 + \left(\frac{T^3}{120C_1} + \frac{T^2}{140}\right)p^2 + \frac{T^2}{12C_1}p + 1}. \tag{21}$$

The transfer function (21) can be reduced to a form which is convenient for taking the logarithm; this makes it possible to plot the logarithmic frequency responses directly from a formula. Such a formula is written as follows:

$$W_{opt}^{**}(p) = \frac{1}{C_1 p}\,\frac{6TC_1 - 12C_1^2}{T^2}\,\frac{\left[\frac{T^2}{140}p^2 + \frac{T^2}{21(T-2C_1)}p + 1\right]}{\left[\frac{T^2}{140}p^2 + \left(\frac{T}{10} + \frac{6C_1}{70}\right)p + 1\right]} \times \frac{1 + \left\{\frac{1}{2}p(T-2C_1)\left[\frac{T^2}{140}p^2 + \frac{T^2}{21(T-2C_1)}p + 1\right]\right\}^{-1}}{1 + \left\{\frac{T^2}{12C_1}p\left[\frac{T^2}{140}p^2 + \left(\frac{T}{10} + \frac{6C_1}{70}\right)p + 1\right]\right\}^{-1}}. \tag{22}$$

From expressions (13) and (14) we have plotted graphs in Fig. 2 which illustrate the dependence of the error coefficient C_2 (the solid line) and the relative MSE $\overline{\eta_*^2}$ (the broken lines) on the error coefficient of the first derivative of the useful signal for certain values of the transient response duration.

4. Examples

We shall study two examples of determining the optimal system from formula (16). Assume that it is necessary to obtain the characteristics of an optimal system for which it is sufficient to treat only the first two derivatives of the useful signal. The following quantities are specified: a) $T = 4$ sec, $C_1 = 0.025$ sec; b) $T = 1.2$ sec, $C_1 = 0.005$ sec. Substituting the specified values of transient response duration T and the error coefficient C_1 into (16), we obtain the following expressions for the optimal transfer function:

$$W_a^*(p) = \frac{40}{p}\,\frac{(1.82p+1)(0.146p+1)}{(52.8p+1)(0.4p+1)},$$

$$W_b^*(p) = \frac{200}{p}\,\frac{(0.045p+1)(0.006p+1)}{(0.11p+1)(0.014p+1)}. \qquad (23)$$

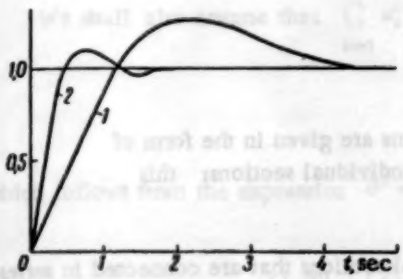

Fig. 4.

Using the transfer functions (23), we plot the logarithmic amplitude-frequency and phase-frequency responses (Fig. 3); curves 1 and 3 apply to the system a, whereas curves 2 and 3 apply to the system b; $A(\omega)$ is the amplitude response, and $\varphi(\omega)$ is the phase response. The shape of these characteristics in the low-frequency and intermediate frequency regions satisfies all the requirements that govern automatic control systems of high quality; in the high frequency region the characteristics must be corrected.

Figure 4 shows the graphs for the transient response of the systems under study; these responses were obtained using an electronic integrator. Curve 1 corresponds to case a. and curve 2 corresponds to case b.

SUMMARY

1. Expressions are derived which make it possible to determine the optimal transfer functions when "white noise" appears at the input of servosystems that have specified values for the figure of merit and the transient response duration which assure a minimum MSE.

2. The resulting formulas are convenient to use in engineering practice when using control systems.

LITERATURE CITED

1. V. A. Karabanov, Computing the Optimal Parameters for Low-Power Systems with a Specified Block Diagram, Transactions of the N. É. Bauman Moscow Higher Technical School, Symposium No. 97 [in Russian] (Machinery Press).
2. V. V. Solodovnikov and P. S. Matveev, "Synthesis of corrective networks for servosystems when noise is present on the basis of specified requirements for dynamic accuracy," Avtomatika i Telemekhanika 16, 3 (1955).
3. K. I. Kurakin, "An analytical method for synthesizing linear automatic control systems when noise is present and the dynamic accuracy is specified," Avtomatika i Telemekhanika 19, 5 (1958).*
4. H. James, N. Nichols, and R. Phillips, Theory of Servosystems [Russian translation] (Foreign Literature Press, 1951).

* Original Russian Pagination. See C. B. translation.

ON THE PROPERTIES OF SINGLE-LOOP CONTROL SYSTEMS

L. G. Sobolov

(Leningrad)

Translated from Avtomatika i Telemekhanika, Vol. 22, No. 4,
pp. 530-535, April,1961
Original article submitted November 18, 1960

The stability conditions for certain types of single-loop control systems are given in the form of an interrelationship between the critical gain and the parameters of individual sections; this makes it possible to establish certain properties of these systems.

Single-loop systems shall be defined as systems that consist of directional sections that are connected in series in a ring. We shall study systems that consist of aperiodic sections of a control circuit that controls an aperiodic object (case "A"), or an integrating object (case "B"). In both cases we shall also study so-called extreme systems in which all the time constants of the control circuit are equal.

A. The characteristic equation for the system is

$$\prod_{i=0}^{n} (T_i p + 1) + K = 0, \tag{1}$$

where $p = d/dt$, $K = \prod_{i=0}^{n} K_i$, $\underline{i}$ is the over-all system gain, T_i for $i > 0$ are the time constants for the sections of the control circuit, T_i for $i = 0$ is the time constant of the object.

For $K = 0$ the Mikhailov root locus for the open-loop system is

$$D(j\omega) = Re^{j\theta'}, \tag{2}$$

where

$$\text{where } R = \prod_{i=0}^{n} R_i,\ \theta' = \sum_{i=0}^{n} \theta_i,\ R_i = \sqrt{\omega^2 T_i^2 + 1},\ \theta_i = \arctan \omega T_i.$$

The maximum gain corresponding to the stability boundary is equal in magnitude to the radius-vector $K_{cr} = R$ of the root locus at its first intersection of the axis of abscissas (i.e., at $\theta' = \pi$). We also have

$$\tan \theta_i = \omega T_i \qquad (i = 0, 1, \ldots, n) \tag{3}$$

for the condition $\theta' < \pi/2$ (since we are seeking the first intersection of the axis of abscissas by the root locus which occurs at the finite frequency ω_1). In solving (3) we also use the well-known trigonometric expression which can be reduced to the following form for $\underline{n}$ terms:

$$\sum_{i=1}^{n} \arctan u_i = \arctan \frac{\overset{n}{\underset{i=1}{C}} u_i^1 - \overset{n}{\underset{i=1}{C}} u_i^3 + \overset{n}{\underset{i=1}{C}} u_i^5 - \ldots}{\overset{n}{\underset{i=1}{C}} u_i^0 - \overset{n}{\underset{i=1}{C}} u_i^2 + \overset{n}{\underset{i=1}{C}} u_i^4 - \ldots}, \tag{4}$$

where

$$\text{where } \overset{n}{\underset{i=1}{C}} u_i^m = \sum_{\substack{i,j,\ldots,m=1 \\ (i<j<\ldots m)}}^{n} u_i u_j \ldots u_m,$$

$$u_i = \omega T_i.$$

It is obvious that

$$\overset{n}{\underset{i=1}{C}} u_i^1 = \sum_{i=1}^{n} u_i; \quad \overset{n}{\underset{i=1}{C}} u_i^n = \prod_{i=1}^{n} u_i$$

We shall also assume that $\overset{n}{\underset{i=1}{C}} u_i^0 = 1$. On the basis of (4) we take into account the relationship

$$\tan \sum_{i=1}^{n} \theta_i = -\tan\theta_0 \tag{5}$$

(which follows from the expression $\theta' = \sum_{i=0}^{n} \theta_i = \pi$) and obtain

$$\overset{n}{\underset{i=0}{C}} T_i^1 - \left(\overset{n}{\underset{i=1}{C}} T_i^3 + T_0 \overset{n}{\underset{i=1}{C}} T_i^2\right)\omega^2 + \left(\overset{n}{\underset{i=1}{C}} T_i^5 + T_0 \overset{n}{\underset{i=1}{C}} T_i^4\right)\omega^4 - \ldots = 0. \tag{6}$$

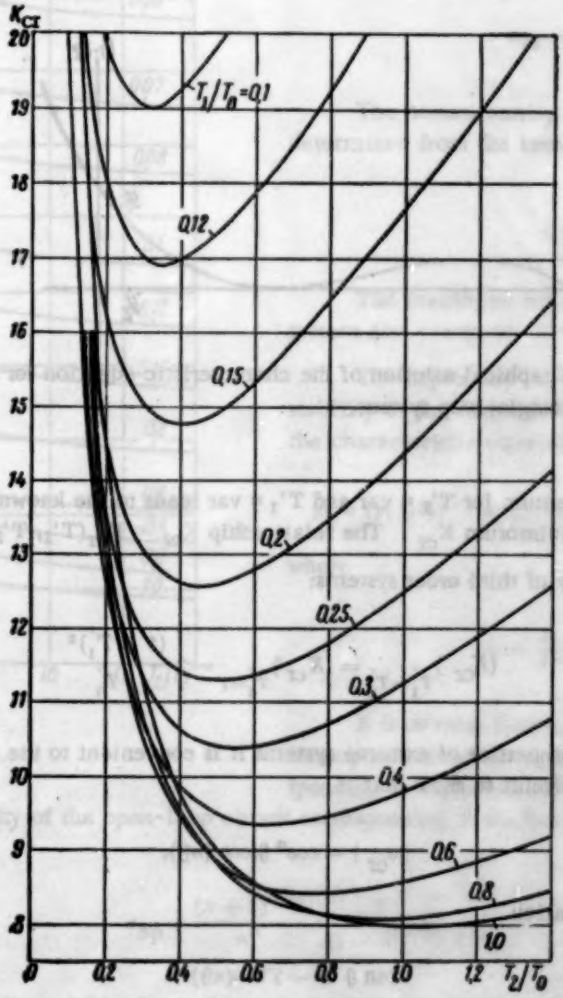

Fig. 1.

Determining the minimal root ω_1 from (6), we find the critical gain of the open-loop system.

Thus, for example, for a third order system (n = 2) we have

$$K_{cr} = (1 + T'_1)(1 + T'_2)\left(\frac{1}{T'_1} + \frac{1}{T'_2}\right), \tag{7}$$

where

$$T'_1 = \frac{T_1}{T_0}, \quad T'_2 = \frac{T_2}{T_0}.$$

By performing an investigation of the extremum for (7) for T'_2 = var, but T'_1 = const we find

$$T'_2 = \sqrt{T'_1}, \tag{8}$$

i.e., the worst case from the point of view of stability is a square-law relationship between the ratios of the time constants for the control circuit sections and the object time constant.

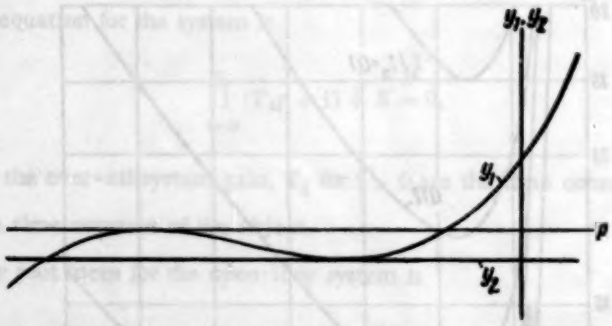

Fig. 2. Graphical solution of the characteristic equation for an extreme single-loop system.

An investigation of the extremum for T'_2 = var and T'_1 = var leads to the known [1, 2] relationships $T'_1 = T'_2 = 1$ corresponding to the minimum-minimorum K_{cr}. The relationship $K_{cr} = K_{cr}(T'_1, T'_2)$ is shown in Fig. 1.

Note the interesting property of third order systems:

$$(K_{cr})_{T'_1 = T'_2} = (K_{cr})_{T'_1 = 1} = 2\frac{(1 + T'_1)^2}{T'_1}. \tag{9}$$

For an investigation of the properties of extreme systems it is convenient to use the critical nonuniformity a_{cr} of the control circuit. It is not difficult to show that

$$|a_{cr}| = \cos^n\theta \cos(n\theta), \tag{10}$$

where θ is the solution of the equation

$$\tan\theta = -T\tan(n\theta) \tag{11}$$

for the condition $\theta < \pi/2$. Here T is the ratio between the time constant of the control circuit section and the object time constant.

In the coordinates aT the curve for the critical nonuniformity of the open-loop system represents a family of single-parameter curves (the parameter is n) emanating from the origin. The maximum for a curve of any order can be found from the condition

$$\frac{da_{cr}}{dT} = 0, \tag{12}$$

which leads to the expression

$$\tan\theta = -\tan(n\theta). \tag{13}$$

A comparison of (11) with (13) shows that the maximum for a curve of any order occurs for T = 1.

Solving (10) and (11), we obtain the following result for a third order system (n = 2):

$$a_{cr} = \frac{T}{2(1+T)^2} \tag{14}$$

and for a fourth order system (n = 3) we obtain

$$a_{cr} = \frac{T(3+T)^2}{8(1+T)^3}. \tag{15}$$

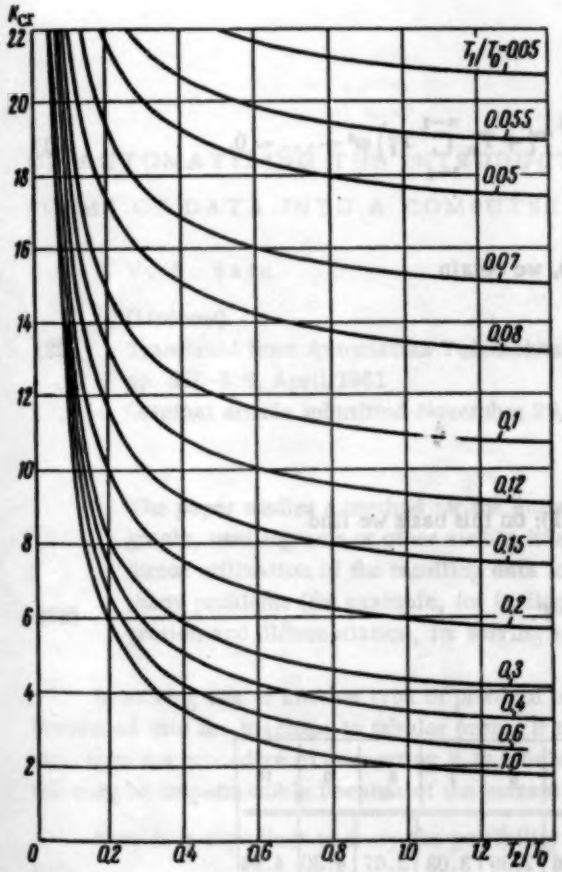

Fig. 3.

The nonuniformity of the closed control loop can be determined from the known relationship

$$\delta = \frac{a}{1+a}.$$

The maximum for the curve δ_{cr} of an nth order system also occurs for T = 1.

The expression for the conditions governing aperiodic stability of the extreme system can easily be obtained if the characteristic equation for the system is written as

$$y_1 = (p_1+1)(Tp_1+1)^n, \quad y_2 = -K, \quad y_1 = y_2, \tag{16}$$

where

$$p_1 = \frac{d}{d\tau}; \quad \tau = \frac{t}{T_0}.$$

It is obvious that the boundary for aperiodic stability corresponds to the case shown in Fig. 2. The ordinates corresponding to the points of tangency between y_1 and y_2 characterize the minimal nonuniformity of the open-loop circuit corresponding to the boundary of aperiodic stability. Therefore

$$a_{ap} = \frac{(n+1)^{n+1}}{n^n} \frac{T}{(1-T)^{n+1}}. \tag{17}$$

In extreme systems aperiodic stability is possible only for systems of order no higher than the third.

B. In analogous fashion it is possible to derive the expression

$$K_{cr} = T_0\omega_1 \prod_{i=1}^{n} \sqrt{\omega_1^2 T_i^2 + 1} \tag{18}$$

or

$$|\delta_{cr}| = \frac{T_n}{T_0} \frac{\prod_{i=1}^{n} \cos \theta_{i1}}{\tan \theta_{n1}}, \tag{19}$$

where θ_{i1} and ω_1 are found from the system of equations

$$2 \sum_{i=1}^{n} \theta_i = \pi, \quad \tan \theta_i = \omega T_i \qquad (i = 1, 2, \ldots, n) \tag{20}$$

for the condition $\theta_i < \pi/2$.

The system (20) is reduced to the equation

$$\overset{n-1}{\underset{i=1}{C}} T_i^0 - \left(\overset{n-1}{\underset{i=1}{C}} T_i^2 + T_n \overset{n-1}{\underset{i=1}{C}} T_i^1\right) \omega^2 + \left(\overset{n-1}{\underset{i=1}{C}} T_i^4 + T_n \overset{n-1}{\underset{i=1}{C}} T_i^3\right) \omega^4 - \ldots = 0. \tag{21}$$

for the specified conditions.

Determining the minimum roots (21) and making use of (18), we obtain

$$K_{cr} = \frac{T_0}{T_1} + \frac{T_0}{T_2}. \tag{22}$$

for third order systems.

The function $K_{cr} = K_{cr}(T_0/T_1, T_0/T_2)$ is shown in Fig. 3.

For extreme systems it is more convenient to use (19) and (21); on this basis we find

$$|\delta_{cr}| = \frac{\cos^n\left(\frac{\pi}{2n}\right)}{\tan\left(\frac{\pi}{2n}\right)} T. \tag{23}$$

Order of the equation	3	4	5	6	7	8	9	10
Value of the slope	0.5	1.125	1.76	2.39	3.03	3.67	4.30	4.94

It is evident from (23) that the boundary stability curves in the coordinates δT consist of rays emanating from the origin with slopes depending only on n; the magnitudes of these slopes are equal to the values of the derivatives of a_{cr} for T = 0 and for the corresponding value of n. The values of the slopes are given in the table as a function of the order of the equation (i.e., as a function of n + 1).

The expression for the aperiodic stability curve for the extreme system is given by

$$\delta_{ap} = AT, \tag{24}$$

where

$$A = \frac{(n+1)^{n+1}}{n^n}.$$

Aperiodic stability is possible for systems of order no higher than the third.

Expression (23) can also be recommended for determining the minimum achievable nonuniformity for non-extreme single-loop systems of arbitrary order.

In conclusion, note that the transient responses for the unit step perturbation in an extreme single-loop system of nth order are completely determined by the two dimensionless quantities T and K (or T and δ); this makes it possible in principle for formulate transient response tables for the system.

LITERATURE CITED

1. M. A. Aizerman, Lectures on Automatic Control Theory [in Russian] (State Technical Press, 1956).
2. A. A. Voronov, Elements of Automatic Control Theory [in Russian] (Military Press, 1954).

ON AUTOMATIZING THE INTRODUCTION OF CERTAIN FORMS OF DATA INTO A COMPUTER

V. S. Fain

(Moscow)

Translated from Avtomatika Telemekhanika, Vol. 22, No. 4,
pp. 536-538, April, 1961
Original article submitted November 29, 1960

The paper studies a method for the automatic transformation of functions specified in the form of graphs, oscillograms, or other visible images into digital (tabular) form. Here the possibility of direct utilization of the resulting data in digital computers is assured for the purpose of solving many problems (for example, for finding interpolation polynomials, for performing numerical ingration and differentiation, for solving a number of differential equation, etc.).

In solving one or another type of problem on automatic digital computers it is necessary to reduce the data introduced into the machine to tabular form. If this data is initially in the form of graphs, oscillograms, photographs, etc., then the procedure of converting it to tabular form by means of a human operator occupies a great deal of time; this may be impermissible because of the current tendency toward increasing the speed of computation (cf. [1, 2]).

Here it is expedient to study the possibility of automatizing the conversion of data from graphical to tabular form.

Principle of Performance of the Transformation

The graph (oscillogram) of a function may be continuous or quantized; a table is of necessity always quantized. This makes it possible to use a type of "retina" system for "seeing" the image; this system is made up of a matrix of individual light detecting elements (receptors). For functions which are given in rectangular coordinates it is convenient to use a rectangular matrix. In such a matrix the distance between the centers of two neighboring receptors on one line (or in one column) can serve simultaneously as a unit length and the measure of the resolving power. Based on this approach, the intervals between neighboring values in the table can contain only an integer number of unit lengths, and the minimum length for such an interval is equal to one unit length. Because of the fact that the functions to be processed $f(x, y) = 0$ may in the general case be functions that are not single-valued relative to x, it is expedient to use a scanning method in which the reference points are taken not along the x axis of the graph, but along the line proper. The table formed in such a case as a result of "reading" the graph corresponds to the expressions $x_i = f_1(s_i)$, $y_i = f_2(s_i)$; i.e., the table "writes" the curve in the form of a pair of natural equations. In practice this means that quantities referring to adjacent reference points on the curves are written in adjacent cells of the table, whereas in taking reference points along the x axis this proposition could be violated. For the engineering

realization of such a scanning method it is necessary to solve the problem of incorporating into the conversion device the capacity to establish whether or not two specified activated receptors correspond to neighboring (along the curve) reference points s_i and s_{i+1}.

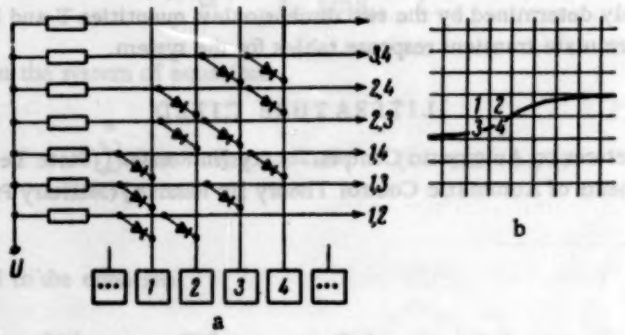

In order to be specific we shall choose the minimum interval between reference points $s_{i+1} - s_i$; i.e., this distance will be chosen equal to the distance between the centers of two adjacent receptors. It can be demonstrated that the reasoning which follows below for the case of the minimum interval between reference points remains valid even for larger intervals, provided that these intervals are chosen according to definite rules and the curves satisfy certain conditions (the Deeny conditions) that are satisfied in the majority of cases [3, 4]. In that case a satisfactory method of solving the problem is one which might be called the method of formulating chains of numbers. The essence of this method is the following.

All possible pairs of numbers of adjacent retina receptors are introduced into the memory section of the unit. We shall define two receptors as neighboring ones if their centers can be connected by a line segment which passes only through areas occupied by these two receptors. It is evident that the number of different pairs of numbers for adjacent receptors is equal to the number of different segments of a straight line connecting the centers of adjacent receptors; such a method for counting pairs makes it possible to assume pairs of number (i, j) and (j, i) to be identical.

The signals arriving from the retina which contain information on the numbers of the activated receptors are compared with the pairs of numbers for the adjacent receptors which are stored in the memory. Only those pairs for which both numbers correspond to activated receptors in the specified image are passed through for further processing. The formulation of the number chains is accomplished in the following manner.

Any of the activated pairs is examined. Assume that the left number in that pair is taken, and among the remaining activated pairs we find a pair which also contains a number. The second number for this pair which we have found is written at the left next to the original pair. Then we take the right number of the original pair and repeat the same process. The second number in the pair that we have found is written next to the original pair on the right. After that the entire procedure described above is performed for the left and right extreme numbers of the resulting chain of four numbers, etc. The process can be stopped in two ways: 1) we come to the end of all the activated pairs; 2) we find no pairs containing the extreme numbers in the chain among the remaining activated pairs. The case where the process is stopped for the first reason corresponds to a graph containing one curve with no discontinuities. In that case we may encounter two variants: a) if in comparing the extreme numbers of the chain these numbers prove to be identical, the curve is closed and when necessary a signal is given to that effect; b) in the contrary case the curve is not closed. If the process has been stopped for the second reason, the chain counter records the termination of one chain; then any of the remaining activated pairs is taken and the next chain of numbers is developed from it. If activated pairs still remain, then the process is repeated, etc. Note that after termination of each chain it is also possible to check for closure of the curve.

For the case where the graph of the curve forms an intersection, the number of the receptor corresponding to the intersection point will belong to more than two activated pairs. The programming for the unit in this case will depend on the particular features of the investigated material. If there is no need to pay any special attention to the act of intersection, we can limit the process to finding only one activated pair containing the required number

and continue the formulation of the chain. However, if it is necessary to fix both the fact of intersection and the intersection point, it is necessary to check all the activated pairs each time in order to choose from them those which contain the specified number. If we find there is more than one such pair (not including the pair which is already incorporated in the chain), then the intersection point is memorized and one of these pairs (any one) is entered into the chain which is being formulated. The other pairs are entered into other chains. Then it is possible to compare the intersection points which are fixed in the memory unit for all the chains and to establish the number of intersection points and the number of intersecting chains at each point.

Each number which is incorporated in the chain contains the coordinates x_i and y_i of the corresponding $\underline{i}$th receptor in coded form. Thus the result of recording each chain actually represents the sought-for tabular recording of the function.

We shall make a brief examination of methods for achieving an engineering realization of the principles presented above. The memorization of the pairs of numbers can be achieved without a memory unit in the conventional sense. In cases where the required memorizations of the information remain permanently the same, the memory function may be performed by the network structure proper. In fact, any network contains in its structure the information on the rules according to which the signal is transformed in the network.

In our case it is possible to use a well-known network for choosing the chain; this network is often used for converting numbers from the binary system to some other system (cf. [5]). An example of a portion of such a network for four receptors is shown in the figure (a). Activation of a receptor in this network corresponds to a positive voltage at its output. For the curve shown in Fig. 6 a positive signal appears at the output 3, 4 (i.e., the pair 3. 4 is activated and is transmitted for use in the operative memory). It is easy to see that all of the remaining processes described above can also be accomplished using universal and widely used computer elements: coincidence networks, noncoincidence networks, shift registers, etc. It can also be demonstrated that when necessary the memory network (a portion of which is shown in Fig. b) can easily be subdivided into individual parts that "service" the corresponding sections of the retina; moreover, in a number of cases these retina sections can be "serviced" alternately by one partial network.

APPENDIX

1. The number of pairs of adjacent receptors can be computed by an obvious method. For a quadratic retina consisting of A^2 receptors the number F of adjacent receptor pairs is equal to

$$B = 2(A-1)(2A-1).$$

Thus for a retina consisting of 100 × 100 receptors, $B \approx 4 \cdot 10^4$.

2. The method for indicating the receptor numbers. Using the binary number system for denoting the numbers (coordinates) of the receptors, it is possible to make use of two methods for denoting the numbers.

A. Assume the retina contains $S = A^2$ receptors. Then in order to denote any receptor number in the binary system (i.e., to denote any number from 1 to S) it is sufficient to use binary numbers containing $\log_2 S$ places. If the curve contains L unit lengths, then its notation based on this method will require $L \log_2 S$ binary places.

B. Assume that S-place numbers are used to denote lines on this same retina; then the notation for any curve will contains S binary places, irrespective of its length L.

It is evident that the use of method "A" for method "B" depends on the relationship between the average length of the investigated curve and the dimensions of the retina:

if $S > L_{av} \log_2 S$ (i.e., $L_{av} < S/\log_2 S$), then we should use method "A";

if $S < L_{av} \log_2 S$ (i.e., $L_{av} > S/\log_2 S$), then we should use method "B."

For the case where the image contains not only a line but also areas which must be taken into account, the method "B" will as a rule be preferable.

LITERATURE CITED

1. M. V. Keldysh, A. A. Lyapunov, and M. R. Shura-Bura, "Mathematical problem in the theory of computers," Vestinik Akad. Nauk SSSR 11 (1956).
2. S. A. Lebedev, Electronic Computery [in Russian] (Academy of Sciences USSR Press, 1956).
3. V. L. Goncharov, Theory of Interpolation and Approximation of Functions [in Russian] (State Technical Press, Moscow, 1954).
4. V. S. Fain, "on abridged notations for absolute description of images", Izvestiya Akad. Nauk SSR, Otdelenie Tekhnicheskikh Nauk, Énergetika i Avtomatika 1 (1961).
5. B. M. Kagan and T. M. Ter-Mikaelyn, Solution of Engineering Problems Using Automatic Digital Computers [in Russian] (State Power Engineering Press, Moscow 1958).

A WIRE FREQUENCY RESONATOR FOR TELEMETERING

Yu. I. Pivovarov and Yu. M. Tsodikov

(Khar'kov)

Translated from Avtomatika i Telemekhanika, Vol. 1, No. 4,
pp. 539-542, April,1961
Original article submitted July 2, 1960

The paper describes the principles of operation for a wire frequency resonator that is used for industrial telemetering. The basic design relationships are cited. The results of experimental investigation are cited along with the circuit diagram for the wire frequency resonator.

One of the most reliable forms of information used in telemetering is the frequency of an ac current whose magnitude depends on the value of the measured parameter. During the last few years a large number of instruments have been designed according to the frequency principle for the purpose of telemetering resistive and reactive power, voltage, current and other quantities. However, a shortcoming of such instruments is the low accuracy with which the measured quantity is converted into the frequency of the ac current. The RC and LC oscillators which are used as transducers to convert the parameter into a frequency have appreciable conversion errors which are caused by variations in the temperature and humidity of the ambient medium, atmospheric pressure, and supply voltage. The electrical properties of the elements in the tank circuit of such oscillators are unstable in time. Therefore frequency methods of telemetering are at present used in those cases where the communication channels employed can pass only quantized information without substantial distortion. Examples of such communication channels are high-voltage power lines, radio-communication channels, and conventional overhead or cable lines whose length amounts to tens or hundreds of kilometers.

The growing requirements imposed on the accuracy of industrial measurements, coupled with the development of digital control machines for which the most convenient form of introducing information is the quantized form (pulse-code, digital-pulse, frequency), have increased the interest in transducers which convert industrial parameters into frequency.

The design of such accurate and reliable transducers will make it possible to realize the advantages of frequency methods over telemetering methods based on identifying features related to intensity in using communication channels with a high noise level.

The conversion of a frequency into readings of a secondary instrument using digital indicators and printers, as well as the conversion of frequency into codes which can be used to introduce information into the control machine, do not at present lead to any particular difficulties.

Below we shall describe certain results of investigations performed on a wire frequency resonator designed to convert a parameter into frequency; these investigations were performed by the authors during a process of designing a digital telemetering system.

The wire frequency resonator (Fig. 1) consists of the metallic wire 1 with one end is fixed to a support 2. The other end of the wire is connected to the kinematic element of the metering instrument and is not coupled rigidly to the frame of the resonator. The force F which stretches the wire is determined by the value of the measured parameter. The proper frequency f_0 of the wire is determined by the relationship [1]

$$f_0 = \frac{1}{2l}\sqrt{\frac{F}{\rho}},$$

where l is the length of the wire, ρ is the linear density of the wire.

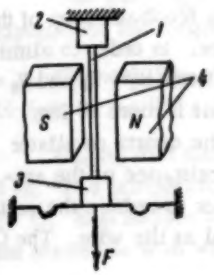

Fig. 1.

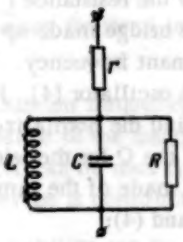

Fig. 2.

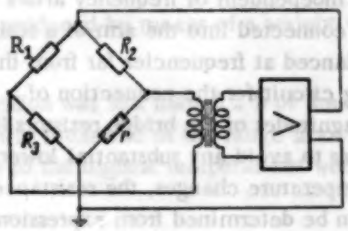

Fig. 3.

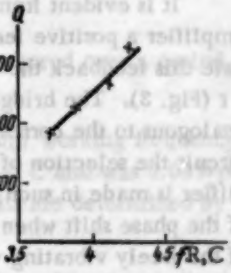

Fig. 4.

From [1] it is evident that for a resonator in which l and ρ are constant quantities, the proper vibration frequency of the wire is determined by the force F. In order to excite vibrations in the wire the latter is placed in a transverse magnetic field produced by the permanent magnet 4; the wire is coupled to an electronic amplifier in such a way that the system forms an oscillator with self-excitation in which the resonator is the wire resonator.

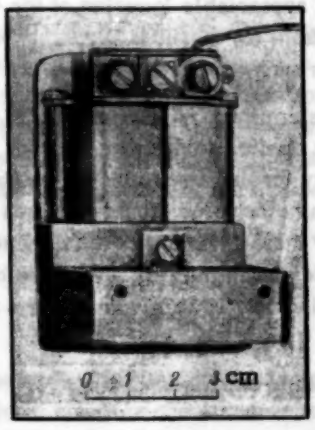

Fig. 5.

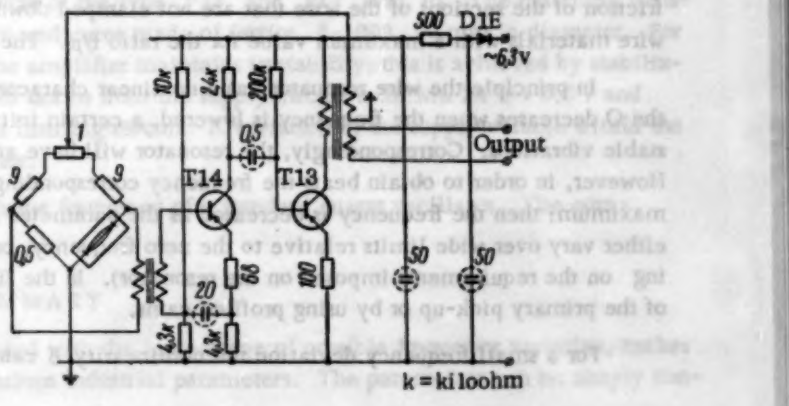

Fig. 6.

The vibrations of the wire are described by a second-order partial derivative equation for small amplitudes; this equation can be reduced to an ordinary differential equation on the assumption that: 1) the vibrations of the wire are sinusoidal, and 2) the distribution of the magnetic flux density along the wire is sinusoidal.

As a result of these simplifications it is possible to develop an equivalent circuit for the vibrating wire; this equivalent LC tank circuit is shown in Fig. 2., and its parameters are determined by the following equations [3]:

$$L = \frac{B^2 l^3}{2\pi^2 F}, \tag{2}$$

$$C = \frac{2\rho}{B^2 l}, \tag{3}$$

$$R = \frac{B^2 l}{4k\rho}, \tag{4}$$

where B is the maximum value of the flux density, k is the coefficient of air friction.

It is evident from the equivalent circuit that when the wire is connected directly into the feedback loop of the amplifier a positive feedback independent of frequency arises due to the resistance r of the wire. In order to eliminate this feedback the wire is connected into the arm of a resistance bridge made up of the resistors $R_1 = R_2$ and $R_3 = r$ (Fig. 3). The bridge is balanced at frequencies far from the resonant frequency. This circuit is more or less analogous to the corresponding circuit for the connection of a quartz oscillator [4]. Just as in the quartz oscillator circuit the selection of the magnitudes of the bridge resistors R_1, R_2, and the normalized input resistance of the amplifier is made in such a way as to avoid any substantial lowering of the Q for the wire. In order to reduce the variation of the phase shift when the temperature changes, the resistance R_3 is made of the same material as the wire. The Q of the freely vibrating wire can be determined from expressions (3) and (4):

$$Q = \omega_0 CR = \frac{\omega_0}{2k} = \frac{\pi}{2lk}\sqrt{\frac{F}{\rho}}. \tag{5}$$

The linear dependence of the Q for the wire on frequency is verified experimentally (Fig. 4). This data is cited for a tungsten wire d = 0.05 mm in diameter and l = 20 mm in length vibrating in air. However, relationship (5) is not completely exact since it does not take into account the viscosity losses in the material of the wire and the friction at its points of attachment (terminals). It should be noted that one of the basic factors affecting the constancy of the vibration frequency for the wire is the method by which it is fixed to its supports. The microscopic unevenesses which are present on the surfaces of the terminals may lead to an appreciable lowering of the Q due to friction of the sections of the wire that are not clamped down. It is evident from (5) that it is advantageous to use wire materials with a maximum value for the ratio F/ρ. The best material for such wire is tungsten.

In principle the wire resonator has a nonlinear characteristic which is determined by relationship (1). Since the Q decreases when the frequency is lowered, a certain initial force must be applied to the wire in order to assure stable vibrations. Correspondingly, the resonator will have an initial frequency for the zero value of the parameter. However, in order to obtain beats the frequency corresponding to the zero parameter value should be taken as the maximum; then the frequency is decreased as the parameter increases. Under these conditions the frequency must either vary over wide limits relative to the zero frequency, or the frequency deviation must be several percent (depending on the requirements imposed on the resonator). In the first case the nonlinearity is eliminated by the nonlinearity of the primary pick-up or by using profiled cams.

For a small frequency deviation the nonlinearity δ can be determined using expansion into a series

$$f_0 = \frac{1}{2l\sqrt{\rho}}\sqrt{F_0 + \Delta F} = \frac{1}{2l}\sqrt{\frac{F_0}{\rho}}\left[1 + \frac{1}{2}\frac{\Delta F}{F_0} - \frac{1}{8}\left(\frac{\Delta F}{F_0}\right)^2 + \frac{1}{16}\left(\frac{\Delta F}{F_0}\right)^3 - \cdots\right], \tag{6}$$

where F_0 is the initial tension, ΔF is the change in tension which is proportional to the measured parameter,

$$\delta = \frac{1}{4}\frac{\Delta F}{F_0} \quad \text{for} \quad \Delta F \ll F_0.$$

An appreciable decrease in the nonlinearity occurs when beats produced by the frequencies of two wires $\Delta f = f_1 - f_2$.

The proper frequencies f_1 and f_2 are determined by an identical initial tension F_0 for both wires and by the differential change in tension ΔF. The nonlinearity is determined from (6) and is equal to

$$\delta = \frac{1}{8}\left(\frac{\Delta F}{F_0}\right)^2,$$

which yields an error of 0.03% of the tension variation ΔF for a frequency deviation of $\pm$ 5 %.

We made an all-around experimental investigation of a wire resonator with the following basic parameters: l = 20 mm, d = 0.05 mm, B = 500 gauss.

The working frequency variation is assumed to be from 2 to 6 kc; however, during the process of the actual experiment the frequency varied from 1.5 to 7.5 kc.

The stability of the frequency for fixed tension produced by means of a weight was monitored over a period of 10 days for $t = 20° \pm 5°$.

During that time the maximum frequency deviation was less than 0.2 % of the maximum working frequency of 6 kc. The temperature dependence of the frequency was measured in the range from 20 to 85° C and was 0.09% per 10 °C. In principle the resonator can be used right up to the highest temperatures whose limits are determined by the materials with which the device is constructed.

Such a high temperature stability can be achieved if the wire resonator is coupled to the primary metering instrument by means of a spring, a membrance, or some other elastic element whose rigidity is very much less than the rigidity of the stretched wire.

The error due to the elongation of the wire when the temperature changes is determined by the coefficient of linear expansion for the wire material; it is appreciably less than the over-all temperature error of a wire resonator.

The use of tungsten wire assures stability of the length and diameter of the wire with time.

A photograph of the resonator with its cover removed is shown in Fig. 5; the dimensions of the resonator are 32 x 32 x 44 mm.

The two-stage amplifier is designed using transistors of the type P13 and P14 (Fig. 6). The matching transformers at the input and output of the amplifier use armored cores made of ferrite F-1000 20 mm in diameter. For temperature variation in the range from +20 to + 80° the amplifier maintains its stability; this is achieved by stabilizing the operating mode of the first stage [5]. The power drawn from the supply circuit is 15 Mw for u = 6.3 v and can be lowered appreciably by using a diode amplitude limiting circuit. A variation of the supply voltage within the limits $\pm$50 % does not affect the accuracy of the resonator.

We measured the frequency by comparing it with the frequency of a standard quartz oscillator. The comparison error did not exceed $\pm$ 0.1%.

SUMMARY

The high Q of the described wire resonator, coupled with the large range of possible frequency variation, makes it possible to use it for the accurate telemetering of various industrial parameters. The parameters can be simply converted into a digital code.

Depending on the required speed of response and passband widths of the communication channels, the resonator can be designed for any frequency band from 100 cps to 10 kc. The resonator is small.

The high reliability of the resonator is assured by the absence of moveable elements which wear, by its simple construction, and by the use of transistor amplifiers.

LITERATURE CITED

1. F. E. Temnikov and R. R. Kharchenko, Electrical Measurements of Nonelectrical Quantities [in Russian] (State Power Engineering Press, 1958).
2. Symposium of Papers. Control and Measurement over Large Distances. II [in Russian] (Foreign Literature Press, 1959).

3. A. W. Dickson and Murden, W. P. Vibrating-Wire High-Q Resonator, Electronics 26, No. 9 (1953).
4. Ya. Groshkovskii, Generation of High-Frequency Oscillations and Frequency Stabilization [in Russian] (Foreign Literature Press, 1958).
5. N. S. Nikolaenko, A Transistorized Signal Amplifier, In the Symposium: Semiconductor Instruments and their Application, No. 3 [in Russian] (Soviet Radio Press).

THE TRANSFER FUNCTIONS AND FREQUENCY RESPONSES OF A CARBON PILE VOLTAGE REGULATOR

D. A. Popov

(Moscow)

Translated from Avtomatika i Telemekhanika, Vol. 22, No. 4, pp. 543-551, April, 1961
Original argicle submitted July 18, 1960

The paper determines the frequency responses of carbon pile voltage regulators for dc and ac generators. Based on an analysis of the transient responses performed in a linear approximation, expressions are derived for the transfer functions of the regulator and for its corresponding frequency responses. A method is developed for the experimental determination of the regulator frequency responses in a closed-loop generator-regulator system. Results are cited for an experimental investigation of one of the standard manufactured voltage regulators.

1. Introduction

Notwithstanding a number of shortcomings of carbon pile voltage regulators which are due to the comparatively rapid wear and low heat resistance of the carbon pile, such regulators have been widely used for the voltage regulation of dc and ac generators, and for converters and rectifiers [1, 2]. Nowadays,carbon pile regulators are being replaced by more reliable voltage regulators based on self-saturating reactors and semiconductor devices. However, in a number cases where the cooling conditions are not the limiting factor carbon pile voltage regulators will still remain in use.

Based on the above, a study of the frequency responses of carbon pile voltage regulators and of the engineering method for determining those responses is of definite interest.

The transient responses in carbon pile voltage regulators have been studied in a linear approximation by a number of authors [1, 3, 4 etc.]. However, in a majority of cases the study is a simplified one: it does not take into account the electromagnetic transient responses [3], or it does not consider the effect of the load equalizer [1, 4]. The problem of an experimental determination of the frequency responses for carbon pile regulators has been treated, as far as we know, only in one paper [4]. However, the method proposed in this paper for determining these responses is so complex that it cannot be applied in engineering practice. A special feature of this method is the fact that the responses are taken for an open-loop regulation circuit, and therefore a complex electronic device of the "hard" feedback regulator type is necessary for stabilizing the initial mode of operation of the regulator.

As will be demonstrated below, for obtaining the responses of a closed-loop regulation system the stabilization of the initial mode of operation is achieved by the regulator proper, and no auxiliary units are required.

A theoretical investigation of the transient responses of a carbon pile regulator shall be performed for a typical voltage and load regulation circuit for parallel operation of dc generators (Fig. 1). The connection of the carbon pile voltage regulator for ac generators differs from the circuit shown only in that the regulated ac voltage is first rectified and then applied to the working winding W_w of the electromagnet.

The signal from the reactive load equalizer is usually introduced into the circuit of the working winding at the input of the rectifier [1]; this simplifies the analysis of the system. In a number of cases generator excitation current equalizers are used for parallel operation of ac generators instead of reactive load current equalizers. In that case the equalizer circuit does not differ in principle from the circuit shown in Fig. 1. It is evident from Fig. 1 that the electromagnet of the regulator (usually of the armored type) is equipped with two windings—the working winding W_w and the equalizing winding W_{eq}. The equalizing circuits of the regulator are connected in parallel for parallel operation of several generators; this assures load regulation of the generators in accordance with the method of imaginary statism.

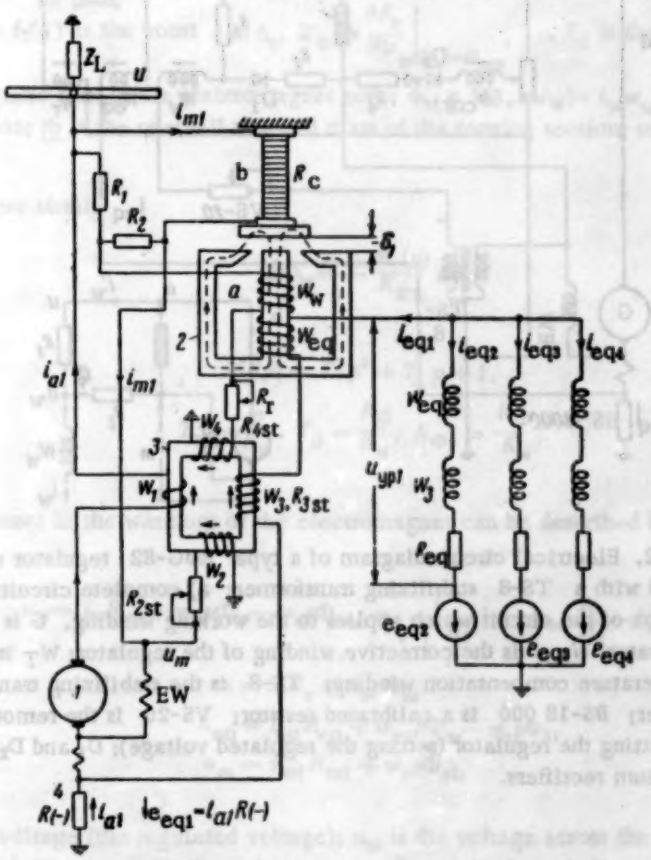

Fig. 1. Circuit diagram for the carbon pile voltage regulator. 1) generator; 2) carbon pile voltage regulator (a is the electromagnet, b is the carbon column); 3) stabilizing transformer; 4) calibrated resistors. EW is the excitation winding of the generator; R_T is a remote resistor for setting the regulator; R_{2st}, R_{3st}, and R_{4st} are the resistances of the windings on the stabilizing transformer.

Besides these two windings, simple carbon pile voltage regulators are usually equipped with several more auxiliary windings which include a temperature compensation winding and a corrective winding (Fig. 2).

The corrective winding is not shown on the original circuit diagram (Fig. 1), since, due to the presence of the rectifier D_2 (Fig. 2) in the circuit of this winding, it operates only for large excitation currents (for small values of the carbon pile resistance R_c). However, these modes of operation for the voltage regulating system are not of great interest from the point of view of stability, since in studying the transient responses the effect of the corrective winding can be neglected.

Regulator circuits usually include a multiplier resistor R_2 which introduces "hard" negative feedback. In the RUG-82 circuit (Fig. 2) this resistor is connected through the rectifier D_1 in such a way that for large excitation currents (i.e., for small generator speeds) no current flows through the resistor; this eliminates any additional lowering of the generator voltage in such a mode due to the presence of "hard" feedback.

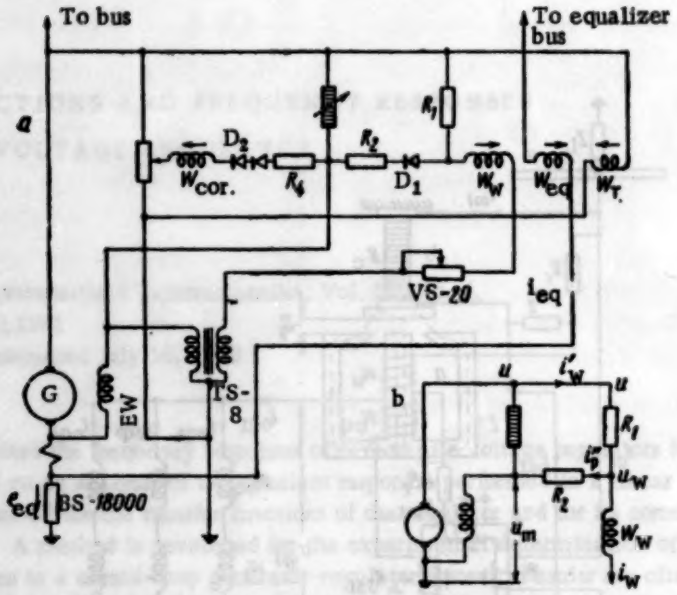

Fig. 2. Electrical circuit diagram of a type RUG-82 regulator combined with a TS-8 stabilizing transformer: a) complete circuit; b) section of the circuit which applies to the working winding. G is the generator; W_{cor} is the corrective winding of the regulator; W_T is the temperature compensation winding; TS-8 is the stabilizing transformer; BS-18 000 is a calibrated resistor; VS-20 is the remote for setting the regulator (setting the regulated voltage); D_1 and D_2 are selenium rectifiers.

The voltage regulator circuit includes stabilizing transformer which in the general case has four windings (Fig. 1): W_1, W_2, W_3, and W_4; they are connected as shown in Fig. 1.

2. The Equation for the Transient Responses of the Regulator

For a theoretical investigation of the regulator transient responses we shall make the following basic original assumptions.

1. The deviation of the variable quantities from their steady-state values are assumed to be small; this corresponds to the problem of developing a method for determining the frequency responses of the controllers for small sinusoidal perturbations.

2. The leakage fluxes of the windings on the regulator electromagnet and stabilizing transformer are neglected.

The resistance R_{cr} of the carbon pile depends, as we know, on its compressive force; the latter is determined by the magnitude of the air gap δ between the armature and core of the electromagnet. Thus, $R_{cr} = f(\delta)$.

For small increments of the variables it is possible to write

$$\Delta R_c = -K_R \Delta\delta, \qquad (1)$$

where

$$K_R = -\frac{\partial R_c}{\partial \delta}\Big|_{\delta=\delta_0}.$$

The equation of motion for the electromagnet armature when small deviations of the variables from their steady-state values occur is written in the following form in operator notation for zero initial conditions:

$$(mp^2 + K_d p + K_M)\,\Delta\delta + K_\Phi \Delta\Phi_W = 0, \tag{2}$$

where $K_M = K_{pr} + K_c = \frac{\partial F_M}{\partial \delta}\Big|_{\delta=\delta_0}$ is the tangent of the slope angle for the mechanical characteristic of the regulator $F_M = F_{pr} - F_{cr} = f_1(\delta)$ at the point $\delta = \delta_0$, $K_\Phi = \frac{\partial F_e}{\partial \Phi_W}\Big|_{\Phi_W=\Phi_{W0}}$, , F_e is the traction force of the electromagnet; Φ_W is the magnetic flux in the electromagnet core; $\Phi_W = f(\delta, aw_W) = i_W w_W + i_{eq} w_{eq} - i_T w_T$; K is the coefficient of viscous friction; m is the over-all reduced mass of the moving sections of the electromagnet, and $\Delta\delta$ is the air-gap increment.

From equation (2) we obtain

$$\Delta\Phi_W = -\frac{M(p)}{K_{\Phi 1}}\Delta\delta, \tag{3}$$

where

$$M(p) = T^2 p^2 + T_d p + 1,$$

$$T_{ar}^2 = \frac{m}{K_M},\quad T_d = \frac{K_d}{K_M},\quad K_{\Phi 1} = \frac{K_\Phi}{K_M}. \tag{4}$$

The transient responses in the windings of the electromagnet can be described by the equations

$$\begin{aligned} u_W &= i_W R_{W1} + w_W p\Phi_W - w_4 p\Phi_{st}, \quad = \frac{1}{1+\frac{R_1}{R_2}}\left(u + u_m\frac{R_1}{R_2} - i_W R_1\right),\\ u &= i_\tau R_\tau + w_\tau p\Phi_W\\ u_{eq} &= i_{eq} R_{eq} + w_{eq} p\Phi_W - w_3 p\Phi_{st},\\ u_m &= i_{2st} R_{2st} + w_2 p\Phi_{st}, \end{aligned} \tag{5}$$

where u is the generator voltage (the regulated voltage); u_W is the voltage across the terminals of the working winding circuit of the regulator (cf. Fig. 2); u_m is the voltage across the excitation winding of the generator; u_{eq} is the voltage in the equalizing circuit which is equal to the potential difference between the equalizing bus and the upper terminal of the calibrated resistor (cf. Fig. 1); R_{W1}, R_{eq} are the resistances in the circuits of the working and equalizing windings (taking into account the resistances of the stabilizing transformer windings); $\Phi_{st} = f(aw_{st})$ is the magnetic flux in the stabilizing transformer, $aw_{st} = i_a w_1 + i_{2st} w_2 - i_{eq} w_3 - i_W w_4$.

Varying the system of equations (5) and solving it relative to $\Delta\Phi_W$, we find the sought for equation for the electromagnetic transient responses in the regulator:

$$\begin{aligned} \frac{w_p}{T_W'} F_1(p)\,\Delta\Phi_W = &-K_5\frac{w_W}{T_W'}(1+pT_{st.e})\Delta\delta + [(1+pT_5) - K_\tau(1+pT_{st.e})]\,\Delta u +\\ &+ \gamma_1(1+pT_6)\,\Delta u_{eq} + K_1 M_{14}\Delta i_a + \left[\frac{R_1}{R_2}(1+pT_5) + K_1\frac{w_4}{w_2}pT_{st\,2}\right]\Delta u_m, \end{aligned}$$

where

$$F_1(p) = (1+pT_{we})(1+pT_{st.e}) - p^2(T_W' + KT_{eq})\left(T_{st\,4}' + \frac{1}{K}T_{st\,2}\right);$$

$$T_{we} = T_W' + T_{eq} - T_\tau;\ T_{st.e} = T_{st\,2} + T_{st\,3}' + T_{st\,1}';\ T_{st\,4}' = T_{st\,4}\left(1+\frac{R_1}{R_2}\right);$$

$$T'_{\mathrm{W}}=T_{\mathrm{W}}\left(1+\frac{R_1}{R_2}\right);\ T_{\mathrm{W}}=\frac{\lambda_{\mathrm{W}}w_{\mathrm{W}}^2}{R_{\mathrm{p0}}};\ T_{\mathrm{eq}}=\frac{\lambda_{\mathrm{W}}w_{\mathrm{eq}}^2}{R_{\mathrm{eq}}};\ T_{\mathrm{T}}=\frac{\lambda_{\mathrm{W}}w_{\mathrm{T}}^2}{R_{\mathrm{T}}};$$

$$T_{\mathrm{st\,2}}=\frac{\lambda_{\mathrm{st}}w_2^2}{R_{2\mathrm{st}}};\ T_{\mathrm{st\,3}}=\frac{\lambda_{\mathrm{st}}w_3^2}{R_{\mathrm{eq}}};\ T_{\mathrm{st\,4}}=\frac{\lambda_{\mathrm{st}}w_4^2}{R_{\mathrm{p0}}};\ M_{14}=\lambda_{\mathrm{st}}w_1w_4;$$

$$T_5=T_{\mathrm{st\,2}}+T_{\mathrm{st\,3}}\left(1-\frac{1}{K}\right);\ T_6=T_{\mathrm{st\,2}}+T'_{\mathrm{st\,4}}(1-K);\ K=\frac{w_3w_{\mathrm{W}}}{w_4w_{\mathrm{eq}}};$$

$$K_\delta=-\left.\frac{\partial\Phi_{\mathrm{W}}}{\partial\delta}\right|_{\delta_0,\,aw_{\mathrm{W}}};\ \lambda_{\mathrm{W}}=\left.\frac{\partial\Phi_{\mathrm{W}}}{\partial aw_{\mathrm{W}}}\right|_{\delta_0,\,aw_{\mathrm{W0}}};\ \lambda_{\mathrm{st}}=\left.\frac{\partial\Phi_{\mathrm{st}}}{\partial aw_{\mathrm{st}}}\right|_{aw_{\mathrm{st0}}},$$

$$R_{\mathrm{W0}}=R_1+\left(1+\frac{R_1}{R_2}\right)R_{\mathrm{W1}};\ K_1=K\frac{T_{\mathrm{eq}}}{T_{\mathrm{W}}}+\left(1+\frac{R_1}{R_2}\right);$$

$$\gamma_1=\frac{T_{\mathrm{eq}}w_{\mathrm{W}}}{T_{\mathrm{W}}w_{\mathrm{eq}}};\ K_{\mathrm{T}}=\frac{T_{\mathrm{T}}w_{\mathrm{W}}}{T_{\mathrm{W}}w_{\mathrm{T}}}.$$

When the equalizing circuit is cut out, we have $i_{eq} = 0$.

Setting $R_{eq} = \infty$ in (6) we find

$$\frac{w_{\mathrm{W}}}{T_{\mathrm{W}}}F'_1(p)\,\Delta\Phi_{\mathrm{W}}=-K_\delta\frac{w_{\mathrm{W}}}{T_{\mathrm{W}}}(1+pT'_{\mathrm{st.e}})\,\Delta\delta+[(1+pT_{\mathrm{st\,2}})-K_{\mathrm{T}}(1+pT'_{\mathrm{st.e}})]\,\Delta u+$$
$$+\left(1+\frac{R_1}{R_2}\right)pM_{14}\Delta i_a+\left[\frac{R_1}{R_2}(1+pT_{\mathrm{st\,2}})+\left(1+\frac{R_1}{R_2}\right)pT_{\mathrm{st\,2}}\frac{w_4}{w_2}\right]\Delta u_m. \tag{8}$$

where

$$F'_1(p)=1+p(T'_{\mathrm{W.e}}+T'_{\mathrm{st.e}})+p^2(T'_{\mathrm{W}}T_{\mathrm{st\,2}}-T_{\mathrm{T}}T_{\mathrm{st.e}}),$$
$$T'_{\mathrm{W.e}}=T'_{\mathrm{W}}-T_{\mathrm{T}};\ T'_{\mathrm{st.e}}=T_{\mathrm{st\,2}}+T'_{\mathrm{st\,4}}. \tag{9}$$

From Eqs. (6) and (9) it is evident that the resistance R_2 introduces "hard" feedback with respect to the voltage u_m into the circuit along with "soft" stabilizing feedback; this worsens the accuracy with which the generator voltage is regulated in steady-state modes.

Therefore the feedback coefficients $K_{fb} = R_1/R_2$ in standard manufactured regulators is made very small (0.013-0.03). Thus in investigating the transient responses the feedback through the resistor R_2 can be neglected.

Solving the system of equations (1), (3), and (6) relative to ΔR_{cr}, we obtain the general equation for the regulator (for $R_1/R_2 = 0$):

$$\Delta R_{\mathrm{c}}=G_{\mathrm{W}}\Delta u+G_{\mathrm{eq}}\Delta u_{\mathrm{eq}}+G_m\Delta u_m+G_a\Delta i_a, \tag{10}$$

where

$$G_{\mathrm{W}}=\frac{F_3(p)}{K_2F_2(p)};\ G_{\mathrm{eq}}=\frac{\gamma(1+pT_6)}{K_2F_2(p)},\ G_m=\frac{K_1}{1-K_{\mathrm{T}}}\frac{w_4}{w_2}\frac{pT_{\mathrm{st\,2}}}{K_2F_2(p)},$$

$$G_a=G_mR_{2\mathrm{st}}\frac{w_1}{w_2},\ K_2=\frac{w_{\mathrm{W}}}{T_{\mathrm{W}}(1-K_{\mathrm{T}})}\frac{1}{K_{\Phi1}K_R},$$

$$F_2(p)=F_1(p)\,M(p)-K_{\mathrm{e}}(1+pT_{\mathrm{st.e}}),\ F_3(p)=1+pT_7, \tag{11}$$

$$K_{\mathrm{e}}=K_{\Phi1}K_\delta=\frac{K_{\delta1}}{K_{\mathrm{M}}},\ K_{\delta1}=-\left.\frac{\partial F_{\mathrm{e}}}{\partial\delta}\right|_{\delta_0,\,aw_{\mathrm{p0}}},$$

$$T_7=T_5-\frac{K_{\mathrm{T}}}{1-K_{\mathrm{T}}}\left(1+K\frac{T_{\mathrm{eq}}}{T_{\mathrm{W}}}\right)T'_{\mathrm{st\,4}}\approx T_5,\ \gamma=\frac{\gamma_1}{1-K_{\mathrm{T}}}.$$

The functions $G_w(p)$, $G_{eq}(p)$, $G_m(p)$, and $G_a(p)$ are the transfer functions for the regulator with respect to the corresponding input signals.

In analogous fashion, for $i_{eq} = 0$ ($R_{eq} = \infty$) we obtain

$$\Delta R_c = G_{p1}\Delta u + G_{m1}\Delta u_m + G_{a1}\Delta i_a, \tag{12}$$

from (10), where

$$G_{w1} = \frac{F_3'(p)}{K_2 F_2'(p)},\quad G_{m1} = \frac{1}{1-K_\tau}\frac{w_4}{w_2}\frac{pT_{st2}}{K_2 F_2'(p)},\quad G_{a1} = G_{m1}R_{2st}\frac{w_1}{w_2},$$
$$F_2'(p) = F_1'(p)M(p) - K_e(1+pT_{st.e}'),\quad F_3'(p) = 1+pT_\tau',\quad T_\tau' = T_{st2} - \frac{K_\tau}{1-K_\tau}T_{st4}' \approx T_{st2} \tag{13}$$

The functions $G_{w1}(p)$, $G_{m1}(p)$, and $G_{a1}(p)$ are the transfer functions for the regulator with respect to the corresponding input signals for an open equalizer circuit.

Replacing the operator p by $j\omega$ in the expressions for the transfer functions, we obtain an analytical expression for the corresponding frequency responses of the regulator. In particular, for $i_{eq} = 0$ and no stabilizing transformer we have

$$G_{w1}'(j\omega) = K_2^{-1}\{[(1-K_e) + \omega^2(T_{w.e}'T_d + T_{ar}^2)] + j\omega(T_{w.e}'T_d - \omega T_{ar}^2)\}^{-1}. \tag{14}$$

In order to use the analytical expression for practical computations it is necessary to know the regulator parameters. However, the experimental determination of these parameters is undoubtedly a much more complex problem than the experimental determination of the frequency responses proper.

It should be noted that experimentally it is sufficient to determine the frequency responses $G_w(j\omega)$ and $G_{w1}(j\omega)$ since the remaining responses can be computed if the indicated frequency responses of the regulator and the stabilizing transformer are known. Thus, for example, from (13) we obtain

$$G_{m1} = \frac{1}{1-K_\tau}\frac{pM_{24}}{R_{2st}(1+pT_{st2})}\frac{(1+pT_{st2})}{K_2F_2'(p)} = \frac{1}{1-K_\tau}G_{st2}G_{w1}, \tag{15}$$

where

$$G_{st2} = \frac{pM_{24}}{R_{2st}(1+pT_{st2})} = \frac{w_4}{w_2}\frac{pT_{st2}}{(1+pT_{st2})}. \tag{16}$$

The frequency response $G_{st}(j\omega)$ is determined as the ratio between the complex amplitude of the emf across the terminals of the winding W_4 of the stabilizing transformer and the complex amplitude of the sinusoidal component of voltage across the terminals of the primary winding W_2 when the remaining windings are energized:

$$G_{st2}(j\omega) = \frac{\Delta\tilde{u}_4}{\Delta\tilde{u}_2} \text{ for } i_a = 0,\ i_w = 0,\ i_{eq} = 0,\quad u_2 = U_{m0} + \Delta U_2 \sin\omega t.$$

Since the stabilizing transformer is not saturated, it follows that in determining the frequency response we can assume $U_{m0} = 0$. Having determined the time constant T_{st2} from the amplitude- and phase-frequency responses of the transformer, and knowing the frequency response of $G_w(j\omega)$ and $G_{w1}(j\omega)$ we can easily obtain all the other frequency responses of the regulator.

3. Experimental Determination of Frequency Responses for the Regulator

The simplest method for experimentally determining the frequency responses of the carbon pile regulator consists of measuring its steady-state response (the amplitudes and phases of the fluctuations in the carbon pile resistance) to constant-amplitude sinusoidal input signals at a number of fixed frequencies.

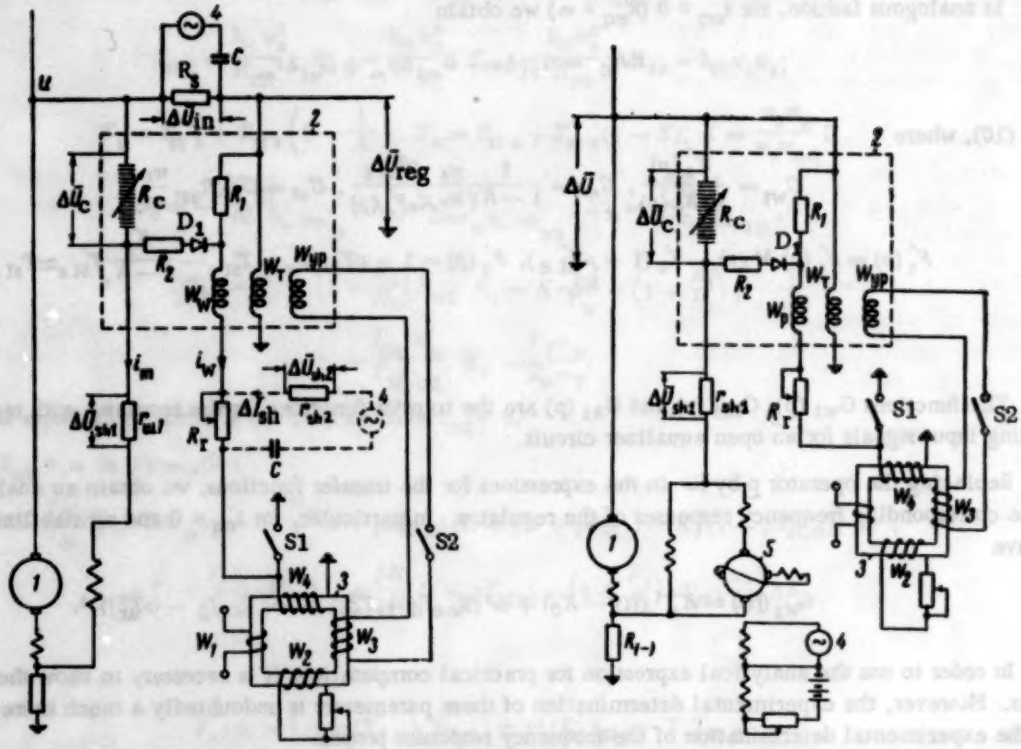

Fig. 3. Circuit diagram for obtaining the frequency responses of a carbon pile voltage regulator when oscillations are excited from the regulator side: 1) generator; 2) regulator; 3) stabilizing transformer; 4) low-frequency signal generator; R_s, r_{sh1}, r_{sh2} are noninductive series resistors; R_r is the remote resistor for setting the regulator.

Fig. 4. Circuit diagram for obtaining the frequency responses of a carbon pile voltage regulator when oscillations are excited from the generator side: 1) generator; 2) regulator; 3) stabilizing transformer; 4) low-frequency signal generator; 5) rotary amplifier.

Here we must keep in mind the fact that since the carbon pile regulator is a nonlinear device its parameters (λ_W, K_R, K_δ, K_M etc.) and frequency responses depend to a substantial extent on the initial unperturbed state (δ_0, R_{cr0}).

Therefore in order to determine the frequency responses it is necessary to create a mode in which small forced oscillations of the electromagnet armature occur relative to the intial state (δ_0).

The high values of gain (for small $\Delta K_e = 1 - K_e$), and the more so for astatic adjustment of the regulator ($K_e = 1$), such a mode can be assured when feedback is present between the carbon pile resistance and the voltage across the working winding of the regulator; i.e., it can only be achieved in a closed-loop voltage regulator circuit. Taking the frequency responses of the regulator as an individual element outside of any regulation system proves to be impossible, since the smallest variations in the intial voltage across the working winding (U_0) leads to full compression or expansion of the carbon pile.

In the paper by Mills [4] a special electronic regulation circuit was used to obtain the frequency responses of the regulator; this special circuit assured stabilization of the initial value of the carbon pile resistance (R_{cr0}) and a mode in which small oscillations in the carbon pile regulator occurred.

However, the use of such a method is unjustifiably complex, since the mode of small forced oscillations can easily be produced in the closed-loop generator-regulator system without using cumbersom auxiliary electronic devices. Under these conditions the stabilization of the initial regulator parameters is assured by the regulator itself.

The excitation of small sinusoidal oscillations in the voltage regulation system can be achieved in two ways: a) from the regulator side (Fig. 3), and b) from the generator side (Fig. 4).

In the first case a small series resistor R_s is connected into the over-all regulator winding circuit; the low-frequency signal generator 4 is connected to the series resistor through an isolating capacitor C. The signal supplied by the generator causes the regulation system to enter a mode of forced small oscillations about the specified steady-state mode.

In order to determine the frequency responses of the regulator it is necessary to maintain a constant amplitude for the voltage Δu_{reg} across the regulator at each frequency, and to measure the amplitudes and phases (relative to $\Delta \bar{u}_{reg}$) of the sinusoidal components of the voltage drops across the carbon pile ($\Delta \bar{u}_c$) and across the resistor r_{sh} connected in series with the carbon pile ($\Delta \bar{u}_{sh}$).

For small sinusoidal oscillations in the system we have (the switch S2 is closed, and S1 is open):

$$\begin{aligned} \Delta \bar{R}_c &= G_w(j\omega)\, \Delta u_{reg} \\ \Delta \bar{u}_c &= \Delta \bar{R}_c\, I_{m0} + \Delta \bar{I}_m R_{c0}, \\ \Delta \bar{u}_{sh} &= \Delta \bar{I}_m r_{sh}. \end{aligned} \tag{17}$$

From this we have

$$G_w(j\omega) = \frac{\Delta \bar{R}_c}{\Delta u_{reg}} = \frac{1}{I_{m0}} \frac{\left(\Delta \bar{u}_c - \dfrac{R_{c0}}{r_{sh}} \Delta \bar{u}_{sh}\right)}{\Delta u_{reg}}. \tag{18}$$

Depending on the position of the switches S1 and S2, we can thus determine the various characteristics of the regulator.

1) If the switch S1 is open and the switch S2 is closed, we obtain the characteristic $G_w(j\omega)$.

2) If S1 and S2 are open, we obtain $G_{w1}(j\omega)$.

3) If S1 is closed and S2 is open, we obtain $G'_{w1}(j\omega)$.

It must be noted that the indicated circuit can also be used for obtaining the frequency responses of the entire voltage regulation system as a whole.

In that case the equalizing circuit of the regulator and the windings W_1 and W_2 of the stabilizing transformer are cut out as shown in Fig. 1. The regulator equation for this circuit can be written in the following form in terms of small increments:

$$\Delta R_c = G_w(\Delta u_{gen} - \Delta u_{in}) + G_c\, \Delta u_c + G_m \Delta u_m + G_a \Delta i_a. \tag{19}$$

In obtaining the frequency responses for the entire system the amplitude of the voltage across the series resistor (Δu_{in}) is maintained constant; the series resistance R_s under these conditions must be made small (1 to 2% of R_{wo}) in order that its connection into the regulator circuit should not cause a noticeable variation of the initial steady-state operating mode of the generator (U_0).

Small oscillations can also be excited in the system when the frequency responses of the regulator and of the entire system are tkane even when the series resistance is not connected into the regulator circuit; this is done by connecting a low-frequency signal generator 4 to the remote resistor R_r which is included in the regulator circuit (cf. the broken line in Fig. 3).

It can be demonstrated that for such regulator circuit its equation for small increments of the variables is written as (for $u_{gen} = u_{reg} = u$):

$$\Delta R_c\ (p) = G_w(p)\,\Delta u - G'_w \Delta u_{in} + G_c\,\Delta u_c + G_m \Delta u_m + G_a \Delta i_a, \tag{20}$$

where

$$\Delta u_{in} = \Delta i_{sh} R_r = \frac{R_r}{r_{sh}}\,\Delta u_{sh},$$

$$G'_w = \frac{G_w}{1 - K_T}\,\frac{1 + pT_5}{1 + pT_7}. \tag{21}$$

Taking into account the fact that $T_5 \simeq T_7$ [cf. (11)] and

$$\frac{1 + pT_5}{1 + pT_7} \simeq 1, \tag{22}$$

Eq. (20) can be written as

$$\Delta R_c = G_w(\Delta u - \Delta u_{in1}) + G_c\,\Delta u_c + G_m \Delta u_m + G_a \Delta i_a, \tag{23}$$

where

$$\Delta u_{in1} = \Delta u_{in}\frac{1}{1 - K_T}. \tag{24}$$

It should be noted that such a method of determining the frequency responses when the winding W_T is present in the regulator is less accurate than the method described above, since Eq. (22) is approximate.

For excitation of oscillations in the system from the generator side, an ac source of low frequency is applied to the generator excitation winding. A rotary amplifier of the type ADU-1300 was used as such a current source at frequencies of up to 40 to 50 cps; one control winding of the rotary amplifier was fed from a low-frequency generator, and the second was fed from a storage battery. At frequencies above 40-50 cps an analagous generator was used for supplying the generator excitation winding; in this case low-frequency modulation of the auxiliary generator voltage achieved by connecting the equalizer winding of the generator regulator to a low-frequency signal generator through an intermediate electronic amplifier.

In all remaining respects the method of obtaining the regulator frequency responses does not differ from that described above.

In order to measure the low-frequency voltages and their phases (relative to a certain reference voltage) we used a phase detecting voltmeter of the type VP-253; the low-frequency master generator consisted of an infra-low-frequency signal generator of the type OS-103 (a "solartron").

Figure 5 shows the frequency responses $G'_{w1}(j\omega)$ determined in this fashion for an RUG-82 regulator when the equalizer winding is connected and no stabilizing transformer is used.

For this experiment the effective value for the voltage was $\Delta u_{reg} = 50$ mv, and $R_{cos} = 11.8$ ohm.

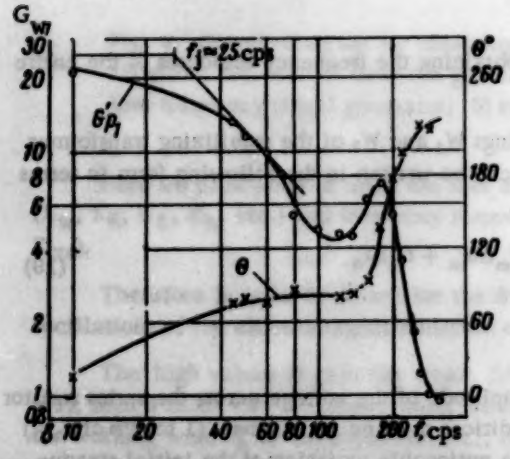

Fig. 5. Logarithmic amplitude- and phase-frequency responses for an RUG-82 carbon pile voltage regulator for an open equalizer winding G'_{w1}.

From Fig. 5 it is evident that in the frequency range from 10 to 100 cps the amplitude G'_{w1} decreases with an increase in frequency, and the phase θ decreases monotonically. The initial segement of the amplitude response is approximated by two straight lines with a junction frequency $f_j = 25$

At a frequency of approximately 120 cps the amplitude response has a clearly defined maximum. The shape of the frequency responses shown in the figure is in full agreement with expression (14).

LITERATURE CITED

1. V. S. Kuiebakin, V. T. Morozovskii, and I. M. Sindeev, Aircraft Electrical Equipment [in Russian] (Defense Press, 1956).
2. Fundamentals of Electrical Equipment in Aircraft and Automobiles, Edited by A. N. Larionov [in Russian] (State Power Engineering Press, 1955).
3. V. D. Konstantinov, On the Problem of Parallel Operation of DC Aircraft Generators [in Russian] (Transactions of the N. E. Zhukovskii All-Union Aircraft Institute, No. 617, 1957).

ON DESIGNING FUNCTIONAL POTENTIOMETERS

V. M. Frygin

(Kuibyshev)

Translated from Avtomatika i Telemekhanika, Vol. 22, No. 4,
pp. 552-555, April,1961
Original article submitted October 3, 1960

The paper describes methods for designing functional potentiometers using unprofiled cases. A graphical method for computing functional potentiometers is given.

Functional potentiometers are widely used in instrumentation, and in automatic and computer devices. At the present time profiled frames are often used to obtain the required functional dependence of the output voltage u_{out} on the position of the movable potentiometer arm. Below we describe methods for designing functional potentiometers with unprofiled frames and a resistance that is uniformly distributed with respect to length. Such frames are more convenient than the profiled ones to manufacture; the winding of the resistance on them and the control of the winding quality can be achieved more simply.

The required functional relationship can be achieved by giving the movable arm a special shape. We shall call this method of obtaining the required functional relationship the shaped-slider method. The principle of operation for such a potentiometer shall be clarified using the example of a linear displacement converter (Fig. 1a). The number 1 on the diagram indicates the resistance wound on an unprofiled frame in this particular case it may be a rheochord in the form of a wire.

Assume that the slider 2 slides along the rheochord made of wire shaped in the form of a flat curve. If the equation for the curve which describes the shape of the slider is $y = f(x)$ in rectangular coordinates and the rheochord is shaped in the form of a straight line segment parallel to the y axis, then when the slider is shifted by the amount x is the output voltage will be expressed by the formula

$$u_{out} = u_{in}\frac{y}{l} = u_{in}\frac{1}{l}f(x), \qquad (1)$$

where u_{in} is the rheochord supply voltage applied to terminals 3 and 4; l is the length of the rheochord.

The positive direction of displacement for the slider is in this case opposite to the positive direction of the x axis. In obtaining formula (1) it is assumed (as it is throughout) that the potentiometer was unloaded. Thus, for obtaining the dependence of u_{out} on x in the form

$$u_{out} = c_1 u_{in} f(x),$$

where $c_1 = \text{const}$, the equation for the shape of the arm must have a similar form.

The functional relationship between u_{out} and $\underline{x}$ can be obtained in the same way if the rheochord is shaped in the form of a flat curve and the slider is shaped in the form of a straight line segment. We shall call this method the shaped rheochord method. It is not difficult to see that in this case

$$u_{out} = u_{in} \frac{s(x)}{l} = c_2 s(x), \qquad (2)$$

where s(x) is the length of the rheochord arc enclosed between the point 0' and the slider; c_2 = const.

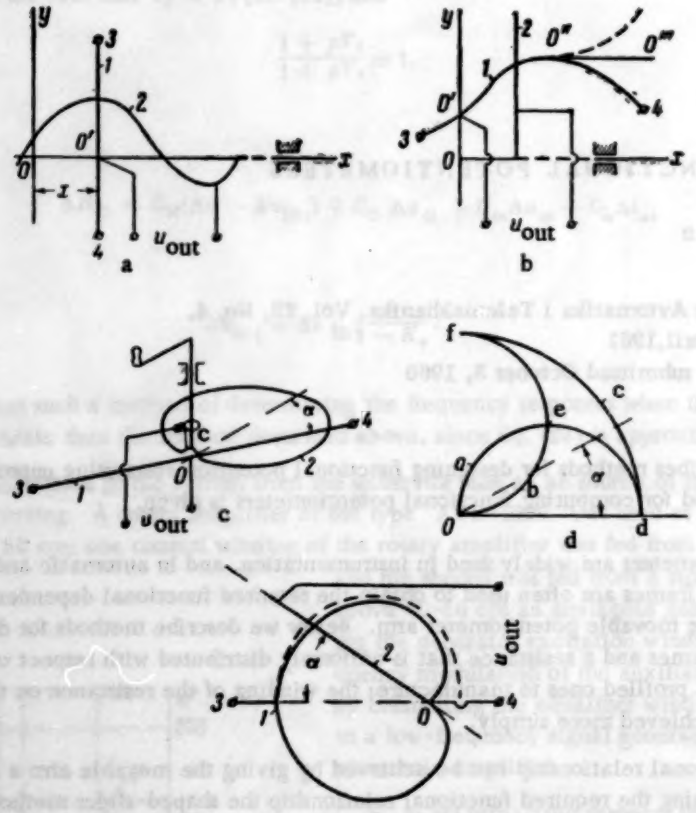

Fig. 1.

The special feature of these potentiometers is the fact that: a) for a rheochord which is not closed and two supply terminals it is possible to obtain only a monotonically varying quantity u_{out} as a function of $\underline{x}$, since s(x) for a monotonic variation of $\underline{x}$ can either only increase or only decrease; b) for obtaining the same functional relationship between u_{out} and $\underline{x}$ it is possible to use various shapes of the rheochord curve. For example, the rheochord shape can be replaced at its end (cf. Fig. 1b) by the broken-line curve which is the mirror image of the segment 0" 0''' that is parallel to the $\underline{x}$ axis. However, all the rheochord curve shapes for which the same function u_{out} (x) is obtained must satisfy Eq. (2).

It is possible to design a functional potentiometer using a combination of the two methods described above. We shall call this the combined method.

All of these methods can be extended to apply to potentiometers with angular displacement of the slider. For example, in order to obtain the required dependence of the output voltage on the angle of rotation α of the slider when the first of the methods above is used, the slider must be given the shape of a curve whose equation in polar coordinates is similar to the output function required under the condition that the rheochord must be a straight

line segment passing through the pole of the polar coordinates (as does the axis of rotation for the slider). For a sine potentiometer, for example, the equation for the circle $\rho = 2R \sin \alpha$ must be obtained, where ρ is the radius-vector, α is the polar angle, R is the radius of the slider circle. Schematically a sine potentiometer with a shaped slider is shown in Fig. 1c.

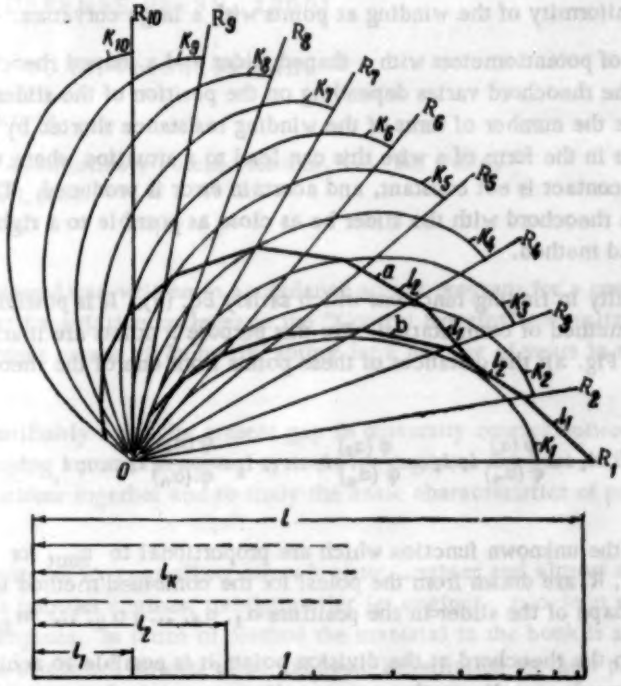

Fig. 2.

When a shaped rheochord is used in potentiometers which convert angular displacement the same function of the output voltage can also be obtained for different shapes of the rheochord curve. For example, in order to obtain a linear dependence of u_{out} on x it is possible to use the following curve shapes (Fig. 1d): the semicircle a; the semicircle b; the quarter of a circle c, and the curve f e d.

The equations for the shapes of the rheochord curves that produce the same output function u_{out} must satisfy the equation

$$\rho^2 + \rho'^2 = (c_3 u_{out})^2 \frac{1}{u_{in}^2}, \qquad (3)$$

where c_3 = const. For example, in order to obtain the function

$$u_{out} = u_{in} \sin\left(\frac{\alpha}{2}\right)$$

the rheochord, in accordance with Eq. (3), must be given the shape of a cardidoid

$$\rho = c_3 \cos^2\left(\frac{\alpha}{2}\right).$$

The arrangement of such a potentiometer is shown in Fig. 1c. Here, just as in the sine potentiometer cited above, it is necessary to isolate the point 0 of the rheochord from the slider for all α except $\alpha = 0$. In both cases

this is achieved by cutting a notch in the slider. In Fig. 1c this notch is denoted by the letter c. The notch permits us to avoid breaking the circuit when the slider passes the value $\alpha = 0$. In order to achieve this in potentiometers with a shaped rheochord it is sometime sufficient to replace the specified rheochord curve shape with another curve which does not pass through the axis of rotation of the slider (cf. for example, the broken line in Fig. 1c).

Other conditions being equal, a shaped rheochord has a higher resistance than the rheochord of a potentiometer with a shaped slider; in some cases this is a positive factor. The shortcoming of a shaped rheochord consists in the possibility of dissipating the uniformity of the winding at points with a large curvature.

A common shortcoming of potentiometers with a shaped slider and a shaped rheochord is the fact that the angle at which the slider intersects the rheochord varies depending on the position of the slider. This latter fact can lead in practice to a situation where the number of turns of the winding resistance shorted by the slider does not remain constant; when the rheochord is in the form of a wire this can lead to a situation where the length of the rheochord section occupied by the slider contact is not constant, and acertain error is produced. Therefore it is desirable that the angle of intersection of the rheochord with the slider be as close as possible to a right angle. This can sometimes be achieved using the combined method.

There is a certain difficulty in finding functions which satisfy Eq. (3). It is possible to find the curve for a shaped rheochord using the graphical method of computation. For this purpose n points are marked on the developed length of the rheochord (segment 1 in Fig. a); the distances of these points from one of the rheochord ends are,respectively, equal to

$$l_1 = \frac{\varphi(\alpha)}{\varphi(\alpha_n)} l;\ l_2 = \frac{\varphi(\alpha_2)}{\varphi(\alpha_n)} l;\ \ldots;\ l_k = \frac{\varphi(\alpha_k)}{\varphi(\alpha_n)} l;\ \ldots;\ l,$$

where $\varphi(\alpha_k)$ are the values of the unknown function which are proportional to u_{out} for $\alpha = \alpha_k$; $k = 1, 2, 3, \ldots$. Then the rays $R_1, R_2, \ldots, R_k, \ldots, R$ are drawn from the poles; for the combined method the curves $K_1, K_2, \ldots, K_k, \ldots \ldots, K_n$, corresponding to the shape of the slider in the positions $\alpha_1, \alpha_2, \ldots, \alpha_k, \ldots, \alpha_n$ are drawn (cf. Fig. 2).

By reproducing "knees" in the rheochord at the division points it is possible to achieve such a deformation of the rheochord that the above-mentioned points lie on the corresponding rays or on the corresponding curves R_k when the combined method is used. The resulting broken line will be the approximate shape of the sought for curve.

Figure 2 shows an example of designing a sine potentiometer with the limits of rotation for the slider ranging from $\alpha = 0$ to $\alpha = \pi/2$. The curve a corresponds to a potentiometer rheochord designed according to the combined method, and curve b corresponds to a potentiometer with a shaped rheochord. For such a graphical computation at the division points the output function will acquire the specified value exactly, and in the interval between those points it will be subject to an error caused by the process of replacing the chord arc. This error will depend on the number of division points and on the specific shape of the curve.

In conclusion it should be noted that for a wire rheochord it is theoretically possible to use the methods cited in this paper to obtain an absolutely exact required relationship between the output voltage and the position of the slider.

REVIEWS

REVIEW OF THE BOOK BY A. A. SHEVYAKOV TITLED "THE AUTOMATION OF AVIATION POWER INSTALLATIONS" (DEFENSE PRESS, 1960)

B. N. Petrov, B. S. Voronkov, and

N. P. Kolpakova

Translated from Avtomatika i Telemekhanika, Vol. 22, No. 4,
pp. 556-557, April,1961

The book being reviewed was written in accordance with a program for a course in aviation power installations and was accepted as a text for aviation colleges in the "Control Systems" specialization. The basic material for this text was drawn from a lecture course given by the author for a number of years in the Ordzhonikidze Moscow Aviation Institute.

The author quite justifiably notes the present gap in university courses between the approach to engine design and to problems of developing automatic control systems for engines. Because of this the book makes an attempt to bring these two problems closer together and to study the basic characteristics of power installations from a unified point of view.

The paper studies systems for controlling aircraft piston engines and almost all types of gas turbine engines – single-shaft and two-shaft turbojet engines, turbopropeller jet engines, two-loop turbojet engines, single-shaft and two-shaft turbopropellar engines. In terms of method the material in the book is arranged in such a way that in the beginning a study is made of control objects when the basic information on their performance characteristics is cited; the equations of motion are derived (in a linear approximation), and the expressions for the coefficients in the equations of motion are derived in terms of the basic parameters which determine the operating mode of the engine. Based on this conclusions are drawn concerning the properties of the engine as a controlled object under all conditions of aircraft flight.

Then a study is made of the possible laws for controlling the engines; the basic requirements which must be imposed on the control systems are formulated, and the problems involving the dynamics of these systems are studied.

For the majority of the engine types examples are given for performing computations with determine the values of the coefficients in the linearized equations of motion and analyze the dynamics of the control system. The problems involving the dynamics of control systems are studied using specific examples of control networks that are used in practice.

The existing educational plans in aviation colleges in the "Control Systems" and "Instrumentation" specialities are laid out in such a way that almost no attention is devoted to problems of engine theory. Moreover, in order to understand the essence of this subject a minimum preliminary knowledge in this field is necessary. In this regard the book under review makes an attempt to approach the subject in a broader fashion; the book thus quite justifiably includes sections devoted to basic information on the performance characteristics of engines.

An important part of the book is devoted to problems involving the dynamics of control systems for turbojet engines with a forcing chamber, since this type of engine is one of the most common used at present. Here a number of possible methods for controlling the forcing loop are studied: regulating the pressure before and after the compressor, regulating the degree of gas expansion onto the turbine, regulating the gas temperature.

For each of the control methods the dynamics problem is solved in such a way that the evaluation of the system is performed according to the transient responses caused by the most substantial perturbations. The same section clarifies problems associated with the process by which the engine enters into a forcing mode. Here studies are also made of several possible methods for controlling the engine when the forcing loop controller acts either on the fuel expenditure in the forcing chamber or on the valve of reactive jet. Under these conditions we take into account different

values for the time shift relative to the beginning of controller operation and the instant at which the forcing mode begins. The transient responses treated in the book permit a proper evaluation of the possibilities of each system.

A significant place in the book is reserved for problems involving the dynamics of control systems for turbopropeller engines; these problems also apply to the basic types of gas turbine engines which are widely used at present. These problems are studied for single-shaft motors with one and two propellers (with a differential reducer), or for two-shaft motors with one propeller. Here a study is made of those control laws for which the number of propeller revolutions is maintained at the specified number by means of controllers which affect the angles at which the propeller blades are set; the specified gas temperature is maintained using controllers which operate in closed and open loops and affect the fuel discharge. The problems associated with the effect of the stabilizing devices in these controllers are clarified along with the effect of the engine torque limiter on the properties of the control system. Data on the transient responses makes it possible correctly to evaluate the advantages and disadvantages of each system which is studied.

An important section of the book is the chapter dealing with problems of autonomous control of gas turbine engines. With respect to single-shaft turbopropeller jet engines and turbopropeller engines with one propeller the book demonstrates the possibilities of such control systems and compares them with nonautonomous systems. Here a study is made of conditions governing complete and partial autonomy, and the advantage of using autonomous control systems is demonstrated.

One of the very important problems which to a great extent determines the basic properties of any aviation power installation is the acceleration characteristic for the engine. The narrow range of operating stability for the compresser and the combustion chamber, as well as the regorous limits with respect to the maximum allowable gas temperature at the turbine input, impose especially difficult conditions on the correct selection of parameters for the acceleration system in the engine. A separate chapter is devoted to this subject, where a study is made of the behavior of an engine acceleration system using a phase plane (since a nonlinear problem is being solved). The method given for computing the acceleration systems of turbojet engines also makes it possible to select the controller parameters in such a way that the necessary margin is achieved with respect to the maximum allowable values of gas temperature and the pumping characteristics of the compressor.

The book compares favorably with others in terms of its completeness, the use of specific examples, and the way in which the problems dealt with coincide with the curriculum.

Besides systematizing previous known material, the book offers a number of new results, including an analysis of the dynamics of two-shaft and two-loop turbojet engines, single-shaft turbopropeller jet engines, turbopropeller engines with a differential reducer and coaxial variable-pitch propellers, autonomous systems for turbojet engines and turbopropeller engines, and acceleration systems for turbojet engines. Investigations of the transient responses are made for all of these case, and the corresponding estimates are given.

The book includes certain clearly identified material which extends beyond the range of the student curriculum; this is done to give the book a scope beyond that of a textbook.

The book is adequately illustrated and is written in easily understandable language.

The book presents extensive material on the classification of aviation engines as controlled objects. However (and this is one of its most substantial shortcomings) the book does not provide any comparison and classification of the automatic control systems for the indicated engines. The author has not made a critical analysis of various types of control systems. Critical remarks should also be made on the way engineering design problems are treated; this applied particularly to problems of designing the automation equipment. The book essentially contains no description of the design and technological solutions, nor does it include a survey of typical engineering specifications and conditions for aviation engine automation systems; problems of improving the control reliability are also not dealt with.

The "auxiliary" aggregates of the control systems—the fuel supply, the starting system for the engine, the safety features, etc.—are treated in a very cursory way. New problems in the theory of aviation engine control are not treated at all (problems of optimization and a consideration of discontinuous perturbations).

As a whole this book is an original text which deals in easily accessible form with the problems set forth in it; its publication is very timely.